Seismic Fragility Formulations for Water Systems

*Web Site Report
Appendices*

*Prepared by:
G&E Engineering Systems Inc.*

*6315 Swainland Road
Oakland, CA 94611
(510) 595-9453 (510) 595-9454 (fax)
eidinger@earthlink.net*

Principal Investigator: John Eidinger, S.E.

Table of Contents

Figures

Tables

Tables (Continued)

A. Commentary - Pipelines

A.1 Buried Pipeline Empirical Data

Section 4 of the main report provides a descriptions and references for empirical damage to buried pipelines from various earthquakes.

Table A.1-1 provides 164 references to damage to buried pipelines from various earthquakes. The references listed in Table A.1-1 are provided section 4.8 of the main report.

Depending upon source, some entries in Table A.1-1 represent duplicated data. Also, some data in Table A-1 include damage to service laterals up to the customer meter, whereas some data points do not. Also, some data points in Table A.1-1 are based on PGA, some on PGV and some of MMI. Some data points in Table A.1-1 exclude damage for pipes with uncertain attributes. For those data points based on PGA or PGV, some are based on attenuation models which predict median level horizontal motions; and some are based on the maximum of two orthogonal horizontal recordings from a nearby instrument.

Table A.1-2 presents the same dataset as in Table A.1-1, but normalized to try to make all data points represent the following condition: damage to main pipes (excludes damage to service laterals up to the utility meter) versus median PGV (average of two horizontal directions).

Table A.1-3 presents damage data for buried pipelines subjected to some form of permanent ground deformations, including liquefaction and ground lurching.

A.2 Buried Pipeline Empirical Data

A.2.1 San Francisco, 1906

1906 San Francisco earthquake (magnitude 8.3) caused the failure of the water distribution system which in turn contributed to the four day long fire storm that destroyed much of the city [Manson].

About 52% of all pipeline breaks occurred inside or within one block of zones experiencing permanent ground deformations, yet these zones accounted for only 5% of the built up areas in 1906 affected by strong ground shaking [Youd and Hoose, Hovland and Daragh, Schussler].

A.2.2 San Fernando, 1971

1971 San Fernando earthquake (magnitude 7.1) caused 23 square miles of residential areas to be without water until 1,400 repairs were made. Over 500 fire hydrants were out-of-service until 22,000 feet of 6 to 10 inch pipe could be repaired [McCaffery and O'Rourke, O'Rourke and Tawfik].

A.2.3 Haicheng, China, 1975

1975 Haicheng, China earthquake (magnitude 7.3) caused damage to buried water piping to four nearby cities resulting in an average pipe repair rate of 0.85 repairs per 1,000 feet of pipe [Wang, Shao-Ping and Shije]. The damage was greatest for softer soil sites closer to the epicenter.

A.2.4 Mexico City, 1985

1985 Mexico City earthquake (magnitude 8.1) caused about 30% of the 18 million people in the area to be without water immediately after the earthquake [Ayala and O'Rourke, O'Rourke and Ayala]. The aqueduct / transmission system was restored to service about six weeks after the event and repairs to the distribution system lasted several months.

There are two water utilities serving Mexico City. The Federal District system experienced about 5,100 repairs to its distribution system (2 to 18 inch diameter pipe, total length of pipe uncertain), and about 180 repairs to its primary system (20 to 48 inch pipe, 570 km of pipe). The State of Mexico water system had over 1,100 repairs to its piping system in addition to about 70 repairs to the aqueduct system. Over 6,500 total repairs resulted from the earthquake.

A.2.5 Other Earthquakes 1933 - 1989

Table A.2-1 presents summary damage statistics for buried pipe for a variety of historical earthquakes. The data shown is limited (where possible) to damage from ground shaking effects only.

Earthquake	Pipe Material	Pipe Repairs	Pipe Length, km	Notes
1933 Long Beach	Cast Iron	130	592	MMI 7-9
1949 Puget Sound	Cast Iron	17	1,319.2	MMI 7
1949 Puget Sound	Cast Iron	24	84.1	MMI 8
1965 Puget Sound	Cast Iron	14	1,906.7	MMI 7
1965 Puget Sound	Cast Iron	13	112.2	MMI 8
1969 Santa Rosa	Cast Iron	7	54 – 219 ?	
1971 San Fernando	Cast Iron	55	5,700	MMI 7
1971 San Fernando	Cast Iron	84	536.2	MMI 8
1979 Imperial Valley	Cast Iron	19	18.5	El Centro
1979 Imperial Valley	Asbestos Cement	6	100	El Centro
1983 Coalinga	Cast Iron	8	13.8	Corrosion?
1989 Loma Prieta	Cast Iron mostly	15	1,740	SFWD

Table A.2-1. Pipe Damage Statistics From Various Earthquakes

Except for the GIS-based analyses done for the EBMUD water system (1989 Loma Prieta) and the LADWP water system (1994 Northridge), damage statistics for the various past earthquakes all suffer from one or more of the following limitations:

- Accurate inventory of existing pipelines (lengths, diameters, materials, joinery) were not completely available.

- Limited (or no) strong motion instruments were located nearby. This makes estimates of strong motions over widespread areas less accurate.

- Accurate counts of damaged pipe locations were not available.

Recognizing these limitations, Toprak [1998] sieved through the available databases to sift out reliable (or semi-reliable) estimates of pipe damage from past earthquakes. Table A.2-2 lists his findings. The PGVs in Table A.2-2 are based on interpreted nearby instruments, listing the highest of the two horizontal components. The average of the two horizontal directions of peak ground velocity motion would be about 83% of the maximum in any one direction.

Earthquake	Pipe Material	PGV (peak) (in/sec)	Pipe Length (km)	Repairs per km	Notes
1989 Loma Prieta	Cast Iron (mostly)	5.3	1,740	0.0086	SFWD
1987 Whittier	Cast Iron	11.0	177.1	0.0791	
1971 San Fernando	Cast Iron	11.8	242.6	0.0412	Zone 1
1971 San Fernando	Cast Iron	7.1	271.6	0.0221	Zone 2
1979 Imperial Valley	Asbestos Cement	15.0	100	0.0600	

Table A.2-2. Pipe Damage Statistics From Various Earthquakes (after Toprak)

Table A.2-3 lists the data shown in Figures A-1 and A-2. The PGV values are based on attenuation relationships.

Earthquake	Pipe Material	PGV (in/sec)	Pipe Length (km)	Repairs per km	Notes
1971 San Fernando	Cast Iron 3 to 6"	11.8		0.155	Pt A
1969 Santa Rosa	Cast Iron 3 to 6"	5.9	219	0.028	Pt B
1971 San Fernando	Cast Iron 3 to 6"	5.9		0.024	Pt C
1965 Puget Sound	Cast Iron 8 to 10"	3.0		0.007	Pt D
1983 Coalinga	Cast Iron 3 to 6"	11.8		0.24	Pt E
1985 Mexico City	AC, Conc CI 20-48"	18.9		0.137	Pt F
1985 Mexico City	AC, Conc CI 20-48"	4.7		0.0213	Pt G
1985 Mexico City	AC, Conc CI 20-48"	4.3		0.0031	Pt H
1989 Tlahuac	PCCP 72"	21.3		0.457	Pt I
1989 Tlahuac	PCCP 72"	9.8		0.0518	Pt J
1983 Coalinga	AC 3 to 10"	11.8		0.101	Pt K

Table A.2-3. Pipe Damage Statistics From Various Earthquakes (From Figures A-1 and A-2)

There are several issues related to the data in Tables A.2-2 and A.2-3, which might suggest how this data might be combined with data from Sections A.3.11 and A.3.12. These are as follows:

- No GIS analysis was performed for the pipeline inventories. Thus, differentiation of pipe damage as a function of PGV is much cruder than that available from GIS analysis.

- The data in Table A.2-2 is based on maximum ground velocity of two horizontal directions for the nearest instrument. The data in Table A.2-3 is based on attenuation functions, and is the expected average ground motion in the two horizontal directions.

- The data for the 1985 Mexico City earthquake is for an event which had strong ground motion reaching 120 seconds. This is 3 to 6 times longer durations of ground shaking than the data from the other earthquakes in the databases. Not

surprisingly, the damage rates for the 1985 / 1989 Mexico data are higher than comparable values from California earthquakes. If repair rate is a function of duration, then a magnitude / duration factor might be needed when combining data from separate types of empirical datasets.

A.3 Buried Pipe Fragility Curves – Past Studies

In this section, we summarize past studies that developed damage algorithms that have been used for the seismic evaluation of water distribution pipes. As the state-of-the-practice in water distribution seismic performance evaluation is rapidly advancing, some of the past studies are no longer considered appropriate. However, many of these past studies are still considered current.

The following sections briefly describe these past studies.

A.3.1 Memphis, Tennessee

Since the late 1980s, several universities, the National Science Foundation and the U.S.G.S. sponsored studies which with regard to seismic pipeline damage for the city of Memphis in Tennessee [Okumura and Shinozuka]. For the most part, the damage algorithms used in these studies were based on expert opinion and a limited amount of empirical evidence.

The damage algorithms used in these studies are based upon simple formulae which were easily applied to all pipes within the water distribution system. The algorithms are functions of the following three parameters:

- Level of shaking, as expressed in terms of Modified Mercalli Intensity. The higher the MMI, the higher the damage rate.

- Pipe diameter. The larger the pipe diameter, the lower the damage rate. The algorithm is based upon limited empirical earthquake damage data (at the time), which tended to show significantly lower damage rates for larger diameter pipe. New empirical data in the 1989 Loma Prieta earthquake confirms the trend of improved performance of large diameter pipe.

- Ground Condition. The ground condition is based upon the Uniform Building Code S1, S2, S3 and S4 descriptions. The damage algorithm in very poor soils (S4) was set at 10 times (arbitrarily chosen) that as stiff soils (S1).

The incidence of breaks is assumed to be a Poisson process and the damage algorithm is as follows:

$$n = C_d \, C_g \, 10^{0.8(\text{MMI}-9)} \qquad\qquad\qquad \text{[A-1]}$$

where, n = the occurrence rate of pipe failure per kilometer; MMI = Modified Mercalli Intensity; and

$$C_d = \begin{cases} 1.0 & \text{Diameter D} \quad < 25 \text{ cm} \\ 0.5 & 25 \le D < 50 \text{ cm} \\ 0.2 & 50 \le D < 100 \text{ cm} \\ 0.0 & 100 \le D \end{cases}$$

$$C_g = \begin{cases} 0.5 & \text{Soil S1} \\ 1.0 & \text{Soil S2} \\ 2.0 & \text{Soil 3S} \\ 5.0 & \text{Soil S4} \end{cases}$$

The probability of a major pipe failure (i.e., complete break with total water loss) is calculated as:

$$Pf_{major} = 1 - e^{-nL} \qquad\qquad\qquad [A-2]$$

where L = the length of pipe and n is defined by the equation above.

The occurrence rate of leakage (minor damage) is assumed to be:

$$Pf_{minor} = 5\,Pf_{major} \qquad\qquad\qquad [A-3]$$

The above damage algorithms are very simple, and capture several of the key features of how seismic hazards affect pipe. Although these damage algorithms are simple to use, they are not considered suitable for "modern" loss estimation efforts as they are based on the MMI scale (instead of PGV and PGD), and omit factors such as pipe construction material, corrosion and amounts (if any) of ground failures.

A.3.2 University-based Seismic Risk Computer Program

Researchers at Princeton University have developed a program [Sato and Myurata] using the same damage algorithm as for Memphis above, except that the Cg factor (ranging from 1.0 to 0.0, depending on ground conditions) is omitted.

The damage algorithm presented in the following table is taken from that reference. Note how the pipe failure rate is strongly dependent upon seismic intensity and pipe diameter. For the same reasons as for the Memphis algorithms, these damage algorithms are not considered suitable for use in "modern" loss estimation studies.

MMI Scale	D < 25 cm	25 ≤ D < 50 cm	50 ≤ D < 100 cm	100 ≤ D
VI	0.003	0.001	0.000	0.000
VII	0.025	0.012	0.005	0.000
VIII	0.158	0.079	0.031	0.000
IX	1.000	0.500	0.200	0.000
X	6.309	3.154	1.261	0.000

Table A.3-1. Occurrence Rate of Pipe Failure (per km)

A.3.3 Metropolitan Water District

In a 1978 study on large diameter (40 to 70 inches) welded seamless pipe for the Los Angeles area Metropolitan Water District (MWD) [Shinozuka, Takada and Ishikawa], a set of damage algorithms was developed based upon analytical calculations of strain levels in the pipe. These algorithms were then applied to the MWD water transmission network.

For wave propagation, the structural strains in the pipe were calculated based upon the free field soil strains. For segments of pipe that cross through areas where soil liquefaction or surface fault rupture are known to occur, the pipe strains are computed using formulas by

[Newmark and Hall] or [in ASCE, 1984]. A series of damage probability matrices were developed for the various units of soil conditions that the large diameter pipe traverses. A typical damage probability matrix is as follows.

MMI Scale	Minor Damage	Moderate Damage	Major Damage
VI	1.00	0.00	0.00
VII	0.96	0.04	0.00
VIII	0.18	0.71	0.11
IX	0.00	0.11	0.89

Table A.3-2. Damage Probability Matrix

This table applies for pipe with curves and connections in poor soil conditions. For Intensity VIII, such pipe will have an 18% chance of being undamaged (minor damage), a 71% chance of leakage (moderate damage), and an 11% chance of a total break (major damage).

These algorithms introduce the concept of uncertainty into the analysis. For example, given Intensity IX, there is some uncertainty whether the damage rates will be "moderate" or "major". The uncertainty arises both from imperfect knowledge of the capacity of individual pipe strengths and the randomness of the earthquake hazard levels.

A.3.4 San Francisco Auxiliary Water Supply System

The damage algorithms suggested by Grigoriu et al [Grigoriu, O'Rourke, Khater] were used in a study on pipeline damage of the Auxiliary Water Supply System (AWSS) for the city of San Francisco, California. The AWSS consists of about 115 miles of pipelines with diameters in the range of 10 to 20 inches.

For modeling expected damage from traveling waves, the authors used a simpler version of the Memphis model. For the AWSS, they adopted the following model:

$$P_f = 1 - e^{-nL} \hspace{3cm} \text{[A-4]}$$

where, P_f = probability that a pipe will have no flow (i.e., complete failure);
n = the mean break rate for the pipe; and, L = the length of the pipe.

No damage algorithms were provided for other seismic hazards (e.g., landslides, surface faulting, liquefaction - although the San Francisco Liquefaction study, described below, considers liquefaction effects on this system). To obtain the mean break rate, the authors of this study summarized pipeline damage statistics for traveling wave effects due to five past earthquakes.

All pipes, independent of size, age, kind or location, were modeled with the same mean break rate value. No "leakage" failure modes were adopted. The range of break rates studied was from 0.02 breaks per kilometer, to 0.325 breaks per kilometer, with six intermediate values. The authors loosely suggest that a break rate of 0.02 / km corresponds to about Intensity VII, and a break rate of 0.10 per km corresponds to about Intensity VIII.

A.3.5 Seattle, Washington

This U.S.G.S. - sponsored study for Seattle, Washington, explicitly differentiates between pipe damage caused by ground shaking and soil failure due to liquefaction [Ballantyne,

Berg, Kennedy, Reneau and Wu]. This is a major refinement as compared to some earlier efforts.

The authors use the following damage algorithms for ground shaking effects:

$$n = a\, e^{b(MMI - 8)} \hspace{5cm} \text{[A-5]}$$

where, n = repairs per kilometer, and a and b are adjusted to fit the scatter in empirical evidence of damage from selected past earthquakes, and engineering judgment. The results are shown in Figure A-3.

The damage algorithm for buried pipelines which pass through liquefied soil zones is described in Table A.3-3. This is also shown graphically in Figure A-4. Figures A-4 and A-5 show the suggested landslide and fault crossing algorithms, respectively.

Pipe Kind	Repairs (Breaks or Leaks) per Kilometer
Asbestos Cement	4.5
Concrete	4.5
Cast Iron	3.3
PVC	2.6
Welded Steel with Caulked Joints	2.6
Welded Steel with Gas or Oxyacetylene Welded Joints	2.4
Ductile Iron	1.0
Polyethylene	0.5
Welded Steel with arc-welded joints	0.5

Table A.3-3. Pipe Damage Algorithms Due to Liquefaction PGDs

In application, the authors compute the damage rate using equation A-5 (based on MMI) and the liquefaction-zone rate (based on soil description). The higher of the two rates is applied to the particular pipe if the pipe is located in a liquefaction zone.

This study also refined some of the historical repair damage statistics to allow differentiation between leak and break damage. Undifferentiated damage is denoted as repairs.

- A leak represents joint failures, circumferential failures (round cracks), and corrosion-related failures (pinhole and small blow-outs).

- A break represents longitudinal cracks, splits and ruptures. A full circle break of Cast Iron or Asbestos Cement pipe, for example, would also be defined as a break.

By reviewing the damage / repair data from the 1949 and 1969 Seattle, 1969 Santa Rosa, 1971 San Fernando Valley, 1983 Coalinga, and 1987 Whittier Narrows earthquakes, the following observations were made:

- In local areas subjected to fault rupture, subsidence, liquefaction or spreading ground, approximately 50% of all recorded repairs/damage have been breaks. The remaining 50% of all repairs / damage have been leaks.

- In local areas only subjected to traveling wave motions, approximately 15% of all recorded repairs / damage have been breaks. The remaining 85% of all repairs have been leaks.

A.3.6 Empirical Vulnerability Models

In this National Science Foundation sponsored study performed by the J. H. Wiggins Company [Eguchi et al], empirical-based damage algorithms were developed for pipe in ground shaking, fault rupture, liquefaction and landslide areas. They were based on review of actual pipe damage from the 1971 San Fernando, 1969 Santa Rosa, 1972 Managua and the 1979 El Centro earthquakes. The algorithms are statistical in nature by computing the number of pipe breaks per 1,000 feet of pipe. The algorithms denote different break rates according to pipe type. Asbestos cement pipe generally was found to have the poorest performance and welded steel having the best performance. The study also indicates that corroded pipe have break rates about three times that of uncorroded pipe.

This empirical evidence forms the basis of some of the more recent efforts, including the Seattle (described above) damage algorithms. The increased repair rate for corroded pipes also serves as partial basis for the pipeline fragility curves in the current study.

A.3.7 San Francisco Liquefaction Study

In this study [Porter et al] the repair rate per 1,000 feet of pipe was related to magnitude of permanent ground deformation (PGD). Data from the 1989 Loma Prieta (Marina District) and the 1906 San Francisco (Sullivan Marsh and Mission Creek) earthquake were used to develop a damage algorithm. Figure A-6 shows the algorithm. A key feature is that the repair rate is proportional, at least in some increasing fashion, to the PGD magnitude.

Most of the San Francisco pipe which broke in the liquefied areas in 1906 and 1989 were cast iron.

A.3.8 Empirical Vulnerability Model – Japanese and U.S. Data

This 1975 study [Katayama, Kubo and Sito] developed an empirical pipeline damage model based on observed repair rates from actual earthquakes. Several of these earthquakes were in Japan (1923 Kanto - Tokyo, 1964 Nigata, 1968 Tokachi-Oki).

The repair rate is related to soil condition (good, average, poor), and peak ground acceleration. It does not distinguish between damage caused by ground shaking (wave propagation), or permanent ground deformations (liquefaction, landslide, fault crossing). Figure A-7 shows the algorithm.

A key conclusion drawn from Figure A-7 is that "poor" to "good" soil conditions bears a critical relationship to overall pipe repair rates. Repair rates in "poor" soils are an order of magnitude higher than repair rates in better soils. Another facet to be pointed out is that this early effort tried to relate peak ground acceleration to pipe repair rates. More recent efforts have shown that peak ground accelerations is not a good predictor of actual energies damaging to pipes. Instead, peak ground velocity (PGV) is a better predictor. PGVs are further discussed in the Barenberg work described below.

A.3.9 Wave Propagation Damage Algorithm - Barenberg

This 1988 study [Barenberg] computes a relation between buried cast iron pipe damage (breaks/km) observed in four past earthquakes and peak ground velocities experienced at the associated sites. The relation is for damage caused by transient ground motions only (i.e., wave propagation effects). Figure A-1 shows the algorithm.

This study makes a major improvement over previous studies. Empirical pipe damage is related to actual levels of ground shaking (peak ground velocity) rather than indirect (and very imperfect) Modified Mercalli Intensity levels. MMIs have often been used in the past, as there were no seismic instruments to record actual ground motions - the MMI scale

relates observed items like broken chimneys to ground shaking levels. With the vastly increasing number of seismic instruments installed, each future earthquake will add to the empirical database of actual ground motions versus actual observed damage rates.

Another important reason to adopt peak ground velocity as the predictor of ground - shaking induced pipe repairs is that there are mathematical models to relate ground velocities to strains induced in pipes. This mathematical model states that peak seismic ground strain is directly proportional to the peak ground velocity. Up to very high strain levels the pipes conform to ground movements, and the strain/deformation in the pipe is correlated to the ground strain. Hence empirical relations relating damage to peak ground velocity have a better physical basis than those using Modified Mercalli Intensity.

A.3.10 Wave Propagation Damage Algorithm – O'Rourke and Ayala

This 1988 study [Barenberg] computes a relation between buried cast iron pipe damage (breaks/km) observed in four past earthquakes and peak ground velocities experienced at the associated sites. The relation is for damage caused by transient ground motions only (i.e., wave propagation effects). Figure A-2 shows the algorithm.

A subsequent work [O'Rourke, M., and Ayala, G., 1994] provides additional empirical data points for pipe damage versus peak ground velocity that were not included in the Barenberg work. The additional data are for large diameter (20 and 48 inch diameter) asbestos cement, concrete, prestressed concrete, as well as distribution diameter cast iron and asbestos cement pipe that were subjected to pipe failures in the 1985 Mexico city, 1989 Tlahuac and 1983 Coalinga earthquakes.

Some detailed pipe data were lost in the 1985 Mexico earthquake (the water company's facility collapsed and records were lost). However, it appears that the bulk of the large diameter transmission pipe that is represented by the data in Figure A-2 is for segmented AC and concrete pipe. Joints were typically cemented. A least squares regression line ($R^2 = 0.71$) is plotted for convenience.

The following observations are made:

1. The empirical evidence (Figures A-1 and A-2) does not clearly suggest a "turn over" point in the damage algorithm, as is suggested in the Seattle study (Figure A-3) at MMI = VIII (or PGV = 20 inches / second after conversion).

2. The empirical data is more severe at very low levels of shaking than suggested in the Seattle study. The differences are smaller at strong levels of shaking. In practice, this may not be a great concern, as being greatly off at very low levels of shaking probably does not meaningfully change the level of overall system damage.

A.3.11 Damage Algorithms – Loma Prieta - EBMUD

This study of the EBMUD water distribution system [Eidinger 1998, Eidinger et al 1995, unpublished work] presents the empirical damage data to over 3,300 miles of pipelines that were exposed to various levels of ground shaking in the 1989 Loma Prieta earthquake. An effort to collate all pipeline damage from the Loma Prieta and Northridge earthquakes is available from http://quake.abag.ca.gov. Using GIS techniques, the entire inventory of EBMUD pipelines was analyzed to estimate the median level of ground shaking at each pipe location. Attenuation models used in this study were calibrated to provide estimates of ground motions approximately equal to those observed at 12 recording stations within the EBMUD service area. Then, careful review was made of each damage location where pipes actually were repaired in the first few days after the earthquake (see Figure A-8 for a map of damage locations).

PGV / Material	Cast Iron RR / 1000 feet	Asbestos Cement RR / 1000 feet	Welded Steel RR / 1000 feet
3 Inches / sec	0.00560	0.00341	0.00253
5 Inches / sec	0.01230	0.00239	0.00841
7 Inches / sec	0.00517	0.00086	0.00610
17 Inches / sec	0.09189	0.01230	0.14826

Table A.3-4. Pipe Repair Rates per 1,000 Feet, 1989 Loma Prieta Earthquake

The damage pipe locations were binned into twelve groups, representing four average levels of PGV, and for three types of pipeline: cast iron, asbestos cement (rubber gasket joints) and welded steel (single lap welded joints). Repair rates were calculated for each bin. The total inventory of pipelines included about 752 miles of welded steel pipe, 1,008 miles of asbestos cement pipe, and 1,480 miles of cast iron pipe. There were 135 pipe repairs to the EBMUD system due to the Loma Prieta earthquake. (Mains: 52 cast iron, 46 steel, 13 asbestos cement, 2 PVC. Service connections: 22 up to meter – damage on customer side of meter not counted). Tables A.3-4 and A.3-5 show the results.

PGV / Material	Cast Iron Miles of Pipe	Asbestos Cement Miles of Pipe	Welded Steel Miles of Pipe
3 Inches / sec	473.2	444.7	374.2
5 Inches / sec	123.2	79.2	45.0
7 Inches / sec	878.8	438.3	279.3
17 Inches / sec	20.6	46.2	60.0

Table A.3-5. Length of Pipe in Each Repair Rate Bin, Loma Prieta Earthquake

The twelve data points from Table A.3-4, are plotted in Figure A-9. An exponential curve fit is drawn through the data. The scatter shown in this plot is not unexpected, in that damage data for three different kinds of pipe are all combined into one regression curve.

The same data in Figure A-9 are plotted in Figure A-10, but this time using three different regression curves, one for each pipe material. Table A.3-6 provides the coefficients for the regression relationships.

Value / Material	Cast Iron RR / 1000 feet	Asbestos Cement RR / 1000 feet	Welded Steel RR / 1000 feet
a	0.000737	0.000725	0.000161
b	1.55	0.77	2.29
PGV	in/sec	in/sec	in/sec
R^2	0.71	0.26	0.90

Table A.3-6. Regression Curves for Loma Prieta Pipe Damage, RR = a (PGV)^b, R^2

One issue that is brought out by examining Figures A-9 and A-10 is whether a pipe fragility curve should be represented by:

- $RR = k \, a \, (PGV)^b$, where k is some set of constants that relate to the specific pipe material, joinery type, age, etc, and (a,b) are constants developed by the entire empirical pipe database (like Figure A-9); or

- RR = a (PGV)^b, where (a,b) are constants specific to the particular pipe type, ideally with all other factors (joinery, age, etc.) being held constant (like Figure A-10).

The standard error terms (R^2) in the regression relationships in Table A.3-6 seem "better" than those in Figure A-9. However, this might be because the regression relationships in Figure A-10 use fewer data points (4) than the regression line in Table A.3-6 and Figure A-9 (12). Based on engineering judgment, R^2 values like 0.90 for the welded steel pipe curve (Figure A-10) appear to be too high, and are considered more of an artifact of a small data set than being a true predictor of uncertainty. This statement is made because the performance of steel pipe is also known to be a factor of age, corrosive soils, quality of construction of the welds, diameter (possibly), etc., which are not accounted for in the two parameter regression models in Figures A-9 or A-10.

Another key observation from Figure A-10 is that Asbestos Cement pipe (with gasketed joints) appears to perform better than cast iron or welded steel pipe, at least for damage induced by ground shaking. This is in contrast to Figure A-3, which ranks welded steel better than cast iron, and asbestos cement the worst. As also demonstrated in Section A.3.12, the same trend is seen in the 1994 Northridge earthquake, where asbestos cement pipe performed better than ductile iron pipe or cast iron pipe. Base on the rigor of the analyses for the Loma Prieta and Northridge data sets, it would appear that the trend for asbestos cement pipe in Figure A-3 is wrong. This might be due to a reliance on engineering judgment (Figure A-3) for the performance of rubber gasketed AC pipe, as the empirical evidence of AC pipe performance from Loma Prieta and Northridge was not available when Figure A-3 was developed.

There has been some researchers that have suggested that pipe damage rates seem to be a function of pipe diameter (for example, see Section 4.4.7). There is debate as to why this might or might not be so.

Tables A.3-7, A.3-8 and A.3-9 provide the EBMUD – Loma Prieta database of pipe lengths and pipe repairs for cast iron, welded steel and asbestos cement pipe, respectively. Figure A-11 summarizes the empirical evidence for the 1989 Loma Prieta earthquake. Tables A.3-10 and A.3-11 provides the length of pipe and number of repairs for each data point in Figure A-11.

Nominal Diameter (inches) / Material	Cast Iron Miles of Pipe	Asbestos Cement Miles of Pipe	Welded Steel Miles of Pipe
4	321		
6	784	663	111
8	218	296	147
10 to 12	114	49	208
16 to 20	43		136
24 to 60			151

Table A.3-10. Pipe Lengths, 1989 Loma Prieta Earthquake, By Diameter

Nominal Diameter (inches) / Material	Cast Iron Number of Repairs	Asbestos Cement Number of Repairs	Welded Steel Number of Repairs
4	12		
6	31	8	29
8	8	5	16
10 to 12	4	1	13
16 to 20	1		2
24 to 60			3

Table A.3-11. Pipe Repair, 1989 Loma Prieta Earthquake, By Diameter

The results in Figure A-11 show a clear trend for an improvement in welded steel pipe performance with increasing pipe diameter; the trend is lesser for cast iron pipe, and opposite for asbestos cement pipe. The following reasons attempt to explain this behavior:

- Welded steel pipe. Small diameter (6" and 8") welded steel pipe are used as distribution lines to customers. The utility used only this kind of pipe in areas prone to "poor" soil conditions. Examination of the actual damage from the earthquake showed evidence of poor weld quality and corrosion. Smaller diameter pipe tends to get less attention in terms of inspection of welds. Pipe wall thickness for smaller diameter pipe are relatively thinner than for large diameter pipe, and a constant rate of corrosion would affect smaller diameter pipe to a greater degree. Larger diameter pipe (16" and higher) rarely has service taps or hydrants, and has fewer valves, making the pipe less constrained, and thus easier to accommodate ground movements without induced stress risers in the pipe. Large diameter pipe tends to be located in areas away from the worst soils; while the damage data in Table 4-7a,b have been sieved to removed damage due to liquefaction, it is possible that some liquefaction-induced data remains in the data set.

- Cast iron pipe. Similar to steel pipe issues, but without the weld quality factor.

- Asbestos cement pipe. There is no weld or corrosion issues related to asbestos cement pipe. The increase in repair rate with increasing diameter might be related to the small number of AC pipe repairs in the data set (14 total), or to factors such as different lay lengths between rubber gasketed joints; different insertion tolerances for each rubber gasketed joint, for different diameter AC pipe. A rigorous analysis of damage rate versus lay lengths and joint geometry has not yet been performed.

To further examine the trends of diameter dependency versus damage rates, the data is recast for cast iron pipe, in Figure A-12. No clear trends can be seen in Figure A-12 that would indicate a diameter dependency for cast iron pipe. As will be seen in Section A.3.12, the Northridge data tends to show a good diameter dependency for cast iron pipe.

Based on the Loma Prieta and prior earthquake datasets, Eidinger and Avila [1999] presented a simplified way to assess the relative performance of different types of buried pipe due to wave propagation and permanent ground deformation. Tables A3.12 and A.3-13 show the results. The information presented in Tables A.3-12 and A.3-13 was based on the empirical database through the 1989 Loma Prieta earthquake. In Tables A.3-12 and A.3-13, the constants K_1 and K_2 are to be multiplied by the following "backbone" fragility curves:

Ground shaking: n = 0.00032 (PGV)$^{1.98}$, (n = repair rate per 1,000 feet of pipe, PGV in inches per second)

Permanent ground deformation: n = 1.03 (PGD)$^{0.53}$ (n = repair rate per 1,000 feet of pipe, PGD in inches)

Pipe Material	Joint Type	Soils	Diam.	K_1	Quality
Cast iron	Cement	All	Small	0.8	B
Cast iron	Cement	Corrosive	Small	1.1	C
Cast iron	Cement	Non corr.	Small	0.5	B
Cast iron	Rubber gasket	All	Small	0.5	D
Welded steel	Lap - Arc welded	All	Small	0.5	C
Welded steel	Lap - Arc welded	Corrosive	Small	0.8	D
Welded steel	Lap - Arc welded	Non corr.	Small	0.3	B
Welded steel	Lap - Arc welded	All	Large	0.15	B
Welded steel	Rubber gasket	All	Small	0.7	D
Asbestos cement	Rubber gasket	All	Small	0.5	C
Asbestos cement	Cement	All	Small	1.0	B
Asbestos cement	Cement	All	Large	2.0	D
Concrete w/Stl Cyl.	Lap - Arc Welded	All	Large	1.0	D
Concrete w/Stl Cyl.	Cement	All	Large	2.0	D
Concrete w/Stl Cyl.	Rubber Gasket	All	Large	1.2	D
PVC	Rubber gasket	All	Small	0.5	C
Ductile iron	Rubber gasket	All	Small	0.3	C

Table A.3-12. Ground Shaking - Constants for Fragility Curve (after Eidinger)

Pipe Material	Joint Type	K_2	Quality
Cast iron	Cement	1.0	B
Cast iron	Rubber gasket, mechanical	0.7	C
Welded steel	Arc welded, lap welds	0.15	C
Welded steel	Rubber gasket	0.7	D
Asbestos cement	Rubber gasket	0.8	C
Asbestos cement	Cement	1.0	C
Concrete w/Stl Cyl.	Welded	0.8	D
Concrete w/Stl Cyl.	Cement	1.0	D
Concrete w/Stl Cyl.	Rubber Gasket	1.0	D
PVC	Rubber gasket	0.8	C
Ductile iron	Rubber gasket	0.3	C

Table A.3-13. Permanent Ground Deformations - Constants for Fragility Curve (after Eidinger)

Eidinger suggested a "quality" factor ranging from B to D. "B" suggested reasonable confidence in the fragility curve based on empirical evidence; "D" suggested little confidence.

The empirical evidence from the 1994 Northridge earthquake (see Section A.3.12) suggests that K_1 for small diameter AC pipe might be about 0.4 times that for cast iron pipe; similarly K_1 for small diameter ductile iron pipe might be around 0.55. The K_1 constant for PVC pipe might be similar to that for AC pipe (0.4), still recognizing the lack of empirical data for PVC pipe. The relative performance of different pipe materials in the Kobe earthquake (Figure A-17) seems to support that DI pipe has a moderately lower break rate

than the "average" pipe material, but possibly only about 50% lower than the average. The poor performance of small diameter screwed steel pipe in the Northridge earthquake would suggest a K_1 value of between 1.1 and 1.5 for that kind of pipe.

A.3.12 Wave Propagation Damage Algorithms – 1994 Northridge – LADWP

A GIS-based analysis of the pipeline damage to the LADWP water system was performed by [after T. O'Rourke and Jeon, 1999]. This GIS analysis is based on the following:

- Data reported herein are for cast iron, ductile iron, asbestos cement and steel pipe, up to 24" in diameter. The pipeline inventory includes: 7,848 km of cast iron pipe; 433 km of ductile iron pipe; and 961 km of asbestos cement pipe.

- A total of 1,405 pipe repairs were reported for the LADWP distribution system based on work orders. Of these, 136 were removed from the statistics, either being due to damage to service line connections on the customer side of meter; non-damage for any other reason (the work crew could not find the leak after they arrived at the site); duplications; non-pipe related. An additional 208 repairs were removed from the statistics, being caused by damage to service connections on the utility side of the meter, at locations without any damage to the pipe main. An additional 48 repairs are removed from the statistics, being for pipes with diameters 24" and larger. Also, 74 repairs were removed from the statistics, as either pipe locations, type or size was unknown at these locations (this introduces a downward bias in the raw damage rates of 7.9% = 74 / 939). The remaining pipe data locations are: 673 repairs for cast iron pipe; 24 repairs for ductile iron pipe; 26 repairs for asbestos cement pipe, 216 repairs for steel pipe.

- Note: Repair data in Section A.3.11 (Loma Prieta) does not remove service line connection repairs, which represent 19.5% (= 22 / 113) of the repairs due to mains. Repair data in A.3.12 (Northridge) does remove service line connection repairs, which represent 20.5% (= 208 / 1,013) of the repairs due to mains. This suggests that the quantity of repairs to service line connections would be about 20% that for mains. The Loma Prieta database includes pipe material, diameter and location at every location; the Northridge database has one or more of these attributes missing at 7.9% of all locations and this data was omitted from the statistical analyses. Combining damage data between the two data sets (Loma Prieta and Northridge) needs to adjust for these difference (total about 28% difference).

- Damage to steel pipelines in the Northridge database of distribution pipelines was about 216 repairs. The average damage rate for steel pipe was twice as high as that for all other types of pipe combined. The reasons for this are several:

  - Steel pipelines are concentrated in hillsides and mountains, owing to a design philosophy that steel pipes should be used rather than cast iron pipes in hillside terrain.

  - Several types of steel pipe are included in the "steel" category, including (as reported by O'Rourke and Jeon): welded joints (43%); screwed joints (9%); elastomeric or victaulic coupling joints (7%); pipes with and without corrosion protection (coatings, sacrificial anodes, impressed current), pipes using different types of steel, including Mannesman and Matheson steel (30%) which are known to be prone to corrosion; and riveted pipe (1%). Pending more study of the steel pipeline database, repairs to these pipes have not yet been completely evaluated by T. O'Rourke and this data is not incorporated into the fragility formulations

in this report. Percentages in this paragraph pertain to the percentage of all steel pipe repairs with the listed attribute. Mannesman and Matheson steel pipes were installed mostly in the 1920s and 1930s without cement lining and coating, and have wall thicknesses generally thinner than modern installed steel pipes of the same diameter.

- 4" diameter steel pipe use screwed fittings; 6" and larger steel pipe use welded slip joints.

- Pipe damage in locales subjected to large PGDs have been "removed" from the database.

- Pipe damage data were correlated (by T. O'Rourke and Jeon) with peak instrumented PGV to the nearest recording (peak instrumented was the highest of the two orthogonal recorded horizontal motions, not the vector maximum). Most other data in this report is presented with regards to the average of the peak ground velocities from two orthogonal directions. This is commonly the measure of ground velocity provided by attenuation relationships.

A comparison of instrumental records revealed that the ratio of peak horizontal velocity to the average peak velocity from the two orthogonal directions was 1.21. Accordingly, we present in this report "corrected" PGV data from the original work (except note that this correction was not applied to the dataset used in Appendix G).

Unpublished work suggests that R^2 coefficients are higher if pipe damage from the Northridge earthquake is correlated with the vector maximum of the two horizontal recorded PGVs.

Tables A.3-14, A.3-15 and A.3-16 summarizes the results. The data set included 4,900 miles of Cast Iron pipe (mostly 4", 6" and 8" diameter, with about 15% of the total for 10" through 24" diameter), 270 miles of Ductile Iron pipe (4", 6", 8" and 12" diameter) and 600 miles of Asbestos Cement pipe (4", 6" and 8" diameter). In order to maintain a minimum length of pipe for each reported statistic, each reported value is based on a minimum length of about 80 miles (cast iron pipe) or 13 miles (ductile iron and asbestos cement). This is done to smooth out spurious repair rate values if the length of pipe in any single bin is very small. At higher PGV values, this required digitization at slightly different PGV values for AC and DI pipe.

PGV (inches/sec)	Cast Iron RR / 1000 feet	Cast Iron Miles of Pipe	Cast Iron Repairs
1.6	0.0	156.8	0
4.9	0.0079	1055.8	44
8.1	0.0230	1370.7	166
11.4	0.0300	699.7	111
14.6	0.0221	503.1	59
17.9	0.0337	313.9	56
21.1	0.0739	222.7	87
24.4	0.0662	111.7	39
27.7	0.0540	87.6	24
32.5	0.0064	117.6	4
39.0	0.0205	101.8	11
45.6	0.0246	84.8	11
52.1	0.1441	78.9	60

Table A.3-14. Pipe Repair Data, Cast Iron Pipe, 1994 Northridge Earthquake

PGV (inches/sec)	Asbestos Cement RR / 1000 feet	Asbestos Cement Miles of Pipe	Asbestos Cement Repairs
1.6	0.0	98.3	0
4.9	0.0020	192.4	2
8.1	0.0193	147.2	15
11.4	0.0051	73.6	2
14.6	0.0	23.6	0
17.9	0.0	21.3	0
21.1	0.0873	15.2	7
29.3	0.0	13.4	0
35.8	0.0	15.8	0

Table A.3-15. Pipe Repair Data, Asbestos Cement Pipe, 1994 Northridge Earthquake

PGV (inches/sec)	Ductile Iron RR / 1000 feet	Ductile Iron Miles of Pipe	Ductile Iron Repairs
1.6	0.0	26.4	0
4.9	0.0026	72.9	1
8.1	0.0196	57.9	6
11.4	0.0150	25.2	2
14.6	0.0282	20.1	3
17.9	0.0167	11.3	1
22.8	0.0887	12.8	6
29.3	0.0283	13.4	2
35.8	0.0131	14.4	1
47.2	0.0236	16.1	2

Table A.3-16. Pipe Repair Data, Ductile Iron Pipe, 1994 Northridge Earthquake

Figure A-13 shows the "backbone" regression curve. The R^2 value is low (0.26), suggesting that by combining all damage data into one plot leads to substantial scatter.

Figure A-14 compares the Loma Prieta (solid line) and Northridge (dashed line) backbone curves. As previously discussed, the Loma Prieta curve includes damage to service connections (about 20%), and the Northridge curve excludes damage due to incompleteness in the damage data set (about 8%). Also, the Loma Prieta database includes cast iron, asbestos cement and steel; the Northridge database include cast iron, asbestos cement and ductile iron. Given these differences, the two curves are not that different: i.e., the curves are mostly within 50% of each other.

A significant concern in developing regression curves of the sort shown in Figures A-9 through A-14 is that the "data points" are based on rates of damage. As such, one data point which is based on 100 miles of pipe is given the same influence as another data point which is based on 20 miles of pipe. Also, data points which have "0" repair rate cannot be included in an exponential-based regression curve. One approach to handle this problem is treated using a Bayesian form of curve fitting, as outlined in Appendix G. Another way to address this is to "weight" the repair data statistics such that each point represents an equal length of pipe. By "weighting", it is meant that the regression analysis is performed with 5 data points representing a sample with 100 miles of pipe, and 1 data point representing a sample with 20 miles of pipe. The results of the "weighted" analysis are shown in Figure A-15. In developing Figure A-15, the Loma Prieta and Northridge data are normalized to account of the way the raw data was developed (service connections, missing main repair data). The main effects of the weighting are as follows:

- The influence of smaller samples of pipe, at the higher PGV levels, has less influence on the regression coefficients.

- The regression curve using a weighted sample is almost linear (power coefficient = 0.99).

Figure A-16 shows a regression analysis (unweighted) for asbestos cement pipe for both the Loma Prieta and Northridge datasets.

Based on comparable levels of shaking, the relative vulnerability of each pipe material (just Northridge data) was evaluated. Table A.3-17 shows the results.

PGV (inch/sec)	Cast Iron RR / 1000 feet	Asbestos Cement RR / 1000 feet	Ductile Iron RR / 1000 feet	Average RR / 1000 feet	CI / Average	AC / Average	DI / Average
5.9	0.0079	0.0020	0.0026	0.0041	1.902	0.476	0.622
9.8	0.0230	0.0197	0.0197	0.0208	1.105	0.948	0.948
13.8	0.0300	0.0052	0.0152	0.0168	1.790	0.307	0.903
17.7	0.0221		0.0288	0.0255	0.869		1.131
21.7	0.0337		0.0167	0.0252	1.338		0.662
25.6	0.0739	0.0894	0.0939	0.0857	0.861	1.043	1.096
Average					1.311	0.693	0.894

Table A.3-17. Pipe Repair Data, 1994 Northridge Earthquake

This suggests the relative vulnerability of these three pipe materials, from the Northridge earthquake for areas subjected to ground shaking and no PGDs, as follows:

- Cast Iron. 30% more vulnerable than average.

- Asbestos Cement. 30% less vulnerable than average

- Ductile Iron. 10% less vulnerable than average.

A.3.13 Relative Pipe Performance – Ballantyne

Ballantyne presents a model to consider the relative performance of pipelines in earthquakes which differentiates between the properties of the pipe barrel from the pipe joint.

- Pipe joints usually fail from extension (pulled joints); compression (split or telescoped joints); or bending or rotation.

- Pipe barrels usually fail from shear; bending; holes in the pipe wall, or splits.

Holes in pipe walls are usually the result of corrosion. Steel or iron pipe can be weakened by corrosion; asbestos cement pipe by decalcification, and PVC pipe by fatigue.

Given these issues, Ballantyne rates various pipe types using four criteria: ruggedness (strength and ductility of the pipe barrel); resistance to bending failure; joint flexibility; and joint restraint. Table A.3-18 presents his findings (1 = low seismic capacity, 5 = high seismic capacity).

Material Type / diameter	AWWA Standard	Joint Type	Ruggedness	Bending	Joint Flexibility	Restraint	Total
Polyethylene	C906	Fusion	4	5	5	5	19
Steel	C2xx series	Arc Welded	5	5	4	5	19
Steel	None	Riveted	5	5	4	4	18
Steel	C2xx series	B&S, RG, R	5	5	4	4	18
Ductile Iron	C1xx series	B&S, RG, R	5	5	4	4	18
Steel	C2xx	B&S, RG, UR	5	5	4	1	15
Ductile iron	C1xx series	B&S, RG, UR	5	5	4	1	15
Concrete with steel cylinder	C300, C303	B&S, R	3	4	4	3	14
PVC	C900, C905	B&S, R	3	3	4	3	13
Concrete with steel cylinder	C300, C303	B&S, UR	3		4	1	12
AC > 8" diameter	C4xx series	Coupled	2	4	5	1	12
Cast Iron > 8" diameter	None	B&S, RG	2	4	4	1	11
PVC	C900, C905	B&S, UR	3	3	4	1	11
Steel	None	Gas welded	3	3	1	2	9
AC ≤ 8" diameter	C4xx series	Coupled	2	1	5	1	9
Cast iron ≤ 8" diameter	None	B&S, RG	2	1	4	1	8
Cast iron	None	B&S, rigid	2	2	1	1	6
B&S = Bell and spigot. RG = rubber gasket. R = restrained. UR = unrestrained							

Table A.3-18. Relative Earthquake Vulnerability of Water Pipe

By comparing the rankings in Tables A.3-18 versus those in Tables A.3-12 and A.3-13, we see the following trends:

- Both tables rank welded steel pipe as about the best pipe. Table A.3-12 provides substantial downgrades for cases were corrosion is likely, and the evidence from the Northridge and Loma Prieta earthquakes strongly indicates that corrosion is an important factor.

- Table A.3-18 presents high density polyethylene pipe (HDPE) as being very rugged. To date, there is essentially no empirical evidence of HDPE performance in water systems, but it appears to have performed well in gas distribution systems. Limited tests on pressurized HDPE pipe have shown strain capacities before leak in excess of 25% (tensile) and 10% (compression), which suggests very good ruggedness. HDPE pipe is not susceptible to corrosion. There remains some

concern about the long term use of resistance of HDPE pipe to intrusion of certain oil-based compounds; should this issue be adequately resolved, then the use of HDPE pipe in areas prone to PGDs may be very effective in reducing pipe damage.

- Table A.3-18 suggests that unrestrained ductile iron pipe is more rugged than AC pipe; this reflects common assumptions about the ductility of DI pipe, but in some cases does not match the empirical evidence (Northridge 1994), where AC pipe performed better than DI pipe.

Ballantyne suggests that in high seismic zones (Z ≥ 0.4g), DI pipe (restrained joints), steel pipe (welded or restrained joints); HDPE with fusion welded joints should be used. For purposes of this report, these recommendations appear sound, although the use of these materials might best be considered for any seismically active region (Z ≥ 0.15g) with local soils prone to PGDs; and in the areas with high PGVs (Z ≥ 0.4g), the use of rubber gasketed (short barrel length, long joint insertions) AC, DI or PVC pipe might still yield acceptably good performance.

A.3.14 Pipe Damage Statistics – 1995 Kobe Earthquake

The 1995 Hanshin-Awaji earthquake (often called the Hyogo-Ken Nanbu (Kobe) earthquake) was a M 6.7 crustal event that struck directly beneath much of the urbanized city of Kobe, Japan. At the time of the earthquake, the pipeline inventory for the City of Kobe's water system included 3,180 km of Ductile Iron pipe (push on joint), 237 km of special Ductile Iron pipe (with special flexible restrained joints), 103 km of high pressure steel welded pipe, 309 km of cast iron pipe with mechanical joints, and 126 km of PVC pipe with push-on gasketed joint [Eidinger et al, 1998].

The City of Kobe's water system suffered 1,757 pipe repairs to mains. The average damage rate to pipe mains was 0.439 repairs per km. The repairs could be classified into one of three types: damage to the main pipe barrel (splitting open); damage to the pipe joint (separated); damage to air valves and hydrants; the damage rate was divided about 20% - 60% - 20% for these three types of repairs, respectively. Average pipe repair rates were about 0.2/km (PVC pipe); 1.3/km (CI pipe); 0.25/km (Ductile Iron pipe with push on or regular restrained joints); and 0.15/km for welded steel pipe.

Figure A-17 shows the damage rates for pipelines in Kobe, along with the wave propagation damage algorithm Tables A.3-4, A.3-14, A.3-15, A.3-16 and Figures A-1 and A-2. The Kobe data is plotted as horizontal lines; meaning the data is not differentiated by level of ground shaking. Also, the Kobe data is not differentiated between damage from PGVs or PGDs. Note that while the ratio of damage between pipeline materials for Kobe is known, to say that one pipe material is that much better than the next may be misleading, as the inventory of different pipe materials may have been exposed to differing levels of hazards. There remains a need to perform a GIS evaluation for the Kobe pipe inventory in a manner similar to that done for Loma Prieta 1989 (Section A.3.11) or Northridge 1994 (Section A.3.12). Shirozu et al [1996] have performed an analysis of the Kobe dataset, and their findings are included in the dataset used for evaluation of the PGV-based pipeline fragility curves; Table A.3-19 provides a complete breakdown of the pipe damage for this earthquake.

There were an additional 89,584 service line repairs in Kobe [Matsushita]. The service line failure rate was 13.8% of all service lines in the city. The high rate of damage to service line connections reflects the large number of structures and roadways that were damaged or destroyed in the earthquake.

The Cities of Kobe and Ashiya had recently installed a special type of ductile iron pipe (so called "S and SII joint pipe". A total inventory of 270 km of this type of pipeline was

installed at the time of the earthquake, and there was no reported damage to this type of pipeline. The key features of this type of pipeline were: ductile iron body; with restrained slip joints at every fitting. Each joint could extent and rotate a moderate amount. This type of pipeline was installed at about a 50% cost premium to regular push-on type joint ductile iron pipeline.

In the neighboring city of Ashiya, the pipeline inventory included 192 km of pipelines. This included 58 km of Ductile Iron pipe with restrained joints, 96 km of Cast Iron pipe, 2 km of steel pipe, 23 km of PVC pipe and 14 km of special Ductile Iron pipe (with flexible restrained joints). There were 303 pipe repairs made for this water system (average 1.58 repairs / km = 0.48 repairs / 1,000 ft) [Eidinger et al, 1998]. The higher damage rate for Ashiya than for Kobe is partially explained in that 100% of Ashiya was exposed to strong ground shaking, whereas perhaps only 2/3 of Kobe was similarly exposed; also, Ashiya has a somewhat higher percentage of Cast Iron pipe.

A.3.15 Pipe Damage Statistics – Recent Earthquakes

The damage to water system pipelines in recent (1999 – 2001) earthquakes is briefly summarized in this section. As of the time of writing this report, sufficiently accurate databases of the pipe damage were unavailable in order for the data to be included in the statistical analyses presented in this report.

1999 Kocaeli – Izmit (Turkey) Earthquake

The M_W 7.4 Kocaeli (Izmit) earthquake of August 17, 1999 in Turkey led to widespread damage to water transmission and distribution systems that serve a population of about 1,500,000 people. Potable water was lost to the bulk of the population immediately after the earthquake, largely due to damage to buried pipelines.

The most common inventories of pipe material were welded steel pipe (large diameter transmission pipelines) and rubber gasketed asbestos cement pipe (most distribution pipelines).

There was heavy damage to both transmission and distribution pipelines by this earthquake. Some of the damage was due to rupture at fault offset, some was due to widespread liquefaction, and some was due to strong ground shaking.

At this time, no precise inventory of pipeline damage is available. However, based on the level of efforts of crews to repair water pipelines, and the percentage of water service restored as of three weeks after the earthquake, it would be reasonable to assume that between 1,000 and 3,000 pipe repairs would be required to completely restore water service. An average repair rate possibly in the range of 0.5 to 1/km was likely to have occurred in the strongest shaking areas, including the cities of Adapazari and Golcuk, and the town of Arifye.

1999 Chi-Chi (Taiwan) Earthquake

The M_W 7.7 Chi-Chi (Ji-Ji) earthquake of September 21, 1999 in Taiwan led to 2,405 deaths and 10,718 injuries. Potable water was lost to 360,000 households immediately after the earthquake, largely due to damage to buried pipelines.

There was about 32,000 km of water distribution pipelines in the country; perhaps a quarter or more was exposed to strong ground shaking. The largest pipes (diameter ≥1.5 meters) are typically concrete cylinder pipe or steel, with ductile iron pipe being the predominant material for moderate diameter pipe and a mix of polyethylene and ductile iron pipe for distribution pipe (≤8 inch diameter).

At this time, there is incomplete analysis of the damaged inventory to pipelines in this earthquake. However, the following trends have been observed from preliminary data [Shih et al, 2000]:

- About 48% of all buried water pipe damage is due to ground shaking (this ratio may change under future analysis). The remainder is due to liquefaction (2%), ground collapse (11%), ground cracking and opening (10%), horizontal ground movements (9%), vertical ground movement (16%), other (4%).

- For the town of Tsautuen, repair rates varied from 0.4/km to 7/km (PGA = 0.2g) to as high as 0.6/km (PGA = 0.6g).

2001 Gujarat Kutch (India) Earthquake

The M_w 7.7 Gujarat (Kutch) earthquake of January 26, 2001 in India led to about 17,000 deaths and about 140,000 injuries. Potable water was lost to over 1,000,000 people immediately after the earthquake, largely due to damage to wells, pump station buildings and buried pipelines.

There was about 3,500 km of water distribution and transmission pipelines in the Kutch District; perhaps 2,500 km was exposed to strong ground shaking. As of the time of writing this report, it is estimated that about 700 km of these pipelines will have to be replaced due to earthquake damage. It may take up to 4 months after the earthquake to complete the pipe repairs.

A.4 References

ASCE, 1984, Guidelines for the Seismic Design of Oil and Gas Pipeline Systems, prepared by the ASCE Technical Council on Lifeline Earthquake Engineering, D. Nyman Principal Investigator, 1984.

Ayala, G. and O'Rourke, M., "Effects of the 1985 Michoacan Earthquake on Water Systems and other Buried Lifelines in Mexico," National Center for Earthquake Engineering Report No. 89-009, 1989.

Ballantyne, D. B., Berg, E., Kennedy, J., Reneau, R., and Wu, D., "Earthquake Loss Estimation Modeling of the Seattle Water System," Report to U.S. Geological Survey, Grant 14-08-0001-G1526, October 1990.

Barenberg, M.D., "Correlation of Pipeline Damage with Ground Motion," Journal of Geotechnical Engineering, ASCE, Vol. 114, No. 6, June 1988.

Eguchi, R., T., Legg, M.R., Taylor, C. E., Philipson, L. L., Wiggins, J. H., "Earthquake Performance of Water and Natural Gas Supply System," J. H. Wiggins Company, NSF Grant PFR-8005083, Report 83-1396-5, July 1983.

Eidinger, J., Maison, B. Lee, D., Lau, R, "EBMUD Water Distribution Damage in the 1989 Loma Prieta Earthquake," 4th U.S. Conference on Lifeline Earthquake Engineering, TCLEE, ASCE, San Francisco, 1995.

Eidinger, J. "Lifelines, Water Distribution System," in The Loma Prieta, California, Earthquake of October 17, 1989, Performance of the Built Environment - Lifelines, US Geological Survey Professional Paper 1552-A, pp A63-A80, A. Schiff Ed. December 1998.

Eidinger, J., Lund, LeVal and Ballantyne, Don, Water and Sewer Systems, in Hyogo-Ken Nanbu (Kobe) Earthquake of January 17, 1995, TCLEE Monograph 14, ASCE, 1998.

Eidinger, J., Avila, E., eds., <u>Guidelines for the Seismic Upgrade of Water Transmission Facilities</u>, ASCE, TCLEE Monograph No. 15, January 1999.

Grigoriu, M., O'Rourke, T., Khater, M., "Serviceability of San Francisco Auxiliary Water Supply System" Proceedings of 5th International Conference on Structural Safety and Reliability, San Francisco, California 1989.

Hovland, H. J., and Daragh, R. D. "Earthquake-Induced Ground Movements in the Mission Bay Area of San Francisco in 1906," Proceedings of the 2nd Specialty Conference of the Technical Council on Lifeline Earthquake Engineering. ASCE, August 1981.

Katayama, T., Kubo, K., and Sito, N., "Earthquake Damage to Water and Gas Distribution Systems," Proceedings—U.S. National Conference on Earthquake Engineering, EERI, 1975.

Manson, M., "Reports on an Auxiliary Water Supply System for Fire Protection for San Francisco, California," Report of Board of Public Works, San Francisco, California 1908.

Matsushita, M., Restoration Process of Kobe Water system from the 1995 Hanshin-Awaji Earthquake, *in* Optimizing Post-Earthquake System Reliability, Proceedings of the 5th US Conference on Lifeline Earthquake Engineering, TCLEE Monograph 16, ASCE, August, 1999.

McCaffery, M. A., and O'Rourke, T. D., "Buried Pipeline Response to Reverse Faulting During the 1971 San Fernando Earthquake," Earthquake Behavior and Safety of Oil and Gas Storage Facilities, Buried Pipelines an Equipment, PVP-Vol.77, New York, ASME, 1983.

Newmark, N.M., and Hall, W. J.,"Pipeline Design to Resist Large Fault Displacement," Presented at the June 1975 U. S. National Conference of Earthquake Engineering, Ann Arbor, Michigan.

O'Rourke, M.J., and Ayala, G., 1993, Pipeline Damage to Wave Propagation, *Journal of Geotechnical Engineering*, ASCE, Vol. 119, No. 9, 1993.

O'Rourke, T.D., and Jeon, S-S., Factors Affecting the Earthquake Damage of Water Distribution Systems, in Optimizing Post-Earthquake Lifeline System Reliability, TCLEE Monograph No. 16, ASCE, 1999.

O'Rourke, T. D., and Tawfik, M.S. "Effects of Lateral Spreading on Buried Pipelines During the 1971 San Fernando Earthquake," Earthquake Behavior and Safety of Oil and Gas Storage Facilities, Buried Pipelines and Equipment, PVC,-Vol.77, New York, ASME, 1983.

Porter, K.A., Scawthorn C., Honegger, D. G., O'Rourke, T.D., and Blackburn, F., "Performance of Water Supply Pipelines in Liquefied Soil," Proceedings—4th U.S.-Japan Workshop on Earthquake Disaster Prevention for Lifeline Systems, NIST Special Publication 840, August 1992.

Sato, Ryo and Myurata, Masahiko, GIS-Based Interactive and Graphic Computer System to Evaluate Seismic Risks on Water Delivery Networks, Dept. of Civil Engineering and Operations Research, Princeton University, December 1, 1990.

Schussler, H., "The Water Supply System of San Francisco, California" Spring Valley Water Company, San Francisco, California, July, 1906.

Shih, B., Chen, W., Hung, J-H., Chen, C-W., Wang, P-H., Chen, Y-C., and Liu, S-Y., The Fragility Relations of Buried Water and Gas Pipes, International Workshop on Annual Commemoration of Chi-chi Earthquake, Taipei, September 18-20. 2000.

Shinozuka, M. Takada, S. Ishikawa, H., <u>Seismic Risk Analysis of Underground Lifeline Systems With the Aid of Damage Probability Matrices</u>, NSF-PFR-78-15049-CU-2, Columbia University, September 1978.

Shirozu, T., Yune, S., Isoyama, R., and Iwamoto, T., "Report on Damage to Water Distribution Pipes Caused by the 1995 Hyogoken-Nanbu (Kobe) Earthquake," *Proceedings from the 6th Japan-U.S. Workshop on Earthquake Resistant Design of Lifeline Facilities and Countermeasures Against Soil Liquefaction*, National Center for Earthquake Engineering Research Report NCEER-96-0012, September 1996.

Toprak, Selcuk, "Earthquake effects on buried pipeline systems," PhD Dissertation, Cornell University, August, 1998.

Wang, Leon, Shao-Ping S.,and Shijie S., "Seismic Damage Behavior of Buried Pipeline Systems During Recent Severe Earthquakes in U.S., China and Other Countries, ODU LEE-02, Old Dominion University, December 1985.

Wang, L., "A New Look Into the Performance of Water Pipeline Systems From 1987 Whittier Narrows, California Earthquake," Department of Civil Engineering, Old Dominion University, No. ODU LEE-05, January 1990.

Youd, T. L. and Hoose, S. N. "Historic Ground Failures in Northern California Associated with Earthquakes," Geological Survey Professional Paper No. 993. U.S. Geological Survey, Washington D. C. GPO 1978.

ID	Earthquake	Material Type	Size	Length	Repairs	Rate	Demand	Comment	Source
1001	1995 Hyogoken-nanbu	MX	DS	NR	NR	0.031	PGA = 0.211	Includes DI & CI from 1011 to 1029	Shirozu et al, 1996 (Fig. 15)
1002	1995 Hyogoken-nanbu	MX	DS	NR	NR	0.207	PGA = 0.306	Includes DI & CI from 1011 to 1029	Shirozu et al, 1996 (Fig. 15)
1003	1995 Hyogoken-nanbu	MX	DS	NR	NR	0.047	PGA = 0.478	Includes DI & CI from 1011 to 1029	Shirozu et al, 1996 (Fig. 15)
1004	1995 Hyogoken-nanbu	MX	DS	NR	NR	0.057	PGA = 0.572	Includes DI & CI from 1011 to 1029	Shirozu et al, 1996 (Fig. 15)
1005	1995 Hyogoken-nanbu	MX	DS	NR	NR	0.227	PGA = 0.595	Includes DI & CI from 1011 to 1029	Shirozu et al, 1996 (Fig. 15)
1006	1995 Hyogoken-nanbu	MX	DS	NR	NR	0.227	PGA = 0.677	Includes DI & CI from 1011 to 1029	Shirozu et al, 1996 (Fig. 15)
1007	1995 Hyogoken-nanbu	MX	DS	NR	NR	0.062	PGA = 0.710	Includes DI & CI from 1011 to 1029	Shirozu et al, 1996 (Fig. 15)
1008	1995 Hyogoken-nanbu	MX	DS	NR	NR	0.202	PGA = 0.792	Includes DI & CI from 1011 to 1029	Shirozu et al, 1996 (Fig. 15)
1009	1995 Hyogoken-nanbu	MX	DS	NR	NR	0.522	PGA = 0.819	Includes DI & CI from 1011 to 1029	Shirozu et al, 1996 (Fig. 15)
1010	1995 Hyogoken-nanbu	MX	DS	NR	NR	0.098	PGA = 0.834	Includes DI & CI from 1011 to 1029	Shirozu et al, 1996 (Fig. 15)
1011	1995 Hyogoken-nanbu	DI	DS	NR	NR	0.092	PGA = 0.306		Shirozu et al, 1996 (Fig. 16a)
1012	1995 Hyogoken-nanbu	DI	DS	NR	NR	0.016	PGA = 0.478		Shirozu et al, 1996 (Fig. 16a)
1013	1995 Hyogoken-nanbu	DI	DS	NR	NR	0.02	PGA = 0.572		Shirozu et al, 1996 (Fig. 16a)
1014	1995 Hyogoken-nanbu	DI	DS	NR	NR	0.14	PGA = 0.595		Shirozu et al, 1996 (Fig. 16a)
1015	1995 Hyogoken-nanbu	DI	DS	NR	NR	0.149	PGA = 0.677		Shirozu et al, 1996 (Fig. 16a)
1016	1995 Hyogoken-nanbu	DI	DS	NR	NR	0.027	PGA = 0.710		Shirozu et al, 1996 (Fig. 16a)
1017	1995 Hyogoken-nanbu	DI	DS	NR	NR	0.054	PGA = 0.792		Shirozu et al, 1996 (Fig. 16a)
1018	1995 Hyogoken-nanbu	DI	DS	NR	NR	0.2	PGA = 0.819		Shirozu et al, 1996 (Fig. 16a)
1019	1995 Hyogoken-nanbu	DI	DS	NR	NR	0.065	PGA = 0.834		Shirozu et al, 1996 (Fig. 16a)
1020	1995 Hyogoken-nanbu	CI	DS	NR	NR	0.099	PGA = 0.211		Shirozu et al, 1996 (Fig. 16b)
1021	1995 Hyogoken-nanbu	CI	DS	NR	NR	0.288	PGA = 0.306		Shirozu et al, 1996 (Fig. 16b)
1022	1995 Hyogoken-nanbu	CI	DS	NR	NR	0.252	PGA = 0.478		Shirozu et al, 1996 (Fig. 16b)
1023	1995 Hyogoken-nanbu	CI	DS	NR	NR	0.171	PGA = 0.572		Shirozu et al, 1996 (Fig. 16b)
1024	1995 Hyogoken-nanbu	CI	DS	NR	NR	0.585	PGA = 0.595		Shirozu et al, 1996 (Fig. 16b)
1025	1995 Hyogoken-nanbu	CI	DS	NR	NR	0.441	PGA = 0.677		Shirozu et al, 1996 (Fig. 16b)
1026	1995 Hyogoken-nanbu	CI	DS	NR	NR	0.099	PGA = 0.710		Shirozu et al, 1996 (Fig. 16b)
1027	1995 Hyogoken-nanbu	CI	DS	NR	NR	1.098	PGA = 0.792		Shirozu et al, 1996 (Fig. 16b)
1028	1995 Hyogoken-nanbu	CI	DS	NR	NR	1.458	PGA = 0.819		Shirozu et al, 1996 (Fig. 16b)
1029	1995 Hyogoken-nanbu	CI	DS	NR	NR	0.189	PGA = 0.834		Shirozu et al, 1996 (Fig. 16b)
1030	1994 Northridge	DI	DS	16.1	2	0.0236	PGV = 47.2	LADWP	ALA Report Table 4-10
1031	1994 Northridge	DI	DS	14.4	1	0.0131	PGV = 35.8	LADWP	ALA Report Table 4-10
1032	1994 Northridge	DI	DS	13.4	2	0.0283	PGV = 29.3	LADWP	ALA Report Table 4-10
1033	1994 Northridge	DI	DS	12.8	6	0.0887	PGV = 22.8	LADWP	ALA Report Table 4-10
1034	1994 Northridge	DI	DS	11.3	1	0.0167	PGV = 17.9	LADWP	ALA Report Table 4-10
1035	1994 Northridge	DI	DS	20.1	3	0.0282	PGV = 14.6	LADWP	ALA Report Table 4-10
1036	1994 Northridge	DI	DS	25.2	2	0.015	PGV = 11.4	LADWP	ALA Report Table 4-10
1037	1994 Northridge	DI	DS	57.9	6	0.0196	PGV = 8.1	LADWP	ALA Report Table 4-10
1038	1994 Northridge	DI	DS	72.9	1	0.0026	PGV = 4.9	LADWP	ALA Report Table 4-10
1039	1994 Northridge	DI	DS	26.4	0	0	PGV = 1.6	LADWP	ALA Report Table 4-10
1040	1994 Northridge	AC	DS	15.8	0	0	PGV = 35.8	LADWP	ALA Report Table 4-9
1041	1994 Northridge	AC	DS	13.4	0	0	PGV = 29.3	LADWP	ALA Report Table 4-9
1042	1994 Northridge	AC	DS	15.2	7	0.0873	PGV = 21.1	LADWP	ALA Report Table 4-9
1043	1994 Northridge	AC	DS	21.3	0	0	PGV = 17.9	LADWP	ALA Report Table 4-9
1044	1994 Northridge	AC	DS	23.6	0	0	PGV = 14.6	LADWP	ALA Report Table 4-9
1045	1994 Northridge	AC	DS	73.6	2	0.0051	PGV = 11.4	LADWP	ALA Report Table 4-9
1046	1994 Northridge	AC	DS	147.2	15	0.0193	PGV = 8.1	LADWP	ALA Report Table 4-9

Table A.1-1. Pipe Damage Statistics (Page 1 of 4)

ID	Earthquake	Material Type	Size	Length	Repairs	Rate	Demand	Comment	Source
1047	1994 Northridge	AC	DS	192.4	2	0.002	PGV = 4.9	LADWP	ALA Report Table 4-9
1048	1994 Northridge	AC	DS	98.3	0	0	PGV = 1.6	LADWP	ALA Report Table 4-9
1049	1994 Northridge	CI	DS	78.9	60	0.1441	PGV = 52.1	LADWP	ALA Report Table 4-8
1050	1994 Northridge	CI	DS	84.8	11	0.0246	PGV = 45.6	LADWP	ALA Report Table 4-8
1051	1994 Northridge	CI	DS	101.8	11	0.0205	PGV = 39.0	LADWP	ALA Report Table 4-8
1052	1994 Northridge	CI	DS	117.6	4	0.0064	PGV = 32.5	LADWP	ALA Report Table 4-8
1053	1994 Northridge	CI	DS	87.6	24	0.054	PGV = 27.7	LADWP	ALA Report Table 4-8
1054	1994 Northridge	CI	DS	111.7	39	0.0662	PGV = 24.4	LADWP	ALA Report Table 4-8
1055	1994 Northridge	CI	DS	222.7	87	0.0739	PGV = 21.1	LADWP	ALA Report Table 4-8
1056	1994 Northridge	CI	DS	313.9	56	0.0337	PGV = 17.9	LADWP	ALA Report Table 4-8
1057	1994 Northridge	CI	DS	503.1	59	0.0221	PGV = 14.6	LADWP	ALA Report Table 4-8
1058	1994 Northridge	CI	DS	699.7	111	0.03	PGV = 11.4	LADWP	ALA Report Table 4-8
1059	1994 Northridge	CI	DS	1370.7	166	0.023	PGV = 8.1	LADWP	ALA Report Table 4-8
1060	1994 Northridge	CI	DS	1055.8	44	0.0079	PGV = 4.9	LADWP	ALA Report Table 4-8
1061	1994 Northridge	CI	DS	156.8	0	0	PGV = 1.6	LADWP	ALA Report Table 4-8
1062	1994 Northridge	CP	LG	NR	NR	0.102	PGV = 50.7	Trunk lines	Toprak, 1998 (Fig. 6-30)
1063	1994 Northridge	S	LG	NR	NR	0.0839	PGV = 54.3	Trunk lines	Toprak, 1998 (Fig. 6-30)
1064	1994 Northridge	S	LG	NR	NR	0.0396	PGV = 33.2	Trunk lines	Toprak, 1998 (Fig. 6-30)
1065	1994 Northridge	S	LG	NR	NR	0.0092	PGV = 19.8	Trunk lines	Toprak, 1998 (Fig. 6-30)
1066	1994 Northridge	S	LG	NR	NR	0.0031	PGV = 13.7	Trunk lines	Toprak, 1998 (Fig. 6-30)
1067	1994 Northridge	S	LG	NR	NR	0.0031	PGV = 9.7	Trunk lines	Toprak, 1998 (Fig. 6-30)
1068	1994 Northridge	AC	DS	NR	NR	0.0183	PGV = 9.8		Toprak, 1998 (Fig. 6-24)
1069	1994 Northridge	AC	DS	NR	NR	0.0031	PGV = 5.9		Toprak, 1998 (Fig. 6-24)
1070	1994 Northridge	DI	DS	NR	NR	0.0122	PGV = 12.5		Toprak, 1998 (Fig. 6-24)
1071	1994 Northridge	S	DS	NR	NR	0.0854	PGV = 21.5		Toprak, 1998 (Fig. 6-25)
1072	1994 Northridge	S	DS	NR	NR	0.0488	PGV = 13.8		Toprak, 1998 (Fig. 6-25)
1073	1994 Northridge	S	DS	NR	NR	0.0549	PGV = 9.9		Toprak, 1998 (Fig. 6-25)
1074	1994 Northridge	S	DS	NR	NR	0.0515	PGV = 5.9		Toprak, 1998 (Fig. 6-25)
1075	1994 Northridge	CI	DS	NR	NR	0.0674	PGV = 29.4		Toprak, 1998 (Fig. 6-8)
1076	1994 Northridge	CI	DS	NR	NR	0.0759	PGV = 25.7		Toprak, 1998 (Fig. 6-8)
1077	1994 Northridge	CI	DS	NR	NR	0.0338	PGV = 21.8		Toprak, 1998 (Fig. 6-8)
1078	1994 Northridge	CI	DS	NR	NR	0.0213	PGV = 17.8		Toprak, 1998 (Fig. 6-8)
1079	1994 Northridge	CI	DS	NR	NR	0.0031	PGV = 13.7		Toprak, 1998 (Fig. 6-8)
1080	1994 Northridge	CI	DS	NR	NR	0.0241	PGV = 9.8		Toprak, 1998 (Fig. 6-8)
1081	1994 Northridge	CI	DS	NR	NR	0.0061	PGV = 5.9		Toprak, 1998 (Fig. 6-8)
1082	1989 Loma Prieta	S	DS	60	47	0.148	PGV = 17.0	EBMUD	ALA Report 9/24
1083	1989 Loma Prieta	S	DS	279	9	0.0061	PGV = 7.0	EBMUD	ALA Report 9/24
1084	1989 Loma Prieta	S	DS	45	2	0.0084	PGV = 5.0	EBMUD	ALA Report 9/24
1085	1989 Loma Prieta	S	DS	374	5	0.0025	PGV = 3.0	EBMUD	ALA Report 9/24
1086	1989 Loma Prieta	AC	SM	46.2	3	0.0123	PGV = 17.0	EBMUD	ALA Report 9/24
1087	1989 Loma Prieta	AC	SM	438	2	0.0009	PGV = 7.0	EBMUD	ALA Report 9/24
1088	1989 Loma Prieta	AC	SM	79.5	1	0.0024	PGV = 5.0	EBMUD	ALA Report 9/24
1089	1989 Loma Prieta	AC	SM	445	8	0.0034	PGV = 3.0	EBMUD	ALA Report 9/24
1090	1989 Loma Prieta	CI	DS	20.6	10	0.0919	PGV = 17.0	EBMUD	ALA Report 9/24
1091	1989 Loma Prieta	CI	DS	879	24	0.0052	PGV = 7.0	EBMUD	ALA Report 9/24
1092	1989 Loma Prieta	CI	DS	123	8	0.0123	PGV = 5.0	EBMUD	ALA Report 9/24
1093	1989 Loma Prieta	CI	DS	473	14	0.0056	PGV = 3.0	EBMUD	ALA Report 9/24

Table A.1-1. Pipe Damage Statistics (Page 2 of 4)

ID	Earthquake	Material Type	Size	Length	Repairs	Rate	Demand	Comment	Source
1094	1989 Loma Prieta	S	DS	NR	NR	0.097	PGV = 16.0	EBMUD	Eidinger et al, 1995
1095	1989 Loma Prieta	S	DS	NR	NR	0.0052	PGV = 7.0	EBMUD	Eidinger et al, 1995
1096	1989 Loma Prieta	S	DS	NR	NR	0.0031	PGV = 2.5	EBMUD	Eidinger et al, 1995
1097	1989 Loma Prieta	AC	DS	NR	NR	0.0122	PGV = 16.0	EBMUD	Eidinger et al, 1995
1098	1989 Loma Prieta	AC	DS	NR	NR	0.0012	PGV = 7.0	EBMUD	Eidinger et al, 1995
1099	1989 Loma Prieta	AC	DS	NR	NR	0.0031	PGV = 2.5	EBMUD	Eidinger et al, 1995
1100	1989 Loma Prieta	CI	DS	NR	NR	0.079	PGV = 16.0	EBMUD	Eidinger et al, 1995
1101	1989 Loma Prieta	CI	DS	NR	NR	0.0055	PGV = 7.0	EBMUD	Eidinger et al, 1995
1102	1989 Loma Prieta	CI	DS	NR	NR	0.0061	PGV = 2.5	EBMUD	Eidinger et al, 1995
1103	1989 Mexico	CP	LG	NR	NR	0.0518	PGV = 9.8		O'Rourke & Ayala,1993 (J)
1104	1989 Loma Prieta	CI	DS	1080	15	0.0026	PGV = 5.3	San Francisco non- liq. Areas	Toprak, 1998 (Table 2-1)
1105	1987 Whittier	CI	DS	110	14	0.0241	PGV = 11.0		Toprak, 1998 (Table 2-1)
1106	1985 Mexico City	CP	LG	NR	NR	0.457	PGV = 21.3		O'Rourke & Ayala, 1993 (I)
1107	1985 Mexico City	MX	LG	NR	NR	0.0031	PGV = 4.3	Mix of CI, CP, AC	O'Rourke & Ayala, 1993 (H)
1108	1985 Mexico City	MX	LG	NR	NR	0.0213	PGV = 4.7	Mix of CI, CP, AC	O'Rourke & Ayala, 1993 (G)
1109	1985 Mexico City	MX	LG	NR	NR	0.137	PGV = 18.9	Mix of CI, CP, AC	O'Rourke & Ayala, 1993 (F)
1110	1983 Coalinga	AC	SM	NR	NR	0.101	PGV = 11.8		O'Rourke & Ayala, 1993 (K)
1111	1983 Coalinga	CI	SM	NR	NR	0.24	PGV = 11.8	Corrosion issue	O'Rourke & Ayala, 1993 (E)
1112	1979 Imperial Val.	AC	DS	NR	NR	0.0183	PGV = 23.7		Toprak, 1998 (Fig. 6-24)
1113	1979 Imperial Val.	CI	DS	11.5	19	0.314	MMI = 7	Corrosion issue	Toprak, 1998 (Table 2-3)
1114	1972 Managua	AC	SM	205	393	0.363	PGA = 0.41	May include PGD effects	Katayama et al, 1975 (Table 4)
1115	1972 Managua	CI	LG	18.8	11	0.11	PGA = 0.41	May include PGD effects	Katayama et al, 1975 (Table 4)
1116	1972 Managua	CI	SM	55.8	107	0.363	PGA = 0.41	May include PGD effects	Katayama et al, 1975 (Table 4)
1117	1971 San Fernando	CI	SM	52.7	3	0.0122	PGA = 0.27	May include PGD effects	Katayama et al, 1975 (Table 9)
1118	1971 San Fernando	CI	SM	60	5	0.0152	PGA = 0.28	May include PGD effects	Katayama et al, 1975 (Table 9)
1119	1971 San Fernando	CI	SM	52.2	7	0.0244	PGA = 0.29	May include PGD effects	Katayama et al, 1975 (Table 9)
1120	1971 San Fernando	CI	SM	48.8	5	0.0183	PGA = 0.29	May include PGD effects	Katayama et al, 1975 (Table 9)
1121	1971 San Fernando	CI	SM	49.1	6	0.0244	PGA = 0.30	May include PGD effects	Katayama et al, 1975 (Table 9)
1122	1971 San Fernando	CI	SM	50.6	9	0.0335	PGA = 0.31	May include PGD effects	Katayama et al, 1975 (Table 9)
1123	1971 San Fernando	CI	SM	59.8	19	0.061	PGA = 0.32	May include PGD effects	Katayama et al, 1975 (Table 9)
1124	1971 San Fernando	CI	SM	40.1	26	0.122	PGA = 0.33	May include PGD effects	Katayama et al, 1975 (Table 9)
1125	1971 San Fernando	CI	SM	31.9	22	0.131	PGA = 0.34	May include PGD effects	Katayama et al, 1975 (Table 9)
1126	1971 San Fernando	CI	SM	18.6	24	0.244	PGA = 0.35	May include PGD effects	Katayama et al, 1975 (Table 9)
1127	1971 San Fernando	CI	SM	16.1	16	0.189	PGA = 0.36	May include PGD effects	Katayama et al, 1975 (Table 9)
1128	1971 San Fernando	CI	SM	19.6	26	0.253	PGA = 0.38	May include PGD effects	Katayama et al, 1975 (Table 9)
1129	1971 San Fernando	CI	SM	20.6	77	0.707	PGA = 0.39	May include PGD effects	Katayama et al, 1975 (Table 9)
1130	1971 San Fernando	CI	SM	21.8	35	0.305	PGA = 0.41	May include PGD effects	Katayama et al, 1975 (Table 9)
1131	1971 San Fernando	CI	SM	16.8	43	0.482	PGA = 0.42	May include PGD effects	Katayama et al, 1975 (Table 9)
1132	1971 San Fernando	CI	SM	15	53	0.668	PGA = 0.44	May include PGD effects	Katayama et al, 1975 (Table 9)
1133	1971 San Fernando	CI	SM	17.8	53	0.564	PGA = 0.46	May include PGD effects	Katayama et al, 1975 (Table 9)
1134	1971 San Fernando	CI	SM	19.3	53	0.521	PGA = 0.48	May include PGD effects	Katayama et al, 1975 (Table 9)
1135	1971 San Fernando	CI	SM	9.1	24	0.5	PGA = 0.50	May include PGD effects	Katayama et al, 1975 (Table 9)
1136	1971 San Fernando	CI	DS	333	84	0.0488	MMI = 8		Toprak, 1998 (Table 2-3)
1137	1971 San Fernando	CI	DS	3540	55	0.0029	MMI = 7		Toprak, 1998 (Table 2-3)
1138	1971 San Fernando	CI	SM	NR	NR	0.0073	PGV = 5.9		O'Rourke & Ayala, 1993 (C)
1139	1971 San Fernando	CI	SM	NR	NR	0.0473	PGV = 11.8		O'Rourke & Ayala, 1993 (A)
1140	1971 San Fernando	CI	DS	169	6	0.0067	PGV = 7.1		Toprak, 1998 (Table 2-1)

Table A.1-1. Pipe Damage Statistics (Page 3 of 4)

ID	Earthquake	Material Type	Size	Length	Repairs	Rate	Demand	Comment	Source
1141	1971 San Fernando	CI	DS	151	10	0.0125	PGV = 11.8		Toprak, 1998 (Table 2-1)
1142	1969 Santa Rosa	CI	DS	136	7	0.0098	MMI = 7		Toprak, 1998 (Table 2-3)
1143	1969 Santa Rosa	CI	SM	NR	NR	0.0085	PGV = 5.9		O'Rourke & Ayala,1993 (B)
1144	1968 Tokachi-oki	AC	DS	24.8	77	0.589	MMI = 6 - 7	May include PGD effects	Katayama et al, 1975 (Table 3)
1145	1968 Tokachi-oki	MX	DS	83.9	22	0.0488	MMI = 6 - 7	Mix of CI & AC, may include PGD	Katayama et al, 1975 (Table 3)
1146	1968 Tokachi-oki	MX	DS	98.1	16	0.0305	MMI = 7 - 8	Mix of CI & AC, may include PGD	Katayama et al, 1975 (Table 3)
1147	1968 Tokachi-oki	MX	DS	101	16	0.0305	MMI = 6 - 7	Mix of CI & AC, may include PGD	Katayama et al, 1975 (Table 3)
1148	1968 Tokachi-oki	MX	DS	150	116	0.146	MMI = 7 - 8	Mix of CI & AC, may include PGD	Katayama et al, 1975 (Table 3)
1149	1968 Tokachi-oki	AC	DS	13.7	58	0.805	MMI = 7 - 8	May include PGD effects	Katayama et al, 1975 (Table 3)
1150	1968 Tokachi-oki	CI	DS	5.6	7	0.238	MMI = 7 - 8	May include PGD effects	Katayama et al, 1975 (Table 3)
1151	1968 Tokachi-oki	MX	DS	33.5	46	0.259	MMI = 7 - 8	Mix of CI & AC, may include PGD	Katayama et al, 1975 (Table 3)
1152	1968 Tokachi-oki	AC	DS	31.1	13	0.0793	MMI = 7 - 8	May include PGD effects	Katayama et al, 1975 (Table 3)
1153	1968 Tokachi-oki	CI	DS	13.7	29	0.403	MMI = 7 - 8	May include PGD effects	Katayama et al, 1975 (Table 3)
1154	1968 Tokachi-oki	MX	DS	60.9	81	0.369	MMI = 7 - 8	Mix of CI & AC, may include PGD	Katayama et al, 1975 (Table 3)
1155	1965 Puget Sound	CI	DS	69.7	13	0.0366	MMI = 8		Toprak, 1998 (Table 2-3)
1156	1965 Puget Sound	CI	DS	1180	14	0.0022	MMI = 7		Toprak, 1998 (Table 2-3)
1157	1965 Puget Sound	CI	SM	NR	NR	0.0021	PGV = 3.0		O'Rourke & Ayala, 1993 (D)
1158	1964 Niigata	CI	SM	293	215	0.14	PGA = 0.16	Non-liq. Area	Katayama et al, 1975
1159	1949 Puget Sound	CI	DS	52.2	24	0.0884	MMI = 8		Toprak, 1998 (Table 2-3)
1160	1949 Puget Sound	CI	DS	819	17	0.004	MMI = 7		Toprak, 1998 (Table 2-3)
1161	1948 Fukui	CI	DS	49.7	150	0.579	PGA = 0.51	May include PGD	Katayama et al, 1975
1162	1933 Long Beach	CI	DS	368	130	0.0671	MMI = 7 - 9		Toprak, 1998 (Table 2-3)
1163	1923 Kanto	CI	LG	39.1	10	0.0488	PGA = 0.31		Katayama et al, 1975
1164	1923 Kanto	CI	SM	570	214	0.0671	PGA = 0.31		Katayama et al, 1975
Comments				19525.7	3350				
DI = ductile iron. AC = asbestoc cement. S = steel. CP = concrete pipe. MX = combined materials (I.e., mixed)									
Size refers to pipe diameter. LG = Large (≥ 12 inches) SM = small (< 12 inches), DS = distirbution system (mostly small diameter, but some large diameter possible)									
Length is in miles of pipeline (NR = not reported)									
Rate is Repairs per 1,000 feet of pipeline length									
Demand is the reported seismic intensity measure associated with the length of pipeline.									
PGV = peak ground velocity (inch/second) PGA = peak ground acceleration (g), MMI = modified Mercalli Intensity									

Table A.1-1. Pipe Damage Statistics (Page 4 of 4)

ID	Earthquake	Magnitude	Material Type	Size	Repair Rate / 1000 f t	PGV, inch/sec	Comment
1001	1995 Hyogoken-nanbu	6.9	MX	DS	0.031	10.5	PGV (c/s)=140xPGA, 0.9xPGV
1002	1995 Hyogoken-nanbu	6.9	MX	DS	0.207	15.2	PGV (c/s)=140xPGA, 0.9xPGV
1003	1995 Hyogoken-nanbu	6.9	MX	DS	0.047	23.8	PGV (c/s)=140xPGA, 0.9xPGV
1004	1995 Hyogoken-nanbu	6.9	MX	DS	0.057	28.4	PGV (c/s)=140xPGA, 0.9xPGV
1005	1995 Hyogoken-nanbu	6.9	MX	DS	0.227	29.6	PGV (c/s)=140xPGA, 0.9xPGV
1006	1995 Hyogoken-nanbu	6.9	MX	DS	0.227	33.6	PGV (c/s)=140xPGA, 0.9xPGV
1007	1995 Hyogoken-nanbu	6.9	MX	DS	0.062	35.3	PGV (c/s)=140xPGA, 0.9xPGV
1008	1995 Hyogoken-nanbu	6.9	MX	DS	0.202	39.3	PGV (c/s)=140xPGA, 0.9xPGV
1009	1995 Hyogoken-nanbu	6.9	MX	DS	---	---	Omit due to possible PGD effects
1010	1995 Hyogoken-nanbu	6.9	MX	DS	0.098	41.4	PGV (c/s)=140xPGA, 0.9xPGV
1011	1995 Hyogoken-nanbu	6.9	DI	DS	---	---	Included in 1001 to 1010
1012	1995 Hyogoken-nanbu	6.9	DI	DS	---	---	Included in 1001 to 1010
1013	1995 Hyogoken-nanbu	6.9	DI	DS	---	---	Included in 1001 to 1010
1014	1995 Hyogoken-nanbu	6.9	DI	DS	---	---	Included in 1001 to 1010
1015	1995 Hyogoken-nanbu	6.9	DI	DS	---	---	Included in 1001 to 1010
1016	1995 Hyogoken-nanbu	6.9	DI	DS	---	---	Included in 1001 to 1010
1017	1995 Hyogoken-nanbu	6.9	DI	DS	---	---	Included in 1001 to 1010
1018	1995 Hyogoken-nanbu	6.9	DI	DS	---	---	Included in 1001 to 1010
1019	1995 Hyogoken-nanbu	6.9	DI	DS	---	---	Included in 1001 to 1010
1020	1995 Hyogoken-nanbu	6.9	CI	DS	---	---	Included in 1001 to 1010
1021	1995 Hyogoken-nanbu	6.9	CI	DS	---	---	Included in 1001 to 1010
1022	1995 Hyogoken-nanbu	6.9	CI	DS	---	---	Included in 1001 to 1010
1023	1995 Hyogoken-nanbu	6.9	CI	DS	---	---	Included in 1001 to 1010
1024	1995 Hyogoken-nanbu	6.9	CI	DS	---	---	Included in 1001 to 1010
1025	1995 Hyogoken-nanbu	6.9	CI	DS	---	---	Included in 1001 to 1010
1026	1995 Hyogoken-nanbu	6.9	CI	DS	---	---	Included in 1001 to 1010
1027	1995 Hyogoken-nanbu	6.9	CI	DS	---	---	Included in 1001 to 1010
1028	1995 Hyogoken-nanbu	6.9	CI	DS	---	---	Included in 1001 to 1010
1029	1995 Hyogoken-nanbu	6.9	CI	DS	---	---	Included in 1001 to 1010
1030	1994 Northridge	6.7	DI	DS	0.0253	47.2	1.07xRate (see Note 7)
1031	1994 Northridge	6.7	DI	DS	0.014	35.8	1.07xRate (see Note 7)
1032	1994 Northridge	6.7	DI	DS	0.0303	29.3	1.07xRate (see Note 7)
1033	1994 Northridge	6.7	DI	DS	0.0949	22.8	1.07xRate (see Note 7)
1034	1994 Northridge	6.7	DI	DS	0.0179	17.9	1.07xRate (see Note 7)
1035	1994 Northridge	6.7	DI	DS	0.0302	14.6	1.07xRate (see Note 7)
1036	1994 Northridge	6.7	DI	DS	0.0161	11.4	1.07xRate (see Note 7)
1037	1994 Northridge	6.7	DI	DS	0.021	8.1	1.07xRate (see Note 7)
1038	1994 Northridge	6.7	DI	DS	0.002	4	Combine w/ 1039, 1.07xRate
1039	1994 Northridge	6.7	DI	DS	---	---	
1040	1994 Northridge	6.7	AC	DS	---	---	
1041	1994 Northridge	6.7	AC	DS	---	---	
1042	1994 Northridge	6.7	AC	DS	0.0216	25.3	Combine w/ 1040, 1041, 1043, 1.07xRate
1043	1994 Northridge	6.7	AC	DS	---	---	
1044	1994 Northridge	6.7	AC	DS	---	---	
1045	1994 Northridge	6.7	AC	DS	0.0042	12.2	Combine w/ 1044, 1.07xRate
1046	1994 Northridge	6.7	AC	DS	0.0207	8.1	

Table A.1-2. Screened Database of Pipe Damage Caused by Seismic Wave Propagation (Page 1 of 4)

ID	Earthquake	Magnitude	Material Type	Size	Repair Rate / 1000 ft	PGV, inch/sec	Comment
1047	1994 Northridge	6.7	AC	DS	0.0014	3.8	Combine w/ 1048, 1.07xRate
1048	1994 Northridge	6.7	AC	DS	---	---	
1049	1994 Northridge	6.7	CI	DS	0.1541	52.1	1.07xRate
1050	1994 Northridge	6.7	CI	DS	0.0263	45.6	1.07xRate
1051	1994 Northridge	6.7	CI	DS	0.0219	39	1.07xRate
1052	1994 Northridge	6.7	CI	DS	0.0068	32.5	1.07xRate
1053	1994 Northridge	6.7	CI	DS	0.0578	27.7	1.07xRate
1054	1994 Northridge	6.7	CI	DS	0.0708	24.4	1.07xRate
1055	1994 Northridge	6.7	CI	DS	0.079	21.1	1.07xRate
1056	1994 Northridge	6.7	CI	DS	0.0362	17.9	1.07xRate
1057	1994 Northridge	6.7	CI	DS	0.0236	14.6	1.07xRate
1058	1994 Northridge	6.7	CI	DS	0.0321	11.4	1.07xRate
1059	1994 Northridge	6.7	CI	DS	0.0246	8.1	1.07xRate
1060	1994 Northridge	6.7	CI	DS	0.0073	4.5	Combine w/ 1061, 1.07xRate
1061	1994 Northridge	6.7	CI	DS	---	---	
1062	1994 Northridge	6.7	CP	LG	0.102	42.3	0.83xPGV (see Note 8)
1063	1994 Northridge	6.7	S	LG	0.0839	45.3	0.83xPGV (see Note 8)
1064	1994 Northridge	6.7	S	LG	0.0396	27.7	0.83xPGV (see Note 8)
1065	1994 Northridge	6.7	S	LG	0.0092	16.5	0.83xPGV (see Note 8)
1066	1994 Northridge	6.7	S	LG	0.0031	11.4	0.83xPGV (see Note 8)
1067	1994 Northridge	6.7	S	LG	0.0031	8.1	0.83xPGV (see Note 8)
1068	1994 Northridge	6.7	AC	DS	---	---	Already in ALA data above
1069	1994 Northridge	6.7	AC	DS	---	---	Already in ALA data above
1070	1994 Northridge	6.7	DI	DS	---	---	Already in ALA data above
1071	1994 Northridge	6.7	S	DS	0.0914	17.9	1.07xRate, 0.83xPGV
1072	1994 Northridge	6.7	S	DS	0.0522	11.5	1.07xRate, 0.83xPGV
1073	1994 Northridge	6.7	S	DS	0.0587	8.3	1.07xRate, 0.83xPGV
1074	1994 Northridge	6.7	S	DS	0.0551	4.9	1.07xRate, 0.83xPGV
1075	1994 Northridge	6.7	CI	DS	---	---	Already in ALA data above
1076	1994 Northridge	6.7	CI	DS	---	---	Already in ALA data above
1077	1994 Northridge	6.7	CI	DS	---	---	Already in ALA data above
1078	1994 Northridge	6.7	CI	DS	---	---	Already in ALA data above
1079	1994 Northridge	6.7	CI	DS	---	---	Already in ALA data above
1080	1994 Northridge	6.7	CI	DS	---	---	Already in ALA data above
1081	1994 Northridge	6.7	CI	DS	---	---	Already in ALA data above
1082	1989 Loma Prieta	6.9	S	DS	0.148	17	Supersedes 1094 to 1096
1083	1989 Loma Prieta	6.9	S	DS	0.0061	7	Supersedes 1094 to 1096
1084	1989 Loma Prieta	6.9	S	DS	0.0084	5	Supersedes 1094 to 1096
1085	1989 Loma Prieta	6.9	S	DS	0.0025	3	Supersedes 1094 to 1096
1086	1989 Loma Prieta	6.9	AC	SM	0.0123	17	Supersedes 1097 to 1099
1087	1989 Loma Prieta	6.9	AC	SM	0.0009	7	Supersedes 1097 to 1099
1088	1989 Loma Prieta	6.9	AC	SM	0.0024	5	Supersedes 1097 to 1099
1089	1989 Loma Prieta	6.9	AC	SM	0.0034	3	Supersedes 1097 to 1099
1090	1989 Loma Prieta	6.9	CI	DS	0.0919	17	Supersedes 1100 to 1102
1091	1989 Loma Prieta	6.9	CI	DS	0.0052	7	Supersedes 1100 to 1102
1092	1989 Loma Prieta	6.9	CI	DS	0.0123	5	Supersedes 1100 to 1102
1093	1989 Loma Prieta	6.9	CI	DS	0.0056	3	Supersedes 1100 to 1102

Table A.1-2. Screened Database of Pipe Damage Caused by Seismic Wave Propagation (Page 2 of 4)

ID	Earthquake	Magnitude	Material Type	Size	Repair Rate / 1000 f t	PGV, inch/sec	Comment
1094	1989 Loma Prieta	6.9	S	DS	---	---	
1095	1989 Loma Prieta	6.9	S	DS	---	---	
1096	1989 Loma Prieta	6.9	S	DS	---	---	
1097	1989 Loma Prieta	6.9	AC	DS	---	---	
1098	1989 Loma Prieta	6.9	AC	DS	---	---	
1099	1989 Loma Prieta	6.9	AC	DS	---	---	
1100	1989 Loma Prieta	6.9	CI	DS	---	---	
1101	1989 Loma Prieta	6.9	CI	DS	---	---	
1102	1989 Loma Prieta	6.9	CI	DS	---	---	
1103	1989 Mexico	7.4	CP	LG	0.0518	9.8	
1104	1989 Loma Prieta	6.9	CI	DS	0.0026	5.3	
1105	1987 Whittier	5.9&5.3	CI	DS	---	---	Main and aftershock magnitudes (Note 10)
1106	1985 Mexico City	8.1&7.5	CP	LG	---	---	Main and aftershock magnitudes (Note 10)
1107	1985 Mexico City	8.1&7.5	MX	LG	---	---	Main and aftershock magnitudes (Note 10)
1108	1985 Mexico City	8.1&7.5	MX	LG	---	---	Main and aftershock magnitudes (Note 10)
1109	1985 Mexico City	8.1&7.5	MX	LG	---	---	Main and aftershock magnitudes (Note 10)
1110	1983 Coalinga	6.7	AC	SM	0.101	11.8	
1111	1983 Coalinga	6.7	CI	SM	---	---	Corrosion bias
1112	1979 Imperial Val.	6.5	AC	DS	0.0183	23.7	
1113	1979 Imperial Val.	6.5	CI	DS	---	---	Corrosion bias
1114	1972 Managua	6.3	AC	SM	---	---	See Note 9
1115	1972 Managua	6.3	CI	LG	---	---	See Note 9
1116	1972 Managua	6.3	CI	SM	---	---	See Note 9
1117	1971 San Fernando	6.7	CI	SM	0.0122	13.8	PGV (c/s)=130xPGA per Wald Figs. 1&2
1118	1971 San Fernando	6.7	CI	SM	0.0152	14.3	PGV (c/s)=130xPGA per Wald Figs. 1&2
1119	1971 San Fernando	6.7	CI	SM	0.0244	14.8	PGV (c/s)=130xPGA per Wald Figs. 1&2
1120	1971 San Fernando	6.7	CI	SM	0.0183	14.8	PGV (c/s)=130xPGA per Wald Figs. 1&2
1121	1971 San Fernando	6.7	CI	SM	0.0244	15.4	PGV (c/s)=130xPGA per Wald Figs. 1&2
1122	1971 San Fernando	6.7	CI	SM	0.0335	15.9	PGV (c/s)=130xPGA per Wald Figs. 1&2
1123	1971 San Fernando	6.7	CI	SM	0.061	16.4	PGV (c/s)=130xPGA per Wald Figs. 1&2
1124	1971 San Fernando	6.7	CI	SM	0.122	16.9	PGV (c/s)=130xPGA per Wald Figs. 1&2
1125	1971 San Fernando	6.7	CI	SM	0.131	17.4	PGV (c/s)=130xPGA per Wald Figs. 1&2
1126	1971 San Fernando	6.7	CI	SM	---	---	See Note 9
1127	1971 San Fernando	6.7	CI	SM	---	---	See Note 9
1128	1971 San Fernando	6.7	CI	SM	---	---	See Note 9
1129	1971 San Fernando	6.7	CI	SM	---	---	See Note 9
1130	1971 San Fernando	6.7	CI	SM	---	---	See Note 9
1131	1971 San Fernando	6.7	CI	SM	---	---	See Note 9
1132	1971 San Fernando	6.7	CI	SM	---	---	See Note 9
1133	1971 San Fernando	6.7	CI	SM	---	---	See Note 9
1134	1971 San Fernando	6.7	CI	SM	---	---	See Note 9
1135	1971 San Fernando	6.7	CI	SM	---	---	See Note 9
1136	1971 San Fernando	6.7	CI	DS	0.0488	26	PGV per Wald el al, 1999 Fig. 2
1137	1971 San Fernando	6.7	CI	DS	0.0029	9.1	PGV per Wald el al, 1999 Fig. 2
1138	1971 San Fernando	6.7	CI	SM	---	---	Same data set as 1140 and 1141
1139	1971 San Fernando	6.7	CI	SM	---	---	Same data set as 1140 and 1141
1140	1971 San Fernando	6.7	CI	DS	0.0067	7.1	

Table A.1-2. Screened Database of Pipe Damage Caused by Seismic Wave Propagation (Page 3 of 4)

ID	Earthquake	Magnitude	Material Type	Size	Repair Rate / 1000 ft	PGV, inch/sec	Comment
1141	1971 San Fernando	6.7	CI	DS	0.0125	11.8	
1142	1969 Santa Rosa	5.6&5.7	CI	DS	---	---	Main and aftershock magnitudes (Note 10)
1143	1969 Santa Rosa	5.6&5.7	CI	SM	---	---	Main and aftershock magnitudes (Note 10)
1144	1968 Tokachi-oki	7.9	AC	DS	---	---	See Note 9
1145	1968 Tokachi-oki	7.9	MX	DS	---	---	See Note 9
1146	1968 Tokachi-oki	7.9	MX	DS	---	---	See Note 9
1147	1968 Tokachi-oki	7.9	MX	DS	---	---	See Note 9
1148	1968 Tokachi-oki	7.9	MX	DS	---	---	See Note 9
1149	1968 Tokachi-oki	7.9	AC	DS	---	---	See Note 9
1150	1968 Tokachi-oki	7.9	CI	DS	---	---	See Note 9
1151	1968 Tokachi-oki	7.9	MX	DS	---	---	See Note 9
1152	1968 Tokachi-oki	7.9	AC	DS	---	---	See Note 9
1153	1968 Tokachi-oki	7.9	CI	DS	---	---	See Note 9
1154	1968 Tokachi-oki	7.9	MX	DS	---	---	See Note 9
1155	1965 Puget Sound	6.5	CI	DS	0.0366	16.7	PGV per Wald el al, 1999 eqn 2
1156	1965 Puget Sound	6.5	CI	DS	0.0022	8.6	PGV per Wald el al, 1999 eqn 2
1157	1965 Puget Sound	6.5	CI	SM	---	---	Data included in 1155 and 1156
1158	1964 Niigata	7.5	CI	SM	0.14	6	PGV (c/s)=95xPGA per Wald Figs. 3&4
1159	1949 Puget Sound	7.1	CI	DS	0.0884	16.7	PGV per Wald el al, 1999 eqn 2
1160	1949 Puget Sound	7.1	CI	DS	0.004	8.6	PGV per Wald el al, 1999 eqn 2
1161	1948 Fukui	7.3	CI	DS	---	---	See Note 9
1162	1933 Long Beach	6.3	CI	DS	0.0671	24.6	PGV per Wald el al, 1999 eqn 2
1163	1923 Kanto	7.9	CI	LG	0.0488	11.6	PGV (c/s)=95xPGA per Wald Figs. 3&4
1164	1923 Kanto	7.9	CI	SM	0.0671	11.6	PGV (c/s)=95xPGA per Wald Figs. 3&4

Notes.

1. DI = ductile iron. AC = asbestoc cement. S = steel. CP = concrete pipe. MX = combined materials (I.e., mixed)

2. Size refers to pipe diameter. LG = Large (> about 12 inches) SM = small (≤ about12 inches).

3. DS = distirbution system (mostly small diameter, but some large diameter possible)

4. Repair rate is repairs per 1,000 of pipe

5. Modified Demand, PGA, inches / second. Peak Ground Velocity. Entry of "---" means that the data point was screened out for reasons cited in this table.

6. Wald et al ([1999] equation 2 is as follows: MMI = 3.47 log(PGV) + 2.35, where PGV is in cm / sec.

7. 1.07 x Rate modification is to account for repairs omitted from Toprak [1998] analysis due to lack of some atttributes, but the damage did occur

8. 0.83 x PGV modification is to adjust peak PGV value of two horizontal directions to average horizontal vale of two directions (for Northridge only)

9. Data point screened out due to possible PGD effects. For San Fernando, only point in the northeast part of the valley were screened out per Barenberg [1988] and NOAA [1973].

10. These entries had aftershocks of similar magnitude as the main shock. The data points were screened out as the amount of damage caused by each event cannot be differentiated.

Table A.1-2. Screened Database of Pipe Damage Caused by Seismic Wave Propagation (Page 4 of 4)

ID	Earthquake	Material Type	Size	Repair Rate / 1000 ft	PGD, inches	Source	Comment
2001	1989 Loma Prieta	CI	DS	3.5	4.6	Porter et al, 1991 (Fig. 9)	
2002	1989 Loma Prieta	CI	DS	3.5	1.3	Porter et al, 1991 (Fig. 9)	
2003	1989 Loma Prieta	CI	DS	2.6	4.6	Porter et al, 1991 (Fig. 9)	
2004	1989 Loma Prieta	CI	DS	2.3	4.5	Porter et al, 1991 (Fig. 9)	
2005	1989 Loma Prieta	CI	DS	2.3	2.8	Porter et al, 1991 (Fig. 9)	
2006	1989 Loma Prieta	CI	DS	2.1	3.8	Porter et al, 1991 (Fig. 9)	
2007	1989 Loma Prieta	CI	DS	2.1	2.3	Porter et al, 1991 (Fig. 9)	
2008	1989 Loma Prieta	CI	DS	1.7	3.7	Porter et al, 1991 (Fig. 9)	
2009	1989 Loma Prieta	CI	DS	1.6	1.1	Porter et al, 1991 (Fig. 9)	
2010	1989 Loma Prieta	CI	DS	1.1	0.6	Porter et al, 1991 (Fig. 9)	
2011	1989 Loma Prieta	CI	DS	0.4	1.4	Porter et al, 1991 (Fig. 9)	
2012	1989 Loma Prieta	CI	DS	0.4	0.8	Porter et al, 1991 (Fig. 9)	
2013	1983 Nihonkai-Chubu	AC	SM	4.6	76.5	Hamada et al, 1986 (Fig. 5-6)	
2014	1983 Nihonkai-Chubu	AC	SM	0.6	48.5	Hamada et al, 1986 (Fig. 5-6)	
2015	1983 Nihonkai-Chubu	AC	SM	3.1	49.5	Hamada et al, 1986 (Fig. 5-6)	
2016	1983 Nihonkai-Chubu	AC	SM	4.2	49.8	Hamada et al, 1986 (Fig. 5-6)	
2017	1983 Nihonkai-Chubu	AC	SM	8.5	41.7	Hamada et al, 1986 (Fig. 5-6)	
2018	1983 Nihonkai-Chubu	AC	SM	11.6	30.4	Hamada et al, 1986 (Fig. 5-6)	
2019	1983 Nihonkai-Chubu	AC	SM	6.9	28.9	Hamada et al, 1986 (Fig. 5-6)	
2020	1983 Nihonkai-Chubu	AC	SM	4.4	30.3	Hamada et al, 1986 (Fig. 5-6)	
2021	1983 Nihonkai-Chubu	AC	SM	1.4	28.1	Hamada et al, 1986 (Fig. 5-6)	
2022	1983 Nihonkai-Chubu	AC	SM	1.6	27.1	Hamada et al, 1986 (Fig. 5-6)	
2023	1983 Nihonkai-Chubu	AC	SM	1.8	25.6	Hamada et al, 1986 (Fig. 5-6)	
2024	1983 Nihonkai-Chubu	AC	SM	1.9	23.4	Hamada et al, 1986 (Fig. 5-6)	
2025	1983 Nihonkai-Chubu	AC	SM	5.3	25.7	Hamada et al, 1986 (Fig. 5-6)	
2026	1983 Nihonkai-Chubu	AC	SM	5.9	14.8	Hamada et al, 1986 (Fig. 5-6)	
2027	1983 Nihonkai-Chubu	AC	SM	2.7	16.1	Hamada et al, 1986 (Fig. 5-6)	
2028	1983 Nihonkai-Chubu	AC	SM	0.5	14.4	Hamada et al, 1986 (Fig. 5-6)	
2029	1983 Nihonkai-Chubu	AC	SM	0.9	13.8	Hamada et al, 1986 (Fig. 5-6)	
2030	1983 Nihonkai-Chubu	AC	SM	3.1	12.1	Hamada et al, 1986 (Fig. 5-6)	
2031	1983 Nihonkai-Chubu	AC	SM	1.5	11.1	Hamada et al, 1986 (Fig. 5-6)	
2032	1983 Nihonkai-Chubu	AC	SM	0.5	7.6	Hamada et al, 1986 (Fig. 5-6)	
2033	1983 Nihonkai-Chubu	CI	SM	15.2	49.8	Hamada et al, 1986 (Fig. 5-4a)	Gas pipe (note 4)
2034	1983 Nihonkai-Chubu	CI	SM	19	30	Hamada et al, 1986 (Fig. 5-4a)	Gas pipe (note 4)
2035	1983 Nihonkai-Chubu	CI	SM	20.5	25.7	Hamada et al, 1986 (Fig. 5-4a)	Gas pipe (note 4)
2036	1983 Nihonkai-Chubu	CI	SM	14.6	9.5	Hamada et al, 1986 (Fig. 5-4a)	Gas pipe (note 4)
2037	1983 Nihonkai-Chubu	CI	SM	12.1	11.9	Hamada et al, 1986 (Fig. 5-4a)	Gas pipe (note 4)
2038	1983 Nihonkai-Chubu	CI	SM	5.9	9.6	Hamada et al, 1986 (Fig. 5-4a)	Gas pipe (note 4)
2039	1983 Nihonkai-Chubu	CI	SM	0.9	11.2	Hamada et al, 1986 (Fig. 5-4a)	Gas pipe (note 4)
2040	1983 Nihonkai-Chubu	CI	SM	0.9	8.4	Hamada et al, 1986 (Fig. 5-4a)	Gas pipe (note 4)
2041	1983 Nihonkai-Chubu	CI	SM	0.5	6.6	Hamada et al, 1986 (Fig. 5-4a)	Gas pipe (note 4)
2042	1983 Nihonkai-Chubu	S	SM	16.5	76.6	Hamada et al, 1986 (Fig. 5-4b)	Gas pipe (note 4)
2043	1983 Nihonkai-Chubu	S	SM	3	51.4	Hamada et al, 1986 (Fig. 5-4b)	Gas pipe (note 4)
2044	1983 Nihonkai-Chubu	S	SM	2.4	28.6	Hamada et al, 1986 (Fig. 5-4b)	Gas pipe (note 4)
2045	1983 Nihonkai-Chubu	S	SM	2.8	26.6	Hamada et al, 1986 (Fig. 5-4b)	Gas pipe (note 4)
2046	1983 Nihonkai-Chubu	S	SM	1.3	9.7	Hamada et al, 1986 (Fig. 5-4b)	Gas pipe (note 4)
2047	1971 San Fernando	MX	LG	1.2	19.5	Barenberg, 1988 (Fig. 2)	
2048	1971 San Fernando	MX	LG	1.9	25.7	Barenberg, 1988 (Fig. 2)	
2049	1971 San Fernando	MX	LG	2.3	27.4	Barenberg, 1988 (Fig. 2)	
2050	1971 San Fernando	MX	LG	3.7	31.1	Barenberg, 1988 (Fig. 2)	
2051	1971 San Fernando	MX	LG	8.2	41	Barenberg, 1988 (Fig. 2)	
2052	1906 San Francisco	CI	DS	9.3	108	Porter et al, 1991 (Fig. 9)	
2053	1906 San Francisco	CI	DS	6.8	60	Porter et al, 1991 (Fig. 9)	
2054	1906 San Francisco	CI	DS	2.9	60	Porter et al, 1991 (Fig. 9)	
2055	1906 San Francisco	CI	DS	3.9	29	Porter et al, 1991 (Fig. 9)	
2056	1906 San Francisco	CI	DS	3.6	12	Porter et al, 1991 (Fig. 9)	
Notes							
1. CI = Cast Iron, AC = Asbestoc Cement, S = steel, MX = mix of CI and S							
2. Size refers to pipe diameter. LG = Large (> about 12 inches) SM = small (≤ about12 inches).							
3. Rate is reported repairs per 1,000 feet of pipeline.							
4. Datapoint notused in statistical analysis							

Table A1-3. Database of Pipe Damage Caused by Permanent Ground Displacements

PGV	Pipe Diameter, Inches																	
inch/sec	4		6		8		10		12		16		20		24		30	
	L	n	L	n	L	n	L	n	L	n	L	n	L	n	L	n	L	n
3	98.32	0	266.07	9	60.73	2	11.59	0	18.22	0	9.5	0	1.9	0	0.35	0	0	0
5	30.15	3	60.87	3	21.25	1	1.35	0	7.79	0	0.46	0	0.28	0	0	0	0.02	0
7	190.28	4	450.57	14	132.05	5	23.84	0	45.55	0	11.23	0	15.13	0	1.93	0	0	0
13	0.47	5	0.79	0	0.49	0	0	0	0.11	0	0.08	0	0	0	0	0	0	0
15	0.6	0	0.32	0	0.83	0	0.7	0	0.52	0	0	0	0.24	0	0	0	0	0
17	1.33	0	3.35	5	2.59	0	1.6	1	2.61	3	0.5	0	0.54	1	0.52	0	0	0
19	0.27	0	0.03	0	0	0	0	0	0	0	0	0	0	0	0	0	0	0
21	0	0	0	0	0	0	0	0	0	0	0	0	0	0	0	0	0	0
Total	321.42	12	782	31	217.94	8	39.08	1	74.8	3	21.77	0	18.09	1	2.8	0	0.02	0
Notes																		
L = length of pipeline in miles within the specified PGV bin																		
n = number of repairs																		
See Section A.3.11 for further description of the data																		

Table A.3-7. Cast Iron Pipe Damage, 1989 Loma Prieta Earthquake, EBMUD

PGV inch/sec	Pipe Diameter, Inches																									
	4		6		8		10		12		16		20		24		30		36		42		48		60	
	L	n	L	n	L	n	L	n	L	n	L	n	L	n	L	n	L	n	L	n	L	n	L	n	L	n
3	1.01	0	71.95	2	77.78	0	0.07	0	112.2	2	48.22	0	20.15	1	19.19	0	6.28	0	8.35	0	1.12	0	4.84	0	0.49	0
5	0.11	0	3.96	1	7.75	0	0.03	0	11.13	0	1.79	0	0.33	0	5.45	0	0.93	0	9.66	0	1.17	0	1.87	0	0.64	1
7	1.11	0	25.68	1	45.17	4	0.16	0	61.58	2	44.82	0	15.08	0	17.73	0	19.9	1	29.48	0	4.82	1	6.02	0	4.52	0
13	0.06	0	0.65	0	1.1	0	0	0	0.49	0	0.43	0	0.19	0	0	0	0.23	0	0	0	0	0	0	0	0	0
15	0.04	0	0.8	0	5.08	0	0.01	0	5.9	2	0.65	0	0.41	0	2.1	0	0	0	1.95	0	1.14	0	0	0	0	0
17	0	0	5.58	25	9.21	12	0.06	0	15.14	7	3.42	0	0.03	1	2.03	1	0.62	0	0.44	0	0	0	0	0	0	0
19	0	0	0.25	0	0.68	0	0	0	1.04	0	0	0	0	0	0	0	0	0	0	0	0	0	0	0	0	0
21	0	0	0	0	0	0	0	0	0	0	0	0	0	0	0	0	0	0	0	0	0	0	0	0	0	0
Total	2.33	0	108.9	29	146.8	16	0.33	0	207.5	13	99.33	0	36.19	2	46.5	1	27.96	1	49.88	0	8.25	1	12.73	0	5.65	1

Notes

L = length of pipeline in miles within the specified PGV bin

n = number of repairs

See Section A.3.11 for further description of the data

Table A.3-8. Welded Steel Pipe Damage, 1989 Loma Prieta Earthquake, EBMUD

PGV	Pipeline Diameter, Inches									
inch / sec	4		6		8		10		12	
	L	n	L	n	L	n	L	n	L	n
3	7.8	0	299.27	5	124.4	2	0.43	0	12.76	1
5	2.87	0	50.91	0	18.11	1	0	0	7.29	0
7	11.89	0	273.69	2	129.89	0	0.1	0	22.6	0
13	0	0	1.36	0	0.63	0	0	0	0	0
15	0.43	0	3.97	1	5.22	1	0.04	0	2.36	0
17	0.68	0	9.66	0	15.2	1	1.28	0	1.41	0
19	0	0	0.86	0	2.36	0	0	0	0.75	0
21	0	0	0	0	0	0	0	0	0	0
Total	23.67	0	639.72	8	295.81	5	1.85	0	47.17	1
Notes										
L = length of pipeline in miles, within the specified PGV bin										
n = number of repairs										
See Section A.3.11 for further description of the data										

Table A.3-9. Asbestos Cement Pipe Damage, 1989 Loma Prieta, EBMUD

Bureau	Type of Pipe	Straight Pipe	Bends	Branches	Other	Subtotal	Slip Out Straight Pipe	Slip Out Fitting	Failure Straight Pipe	Failure Fitting	Intrusion Straight Pipe	Intrusion Fitting	Unknown	Subtotal	Unknown Subtotal	Total	Length, km	Damage Rate (Repairs / km)	Air Valves	Gate Valves	Fire Hydrants	Snap taps and others	Unknown	Subtotal	Total Repairs
Kobe City	DI A K T	9	0	1	0	10	669	23	0	0	5	0	3	700	0	710	3452.1	0.206							
	CI lead, rubber	155	44	36	18	253	118	13	6	3	0	0	1	141	0	394	316.4	1.245							
	PVC TS	11	0	0	0	11	11	1	1	0	0	0	0	13	0	24	128.6	0.187							
	Welded Steel SP	9	1	0	0	10	0	0	3	0	0	0	0	3	0	13	104.9	0.124							
	Steel Threaded SGP	0	0	0	0	0	0	0	0	0	0	0	0	0	0	0	0								
	AC rubber gasket	0	0	0	0	0	0	0	0	0	0	0	0	0	0	0	0								
	Unknown	16	1	3	0	20	99	2	1	1	0	0	0	103	0	123	0								
	Subtotals	200	46	40	18	304	897	39	11	4	5	0	4	960	0	1264	4002	0.316	127	281	60	25	0	493	1757
Ashiya City	DI A K T	0	0	0	0	0	65	18	0	0	0	0	3	86	4	90	72.1	1.248							
	CI lead, rubber	54	3	9	1	67	3	0	14	0	0	0	0	17	4	88	89.4	0.984							
	PVC TS	33	2	2	0	37	10	0	61	2	0	0	1	74	5	116	22.9	5.066							
	Welded Steel SP	1	0	0	0	1	0	0	0	0	0	0	1	1	0	2	0.35	5.797							
	Steel Threaded SGP	0	0	0	0	0	0	0	1	0	0	0	0	1	0	1	0								
	AC rubber gasket	0	0	0	0	0	0	0	0	0	0	0	0	0	0	0	0								
	Unknown	0	0	0	0	0	0	0	0	0	0	0	0	0	0	0	0								
	Subtotals	88	5	11	1	105	78	18	76	2	0	0	5	179	13	297	184.745	1.608	2	53	0	10	0	65	362
Nishinomiya City	DI A K T	0	0	0	0	0	234	10	0	0	4	0	8	256	0	256	635.1	0.403							
	CI lead, rubber	68	8	10	0	86	85	2	2	0	1	0	0	90	0	176	97.7	1.801							
	PVC TS	52	24	12	0	88	51	15	56	0	3	0	3	128	0	216	185.9	1.162							
	Welded Steel SP	1	0	0	0	1	0	0	0	0	0	0	0	0	0	1	29.1	0.034							
	Steel Threaded SGP	2	1	0	0	3	1	0	1	0	0	0	0	2	0	5	2.3	2.174							
	AC rubber gasket	30	0	1	0	31	9	0	2	0	0	0	1	12	0	43	16.2	2.654							
	Unknown	0	0	0	0	0	0	0	0	0	0	0	0	0	0	0	0								
	Subtotals	153	33	23	0	209	380	27	61	0	8	0	12	488	0	697	966.3	0.721	12	80	11	24	0	127	824
Takarazuka City	DI A K T	0	0	0	0	0	97	0	0	0	0	0	1	98	6	104	732	0.142							
	CI lead, rubber	2	6	7	0	15	0	0	2	0	0	0	0	2	3	20	117	0.171							
	PVC TS	29	0	0	0	29	1	0	0	0	0	0	0	1	0	30	6.9	4.348							
	Welded Steel SP	0	0	0	0	0	0	0	0	0	0	0	0	0	0	0	0								
	Steel Threaded SGP	0	0	0	0	0	1	0	0	0	0	0	0	1	0	1	17	0.059							
	AC rubber gasket	44	0	0	0	44	0	0	0	0	0	0	0	0	0	44	1.3	33.846							
	Unknown	2	0	0	0	2	0	0	0	0	0	0	0	0	2	4	0								
	Subtotals	77	6	7	0	90	99	0	2	0	0	0	1	102	11	203	874.2	0.232	0	16	1	5	0	22	225
Amagasaki City	DI A K T	0	0	0	0	0	35	4	0	0	0	0	0	39	0	39	721.3	0.054							
	CI lead, rubber	31	5	8	0	44	8	2	2	1	0	0	0	13	0	57	110.9	0.514							
	PVC TS	0	0	0	0	0	1	0	3	0	0	0	0	4	0	4	6.9	0.580							
	Welded Steel SP	2	0	0	0	2	0	0	2	0	0	0	0	2	0	4	7.3	0.548							
	Steel Threaded SGP	0	0	0	0	0	0	0	0	0	0	0	0	0	0	0	0								
	AC rubber gasket	8	0	0	0	8	0	0	0	0	0	0	0	0	0	8	0.3	26.667							
	Unknown	0	0	0	0	0	0	0	0	0	0	0	0	0	0	0	0								
	Subtotals	41	5	8	0	54	44	6	7	1	0	0	0	58	0	112	846.7	0.132	0	12	1	5	0	18	130
Osaka City	DI A K T	0	0	0	0	0	17	0	0	0	0	0	2	19	1	19	3508	0.005							
	CI lead, rubber	139	2	1	0	142	29	1	6	1	0	0	18	55	0	197	1374	0.143							
	PVC TS	0	0	0	0	0	0	0	0	0	0	0	0	0	0	0	0								
	Welded Steel SP	0	0	0	0	0	0	0	0	0	0	0	0	0	1	1	110	0.009							
	Steel Threaded SGP	0	0	0	0	0	0	0	0	0	0	0	0	0	0	0	0								
	AC rubber gasket	0	0	0	0	0	0	0	0	0	0	0	0	0	0	0	0								
	Unknown	1	0	0	0	1	0	0	0	0	0	0	0	0	0	1	0								
	Subtotals	140	2	1	0	143	46	1	6	1	0	0	20	74	1	218	4992	0.044	0	0	0	4	13	17	235
Hokudan-cho	DI A K T	1	0	0	0	1	9	0	0	0	1	0	1	11	3	15	40.7	0.369							
	CI lead, rubber	0	0	0	0	0	0	0	0	0	0	0	0	0	0	0	1.7	0.000							
	PVC TS	22	5	5	0	32	7	0	7	0	0	0	1	15	0	47	80.1	0.587							
	Welded Steel SP	1	0	0	0	1	0	0	0	0	0	0	0	0	0	1	8.9	0.112							
	Steel Threaded SGP	1	0	0	0	1	0	0	0	0	0	0	0	0	0	1	0								
	AC rubber gasket	4	0	2	0	6	0	0	0	0	0	0	0	0	3	9	22.7	0.396							
	Unknown	0	0	1	0	1	0	0	1	0	0	0	0	1	19	21	0								
	Subtotals	29	5	8	0	42	16	0	8	0	1	0	2	27	25	94	154.1	0.610	1	1	0	1	0	3	97
Total 7 Cities	DI A K T	10	0	1	0	11	1126	55	0	0	10	0	18	1209	13	1233	9161.3	0.135							
	CI lead, rubber	449	68	71	19	607	243	18	32	5	1	0	19	318	7	932	2107.1	0.442							
	PVC TS	147	31	19	0	197	81	16	128	2	3	0	5	235	5	437	431.3	1.013							
	Welded Steel SP	14	1	0	0	15	0	0	5	0	0	0	1	6	1	22	260.545	0.084							
	Steel Threaded SGP	3	1	0	0	4	2	0	2	0	0	0	0	4	0	8	19.3	0.415							
	AC rubber gasket	86	0	3	0	89	9	0	2	0	0	0	1	12	3	104	40.5	2.568							
	Unknown	19	1	4	0	24	99	2	2	1	0	0	0	104	21	149	0								
	Subtotals	728	102	98	19	947	1560	91	171	8	14	0	44	1888	50	2885	12020.05	0.240	142	443	73	74	13	745	3630

Table A-3.19. Pipe Damage Statistics - 1995 Hanshin Earthquake
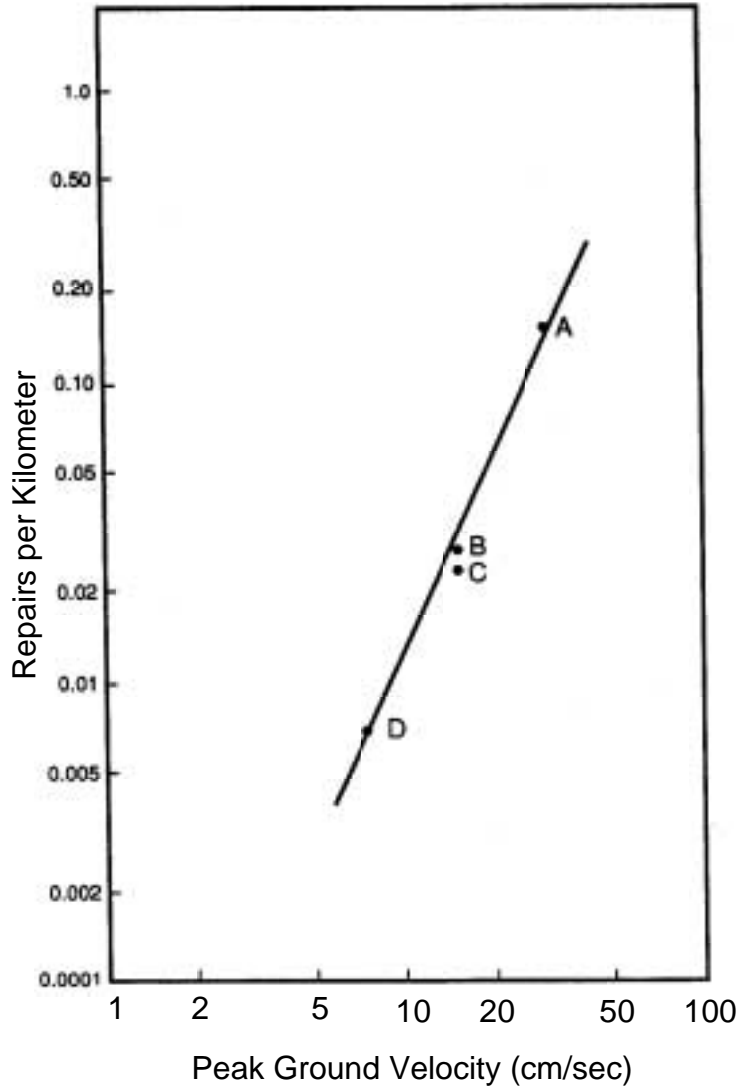
Figure A-1. Wave Propagation Damage to Cast Iron Pipe [from Barenberg, 1988]

A. 1971 San Fernando. Most common - 3 to 6 inch diameter pipes. PGV = 30 cm/sec.
Observed repair rate = 0.155 repairs / km

B. 1969 Santa Rosa. Most common - 3 to 6 inch diameter pipes. PGV = 15 cm/sec.
Observed repair rate = 0.028 repairs / km

C. 1971 San Fernando. Most common - 3 to 6 inch diameter pipes. PGV = 15 cm/sec.
Observed repair rate = 0.024 repairs / km

D. 1965 Puget Sound. Most common - 8 to 10 inch diameter pipes. PGV = 7.5 cm/sec.
Observed repair rate = 0.007 repairs / km

Note - all data from: O'Rourke, T.D., Factors affecting the performance of cast iron pipelines:
A review of U.S. observations and research investigations,
Contractor Report 18, Transport and Road Res. Lab., Crowthorne, U.K.

Best Fit: n=(0.00478)exp(.221 * PGV)

E. 1983 Coalinga. CI 3-6". PGV = 11.8 in/sec. RR = 0.238/1000 ft
F. 1985 Mexico City Lake Zone. AC, CONC, CI 20 and 48". PGV = 18.9 in/sec. RR = 0.136/1000 ft
G. 1985 M.C. Transision Zone. AC, CONC, CI 20" and 48". PGV =4.72 in/sec. RR = 0.021/1000 ft
H. 1985 M.C. Hill Zone. AC, CONC, CI 20" and 48". PGV=4.33 In/sec. RR = 0.003/1000 ft
I. 1989 Mexico Tlahuac. PCCP. 72". PGV=21.3 in/sec. RR=0.455/1000 ft.
J. 1989 Mexico Tlahuac. PCCP. 72". PGV=9.84 in/sec. RR=0.0515/1000 ft.
K. 1983 Coalinga. AC 3-10". PGV=11.8 in/sec. RR=0.10/1000 ft.

**Figure A-2. Pipe Damage - Wave Propagation
[from O'Rourke and Ayala, 1994]**

R47.01.02 Rev. 0
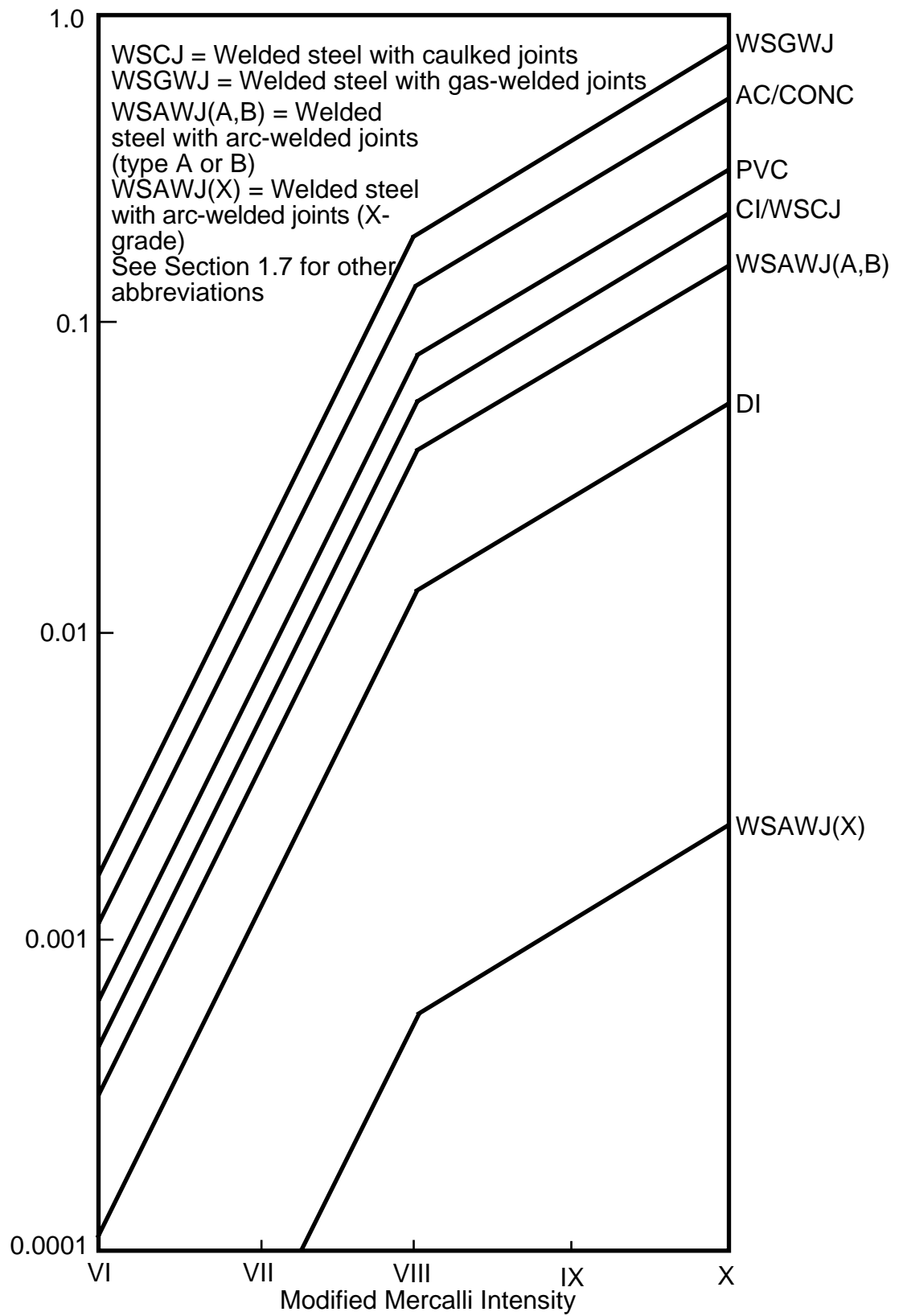
Figure A-3. Pipe Fragility Curves for Ground Shaking Hazard Only [From Ballantyne et al]

**Figure A-4. Earthquake Vulnerability
Models for Buried Pipes
for Landslide and Liquefaction**

See Section 1.7 for abbreviations
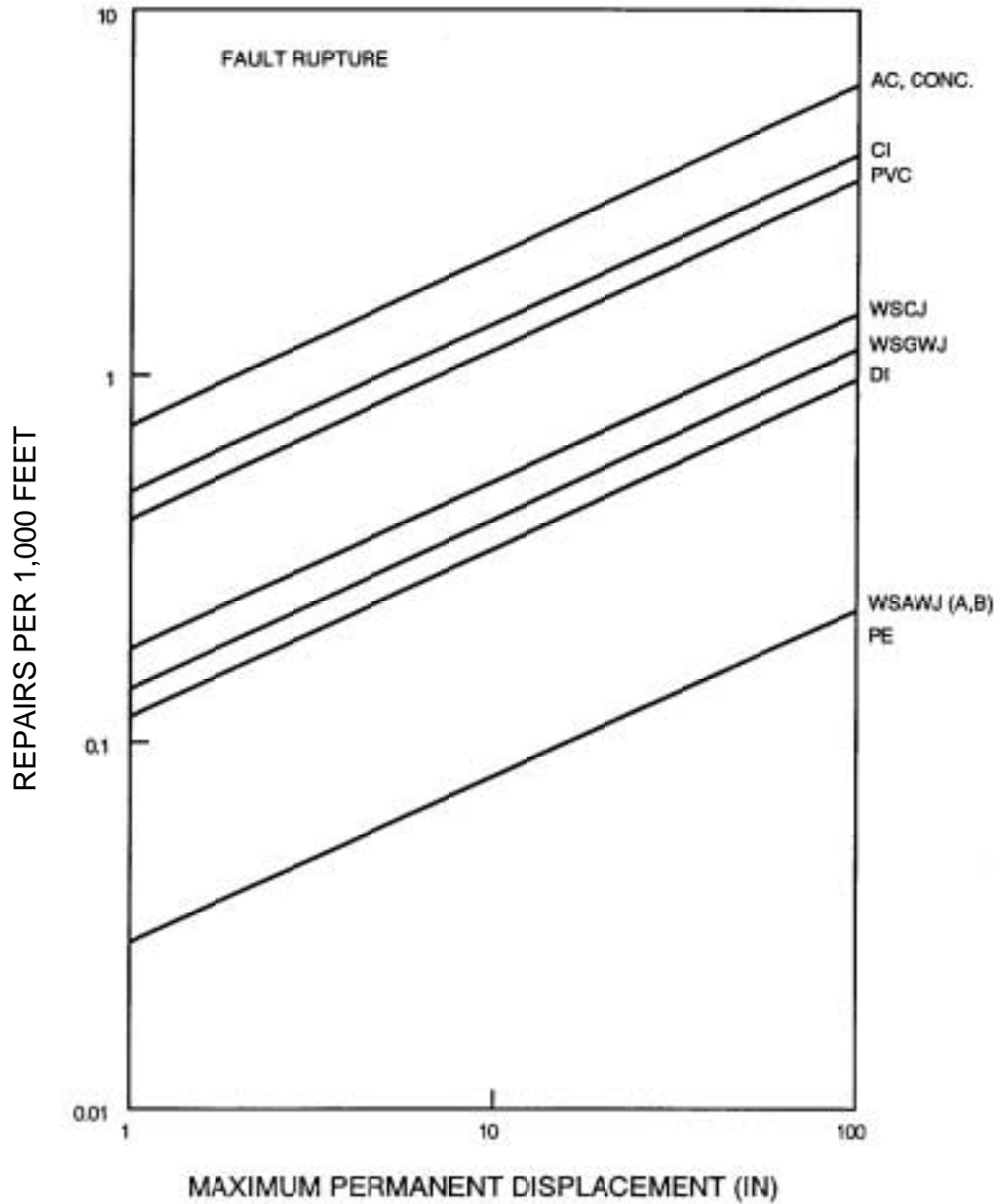
**Figure A-5. Earthquake Vulnerability
Models for Buried Pipes for Fault Offset**
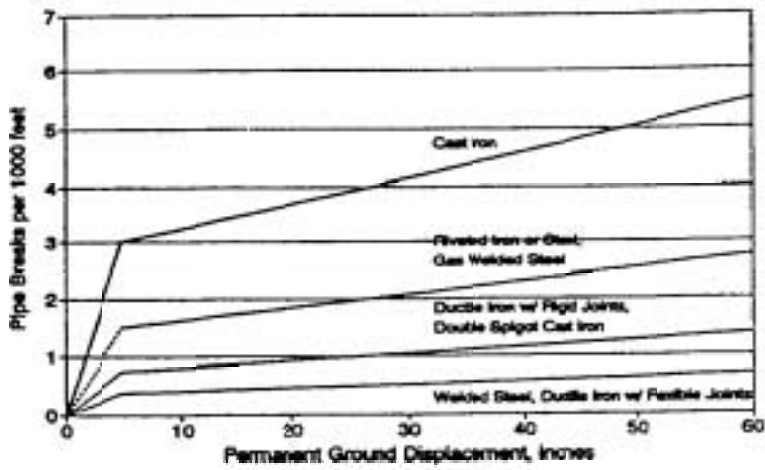
Figure A-6. PGD Damage Algorithm [from Harding and Lawson, 1991]
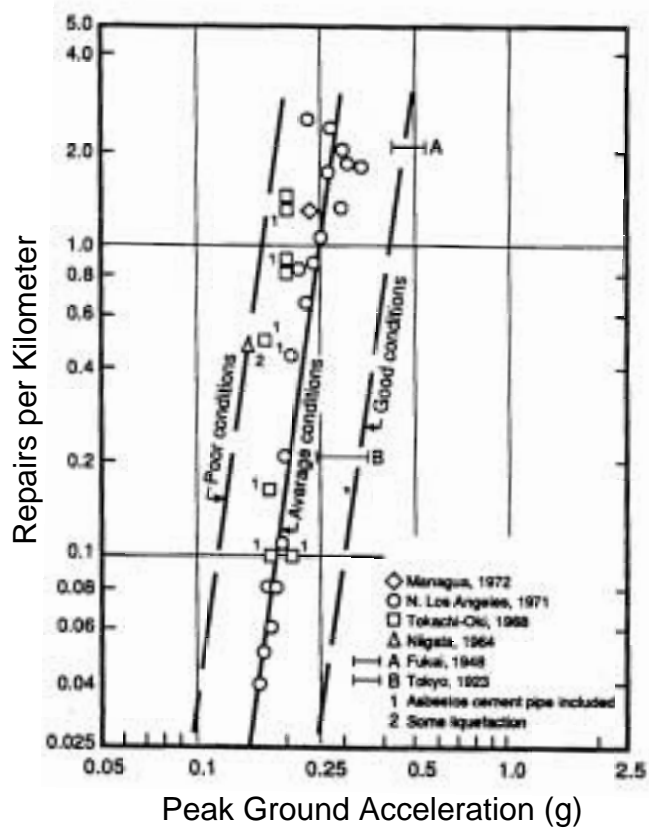
Figure A-7. Pipe Damage [from Katayama et al, 1975]
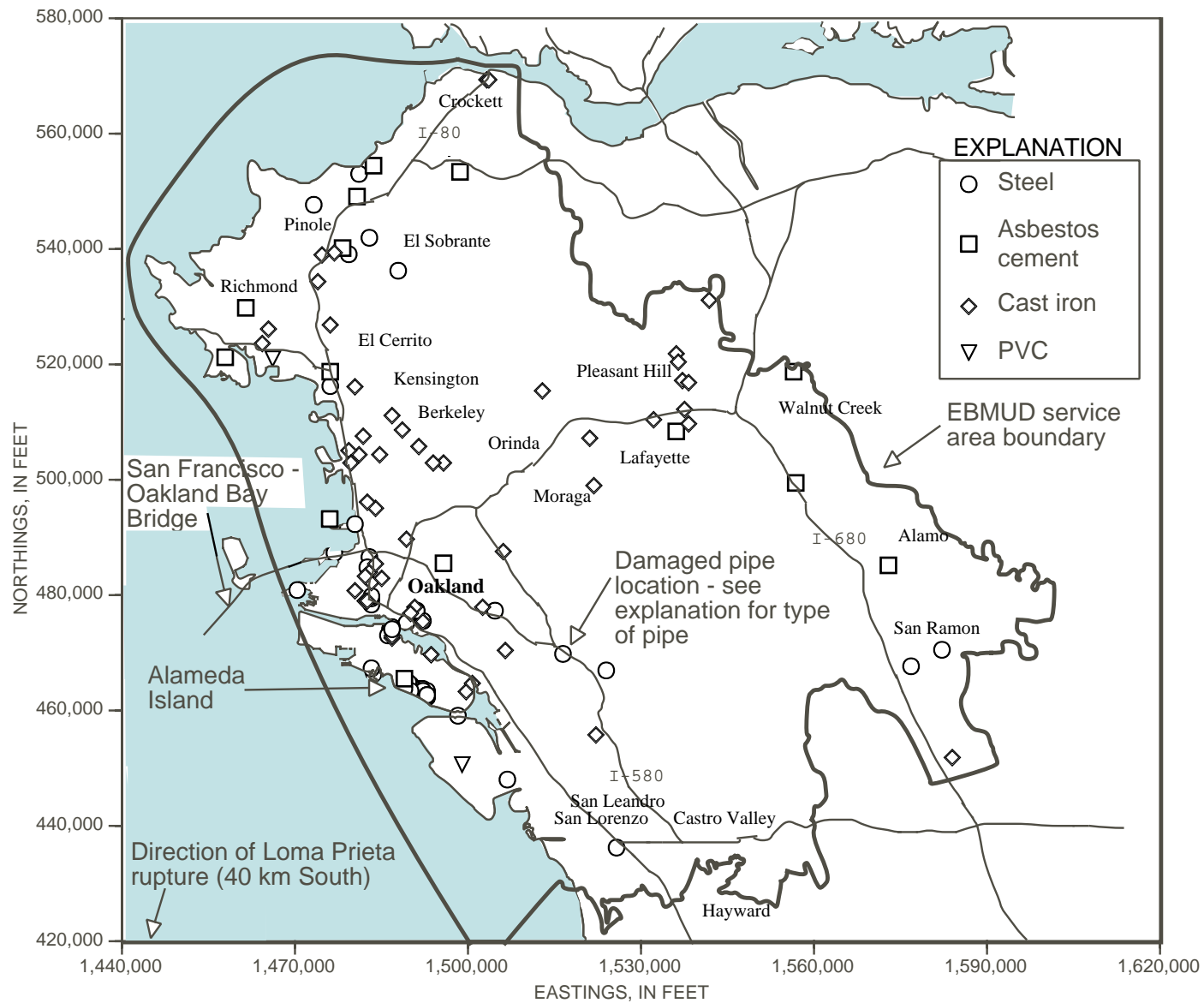
Figure A-8. Location of Pipe Repairs in EBMUD System, 1989 Loma Prieta Earthquake [after Eidinger, 1998]
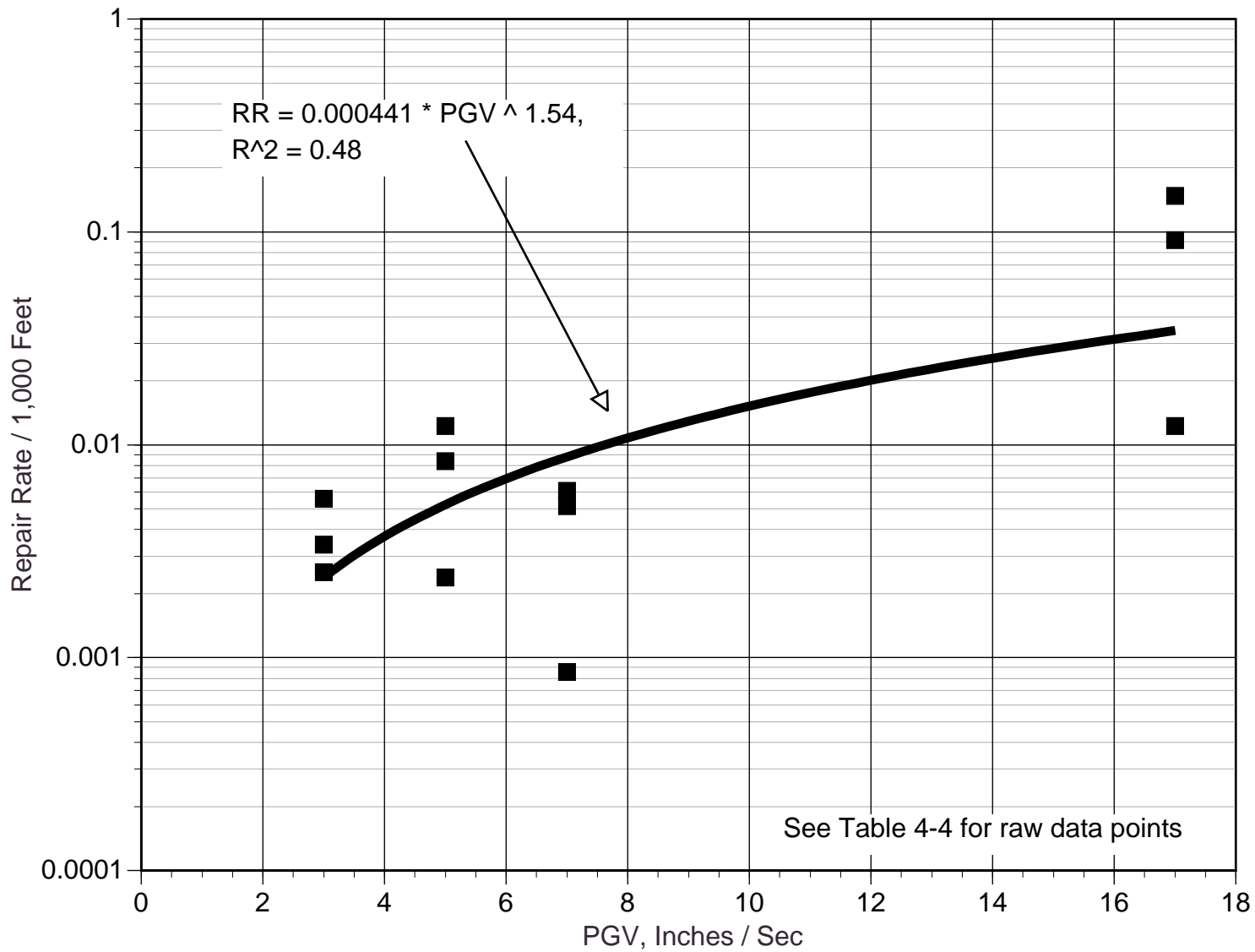
Figure A-9. Repair Rate, Loma Prieta (EBMUD), Ground Shaking, All Materials (CI + AC + WS)

RR = 0.000441 * PGV ^ 1.54, R^2 = 0.48

See Table 4-4 for raw data points
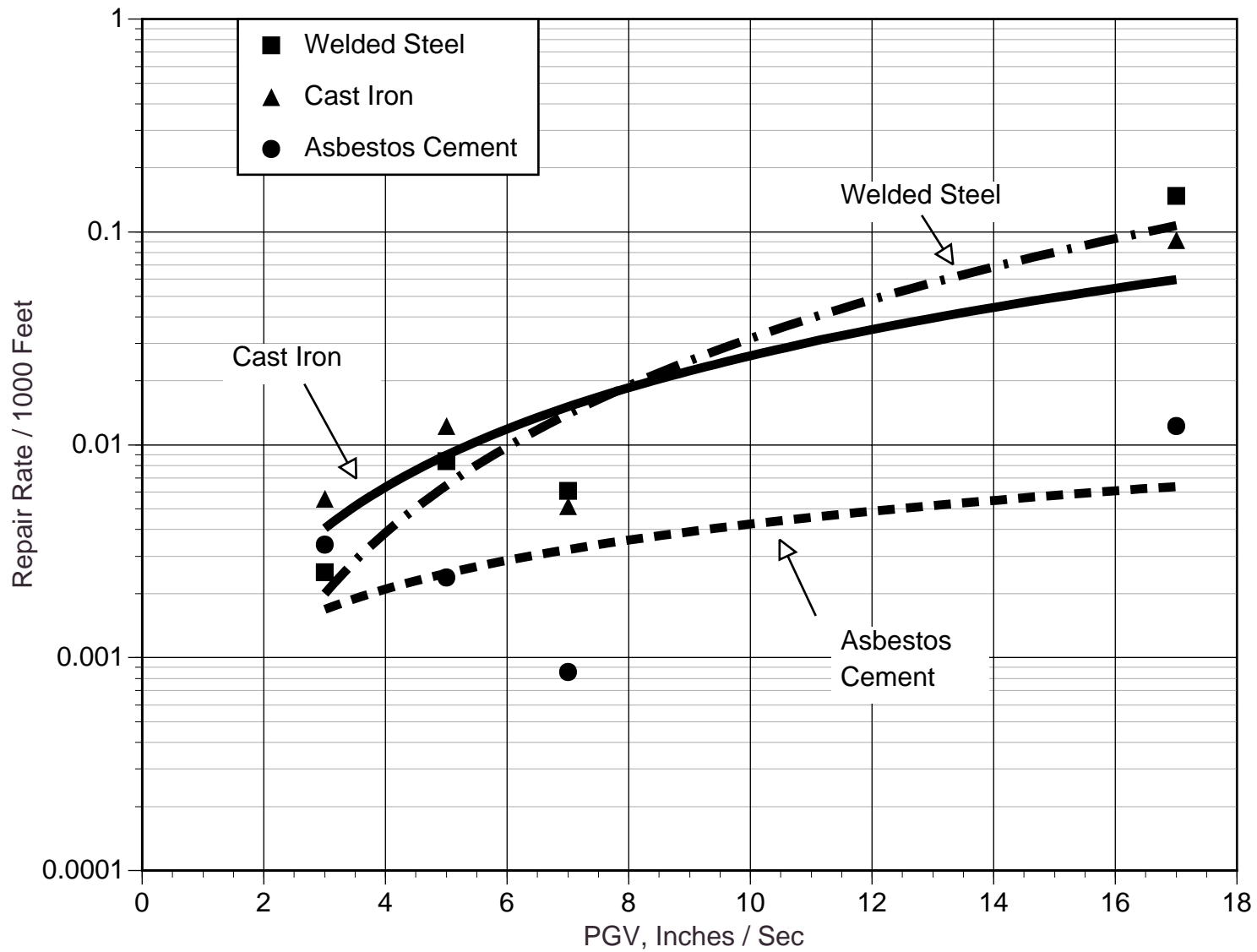
Figure A-10. Repair Rate, Loma Prieta (EBMUD), Ground Shaking, By Material (CI + AC + WS)

R47.01.02 Rev. 0
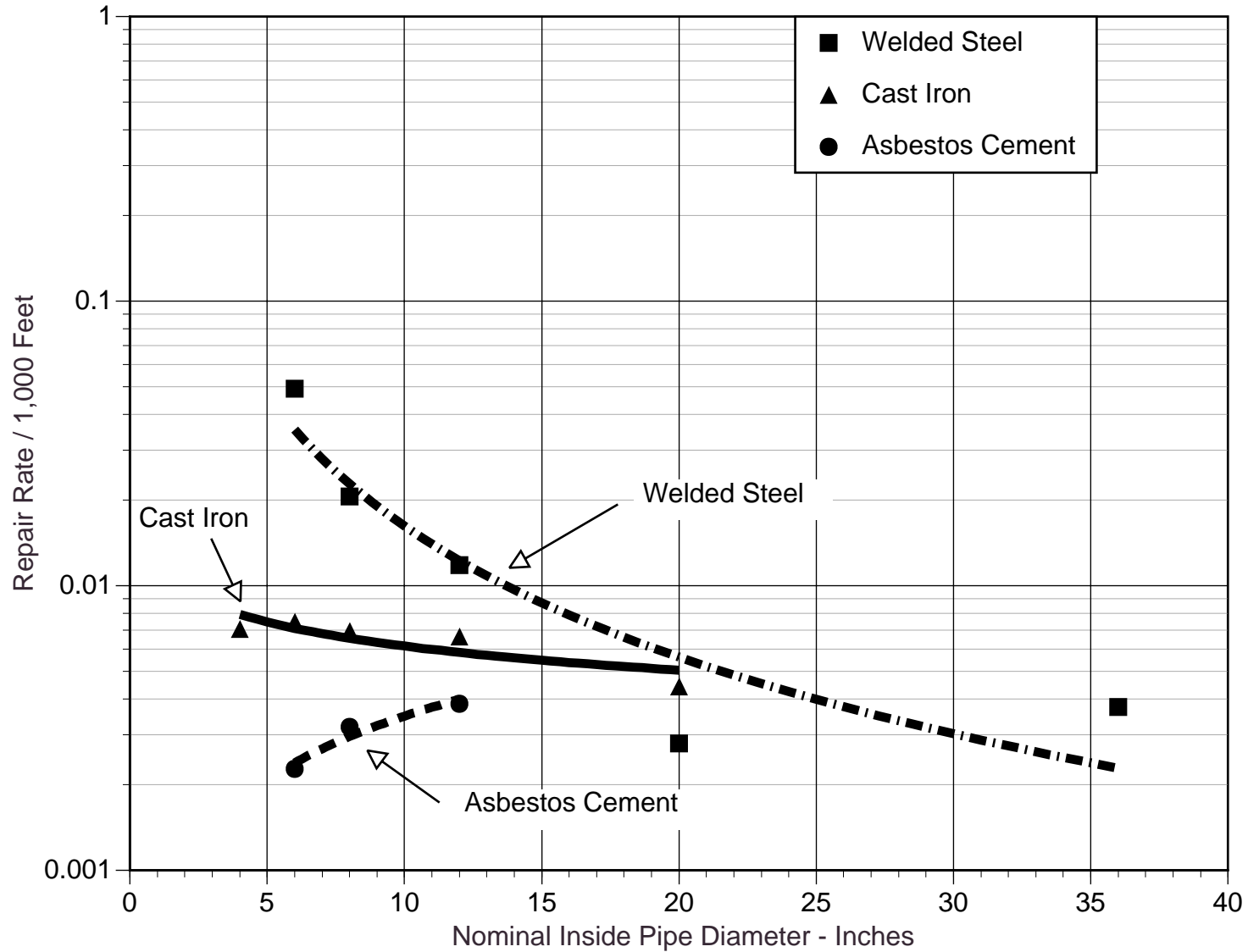
**Figure A-11. Repair Rate - As a Function of
Pipe Diameter, Loma Prieta - EBMUD Data**
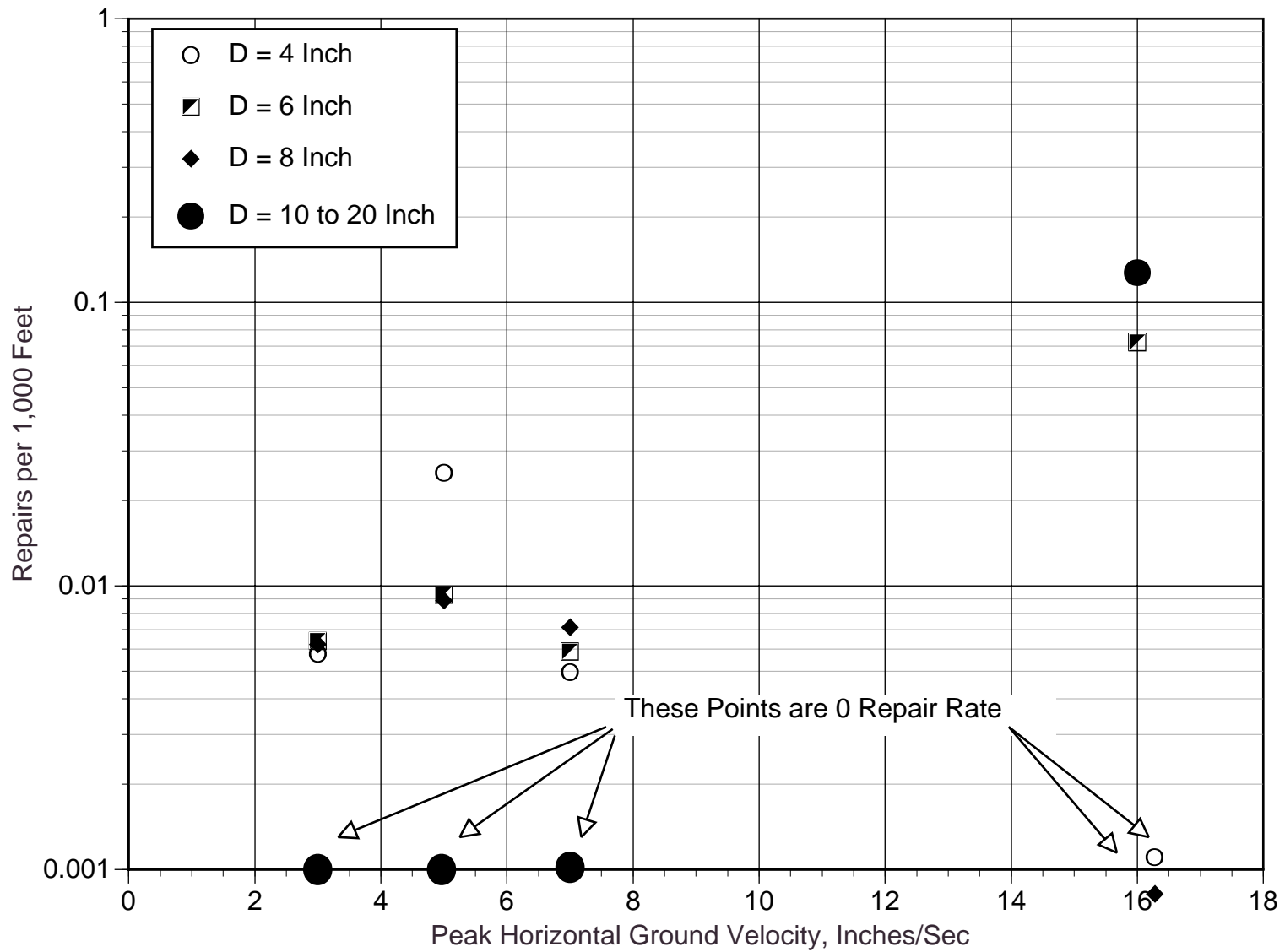
**Figure A-12. Pipe Damage - Wave Propagation -
Cast Iron - Loma Prieta - By Diameter**
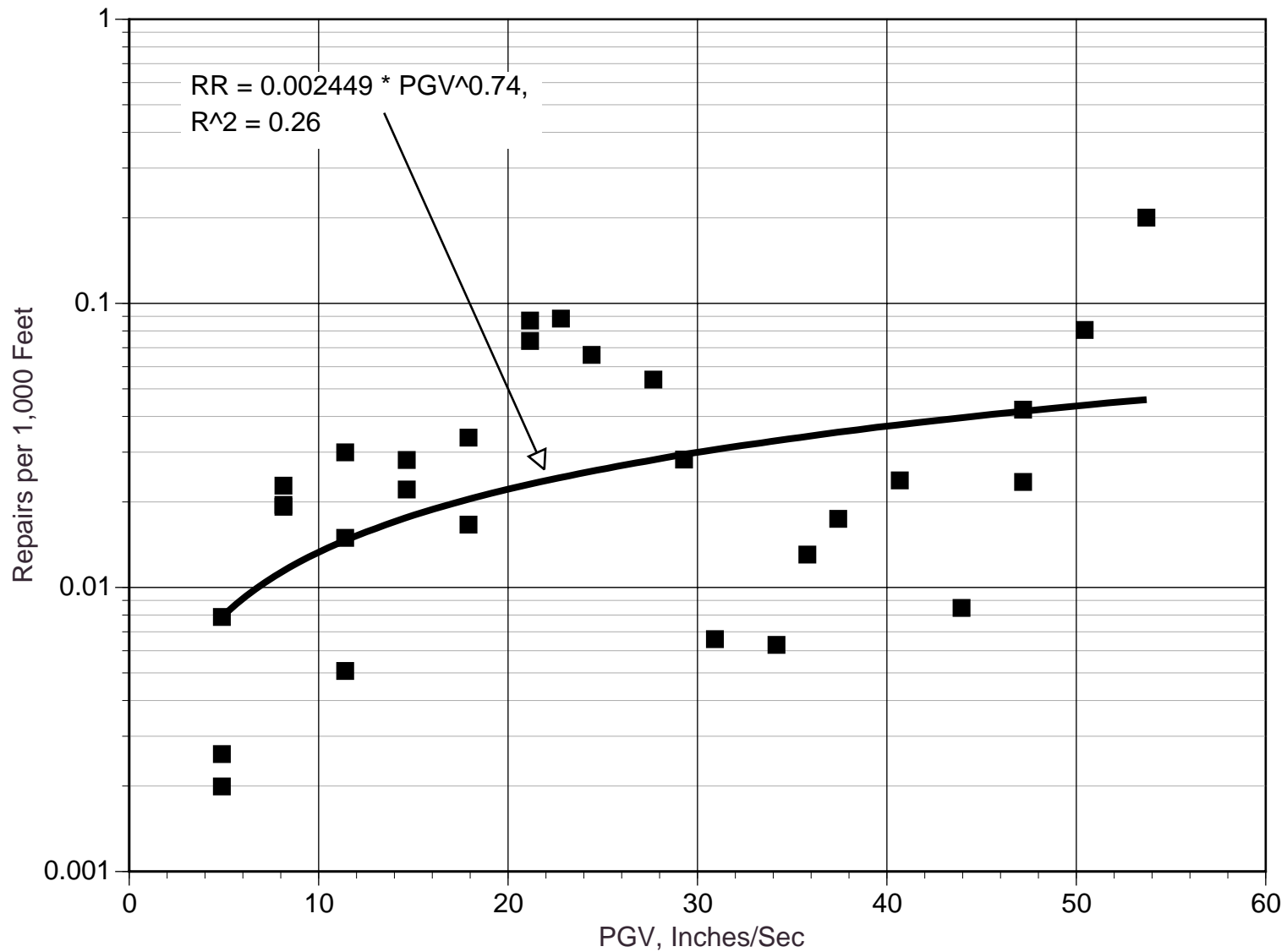
Figure A-13. Repair Rate, Northridge (LADWP), All Materials, Ground Shaking

RR = 0.002449 * PGV^0.74,
R^2 = 0.26
Northridge

RR = 0.000441 * PGV^0.1.54,
R^2 = 0.48
Loma Prieta
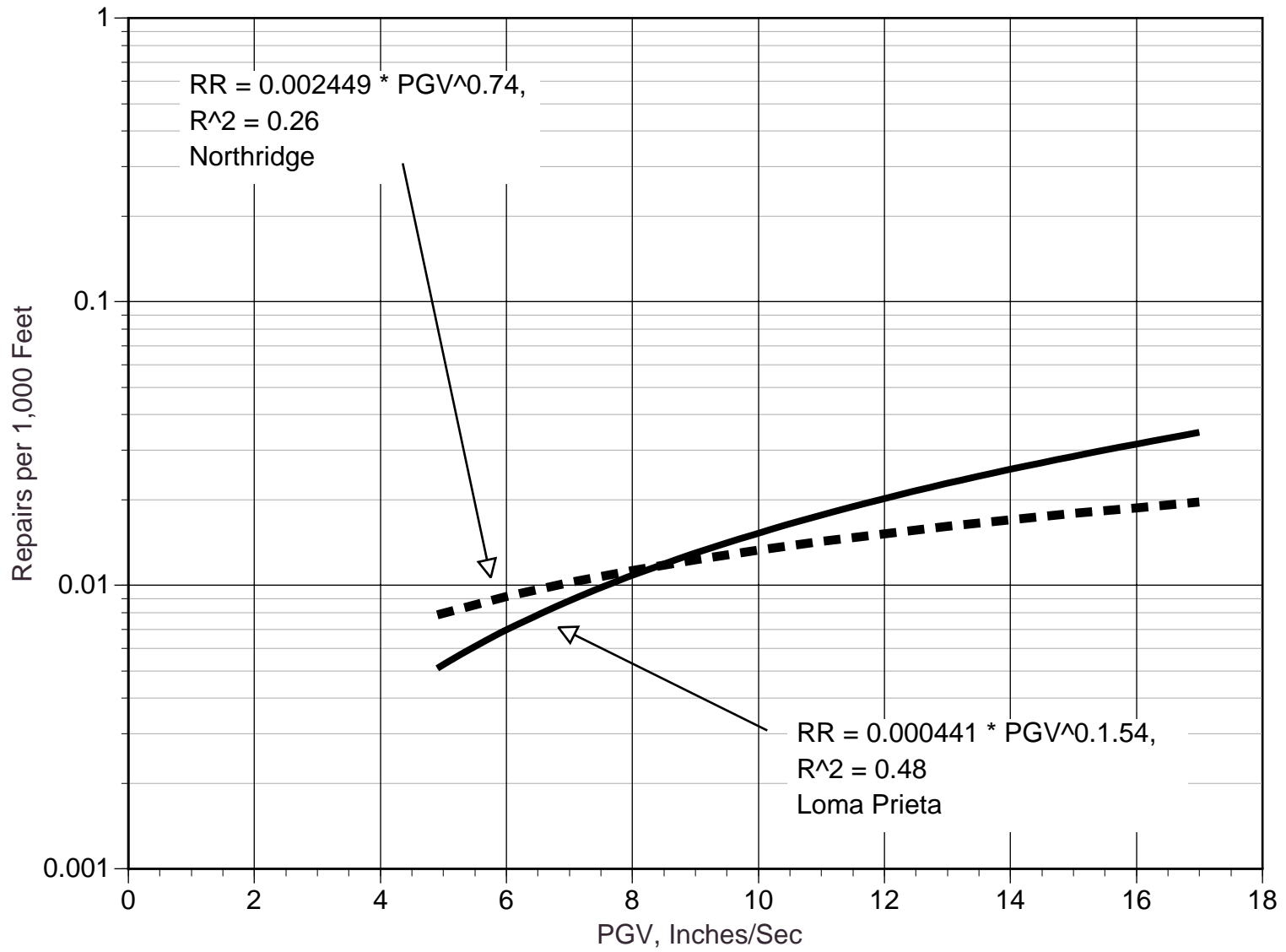
Figure A-14. Repair Rate, Northridge (LADWP) vs. Loma Prieta (EBMUD), all data
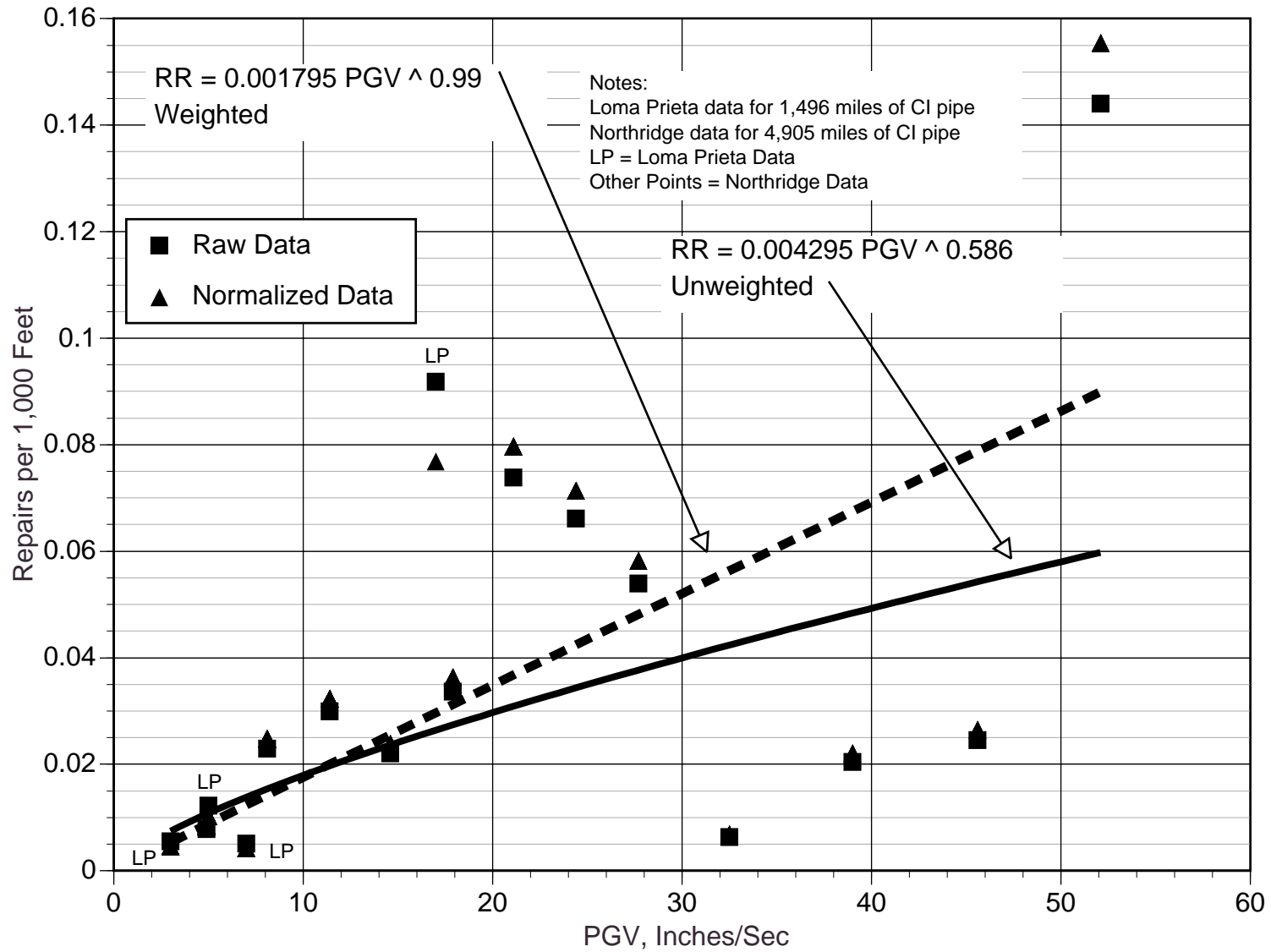
Figure A-15. Repair Rate, Northridge (LADWP) and Loma Prieta (EBMUD), Cast Iron Pipe Only

Raw data: Loma Prieta data includes service repairs, Northridge does not
Raw data: Northridge data excludes certain main repairs due to insufficient attributes
Normalized data: LP data reduced for service repairs, Northridge data increased for missing main repairs

R47.01.02 Rev. 0
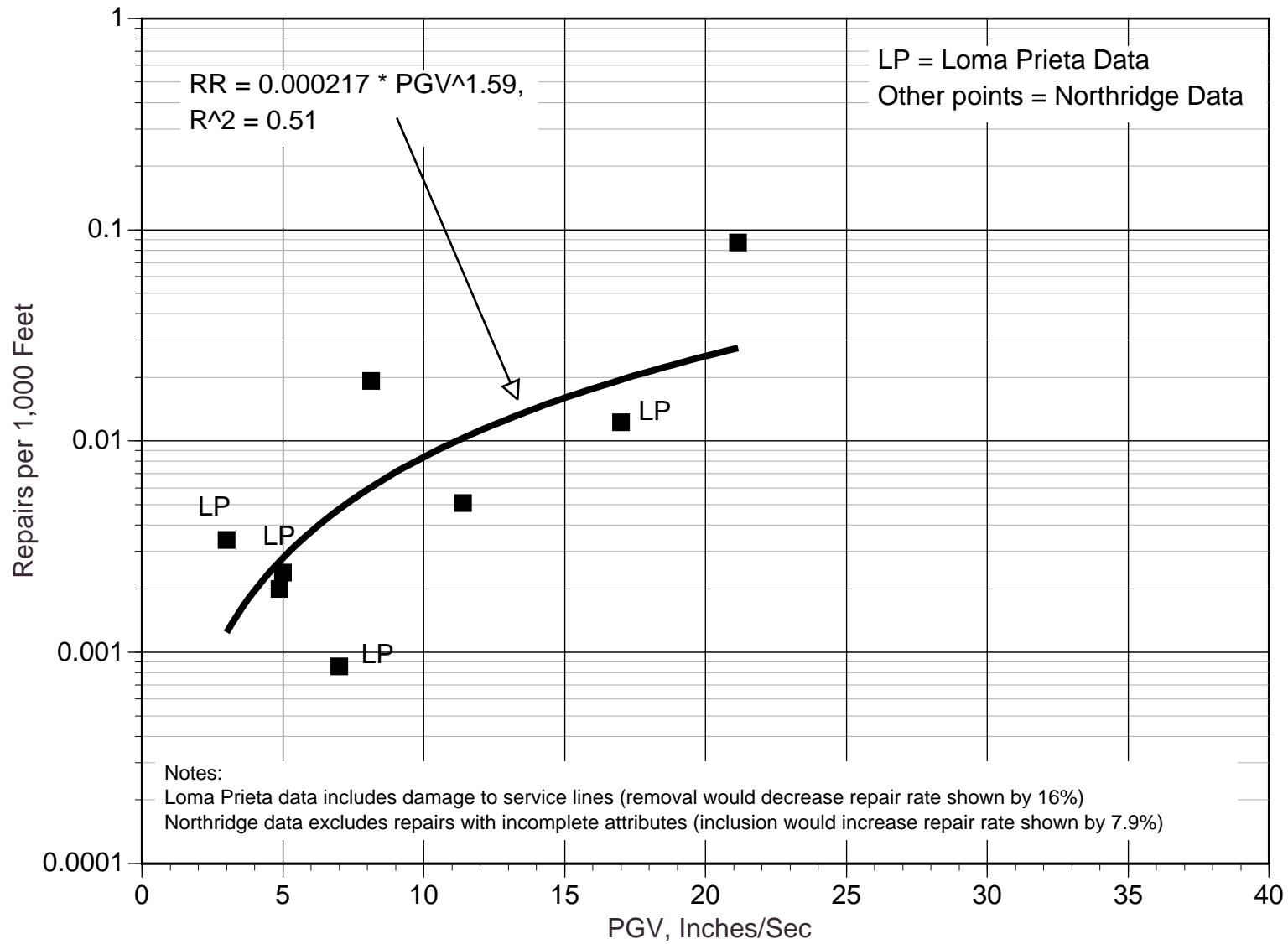
Figure A-16. Repair Rate, Northridge (LADWP) and Loma Prieta (EBMUD), Asbestos Cement Pipe Only

Chart text:

RR = 0.000217 * PGV^1.59, R^2 = 0.51

LP = Loma Prieta Data
Other points = Northridge Data

Y-axis: Repairs per 1,000 Feet

X-axis: PGV, Inches/Sec

Notes:
Loma Prieta data includes damage to service lines (removal would decrease repair rate shown by 16%)
Northridge data excludes repairs with incomplete attributes (inclusion would increase repair rate shown by 7.9%)
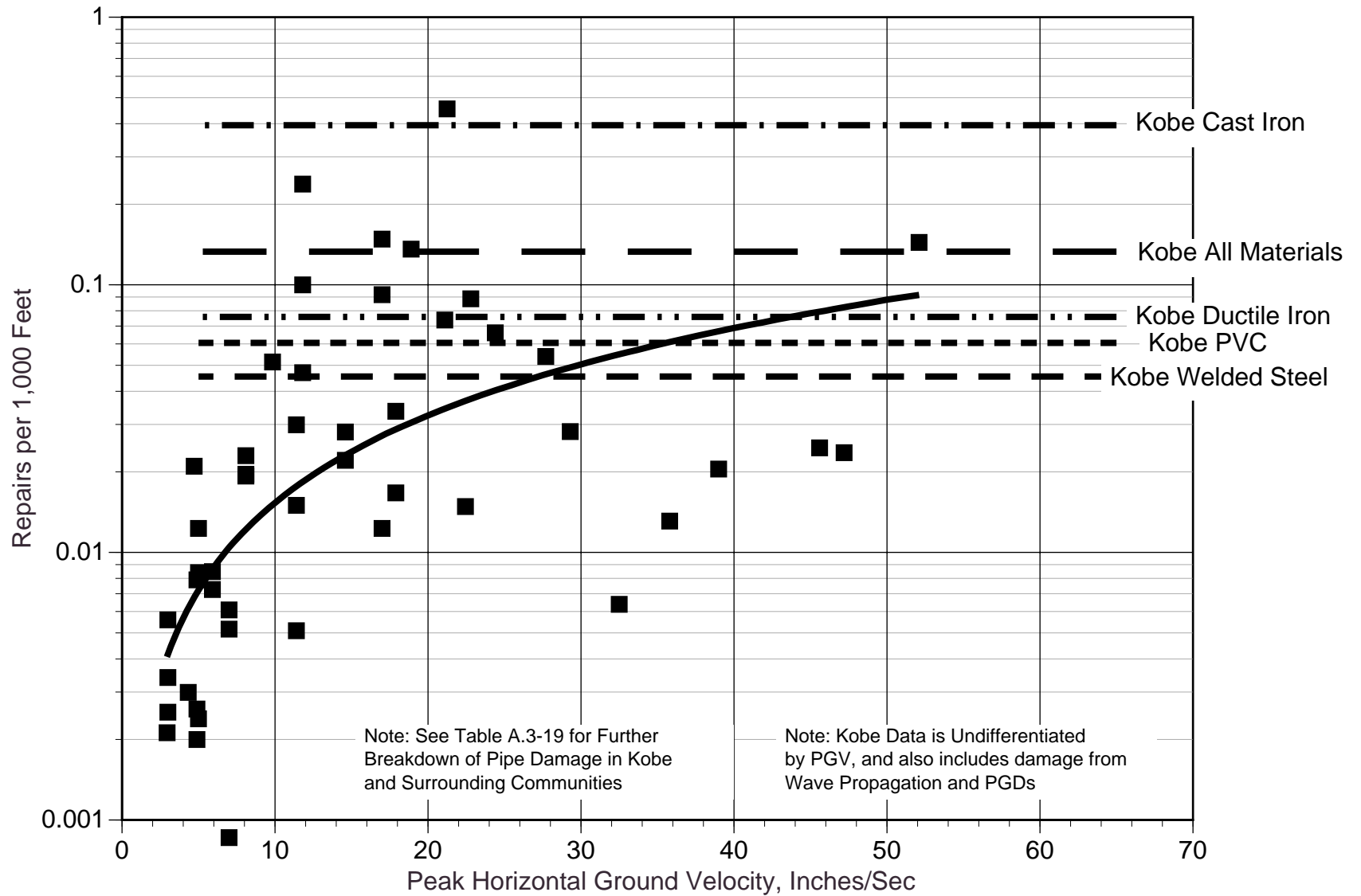
Figure A-17. Pipe Damage - Ground Shaking Data in Tables A.3-4, A.3-14, A.3-15, A.3-16, Figures A-1 and A-2, plus All Data (PGV and PGD) from Kobe, 1995

R47.01.02 Rev. 0

B. Commentary - Tanks

B.1 Damage States for Fragility Curves

In developing the fragility curves presented in Section 5 of the main report, consideration was made to match the fragility curves to match, as close as feasible, to those used in the HAZUS [HAZUS, 1997] computer program. Essentially, this requires the use of five damage states:

- Damage State 1 (DS1): No damage

- DS2: Slight damage

- DS3: Moderate damage

- DS4: Extensive damage

- DS5: Complete (collapse) damage

Section 5.2 of the report provides descriptions of the actual damage states that have been seen or envisioned for on-grade steel tanks. These damage states include:

- Shell buckling (elephant foot buckling)

- Roof damage

- Anchorage failure

- Tank support / column system failure (pertains to elevated tanks)

- Foundation failure (largely a function of soil failures)

- Hydrodynamic pressure failure

- Connecting pipe failure

- Manhole failure

There is an inherent problem with mapping the actual damage states to the HAZUS DS1 through DS5 damage states. The main problem is that the HAZUS damage states have been developed to be used for building type structures, and the same format has been adopted for utility systems.

- For buildings, it is reasonable to assume that increasing damage states also relate to increasing direct damage rates (loss ratios) and decreased functionality. For example, for DS2, a building is in "slight" damage state, and might suffer a 1% to 5% loss (the cost to repair is 1% to 5% of the replacement cost of the building), and suffers almost no functional loss.

- For tanks, the type of damage that occurs could be low cost to repair, but have big impact on functionality; or vice versa. For example, DS=3 in this report means that the tank has suffered elephant foot buckling, but the tank is still leak tight. To repair this type of damage, the owner could replace the buckled lower course of the shell with a

new lower course, which might cost between 20% and 40% of the replacement cost of the entire tank; yet the tank has not lost any immediate post-earthquake functionality. Another damage state, DS=2, could pertain to damage to an attached pipe, which would entail repair costs of only 1% to 2% of the replacement value of the tank; but put the tank completely out of service immediately after the earthquake.

A case can be made that the form of the fragility curves for tanks should be altered from the generic form used in HAZUS. The following improved set of damage states are suggested:

Damage State (Most common damage modes)	Repair Cost as a Percentage of Replacement Cost	Impact on Functionality as a Percentage of Contents Lost Immediately After the Earthquake
Elephant Foot Buckling With Leak	40% to 100%	100%
Elephant Foot buckling with No Leak	30% to 80%	0%
Upper Shell Buckling	10% to 40%	0% to 20%
Roof System Partial Damage	2% to 20%	0% to 10%
Roof System Collapse	5% to 30%	0% to 20%
Rupture of Overflow Pipe	1% to 2%	0% to 2%
Rupture of Inlet / Outlet Pipe	1% to 5%	100%
Rupture of Drain Pipe	1% to 2%	50% to 100%
Rupture of Bottom Plate from Bottom Course	2% to 20%	100%

Table B.1-1. Water Tank Damage States

As can be seen in the above table, there is no direct correlation between repair cost and functionality. As presented in the main report, the damage states are ranked according to increased repair costs for a tank (i.e., DS=2 is for roof damage and pipe damage, generally 1% to 20% loss ratios; DS = 3 is for elephant foot buckling with no leak, generally 40% loss ratio; DS = 4 for elephant foot buckling with leak, generally 40% to 100% loss ratio; and DS=5 is for complete collapse, generally 100% loss ratio.

The use of this document is cautioned that adequate functional performance of a tank which reaches DS=2 is not assured. A review of the empirical tank database (Tables B-8 through B-15) confirms this.

B.2 Replacement Value of Tanks

For cases where the user wishes to make an estimate as to the costs to repair a tank, given it has reached a particular damage state, the following is a rough guideline for the replacement value of water tanks in Year 2000 dollars:

• Tanks under 1,000,000 gallons: $1.50 per gallon

• Tanks from 1,000,000 gallons to 5,000,000 gallons: $1.25 per gallon

• Tanks over 5,000,000 gallons: $1.00 per gallon

• Open cut reservoirs. Open cut reservoirs can vary in volume from 500,000 gallons to over 100,000,000 gallons. Large open cut reservoirs can cost much less, on a per-gallon basis, than tanks.

- Concrete versus steel tanks. Modern tanks are almost always built from either steel or concrete. There are cost differences between the two styles of materials. Concrete tanks can have higher initial capital costs than that for steel tanks, but lower lifetime operational costs. The economic lifetime of concrete or steel tanks is usually in the range of 40 to 75 years. There is unresolved debate in the industry as to which style of tank is "better", and it is beyond the scope of this document to suggest any direction as to which form of tank design is better.

These cost values are geared to hillside tank sites in urbanized areas in California. The costs can often vary by +50% to –50% for specific locations within high density urbanized California. The costs will further vary by regional cost factors for different parts of the country. Examples of regional cost factors are provided in the technical manual for HAZUS [HAZUS, 1999].

B.3 Hazard Parameter for Tank Fragility Curves

The fragility curves presented in Section 5 of the main report use PGA as the predictive parameter for damage to tanks. The choice of PGA was based on the best available parameter from the empirical database. However, engineering properties of tanks would suggest that the following improvements could be made if tank-specific fragility curves are to be developed:

- For damage states associated with tank overturning, elephant foot buckling, etc. Use the 2% spectral ordinate at the impulsive mode of the tank-liquid system, assuming the tank is at the full fill depth. The 2% damping value is recommended as experimental tests suggest that the 2% value more closely matches actual tank-contents motions than the 5% damping assumed in typical code-based design spectra. The site-specific response spectral shape should reflect the soil conditions for the specific tank (rock sites will often have less energy than soil sites at the same frequency, even if the sites have the same PGA).

- For damage states associated with roof damage, etc. Use the 0.5% spectral ordinate at the convective mode of the tank-liquid system, assuming the tank is at the full fill depth. The 0.5% damping value is recommended for fluid sloshing modes. For some tanks with low height to depth ratios, the fluid convective mode may significantly contribute to overturning moment, and a suitable ratio of the impulsive and convective components to overturning should be considered.

- For damage states associated with soil failure at the site. At present time, there is insufficient empirical data to develop fragility curves which relate the performance of tanks to ground settlements, lateral spreads, landslide or surface faulting. These hazards could occur at some sites. Ground failure can impose differential movements for attached pipes leading to pipe failure. The PGD fragility curves provided in HAZUS are based on engineering judgment, and lacking site specific evaluation, appear reasonable.

B.4 Tank Damage – Past Studies and Experience

There are three methods to develop damage algorithms: expert opinion, empirical data, and analysis. In this section, we summarize several previous studies that discuss tank damage using expert opinion (Section B.4.1), or empirical data (Sections B.4.2, B.4.3, B.4.4).

B.4.1 Earthquake Damage Evaluation Data for California

ATC-13 [ATC, 1985] develops damage algorithms for a number of types of structures, including tanks. The damage algorithms in ATC-13 were based on expert opinion. Since the 1985 publication of ATC-13, there has been an expanded body of knowledge about the earthquake performance of tanks, and some of the findings in ATC-13 are outdated. However, it is useful to examine the ATC-13 information, in part as it serves as a point of comparison with more the more current information presented in this report.

ATC-13 provided damage algorithms for 3 categories of liquid storage tanks:

- Underground

- On Ground

- Elevated

For example, the ATC-13 damage algorithm for an On-Ground Tank is as follows:

CDF	MMI=VI PGA=0.12g	VII 0.21g	VIII 0.35g	IX 0.53g	X 0.70g	XI 0.85g	XII 1.15g
0 %	94.0	2.5	0.4				
0.5	6.0	92.9	30.6	2.1			
5		4.6	69.0	94.6	25.7	2.5	0.2
20				3.3	69.3	58.1	27.4
45					5.0	39.1	69.4
80						0.3	3.0
100							

Table B-1. Damage Algorithm – ATC-13 – On Ground Liquid Storage Tank

Explanation of the above table is as follows:

- CDF. Central Damage Factor. This represents the percentage damage to the tank (percent of replacement cost).

- MMI. Modified Mercalli Scale. This represents the input ground shaking intensity to the tank.

- PGA. Peak Ground Acceleration. (g). ATC-13 does not provide damage algorithms versus input PGA. The PGA values in the above table have been added to assist the reader in interpretation of ATC-13 damage algorithms versus those used in the present study. The MMI / PGA relationship listed in Table B-1 represents an average of five researchers MMI / PGA conversion relationships, as described in further detail in [McCann, Sauter and Shah, 1980].

- Damage probabilities. The sum of each column is 100.0%. Table entries with no value have very small probability of occurring, given the input level of shaking (less than 0.1%).

ATC-13 makes no distinction between material types used for construction, whether the tanks are anchored or not, the size or aspect ratio of the tank, or the type of attached appurtenances. The ATC-13 damage algorithms for elevated and buried tanks indicate that elevated tanks are more sensitive to damage than on-grade tanks; and buried tanks are less sensitive to damage than on-grade tanks.

ATC-13 does not provide guidance to relate the cause of damage (like breakage of attached pipes, buckling, weld failures, roof damage, etc.) to the CDF. ATC-13 does not provides guidance as to how CDFs relate to tank functionality.

These limitations in the ATC-13 damage algorithm require the end user to make arbitrary assumptions like: a CDF of 20% or below means the tank is functional (holds water), and a CDF of 45% or above means that the tank is not functional (does not hold water). If this is in fact the rule that the user applies, then the ATC-13 damage algorithm above would say that no tank would become non-functional at any ground motion up to about MMI IX (PGA = 0.53g). This may not be true, and the reader is cautioned not to use the ATC-13 tank damage functions without further consideration of tank-specific features.

An applied version of ATC-13 was developed specifically for water systems by Scawthorne and Khater [1992]. This report uses the same damage algorithms in ATC-13 for water tanks located in the highest seismic regions of California, and makes the following suggestions as to how to apply these damage algorithms for water tanks located in lower seismic hazard areas of the United States:

- For moderate seismic zones (including the west coast of Oregon, Washington State, the Wasatch front area of Utah, etc. Use the damage algorithms in Table 5-1, except shift the MMI scale down by 1. In other words, if the predicted MMI for a particular site was IX, apply the damage algorithm from Table B-1 for MMI X.

- For cases where tanks are to be seismically upgraded (retrofitted). ATC 25-1 suggests using the damage algorithms of Table B-1, except shift the MMI scale up by 1 or 2 intensity units. In other words, if the predicted MMI for a particular site with an upgraded tank was IX, apply the damage algorithm from Table B-1 for MMI VII.

B.4.2 Experience Database for Anchored Steel Tanks in Earthquakes Prior to 1988

Section B.4.2 summarizes the actual observed performance for 43 above ground, anchored liquid storage tanks, due to 11 earthquakes through 1987 [Hashimoto, and Tiong, 1989]. Tables B-2, B-3 and B-20 provide listings and various attributes of the tanks.

Of these 43 tanks, only one tank probably lost its entire fluid contents. The likely cause was failure of a stiff attached pipe that experienced larger seismic displacements after anchor failure.

Other tanks were investigated in this effort, including thin-walled stainless steel tanks and elevated storage tanks. These types of tanks had more failures than for above ground, anchored storage tanks. It should be noted that thin walled stainless steel storage tanks are not commonly used in water system lifelines, but are more common to the wine and milk industries. Tanks excluded from this report include: those with peak ground acceleration (PGA) less than 0.15g; fiberglass tanks; tanks with thin course thickness (< 3/16 inch); tanks with fill less than 50%; and unanchored tanks.

The earthquakes considered include: San Fernando 1971, Managua 1972, Ferndale 1975, Miyagi-ken-oki 1978, Humboldt County, 1980, Greenville, 1980, Coalinga 1983, Chile 1985, Adak 1986, New Zealand 1987, Whittier 1987. Key results are given in Table B-2.

PGA	Total	No Damage	Anchor Damage	Shell Buckling	Minor Leakage at Valve or Pipe	Total Loss of Contents
0.17g-0.20g	12	12	0	0	0	0
0.25g-0.30g	15	14	1	1	0	0
0.35g-0.40g	5	3	2	0	1	1*
0.50g-0.60g	11	7	4	1	1	0
Total	43	36	7	2	2	1

Table B-2. Earthquake Experience Database (Through 1988) for At Grade Steel Tanks

* Note: Total loss of contents was likely due to increased displacements of attached pipe after anchor failure. The tank shell remained intact.

Thin walled stainless steel tanks (wall thickness ≤ 0.1 inch) have behaved poorly in past earthquakes (even if anchored). There have been instances of shell buckling, leakage and even total collapse and rupture. Although damage is much more common than for thicker-walled tanks, leakage and total loss of contents is still infrequent. Even for thin walled tanks, tank shell buckling does not necessarily lead to leakage.

Most of the Table B-2 tanks have diameters between 10 and 30 feet, with heights from between 10 and 50 feet, capacities between 4,400 gallons and 1,750,000 gallons, are made of steel or aluminum, and were at least 50% full at the time of the earthquake. Foundations are believed to be either concrete base mats or concrete ring walls. Known bottom shell course thicknesses range from 3/16 inch to over 5/8 inch.

The tanks in Table B-2 are generally smaller than many water agency storage tanks, which often have capacities greater than 2,000,000 gallons.

Earthquake	Facility	PGA (G)	Component	Capacity (Gallons)
Adak 1986	Fuel Pier Yard	0.20	Small Craft Refuel Tank	315000
Adak 1986	Power Plant # 3	0.20	Tank No. 4	50000
Adak 1986	Power Plant #3	0.20	Tank No. 5	50000
Chile 1985	Las Ventanas Power Plant	0.25		70000*
Chile 1985	Las Ventanas Power Plant	0.25		70000*
Chile 1985	Las Ventanas Power Plant	0.25		70000*
Chile 1985	Las Ventanas Power Plant	0.25	Oil Storage Day Tank	250000*
Chile 1985	Las Ventanas Power Plant	0.25	Oil Storage Day Tank	250000*
Coalinga 1983	Coal.Water Filtration Plant	0.60	Wash Water Tank	300000
Coalinga 1983	Kettleman Gas Compressor Stn	0.20	Lube Oil Fuel Tank #2	7200
Coalinga 1983	Kettleman Gas Compressor Stn	0.20	Lube Oil Fuel Tank #3	7200
Coalinga 1983	Kettleman Gas Compressor Stn	0.20	Lube Oil Fuel Tank #6	7200
Coalinga 1983	Pleasant Valley Pumping Station	0.56	Surge Tank	400000
Coalinga 1983	San Lucas Canal Pmp. Stn 17-R	0.35	Surge Tank	10000
Coalinga 1983	Union Oil Butane Plant	0.60	Diesel Fuel Oil Tank	4400
Coalinga 1983	Union Oil Butane Plant	0.60	Diesel Fuel Oil Tank	4400
Ferndale 1975	Humboldt Bay Unit 3	0.30	Condensate Storage Tank	34500
Ferndale 1980	Humboldt Bay Unit 3	0.25	Condensate Storage Tank	34500
Greenville 1980	Sandia	0.25	Fuel Oil Storage Tank	170000
Managua 1972	Asososca Lake	0.50	Surge Tank	105000*
Miyagi-ken-oki '78	Sendai Refinery	0.28	Fire Water Storage Tank	500000*
New Zealand 1987	Caxton Paper Mill	0.40	Chip Storage Silo	450000*
New Zealand 1987	Caxton Paper Mill	0.40	Hydrogen Peroxide Tank	5700*
New Zealand 1987	Caxton Paper Mill	0.40	Secondary Bleach Tower	50000*
New Zealand 1987	New Zealand Distillery	0.50	Bulk Storage Tank #2	65000*
New Zealand 1987	New Zealand Distillery	0.50	Bulk Storage Tank #5	15000*
New Zealand 1987	New Zealand Distillery	0.50	Bulk Storage Tank #6	15000*
New Zealand 1987	New Zealand Distillery	0.50	Bulk Storage Tank #7	105000*
New Zealand,1987	New Zealand Distillery	0.50	Receiver Tank #9	5700*
New Zealand 1987	Whakatane Board Mills	0.30	Pulp Tank	150000*
New Zealand 1987	Whakatane Board Mills	0.30	Pulp Tank	150000*
New Zealand 1987	Whakatane Board Mills	0.30	Pulp Tank	150000*
San Fernando 1971	Glendale Power Plant	0.28	Distilled Water Tank #1A	14700
San Fernando 1971	Glendale Power Plant	0.28	Distilled Water Tank #1B	14700
San Fernando 1971	Glendale Power Plant	0.28	Distilled Water Tank #2	20000*
San Fernando 1971	Glendale Power Plant	0.28	Fuel Oil Day Tank #1	14700
San Fernando 1971	Jensen Filtration Plant	0.50	Washwater Tank	1750000
San Fernando 1971	Pasadena Power Plant Unit B1	0.20	Distilled Water Tank	120000
San Fernando 1971	Pasadena Power Plant Unit B2	0.20	Distilled Water Tank	120000
San Fernando 1971	Pasadena Power Plant Unit B3	0.20	Distilled Water Tank	86000
Whittier 1987	Pasadena Power Plant Unit B1	0.17	Distilled Water Tank	120000
Whittier 1987	Pasadena Power Plant Unit B2	0.17	Distilled Water Tank	120000
Whittier 1987	Pasadena Power Plant Unit B3	0.17	Distilled Water Tank	86000

Table B-3. Database Tanks (Through 1988)

* Estimated capacity .

The actual tanks that comprise the results given in Table B-2 are the 39 tanks given in Table B-3. Four of these tanks have experienced two earthquakes. No tanks in this database are thin-walled stainless steel (shell thickness < 3/16 inch) or fiberglass tanks. The following paragraphs describe the actual damage for the tanks in Table B-3.

- Jensen Filtration Plant washwater tank, San Fernando, 1971. This tank was 100 feet in diameter, 36.5 feet high, and filled about half full. This tank had twelve 1 inch diameter anchor bolts which were used as tie down points during construction and not as restraints against uplift. Anchor bolt pullout ranged from 1.375 inches to 13 inches. The tank shell buckled at the upper courses, particularly in the vicinity of the stairway. No loss of contents was reported.

- Asososca Lake Water Pumping Plant surge tank, Managua, 1972. This tank was 22 meters high, 5 meters in diameter, and about two-thirds full at the time of the earthquake. The sixteen 1.5 inch diameter anchor bolts stretched between 0.5 inches to 0.75 inches. No loss of contents was reported.

- Sendai Refinery fire water tank, Miyagi-ken-oki 1978. This tank was about 60 feet high and 40 feet in diameter. Anchor bolts stretched or pulled out from 1 to 6 inches. The tank was leaking at a valve after the earthquake, but buckling or rapid loss of contents did not occur. This leakage was probably due to relative displacement of attached piping.

- Sandia National Laboratory fuel oil storage tank, Greenville, 1980. This tank was 50 feet tall, 25 feet in diameter, and full at time of the earthquake. All of the 20, 0.625 inch diameter Wej-it expansion anchors failed. The shell suffered elephant's foot buckling, but did not rupture.

- San Lucas Canal pumping stations surge tanks, Coalinga, 1983. A series of pumping station are distributed along the San Lucas Canal. All of these stations have surge tanks of different designs. Tank diameters typically range from 10 feet to 15 feet, and shell heights vary from 22 feet to 30 feet. The surge tanks are skirt supported with anchorage (probably expansion anchors) bolted through the skirt bottom flange. Various tanks had anchors pulled or broken. At Station 17-R, rocking motion of one surge tank was sufficient to stretch or break most of its anchors. The 24 inch diameter supply/discharge line routed out of the ground into the bottom of this tank reportedly failed. While actual details of this pipe failure are not available, it is probable that a loss of tank contents resulted. An average horizontal PGA of 0.35g has been estimated for the San Lucas Canal pumping stations. This is an average value for all the pumping stations which are distributed along the canal. Since Station 17-R suffered greater damage than other stations, including ground failures, the ground motion experienced was probably greater than the average value of 0.35g.

- Pleasant Valley Pumping Station surge tower, Coalinga, 1983. This tower is 100 feet high and anchored by 1.5 inch diameter J-bolts. An average horizontal PGA of 0.56g was recorded near this station. Because the anchor bolts were equally stretched about 1.5 inches, there is speculation that water hammer in the pipeline feeding this tower caused water to impact the roof with resulting uplift. No loss of contents was reported.

- Coalinga Water Filtration Plant washwater tank, Coalinga 1983. This tank is 60 feet high and 30 feet in diameter, made of A36 steel. Bottom plate is 0.25 inch thick. Fluid height is 45 feet. Anchorage is 24 1.5 inch diameter bolts, A325 steel,

attached by lugs. Shell thickness ranges from 0.375 inch (lowest course) to 0.25 inch (upper course). The foundation is a concrete ring wall. Foundation motion pushed soil away and caused a gap of about 0.5 inches between the southwest and northeast sides of the concrete ring wall and adjacent soil. Some minor leakage, which was not enough to take the tank out of service, was noted at a pipe joint after the earthquake, but was easily stopped by tightening the dresser coupling. Water leakage was observed at the base of the tank. After the earthquake, the tank was drained, the shell to bottom plate welds were sandblasted, and the tank was vacuum tested with no apparent leakage. The water has since been attributed to sources other than tank leakage. The anchor bolts were stretched. They were torqued down after the earthquake and the tank remains functional.

B.4.3 Tank Damage Description in the 1989 Loma Prieta Earthquake

There were numerous reports of damage to liquid storage tanks due to the Loma Prieta 1989 earthquake [EERI, 1990]. Most of the damage was to unanchored storage tanks, at refineries and wineries, with most of the tanks having lost their contents. Content loss was most often due to failures in attached piping, caused by excessive displacements at the tank - pipe connections, due to tank uplifting motions. The following paragraphs describe some tanks that failed with water content loss, which are similar to water system tanks, with the following characteristics: anchored concrete or steel tanks; and unanchored redwood tanks. Thin walled stainless steel tanks are excluded. Typical damage to some unanchored tanks is described.

Concrete Tanks. In the Los Altos hills, a 1,100,000 gallon prestressed concrete tank failed. The tank was built of precast concrete panels, and post tensioned with wire. The outermost surface was gunnite. The earthquake caused a 4 inch vertical crack in the tank wall, which released the water contents. Corrosion in the wires may have contributed to the failure. Estimated ground accelerations were in the 0.25g to 0.35g range.

Wood Tanks. In the San Lorenzo valley, near Santa Cruz, 5 unanchored redwood tanks (10,000 gallons to 150,000 gallons) were lost.   Estimated ground motions were in the 0.20g to 0.40g range.

In the Los Gatos region, a 10,000 gallon redwood tank collapsed. Estimated ground motions were in the 0.10g to 0.30g range.

Near Santa Cruz, 20 unanchored 8,000 gallon oak tanks, at a winery, rocked on unanchored foundations. One tank was damaged after it rocked off its foundation support beams and hit a nearby brick wall. Estimated ground accelerations were in the 0.2g to 0.4g range, for about 10 seconds.

Steel Tanks. At the Moss Landing power plant, there was rapid loss of contents from a 750,000 gallon raw water storage tank. Rupture was at the welded seam of the base plate and shell wall that had been thinned by corrosion. Several dozen other tanks at the Moss Landing plant, ranging from very small, up to 2,000,000 gallons, did not lose their contents. Estimated peak ground acceleration was 0.39g.

At the Hunters Point power plant, there was a small leak at a flange connection to a distilled water tank. Estimated ground acceleration was 0.10g.

In Watsonville, a 1,000,000 gallon welded steel tank, built in 1971, buckled at the roof - shell connection. Electronic water-level-transmitting devices were damaged due to wave action. A pilot line to altitude valve broke, causing a small leak. Overall, the tank did not otherwise leak. There were 9 other tanks at this site that did not leak.

At Sunny Mesa, a 200,000 gallon unanchored welded steel tank tilted, with 2 inch settlement on one side, and base lift-off on the other side. The tank did not leak - however, the attached 8 inch diameter line broke, causing release of the entire tank's contents above the tank outlet.

In Hollister, a 2,000,000 gallon welded steel tank performed well, except that a pulled pipe coupling in a 6 inch diameter line almost drained the tank.

B.4.4 Tank Damage Description in the 1994 Northridge Earthquake

Observations based on a the Los Angeles Department of Water and Power's inspection reports (January 21, 1994) is described below. The inventory of tanks and reservoirs in the entire water system: 13 riveted steel; 38 welded steel; 8 concrete; 9 prestressed concrete; 29 open cut. Note: most of these tanks and reservoirs are located at substantial distances from the zone of highest shaking.

- Tank A. Top panel was slightly buckled, as was the roof. It was uncertain whether the tank leaked its contents, as it was empty at time of inspection. (Steel tank).

- Tank B. Apparent that some seepage occurred at the bottom of the tank. Some tank shell and roof steel plates were slightly buckled. (Steel tank).

- Open Cut Reservoir C. Significant damage to the connections of the roof beams to the walls. (Open cut reservoir).

- Tank D. Tank roof almost completely collapsed. Top course severely bent. Second to top course warped and buckled. Settlement of 6 inches on one side. Inlet and outlet pipes broken.   Some soil erosion around the inlet and outlet pipes, undermining a small portion of the tank. Overflow pipe broken completely free of the outside of the tank shell. Roof debris at the bottom of the tank. Roof debris may include hazardous materials, requiring special disposal. (Steel tank with wood roof).

- Tank E. Tank roof shifted to one side about 10 feet, has partial collapse, but is otherwise largely intact. Shell is structurally sound, but top course buckled in one area. Suspected crack of tank shell to inlet / outlet pipe connection. Possible rupture at the bottom of the tank. Inlet outlet pipe pulled out of its mechanical couplings. A 12-inch gate valve failed. The overflow pipe separated from the tank wall. Severe soil erosion due to loss of water contents.   (Steel tank with wood roof).

- Tank F. All anchor bolts were stretched and hold down plates were bent. The shell was slightly buckled. (Steel tank).

- Tank G. No major structural damage, but the tank was empty at time of inspection. Minor damage at roof joints. No sign of leakage.

- Tank H. A 8-inch gate valve failed and the tank was empty at time of inspection.

- Tank I. A 12-inch gate valve failed. The roof was dislocated from the tank. Roof trusses failed at the center of the tank. The top of the tank buckled at every roof-connection point. The tank was empty at time of inspection.

- Tank J. Tank deflection and settlement severed piping. The slope adjacent to the tank either slid or shows signs of impending slide. All piping, including inlet outlet lines, overflow line severed. This tank apparently suffered a non-leaking elephant foot buckle in the 1971 San Fernando earthquake, and had been kept in service. (Riveted steel tank).

B.4.5 Performance of Petroleum Storage Tanks

In a report for the National Institute of Standards and Technology (NIST), Cooper [1997] examined the performance of steel tanks in 10 earthquakes: 1933 Long Beach, 1952 Kern County, 1964 Alaska, 1971 San Fernando, 1979 Imperial Valley, 1983 Coalinga, 1989 Loma Prieta, 1992 Landers, 1994 Northridge, 1995 Kobe. Most of the tanks were on-grade steel tanks and contained petroleum; a few contained water.

For each of the ten earthquakes, Cooper describes the location of each tank observed; the diameter and height of each tank, and the damage (or no damage) observed. Many pictures are provided of damaged tanks. Where available, instrumented recordings of ground motion are provided.

A numerical analysis of the results from Cooper's data collection is provided in Section B.4.6 below. The more qualitative conclusions of this study are as follows:

- The extent of damage is strongly correlated with the level of fill of the contents. Many oil tanks are only partially filled at any given time. Tanks with low levels of fill appear to suffer less damage than full tanks, all other factors being equal.

- All of the damage modes described in Section B.2 have been observed in these earthquakes.

- As the ratio of the tank height to tank diameter (H / D) increases, the propensity to elephant foot buckle increases. Unanchored tanks with H / D less than 0.5 were not observed to elephant foot buckle.

- Oil tanks with frangible roof / shell joints have often suffered damage, especially those with low H / D ratios. Roof damage is a common damage mode in water tanks, too.

- Small bolted steel tanks with high H/D ratios have not performed well in earthquakes. This may be due to high H / D ratios, thinner wall construction, lack of anchorage, or lack of seismic design in older tanks is not clear.

- Unanchored tanks with low H / D ratios have uplifted in past earthquakes, but have not been damaged. The need to anchor these tanks is questioned.

- Increased thickness annulus rings near the outside of the bottom plate appear to be a good design measure.

- More flexibility is needed to accommodate relative tank / foundation movements for attached pipes.

B.4.6 Statistical Analysis of Tank Performance, 1933-1994

A statistical analysis of on grade steel tanks was reported by O'Rourke and So [1999], which is based on a thesis by So [1999]. The seismic performance for 424 tanks were considered, from the following earthquakes: 1933 Long Beach, 1952 Kern County, 1964 Alaska, 1971 San Fernando, 1979 Imperial Valley, 1983 Coalinga, 1989 Loma Prieta,

1992 Landers, 1994 Northridge. The damage descriptions from Cooper [1997] were used to establish most of the empirical database, with some supplemental material from other sources.

Quantitative attributes were assigned to each database tank, summarized in Table B-4.

Parameter	Range	Median	No. of Tanks
Diameter D, (feet)	10 to 275	62	343
Height H, (feet)	16 to 63	40	343
Percent Full, % Full	0% to 100%	50%	247

Table B-4. Physical Characteristics of Database Tanks (after O'Rourke and So)

Of the 424 tanks in the database, some were missing attributes. Table B-5 lists the tanks from each earthquake.

Event	No. of Tanks Affected	PGA Range (g)	Median PGA (g)	PGA Source
1933 Long Beach	49		0.17	Cooper 1997
1952 Kern County	24		0.19	Cooper 1997
1964 Alaska	26			Not available
1971 San Fernando	20	0.30 to 1.20	0.60	Wald et al 1998
1979 Imperial Valley	24	0.24 to 0.49	0.24	Haroun 1983
1983 Coalinga	38	0.71	0.71	Cooper 1997
1989 Loma Prieta	140	0.11 to 0.54	0.13	Cooper 1997
1992 Landers	33	0.10 to 0.56	0.20	Cooper 1997, Ballantyne and Crouse 1997, Wald et al 1998
1994 Northridge	70	0.30 to 1.00	0.63	Brown et al 1995, Wald et al 1998

Table B-5. Earthquake Characteristics for Tank Database (after O'Rourke and So)

Table B-5 lists the assumed PGA values (or range of values) for the 424 tanks in the database of O'Rourke and So. It is noted that the PGA values used in Table B-5 do not always match the PGA values in Table B-3. For example, for the 8 anchored steel tanks in Table B-3 for the 1983 Coalinga earthquake, tank-specific PGAs ranged from 0.20g to 0.60g; while for the 38 tanks in Table B-5 for the same earthquake, all tanks are assigned a PGA of 0.71g.

Using the data in Table B-5, O'Rourke and So prepared fragility curves using this database using the following procedure:

Each tank was assigned one of five damage states (1, 2, 3, 4, 5). If a tank had multiple types of damage, the damage state with the highest number (most severe) was assigned to the tank. The damage states are as follows:

- Damage state 1: no damage

- Damage state 2: damage to roof, minor loss of content, minor shell damage, damage to attached pipes, no elephant foot failure

- Damage state 3: elephant foot buckling with no leak or minor loss of contents

- Damage state 4: elephant foot buckling with major loss of content, severe damage

- Damage state 5: total failure, tank collapse

Each tank was then assigned into one of 8 PGA bins, ranging from 0.1g to 1.3g.

Using a logistic regression model, a cumulative density function was fitted through the data, which relates PGA versus the probability of reaching or exceeding a particular damage state. O'Rourke and So found that the upward trend of damage is very relevant (i.e., increasing PGA leads to a higher chance of reaching a higher damage state), but there is considerable scatter of the data.

The most relevant dataset for tanks in water distribution systems are for those steel tanks which had fill levels between 50% and 100% of capacity at the time of the earthquake. Table B-6 shows this dataset.

PGA (g)	All Tanks	DS ≥ 1	DS ≥ 2	DS ≥ 3	DS ≥ 4	DS = 5
0.15	28	28	26	8	0	0
0.30	29	29	22	6	1	0
0.45	4	4	2	0	0	0
0.60	37	37	21	8	5	2
0.75	26	26	17	10	4	2
0.90	8	8	3	3	3	0
1.05	1	1	1	1	1	1
Total	133	133	92	36	14	5

Table B-6. Damage Matrix for Steel Tanks with 50% ≤ Full ≤ 100%

Fragility curves were then fitted into this dataset. The fragility curve form is the two parameter fragility model, with the two parameters being the median and a lognormal standard deviation. To fit the two parameters, the median was selected as the 50th percentile PGA value to reach a particular damage state. The lognormal standard deviation was computed by assuming that the cumulative density function value at the 80th percentile fitted the lognormal function. So [1999] found that the goodness of fit (R^2) term of the lognormal distribution function ranged from 0.31 (damage state 2) to 0.83 (damage state 4), indicating that there is a lot of scatter in the data and that the indicator of damage, PGA, may not be an ideal predictor. Given the difficulty in establishing the dataset, the uncertainty involved in selecting the PGA for each tank, omission of key tank design variables (tank wall thickness, for example), is it not surprising that the lognormal fragility curve would not be a "tight" fit to the observed tank performance. However, the form of the fragility curve (median, beta) is the same as used in the HAZUS program, which allows comparisons. The results are in Table B-7.

Damage State	Empirical Median (Fill ≥50%) (g)	Empirical Standard Deviation (β)	HAZUS Unanchored, Near Full Median (g)	HAZUS Unanchored, Near Full Beta (β)	HAZUS Anchored, Near Full Median (g)	HAZUS Anchored, Near Full Beta (β)
DS ≥ 2	0.49	0.55	0.15	0.70	0.30	0.60
DS ≥ 3	0.86	0.39	0.35	0.75	0.70	0.60
DS ≥ 4	0.99	0.27	0.68	0.75	1.25	0.65
DS = 5	1.17	0.21	0.95	0.70	1.60	0.60

Table B-7. Fragility Curves – O'Rourke Empirical Versus HAZUS

It should be noted that the HAZUS fragility curves for DS=2 cover the case with only slight leaks in attached pipes (say to an overflow pipe); while the empirical dataset by O'Rourke and So assume that any pipe damage is in damage state 2 (minor leak or gross pipe break). Also, the HAZUS curves are applicable only for water tanks which are at least 80% full at the time of the earthquake.

The empirical work of O'Rourke and So suggests the following limitations:

- The empirical fragility curves are based on using the PGA. The PGA in the empirical dataset is sometimes the maximum PGA of two horizontal motions, for sites near instrumental recordings, and sometimes based on attenuation models (average PGA of two horizontal motions).

- The empirical dataset includes tanks from 50% full to 100% full, mostly oil tanks, and mostly unanchored tanks. It is common for oil tanks to less than completely full. It is uncommon for water tanks to be less than 80% full (most water tanks are kept between 80% and 100% full, based on time of day). The higher the fill level, the higher the forces and movements in a tank.

- The empirical dataset includes a lot of oil tanks located on soil sites. Many water tanks are located in hillside areas, which are better characterized as rock sites. The difference in spectral shapes for the impulsive and convective mode periods is considerable between rock and soil sites, which would suggest that tanks located on rock sites should perform better than tanks located on soil sites, if both sites are predicted to have the same PGA and all other factors being equal.

B.5 Tank Database

Tables B-8 through B-19 provide the tank database used in the development of the tank fragility data in the main report. The references quoted in these tables can be found in the reference portion of Section 5 of the main report.

Table B-20 provides a summary of the various abbreviations used in these tables.

B.6 Fragility Curve Fitting Procedure

The empirical data in Tables B-8 through B-18 are assembled into one database. Fragility curves are then fitted into this dataset.

Fragilities were developed using the complete tank database as follows:

- First, a subset of the complete database was developed, for only those tanks with the attributes desired. If a particular tank did not have the attribute known, then it was excluded from the analysis.

- Second, the tanks were "binned" into PGA bins. Each bin was for a range of 0.1g, with the exception of 0.71 to 0.90g and 0.91g to 1.20g. The higher g bins were wider, as there were fewer tanks in these PGA ranges. There are 9 bins. The PGA for each bin was set at the average of the PGA values for each tank in that bin. The percent of tanks reaching or exceeding a particular damage state was calculated for each bin.

- Third, a lognormal fragility curve was calculated for each of the four damage state ranges. For example, a fragility curve was calculated for all tanks which reached damage state 2 (DS2) or above, DS3 or above, DS4 or above and DS5. the fragility curve uses two parameters: the median acceleration to reach that damage state or above; and a lognormal dispersion parameter, β. The "best fit" fragility curve was selected by performing a least square regression for all possible fragility curves in the range of A=0.01g to 5.00g (in 0.01g steps) and β=0.01 to 0.80 (in 0.01 steps).

- Since there are an unequal number of tanks in each bin, the analysis was performed using just an unweighted regression analysis (nine data points for the nine bins), and also a weighted regression analysis (the number of data points in each bin reflecting the actual number of tanks in each bin). The weighted analysis is considered a better representation: for example using the data in Table 5-9 of the main report, there are 263 tanks in the 0.16g bin, and just 10 tanks in the 1.18g bin; in the weighted analysis, the 0.16g bin is given about 26 times more weight in the regression analysis.

B.7 Analytical Formulation for Steel Tank Fragility Curves

Section 5.7 of the main report presents representative fragility curves for various classes of water tanks (steel, concrete, wood, elevated). The procedures used to developed analytical (stress based) fragility curves is described in some detail by Bandpadhyay et al [1993] and Kennedy et al [1989] (see Section 5.8 of the main report for references).

Section B.7 provides some examples to show how analytical-based fragility curves can be developed for specific tank geometries.

Example. Steel tank with a wood framed roof (see Figure B-1). The tank is 75 feet in diameter and 32 feet high. Maximum water depth is 31 feet above the base plate, with a maximum capacity of 1 million gallons. The tank wall thickness is sized to achieve a 15,000 psi hoop tensile stress under normal static conditions. The tank is supported in a reinforced concrete ring beam with embedded hold down anchors spaced at 6.5 feet intervals around the circumference of the tank.

The wood framed roof consists of 3/4 inch plywood sheathing supported by 3-by-12 radial joists at 4 feet on center and by 4-by-12 radial beams. The beams are supported by the perimeter of the tank and by interior pipe columns.

The following calculations are based on developing the overturning moment for the tank. Minor adjustments to the calculations to account for inner and outer radius, etc. are left for detailed design. See AWWA D100 [AWWA] for the nomenclature used in this example.

R = 37.5 feet (tank radius)

L = 32 feet (tank height)

H = 31 feet (water height)

t = 0.375 inches (weighted average over height)

E = 29,000 ksi (modulus of elasticity, steel)

rho = 0.490 kcf (density of steel, kip per cubic foot)

H / R = 0.827

t / R = 0.000833

From Figure C.1 of ASCE [1984], ef = 0.05, es = 0.15, ea = 0.465.

For the tank filled with water, the impulsive first mode frequency is 7.1 Hz, following ASCE 1984 procedures. Note that a slightly different frequency would be computed using AWWA D100 simplified rules.

The convective first mode frequency is 0.19 Hz using equation (7-8) of ASCE [1984].

The shell has four equal height courses. Each course is 8 feet high. The bottom course has t = 0.5 inches, the second course has t = 0.375 inches, and the top two courses have t = 0.25 inches. Note that the t to be used in calculating the fundamental impulsive frequency is weighted over the height, with a parabolic weighting function. More detailed analysis can be performed to refine the first mode frequency if the situation warrants.

Note that the top course t need only be 0.104 inches thick, if the shell is designed using hoop stress as the only criteria; some tank owners specify that t = 0.25 inches is the minimum.

The average dead weight of the wood roof is assumed to be 10 pounds per square foot. Wr = 10 psf. Wr = 44.2 kips. Xr = 33 feet.

The dead weight of the tank shell is 0.449 kips per linear foot of circumference. Ws = 0.449 klf. Ws = 105.8 kips. Xs = 13.45 feet.

The weight of water when the tank is full (31 foot depth) is Ww = 1.934 ksf. Ws = 8,546 kips.

The total weight of roof, water and shell Wt = 8,546 kips.

Following AWWA D100:

W1 / Wt = 0.47. X1 / H = 0.38 (impulsive component)

W1 = 4,017 kips, X1 = 11.78 feet

W2 / Wt = 0.51. X2 / H = 0.58 (convective component)

W2 = 4,358 kips. X2 = 17.98 feet.

To establish the overturning moment for purposes of assessing elephant foot buckling, the following assumptions are made.

- A "SRSS" combination of the impulsive and convective components is assumed the be the best fit. Current codes use an absolute sum method, which will generally over predict the true maximum overturning moment by a slight amount.

- The spectral acceleration of the convective mode is assumed to be 10% of the impulsive mode. This is a simplified generalization, and will depend upon actual shape of the response spectra for the tank specific site. However, this simplification is reasonable for many situations, and allows the estimation of overturning moment as a function of only one spectral ordinate.

- For purposes of developing a fragility, the input demand will be the 5% damped spectral ordinate at the impulsive mode frequency.

$$OTM = \sqrt{\left[\frac{S_{ai}}{g}\left(W_s X_s + W_r X_r + W_1 X_1\right)\right]^2 + \left[\frac{S_{ac}}{g}\left(W_2 X_2\right)\right]^2}$$

Using the above values, OTM = 50,810 foot-pounds times (Sai) / (g) where Sai = 5% damped spectral acceleration at the impulsive mode frequency, and g is in the same units as Sai.

Using the allowable compressive stresses for the lowest course shell (t = 0.5 inch) based on AWWA D100 Section 13.3.3.4.1(1991 edition, not the 1996 edition), we get:

fa = 2.14 ksi (ignoring internal water pressure)

delta fc = 5.16 ksi (increase in compressive allowable to reflect internal hoop pressure)

fc = 6.29 ksi (includes the effect of internal hoop pressure, plus 1.33 seismic increase factor)

The overturning moment to reach fc = 6.29 ksi is M = 164,385 kip-feet. As the actual OTM is 50,810 kip-feet for a 1g spectral acceleration at 7.1 Hz, the required spectral acceleration needed to reach the code-limit fc is 3.24g (=164,385 / 50,810).

Table B-21 provides a summary of the various over strength factors and uncertainties that are implied in the above calculations.

Factor	F	βu	βr
F_strength	1.5	0.05	0.05
F_ductility	1.0	0.0	0.0
F_workmanship	1.0	0.15	0.0
F_damping	1.0	0.1	0.1
F_period	1.0	0.2	0.1
F_model	0.75	0.25	0.2
F_total	1.13	0.37	0.25

Table B-21. Probabilistic Factors for Sample Steel Tank – Elephant foot Buckling

F_total is the multiplicative sum of the various items under column F (=1.5 * 1.0 * 1.0 * 1.0 * 1.0 * 0.75 = 1.13). Note that the strength value of 1.5 factors in that the true dynamic buckling capacity is estimated at 50% higher than the code-specified value. The value of 0.75 recognizes that the modeling approach taken here may have underestimated the true seismic forces by 25% (the cantilever beam model is only a crude representation of the complex state of response of a tank shell that is subject to uplift, and may not predict the true highest compressive stress; vertical earthquake issues were ignored, etc.). Also note that in this calculation for elephant foot buckling, there is no obvious analytical justification for the code-specified Rw values from 3.5 to 4.5. The above calculation is to predict the onset of buckling, and there is some margin before a buckle extends far enough to rupture

the steel, which depends on the ductility of the steel, lack of stress discontinuities that would be impacted by the buckle (but note that manhole location in Figure B-1, where a tear could be expected at only moderate buckled deformation), and the dynamic behavior of the tank which would tend to limit the formation of the buckle if the overturning moment is due to high frequency loading.

βu total is the square root of the sum of the squares of the βu column, = 0.37. βr total is the square root of the sum of the squares of the βr column, = 0.25. See Section B.2 for further description. The beta values represent uncertainty and randomness in the calculation above, but assume perfect knowledge of the ground motion response spectra. Beta total (for the tank only) is 0.45, which is the square root of the sum of the squares of βu and βr.

If the ground motion beta is 0.40, and if the user wishes to compute a single overall beta, then βu would increase to 0.55, and the total beta would be βt = 0.60.

The overall fragility curve for this damage state would be: A (median) = 3.65g (5% spectral acceleration) and βt = 0.60.

In a similar manner, this tank should be checked for other damage states such as: roof damage due to water sloshing (tank remains functional but sustains large repair cost); anchor bolt damage due to uplift forces (tank remains functional but sustains small repair cost); bottom plate to bottom course weld damage due to uplift once anchor bolts are stretched / fail (tank is non-functional and sustains moderate repair cost); damage to the top courses of the shell due to excessive roof damage (tank remains partially functional and sustains moderately high repair cost); sliding of the tank which would lead to damage of the attached pipes (tank is non functional and sustains moderate repair cost).

B.8 References

American Water Works Association, Welded Steel Tanks for Water Storage, AWWA Standard D100, Denver, Colorado.

ATC, *Earthquake Damage Evaluation Data for California*, ATC 13, Applied Technology Council, 1985.

Ballantyne, D., Crouse, C., Reliability and Restoration of Water Supply Systems for Fire Suppression and Drinking Following Earthquakes, prepared for National Institute of Standards and Technology, NIST GCR 97-730, 1997.

Bandyopadhyay, K., Cornell, A., Costantino, C., Kennedy, R.P., Miller, C. and Veletsos, A., Seismic Design and Evaluation Guidelines for The Department of energy high-Level Waste Storage Tanks and Appurtenances, Brookhaven National Laboratory, BNL 52361, January, 1993.

Brown, K., Rugar, P., Davis, C., Rulla, T., Seismic Performance of Los Angeles Water Tanks, Lifeline Earthquake Engineering, *in* Proceedings, 4th U.S. Conference, ASCE, TCLEE Monograph No. 6, San Francisco, 1995.

Cooper, T. W., A Study of the Performance of Petroleum Storage Tanks During Earthquakes, 1933 – 1995, prepared for the National Institute of Standards and Technology, Gaithersburg, MD, June, 1997.

EERI, Loma Prieta Reconnaissance Report, Earthquake Spectra, Earthquake Engineering Research Institute, Supplement to Vol. 6, May 1990.

Haroun, M., Behavior of Unanchored Oil Storage Tanks: Imperial Valley Earthquake, Journal of Technical Topics in Civil Engineering, ASCE, Vol. 109, No. 1, April, 1983.

Hashimoto, P.S., and Tiong, L.W., "Earthquake Experience Data on Anchored Ground Mounted Vertical Storage Tanks", EPRI Report NP-6276, March, 1989.

HAZUS, Earthquake Loss Estimation Methodology, National Institute of Building Sciences, prepared by Risk Management Solutions, Menlo Park, CA, 1997.

Kennedy, R. P. and Kassawara, R. P., "Seismic Evaluation of Large Flat-Bottomed Tanks", Second Symposium on Current Issues Related to Nuclear Power Plant Structures, Equipment, and Piping with Emphasis on Resolution of Seismic Issues in Low-Seismicity Regions, EPRI NP-6437-D, May, 1989.

McCann, M., Sauter, F., and Shah, H.C., "A Technical Note on PGA-Intensity Relationship with Applications to Damage Estimation," *BSSA*, Vol. 7, No. 2, pp 631-637, 1980.

O'Rourke, M. and So, P., Seismic Behavior of On-Grade Steel Tanks; Fragility Curves, *in* Optimizing Post-Earthquake Lifeline System Reliability, ed. W. Elliott and P. McDonough, Technical Council on Lifeline Earthquake Engineering, Monograph No. 16, ASCE, August, 1999.

Scawthorne, C., and Khater, M., *A Model Methodology for Assessment of Seismic Vulnerability and Impact of Disruption of Water Supply Systems*, C. Rojahn, Principal Investigator, Applied Technology Council, ATC-25-1, 1992.

So, Pak, Seismic Behavior of On-Grade Steel Tanks; Fragility Curves, thesis submitted to the Graduate Faculty of Rensselaer Polytechnic Institute, RPI, Troy, NY, April 1999.

Wald, J., Quitoriano, V., Heaton, T., Kanamori, H., and Scrivner, C., TRINET Shakemaps: Rapid Generation of Peak Ground Motion and Intensity Maps for Earthquakes in Southern California, Earthquake Spectra, October 1998.

No.	Tank ID	PGA (g)	Diameter, D (m)	Height, H (m)	H / D	H Liq (m)	Pct Full	DS	Damage Observed	Remarks	Tank Anchors	Source
1	A	0.17	28.90	8.80	0.30	8.62	0.98	4	Failed, also oil splashed from top	Riveted. Used same PGA for all Long Beach Tanks. The 0.17g value is from an instrument 29 km from epicenter.	U	Cooper, 1997
2	1 of 3	0.17	28.90	8.80	0.30	4.40	0.50	1	No Damage	Used same PGA for all Long Beach Tanks	U	Cooper, 1997
3	2 of 3	0.17	28.90	8.80	0.30	4.40	0.50	1	NoDamage	Used same PGA for all Long Beach Tanks	U	Cooper, 1997
4	3 of 3	0.17	28.90	8.80	0.30	4.40	0.50	1	No Damage	Used same PGA for all Long Beach Tanks	U	Cooper, 1997
5	B	0.17	U	U	U	U	U	5	Total failure	Riveted. Used same PGA for all Long Beach Tanks	U	Cooper, 1997
6	1 of 43	0.17	U	U	U	U	U	1	No Damage	Used same PGA for all Long Beach Tanks	U	Cooper, 1997
7	2 of 43	0.17	U	U	U	U	U	1	No Damage	Used same PGA for all Long Beach Tanks	U	Cooper, 1997
8	3 of 43	0.17	U	U	U	U	U	1	No Damage	Used same PGA for all Long Beach Tanks	U	Cooper, 1997
9	4 of 43	0.17	U	U	U	U	U	1	No Damage	Used same PGA for all Long Beach Tanks	U	Cooper, 1997
10	5 of 43	0.17	U	U	U	U	U	1	No Damage	Used same PGA for all Long Beach Tanks	U	Cooper, 1997
11	6 of 43	0.17	U	U	U	U	U	1	No Damage	Used same PGA for all Long Beach Tanks	U	Cooper, 1997
12	7 of 43	0.17	U	U	U	U	U	1	No Damage	Used same PGA for all Long Beach Tanks	U	Cooper, 1997
13	8 of 43	0.17	U	U	U	U	U	1	No Damage	Used same PGA for all Long Beach Tanks	U	Cooper, 1997
14	9 of 43	0.17	U	U	U	U	U	1	No Damage	Used same PGA for all Long Beach Tanks	U	Cooper, 1997
15	10 of 43	0.17	U	U	U	U	U	1	No Damage	Used same PGA for all Long Beach Tanks	U	Cooper, 1997
16	11 of 43	0.17	U	U	U	U	U	1	No Damage	Used same PGA for all Long Beach Tanks	U	Cooper, 1997
17	12 of 43	0.17	U	U	U	U	U	1	No Damage	Used same PGA for all Long Beach Tanks	U	Cooper, 1997
18	13 of 43	0.17	U	U	U	U	U	1	No Damage	Used same PGA for all Long Beach Tanks	U	Cooper, 1997
19	14 of 43	0.17	U	U	U	U	U	1	No Damage	Used same PGA for all Long Beach Tanks	U	Cooper, 1997
20	15 of 43	0.17	U	U	U	U	U	1	No Damage	Used same PGA for all Long Beach Tanks	U	Cooper, 1997
21	16 of 43	0.17	U	U	U	U	U	1	No Damage	Used same PGA for all Long Beach Tanks	U	Cooper, 1997
22	17 of 43	0.17	U	U	U	U	U	1	No Damage	Used same PGA for all Long Beach Tanks	U	Cooper, 1997
23	18 of 43	0.17	U	U	U	U	U	1	No Damage	Used same PGA for all Long Beach Tanks	U	Cooper, 1997
24	19 of 43	0.17	U	U	U	U	U	1	No Damage	Used same PGA for all Long Beach Tanks	U	Cooper, 1997
25	20 of 43	0.17	U	U	U	U	U	1	No Damage	Used same PGA for all Long Beach Tanks	U	Cooper, 1997
26	21 of 43	0.17	U	U	U	U	U	1	No Damage	Used same PGA for all Long Beach Tanks	U	Cooper, 1997
27	22 of 43	0.17	U	U	U	U	U	1	No Damage	Used same PGA for all Long Beach Tanks	U	Cooper, 1997
28	23 of 43	0.17	U	U	U	U	U	1	No Damage	Used same PGA for all Long Beach Tanks	U	Cooper, 1997
29	24 of 43	0.17	U	U	U	U	U	1	No Damage	Used same PGA for all Long Beach Tanks	U	Cooper, 1997
30	25 of 43	0.17	U	U	U	U	U	1	No Damage	Used same PGA for all Long Beach Tanks	U	Cooper, 1997
31	26 of 43	0.17	U	U	U	U	U	1	No Damage	Used same PGA for all Long Beach Tanks	U	Cooper, 1997
32	27 of 43	0.17	U	U	U	U	U	1	No Damage	Used same PGA for all Long Beach Tanks	U	Cooper, 1997
33	28 of 43	0.17	U	U	U	U	U	1	No Damage	Used same PGA for all Long Beach Tanks	U	Cooper, 1997
34	29 of 43	0.17	U	U	U	U	U	1	No Damage	Used same PGA for all Long Beach Tanks	U	Cooper, 1997
35	30 of 43	0.17	U	U	U	U	U	1	No Damage	Used same PGA for all Long Beach Tanks	U	Cooper, 1997
36	31 of 43	0.17	U	U	U	U	U	1	No Damage	Used same PGA for all Long Beach Tanks	U	Cooper, 1997
37	32 of 43	0.17	U	U	U	U	U	1	No Damage	Used same PGA for all Long Beach Tanks	U	Cooper, 1997
38	33 of 43	0.17	U	U	U	U	U	1	No Damage	Used same PGA for all Long Beach Tanks	U	Cooper, 1997
39	34 of 43	0.17	U	U	U	U	U	1	No Damage	Used same PGA for all Long Beach Tanks	U	Cooper, 1997
40	35 of 43	0.17	U	U	U	U	U	1	No Damage	Used same PGA for all Long Beach Tanks	U	Cooper, 1997
41	36 of 43	0.17	U	U	U	U	U	1	No Damage	Used same PGA for all Long Beach Tanks	U	Cooper, 1997
42	37 of 43	0.17	U	U	U	U	U	1	No Damage	Used same PGA for all Long Beach Tanks	U	Cooper, 1997
43	38 of 43	0.17	U	U	U	U	U	1	No Damage	Used same PGA for all Long Beach Tanks	U	Cooper, 1997
44	39 of 43	0.17	U	U	U	U	U	1	No Damage	Used same PGA for all Long Beach Tanks	U	Cooper, 1997
45	40 of 43	0.17	U	U	U	U	U	1	No Damage	Used same PGA for all Long Beach Tanks	U	Cooper, 1997
46	41 of 43	0.17	U	U	U	U	U	1	No Damage	Used same PGA for all Long Beach Tanks	U	Cooper, 1997
47	42 of 43	0.17	U	U	U	U	U	1	No Damage	Used same PGA for all Long Beach Tanks	U	Cooper, 1997
48	43 of 43	0.17	U	U	U	U	U	1	No Damage	Used same PGA for all Long Beach Tanks	U	Cooper, 1997
49	C	0.17	45.50	19	0.42	14.5	0.76	4	Damage to upper shell course but no elephant foot buckle. Portions of shell 200 ft from tank after failure	Riveted. Used same PGA for all Long Beach Tanks	U	Cooper, 1997
Comments.												
There is shell / roof damage mentioned in Cooper 1997 but not reflected in the database												
The 0.17g ground motion is from an instrument in Long Beach (location unknown), with 0.2g vertical and only 0.17g known in one horizontal direction												
The damage mode for Tank 49 was listed as "2" by So, but the shell ended up 200 feet from the tank. Changed to 4 (extensive damage, possibly partially salvagable)												
The 0.17g motion might be low for these tanks.												

Table B-8. Long Beach 1933 M6.4

No.	Tank ID	PGA (g)	Diameter, D (m)	Height, H (m)	H / D	H Liq (m)	Pct Full	DS	Damage Observed	Remarks	Tank Anchors	Source
1	550x81	0.19	34.90	9.14	0.26	1.22	0.13	3	Bottom ring bulged 1/4"	Used same PGA for all Kern County Tanks	U	Cooper, 1997
2	550x82	0.19	34.90	9.14	0.26	5.79	0.63	1	No Damage	Used same PGA for all Kern County Tanks	U	Cooper, 1997
3	550x83	0.19	34.90	9.11	0.26	0.79	0.09	2	Earth imprints on bottom edge	Used same PGA for all Kern County Tanks	U	Cooper, 1997
4	550x84	0.19	34.90	9.14	0.26	5.52	0.60	2	Some oil splashed onto top	Used same PGA for all Kern County Tanks	U	Cooper, 1997
5	550x85	0.19	34.90	9.05	0.26	2.87	0.32	1	No Damage	Used same PGA for all Kern County Tanks	U	Cooper, 1997
6	550x86	0.19	34.90	9.08	0.26	8.29	0.91	2	Approx. 15 seals damaged, oil splashed over side, earth imprints by bottom edge	Used same PGA for all Kern County Tanks	U	Cooper, 1997
7	37003	0.19	28.71	9.2	0.32	2.68	0.29	2	Oil splashed onto roof	Used same PGA for all Kern County Tanks	U	Cooper, 1997
8	37014	0.19	28.71	9.14	0.32	5.73	0.63	1	No Damage	Used same PGA for all Kern County Tanks	U	Cooper, 1997
9	550x79	0.19	34.99	9.11	0.26	1.4	0.15	1	No Damage	Used same PGA for all Kern County Tanks	U	Cooper, 1997
10	800x11	0.19	35.72	12.74	0.36	3.08	0.24	1	No Damage	Used same PGA for all Kern County Tanks	U	Cooper, 1997
11	37004	0.19	28.71	9.17	0.32	6.04	0.66	3	Tank settled, lower course budlged, oil splashed on shell	Used same PGA for all Kern County Tanks	U	Cooper, 1997
12	37015	0.19	28.71	9.17	0.32	2.26	0.25	1	No Damage	Used same PGA for all Kern County Tanks	U	Cooper, 1997
13	37005	0.19	28.71	9.17	0.32	6.49	0.71	2	Bottom leaked, oil splaashed over wind girder	Used same PGA for all Kern County Tanks	U	Cooper, 1997
14	37016	0.19	28.71	9.17	0.32	0.73	0.08	1	No Damage	Used same PGA for all Kern County Tanks	U	Cooper, 1997
15	37006	0.19	28.65	9.2	0.32	4.82	0.52	2	Oil splahed onto roof	Used same PGA for all Kern County Tanks	U	Cooper, 1997
16	370x13	0.19	28.93	9.08	0.31	4.82	0.53	2	Earth imprints by bottom edge	Used same PGA for all Kern County Tanks	U	Cooper, 1997
17	55021	0.19	34.93	9.11	0.26	3.78	0.41	1	No Damage	Used same PGA for all Kern County Tanks	U	Cooper, 1997
18	55022	0.19	34.93	9.11	0.26	1.68	0.18	1	No Damage	Used same PGA for all Kern County Tanks	U	Cooper, 1997
19	55047	0.19	34.93	9.14	0.26	0.98	0.11	1	No Damage	Used same PGA for all Kern County Tanks	U	Cooper, 1997
20	80105	0.19	35.69	12.74	0.36	0	0.00	1	No Damage	Used same PGA for all Kern County Tanks	U	Cooper, 1997
21	PG&E 1	0.19	36.60	6.25	0.17	U	U	2	Damage to roof truss	Used same PGA for all Kern County Tanks	U	Cooper, 1997
22	PG&E 2	0.19	23.80	8.93	0.38	U	U	2	Damage to roof truss	Used same PGA for all Kern County Tanks	U	Cooper, 1997
23	PG&E 3	0.19	23.80	13.5	0.57	U	U	2	Seal damage	Used same PGA for all Kern County Tanks	U	Cooper, 1997
24	PG&E 4	0.19	36.60	8.9	0.24	U	U	2	Damage to roof truss	Used same PGA for all Kern County Tanks	U	Cooper, 1997
Comments.												
Most tanks bolted steel or riveted steel (tanks 1 through 20)												
A number of smaller diameter bolted steel tanks either failed in elephant foot buckling, or at least in one case, collapsed and fell over; the collapsed tank was nearly full												
Corrections made for tanks 21, 22, 23,24 for D and H information												
The 0.19g PGA value by So is based on the Taft instrument, located 41 km NW of epicenter												
The Cooper report talks about a lot of other tanks that were damaged in this event, but these are not included in the table												

Table B-9. Kern County 1952 M7.5

No.	Tank ID	PGA (g)	Diameter, D (m)	Height, H (m)	H / D	H Liq (m)	Pct Full	DS	Damage Observed	Remarks	Tank Anchors	Source
1	B	0.20	30.50	9.60	0.31	9.12	1.00	2	Damage to roof, top wall, roof columns		U	Hanson 1973
2	C, Shell Oil at Anchorage airport	0.20	13.70	9.60	0.70	9.12	1.00	4	Damage to roof, top wall, roof rafters, bottom wall buckled EFB		U	Hanson 1973
3	D, Shell Oil at Anchorage Port Area	0.20	36.60	9.60	0.26	9.12	1.00	2	Damage to roof and top shell and columns		U	Hanson 1973
4	E	0.20	36.58	9.75	0.27		0.10	1	No damage		U	Hanson 1973
5	F	0.20	36.60	9.75	0.27		0.10	1	No damage		U	Hanson 1973
6	G-1	0.20	33.50	9.75	0.29		0.10	1	No damage		U	Hanson 1973
7	G-2	0.20	33.50	9.75	0.29		0.10	1	No damage	Assumed almost empty	U	Photo
8	H	0.20	27.40	9.75	0.36	9.12	0.66	1	No damage except to swing joint in floating section		U	Hanson 1973
9	I	0.20	16.70	7	0.42	6.65	1.00	2	Damage to roof rafters and top wall		U	Hanson 1973
10	J	0.20	9.10	12.2	1.34	12.2	1.00	4	Extensive bottom shell buckling, loss of contents		U	Hanson 1973
11	K	0.20	9.10	12.2	1.34	12.2	1.00	4	Extensive bottom shell buckling, loss of contents		U	Hanson 1973
12	L	0.20	9.10	12.2	1.34	12.2	1.00	4	Extensive bottom shell buckling, loss of contents		U	Hanson 1973
13	M, Chevron	0.20	8.50	12.2	1.44	12.2	1.00	5	Collapsed, failed		U	Hanson 1973
14	N	0.20	12.80	12.2	0.95	11.59	0.95	3	Bottom shell buckling		U	Hanson 1973
15	O	0.20	6.10	12.2	2.00	11.59	0.95	4	Bottom shell buckling, broken shell/ bottom weld		U	Hanson 1973
16	P	0.20	43.90	17.1	0.39	16.25	0.95	2	Floating roof buckled, large waves		U	Hanson 1973
17	Q	0.20	34.10	17.1	0.50	16.25	0.95	2	Floating roof pontoon damaged		U	Hanson 1973
18	R	0.20	14.90	14.6	0.98	13.87	0.95	3	Bottom buckled, 12-inch uplift		U	Hanson 1973
19	S	0.20	27.40	14.6	0.53	10.95	0.75	2	3/4 full, roof and roof/shell damage	Over 3/4 full	U	Hanson 1973
20	T	0.20	48.80	17.1	0.35		0.50	2	Support columns twisted and rafters damaged	Assumed 50% full based on damage		Hanson 1973
21	U	0.20	48.80	17.1	0.35		0.50	1	No damage	Assumed 50% full		Hanson 1973
22	R200	0.20	9.10	14.6	1.60	14.6	1.00	5	Water, full, failed	Tank fell over. EFB, bottom plate tore from wall, cone roof ripped off completely	U	Cooper 1997
23	R162	0.20	27.40	14.6	0.53	14.6	1.00	2	Full, cone roof damage no elephant foot		U	Cooper 1997
24	R163	0.20	27.40	14.6	0.53	14.6	1.00	2	Full, cone roof damage no elephant foot		U	Cooper 1997
25	R100	0.20	34.10	17.1	0.50	2.85	0.17	2	Floating roof, 1/6 full, roof damage		U	Cooper 1997
26	R120	0.20	21.30	14.6	0.69	4.87	0.33	2	Floating roof, 1/3 full, roof damage		U	Cooper 1997
27	R110	0.20	43.90	17.1	0.39	11.97	0.50	2	Floating roof, roof damage, 39 feet	Assumed 50% full	U	Cooper 1997
28	R140	0.20	14.90	14.6	0.98	U	0.50	3	Elephant foot buckling, no leak	Assumed 50% full	U	Cooper 1997
29	AA4	0.20	3.20	9.1	2.84	3.03	0.33	1	1/3 full, walked, no damage		U	Cooper 1997
30	AA7	0.20	12.1	13	1.07	U	0.75	4	Severe elephant foot buckling	Assumed .75 full based on damage	U	Cooper 1997
31	AA5	0.20	8.5	12.2	1.44	U	0.75	5	Failed, collapsed	Assumed .75 full based on damage	U	Cooper 1997
32	Army 1	0.30	93	28	0.30		0.7	3	Slight EFB, remained in service. EFB occurred only to non-full tanks	Designed to Z=0.3g. PGA inferred from MMI VII-VIII	UA	Belanger 1973
33	Army 2	0.30	93	28	0.30		0.7	3	Slight EFB, remained in service. EFB occurred only to non-full tanks	Designed to Z=0.3g. PGA inferred from MMI VII-VIII	UA	Belanger 1973
34	Army 3	0.30	93	28	0.30		0.7	3	Slight EFB, remained in service. EFB occurred only to non-full tanks	Designed to Z=0.3g. PGA inferred from MMI VII-VIII	UA	Belanger 1973
35	Army 4	0.30	93	28	0.30		0.7	3	Slight EFB, remained in service. EFB occurred only to non-full tanks	Designed to Z=0.3g. PGA inferred from MMI VII-VIII	UA	Belanger 1973
36	Army 5	0.30	93	28	0.30		0.95	2	Damage to side pipes, sloshing	Designed to Z=0.3g. PGA inferred from MMI VII-VIII	UA	Belanger 1973
37	Army 6	0.30	93	28	0.30		0.95	2	Damage to side pipes	Designed to Z=0.3g. PGA inferred from MMI VII-VIII	UA	Belanger 1973
38	Army 7	0.30	93	28	0.30		0.95	2	Damage to side pipes	Designed to Z=0.3g. PGA inferred from MMI VII-VIII	UA	Belanger 1973
39	Army 8	0.30	93	28	0.30		0.95	2	Damage to side pipes	Designed to Z=0.3g. PGA inferred from MMI VII-VIII	UA	Belanger 1973

Comments
Tanks B - T are in Anchorage area, 130 km from epicenter
Tanks R200 - R140 believed to be Nikiska Refinery. 210 km from epicenter.
Tanks AA are at Anchorage airport
Tanks D, E, F, G are at Anchorage port area, 150 yards from waterfront. 1 in 5 was damaged (Tank G2 based on observation from photo)
Tanks M, N, O are at Anchorage airport area.
PGA ground motion = 0.2g is taken to be the estimated maximum ground acceleration in Anchorage (ref. Hanson, 1973)

Table B-10. Alaska 1964 M8.4

No.	Tank ID	PGA (g)	Diameter, D (m)	Height, H (m)	H / D	H Liq (m)	Pct Full	DS	Damage Observed	Remarks	Tank Anchors	Source
1	MWD Jensen FP Washwater	0.60	31.00	11.00	0.35	5.50	0.58	3	Roof, upper shell damaged due to wrinkling, uplifted 13 inches max based on observed anchor bolt stretch. No efb (Cooper),	Welded steel. Assumed 1/2 to 2/3 full - 50%. PGA from Wald. Anchor bolts were for installation, not for seismic design	A	Cooper 1997, Wald 1998, CDMG 1975
2	OV Hospital	0.60	17.00	12.00	0.71	10.80	0.90	4	Elephant foot buckle, 3 m long floor / shell tear; inlet / outlet piping damage; loss of contents. Roof rafters buckled	Welded steel tank	U	Cooper, Wald
3	Vet Hosp 1	1.20					0.90	2	I/O pipe damage, anchor bolt stretch . Buckled anchorage system	Small Riveted steel tank. Assumed near full	A	Cooper, Wald
4	Vet Hosp 2	1.20					0.90	1	No significant damage	Small Welded steel tank. Assumed near full	U	Cooper, Wald
5	Alta Vista 1, LADWP	1.20	16.60	8.6	0.52	7.74	0.90	2	Damage to inlet / outlet fittings	Riveted steel tank, built 1931	U	Cooper, Wald
6	Alta Vista 2, LADWP	1.20	29.20	11.2	0.38	10.08	0.90	2	Damage to inlet / outlet fittings	Welded Steel Tank, built 1954	U	Cooper, Wald
7	Newhall CWD 1	0.60					0.90	3	Floor plate ruptures and shell buckling	Assumed near full	U	Cooper, Wald
8	Newhall CWD 2	0.60					0.90	3	Floor plate ruptures and shell buckling	Assumed near full	U	Cooper, Wald
9	Mutual Water Co 1	1.20	6.20	6.2	1.00	5.58	0.90	5	Failed	Small bolted tank	U	Cooper, Wald
10	Mutual Water Co 2	1.20	6.20	6.2	1.00	5.58	0.90	5	Failed	Small bolted tank	U	Cooper, Wald
11	Mutual Water Co 3	1.20	6.20	6.2	1.00	5.58	0.90	5	Failed	Small bolted tank	U	Cooper, Wald
12	Mutual Water Co 4	1.20	6.20	6.2	1.00	5.58	0.90	5	Failed	Small bolted tank	U	Cooper, Wald
13	Mutual Water Co 5	1.20	6.20	6.2	1.00	5.58	0.90	5	Failed	Small bolted tank	U	Cooper, Wald
14	Sesnon, LADWP	0.30	28.04	12.8	0.46	12.35	0.96	3	Developed a buckle 7.4 m above the bottom on a 150 degree arc. Uplifted. Damage to wood roof	1" thick bottom course, built 1956	UA	Cooper 1997, Wald 1998, CDMG 1975
15	Granada High, LADWP	0.40	16.77	13.8	0.82	12.42	0.90	2	Roof collapse and shifting of wood roof	Riveted steel, 1929 construction, wood roof	U	Cooper, Wald
16	Newhall 1	0.60	18.50	12.2	0.66	12.2	1.00	3	Elephant foot buckle on one side		U	Cooper, Wald
17	Newhall 2	0.60	18.50	12.2	0.66	12.2	1.00	3	Elephant foot buckle on one side		U	Cooper, Wald
18	Newhall 3	0.60	18.50	12.2	0.66	12.2	1.00	3	Elephant foot buckle on one side		U	Cooper, Wald
19	Newhall 4	0.60	37.00	12.2	0.33		0.90	2	Minor pipe damage	Assumed near full	U	Cooper, Wald
20	Newhall 5	0.60	37.00	12.2	0.33		0.90	2	Minor pipe damage	Assumed near full	U	Cooper, Wald
Comments												
MWDJP. Water tank at Jensen Filter plant (MWD). Fill data corrected from So												
Location of Mutual Water Co is unknown. Why PGA = 1.2g not verified												
Fill Levels for tanks 2, 3, 4, 5, 6, 7, 8, 9, 10,11,12,13, 15 set to 90%, based on normal water system operations procedures (je)												

Table B-11. San Fernando 1971 M6.7

No.	Tank ID	PGA (g)	Diameter, D (m)	Height, H (m)	H / D	H Liq (m)	Pct Full	DS	Damage Observed	Remarks	Tank Anchors	Source
1	IID El Centro 1 of 6	0.49	41.20	13.70	0.33	13.56	0.99	2	Roof damage and spill due to sloshing. Tank may have uplifted	PGA from Haroun	UA	Cooper 1997, Haroun 1983, EERI 1980
2	IID El Centro 2 of 6	0.49	22.30	6.10	0.27	6.04	0.99	1	No damage per EERI 1980	PGA from Haroun	UA	Cooper 1997, Haroun 1983, EERI 1980
3	IID El Centro 3 of 6	0.49	U	U		U		1	No apparent damage. "some" damage reported in EERI, 1980	PGA from Haroun	UA	Cooper 1997, Haroun 1983, EERI 1980
4	IID El Centro 4 of 6	0.49	U	U		U		2	A cracked weld at roof / wall allowed some oil sloshing to leak out	PGA from Haroun	UA	Cooper 1997, Haroun 1983, EERI 1980
5	IID El Centro 5 of 6	0.49	U	U		U		1	No apparent damage. "some" damage reported in EERI, 1980	PGA from Haroun	UA	Cooper 1997, Haroun 1983, EERI 1980
6	IID El Centro 6 of 6	0.49	U	U		U		1	No apparent damage	PGA from Haroun	UA	Cooper 1997, Haroun 1983, EERI 1980
7	IP 1	0.24	24.40	14.6	0.60	6.28	0.43	2	Roof seal damage, broken anti-rotation devi ces, relief piping damage, settlement	PGA from Haroun. Tank built to API 650	UA	Cooper 1997, Haroun 1983
8	IP 2	0.24	24.40	14.6	0.60	7.15	0.49	2	Roof seal damage, broken anti-rotation devi ces, relief piping damage, settlement	PGA from Haroun. Tank built to API 650	UA	Cooper 1997, Haroun 1983
9	IP 3	0.24	20.40	12.3	0.60	4.8	0.39	1	No apparent damage	PGA from Haroun. Tank built to API 650	UA	Cooper 1997, Haroun 1983, EERI 1980
10	IP 4	0.24	14.60	14.6	1.00	7.74	0.53	3	Roof seal damage, broken anti-rotation devi ces, relief piping damage, settlement. Small EFB with no leak	PGA from Haroun. Tank built to API 650	UA	Cooper 1997, Haroun 1983, EERI 1980
11	IP 5	0.24	14.60	14.6	1.00	10.6	0.73	3	Anito rotation devices disconnected; EFB no leak, roof drains leaks, settlement of tank 1 inch	PGA from Haroun. Tank built to API 650	UA	Cooper 1997, Haroun 1983, EERI 1980
12	IP 6	0.24	13.00	12.2	0.94	4.64	0.38	2	Primary seal on floating roof damaged	PGA from Haroun. Tank built to API 650	UA	Cooper 1997, Haroun 1983, EERI 1980
13	IP 7	0.24	13.00	12.2	0.94	4.88	0.40	1	No apparent damage	PGA from Haroun. Tank built to API 650	UA	Cooper 1997, Haroun 1983, EERI 1980
14	IP 8	0.24	24.70	14.6	0.59	11.97	0.82	3	Primary seal on floating roof damaged. Stair platform damaged. Settlement of tank 1 inch, roof drain leaks, leak in tank where floor plates overlap and join shell	PGA from Haroun. Tank built to API 650	UA	Cooper 1997, Haroun 1983, EERI 1980
15	IP 9	0.24	13.00	12.2	0.94	7.93	0.65	2	Roof drain leaks, swingline cable broke	PGA from Haroun. Tank built to API 650	UA	Cooper 1997, Haroun 1983, EERI 1980
16	IP 10	0.24	13.00	12.2	0.94	9.27	0.76	2	Roof drain leaks	PGA from Haroun. Tank built to API 650	UA	Cooper 1997, Haroun 1983, EERI 1980
17	IP 11	0.24	14.20	12.2	0.86	10.49	0.86	2	Relief piping damaged, grounding cable disconnected, settlement of tank 1 to 2 inches, swingline leaking	PGA from Haroun. Tank built to API 650	UA	Cooper 1997, Haroun 1983, EERI 1980
18	IP 12	0.24	13.00	12.2	0.94	10.49	0.86	2	Swingline cable broke, swingline jumped track can caused floating roof to hang, gauge-antirotation pipe broke from floor and bent severely, roof drain leaks	PGA from Haroun. Tank built to API 650	UA	Cooper 1997, Haroun 1983, EERI 1980
19	IP 13	0.24	12.60	14.9	1.18	10.43	0.70	4	Elephant foot buckling 6 to 8 inches outwards over 90 degree arc, shell / bottom separation, relief piping damaged, cracks in epoxy coating on floor, gauge-antirotation pipe broke from floor, floating roof level indicator cable broke	PGA from Haroun. Tank built to API 650. Possibly nearly full per EERI 1980	UA	Cooper 1997, Haroun 1983, EERI 1980
20	IP 14	0.24	14.70	14.9	1.01	9.09	0.61	2	Cracks in concrete ringwall	PGA from Haroun. Tank built to API 650	UA	Cooper 1997, Haroun 1983, EERI 1980
21	IP 15	0.24	15.20	14.9	0.98	9.09	0.61	2	Cracks in concrete ringwall	PGA from Haroun. Tank built to API 650	UA	Cooper 1997, Haroun 1983, EERI 1980
22	IP 16	0.24	14.60	14.6	1.00	12.12	0.83	3	Elephant foot buckling 6 inches outward, no tearing of the bottom plate to bottom course, swingline moutings broke, grounding cable pulled out of ground, relief pipng broke, cracks in concrete ringwall foundation	PGA from Haroun. Tank built to API 650	UA	Cooper 1997, Haroun 1983, EERI 1980
23	IPC-1	0.24	6.50	7.3	1.12	2.19	0.30	1	No apparent damage	PGA from Haroun. Tank built to API 650	UA	Cooper 1997, Haroun 1983, EERI 1980
24	IPC-2	0.24	6.50	7.3	1.12	2.85	0.39	1	No apparent damage	PGA from Haroun. Tank built to API 650	UA	Cooper 1997, Haroun 1983, EERI 1980

Comments
IP 1 to IP 16 are at the SPPL terminal (now SFPPL - Santa Fe Pacific Pipelines). Built 1958 to 1965 with EQ design considerations
IP 13. DS changed from 3 (So) to 4, as the weld separation led to loss of contents
Valley Nitrogen, 20 km from epicenter and 12 km from fault and no significant damage to 4 or 5 tanks at that site (these tanks are not in the above table)
City of El Centro had 2 elevated water steel tanks (150,000 gal and 250,000 gal).
  The smaller tank (built 1940) suffered moderate structural damage to support members and was subsequently emptied, eventually repaired and put back in service.
  The larger tank (250,000 gal, built 1970s) was not damaged, and was 40% full at the time of the earthquake (ref. EERI, Feb 1980 D. Leeds, Ed.)
The Calcot Industries elevated water tank suffered minor damage to diagonal bracing (100,000 gallons, full at time of earthquake), designed 1962.
South of Brawley, a 100,000 gallon elevated steel tank collapsed. The tank was designed and built in 1961 using V = 0.1W.

Table B-12. Imperial valley 1979 M6.5

No.	Tank ID	PGA (g)	Diameter, D (m)	Height, H (m)	H / D	H Liq (m)	Pct Full	DS	Damage Observed	Remarks	Tank Anchors	Source
1	Site A 1	0.47	U	U		U	0.95	2	Roof damage	Large tank	U	Cooper 1997
2	Site A 2	0.47	U	U		U	0.95	2	Roof damage	Large tank	U	Cooper 1997
3	Site A 3	0.47	U	U		U	U	1	No apparent damage	Not full	U	Cooper 1997
4	Site A 4	0.47	U	U		U	U	1	No apparent damage	Not full	U	Cooper 1997
5	Site A 5	0.47	U	U		U	U	1	No apparent damage	Not full	U	Cooper 1997
6	Site A 6	0.47	U	U		U	U	1	No apparent damage	Not full	U	Cooper 1997
7	Site A 7	0.47	U	U		U	U	1	No apparent damage	Not full	U	Cooper 1997
8	Site A 8	0.47	U	U		U	U	1	No apparent damage	Not full	U	Cooper 1997
9	Site A 9	0.47	U	U		U	U	1	No apparent damage	Not full	U	Cooper 1997
10	Site A 10	0.47	U	U		U	U	1	No apparent damage	Not full	U	Cooper 1997
11	Site A 11	0.47	U	U		U	U	1	No apparent damage	Not full	U	Cooper 1997
12	Site A 12	0.47	U	U		U	U	1	No apparent damage	Not full	U	Cooper 1997
13	Site A 13	0.47	U	U		U	U	1	No apparent damage	Not full	U	Cooper 1997
14	Site A 14	0.47	U	U		U	U	1	No apparent damage	Not full	U	Cooper 1997
15	Site A 15	0.47	U	U		U	U	1	No apparent damage	Not full	U	Cooper 1997
16	Site A 16	0.47	U	U		U	U	1	No apparent damage	Not full	U	Cooper 1997
17	Site A 17	0.47	U	U		U	U	1	No apparent damage	Not full	U	Cooper 1997
18	Site A 18	0.47	U	U		U	U	1	No apparent damage	Not full	U	Cooper 1997
19	Site A 19	0.47	U	U		U	U	1	No apparent damage	Not full	U	Cooper 1997
20	Site B 1 of 6	0.57	43.00	14.8	0.34	14.8	1.00	2	Splashing, some roof secondary seal damage	Constructed per API 650, 1956	UA	Cooper 1997
21	Site B 2 of 6	0.57	43.00	14.8	0.34	14.8	1.00	2	Splashing, some roof secondary seal damage	Constructed per API 650, 1956	UA	Cooper 1997
22	Site B 3 of 6	0.57	43.00	14.8	0.34	7.4	0.50	1	No apparent damage	Constructed per API 650, 1956	UA	Cooper 1997
23	Site B 4 of 6	0.57	43.00	14.8	0.34	7.4	0.50	1	No apparent damage	Constructed per API 650, 1956	UA	Cooper 1997
24	Site B 5 of 6	0.57	43.00	14.8	0.34	7.4	0.50	1	No apparent damage	Constructed per API 650, 1956	UA	Cooper 1997
25	Site B 6 of 6	0.57	43	14.8	0.34	0.74	0.05	2	Roof seal damage	Constructed per API 650, 1956	UA	Cooper 1997
26	Site B	0.57	18.5	12	0.65	12	1.00	1	Settled uniformly about 2 inches, but no visible damage	Firewater tank	U	Cooper 1997
27	Site C Tank 7	0.39	61.5	14.8	0.24	10.7	0.72	4	Roof seal damage, oil splashed over top. Tank pounded into foundation 4 inches, uplifted and with steel tear and significant leak of contents where pipe entered through bottom plate. Pipe support moved 4 inches	Built to API 650	UA	Cooper 1997
28	Site C Tank 8	0.39	61.5	14.8	0.24	3	0.20	2	Roof seal damage, wind girder buckled on south side	Built to API 650	UA	Cooper 1997
29	Site C Tank 13	0.39	61.5	14.8	0.24	3	0.20	2	Roof seal damage	Built to API 650	UA	Cooper 1997
30	Site C Tank 13	0.39	61.5	14.8	0.24	3	0.20	2	Roof seal damage	Built to API 650	UA	Cooper 1997
31	Site C	0.39	37	12	0.32	U		3	Slight bulge in bottom course but not elephant foot buckling	Riveted shell, open top, firewater	UA	Cooper 1997
32	Site D 1 of 2	0.70	U	U		U		3	Buckling of top bolted ring	Riveted shell, old	U	Cooper 1997
33	Site D 2 of 2	0.70	U	U		U		2	Broken valves / fittings	Riveted shell, old	U	Cooper 1997
34	Site E 1 of 2	0.62	U	U		U		2	Broken cast iron valves / fittings, pulled Dresser couplings, minor tank settlement	Small Bolted tank	U	Cooper 1997
35	Site E 2 of 2	0.62	U	U		U		2	Broken cast iron valves / fittings, pulled Dresser couplings, minor tank settlement	Small Bolted tank	U	Cooper 1997
36	Site F 1	0.57	34	12	0.35	7.9	0.66	1	No apparent damage	AWWA D100, Built 1971	U	Cooper 1997
37	Site G 1 of 2	0.43	17	10	0.59	7.5	0.75	3	Elephant foot buckling	Bolted steel	U	Cooper 1997
38	Site G 2 of 2	0.43	17	10	0.59	7.5	0.75	3	Elephant foot buckling	Bolted steel	U	Cooper 1997
39	Filter Plant Backwash	0.39	9.14	18.3	2.00	13.71	0.75	2	Minor leaks at outlet pipe due to rocking of tank (possibly not from EQ). Stretched anchor bolts	A36 steel, 0.25" bottom plate, .375" bottom course	A	Hashimoto 1989, EERI 1984
40	Main Tank	0.23					0.50	1	Slight	Southwest of epicenter		EERI 1984
41	East Tank	0.45					0.50	2	Broken CI inlet/outlet pipe	South of epicenter		EERI 1984
Comments												
O'Rourke and So [1999] use PGA = 0.71g, which is average of the peak accelerations given in Cooper (0.6g to 0.82g). PGAs in this table based on attenuation, and to be consistent with Hashimoto [1989]												
Site A had 19 tanks, mostly riveted steel tanks. Site C is mainline pumping station												
Tank 27. DS set to 4 to reflect tear of bottom plate and loss of contents												
Tank 31. DS (2) per So changed to 3 to relfect initiation of elephant foot buckling without leak												
Site G had other bolted steel tanks with leakage at bolt holes and other minor damage												
Sites H and I located 16 km from epicenter (not in table). Damge not extensive at these sites, including sloshing losses and some damage to piping												

Table B-13. Coalinga 1983 M6.7

No.	Tank ID	PGA (g)	Diameter, D (m)	Height, H (m)	H / D	H Liq (m)	Pct Full	DS	Damage Observed	Remarks	Tank Anchors	Source
1	Jackson Oaks	0.50	14.00	8.54	1.00	U	0.95	3	Broken pipe coupling, slight EFB	H/D ratio based on photo	UA	EERI 1985
2	United Technology 1	0.40						2	Tank slid 2-3 inches, rupturing pipes		UA	EERI 1985
3	United Technology 2	0.40						2	Tank slid 2-3 inches, rupturing pipes		UA	EERI 1985
4	Tank 2	0.25						1	No damage	PGA estimated - opposite side of valley	U	EERI 1985
5	Tank 3	0.25						1	No damage	PGA estimated - opposite side of valley	U	EERI 1985
6	Tank 4	0.25						1	No damage	PGA estimated - opposite side of valley	U	EERI 1985
7	Tank 5	0.25						1	No damage	PGA estimated - opposite side of valley	U	EERI 1985
8	Tank 6	0.25						1	No damage	PGA estimated - opposite side of valley	U	EERI 1985
9	Tank 7	0.25						1	No damage	PGA estimated - opposite side of valley	U	EERI 1985
10	Tank 8	0.25						1	No damage	PGA estimated - opposite side of valley	U	EERI 1985
11	Tank 9	0.25						1	No damage	PGA estimated - opposite side of valley	U	EERI 1985
12	Tank 10	0.25						1	No damage	PGA estimated - opposite side of valley	U	EERI 1985
Comments												
The Jackson Oaks tank is one of 10 tanks in the Morgan Hill water system												
Damage to the water system was confined to an area near Jackson Oaks, with the most intense shaking												
Damage to the pipe at the Jackson Tank is assumed to have occurred due to rocking of the tank (likely unanchored)												
The location of the other 9 tanks is presumed more distant from the Calaveras fault, with no reported damage												
United Technologies. PGA estimated from nearby instruments. Tanks located on hillside.												
2 Redwood tanks fell at San Martin winery (PGA about 0.3 - 0.4 g)												
40 of 100 small stainless steel tanks at San Martin wintery were buckled; 13 of these 40 leaked												

Table B-14. Morgan Hill 1984 M6.2

No.	Tank ID	PGA (g)	Diameter, D (m)	Height, H (m)	H / D	H Liq (m)	Pct Full	DS	Damage Observed	Remarks	Tank Anchors	Source
1	Richmond 1	0.13	18.85	15.10	0.80	7.55	0.50	3	Elephant foot buckling, pipe supports pulled from tank shell	Tanks assumed 50% full, average dimensions	U	Cooper 1997
2	Richmond 2	0.13	18.85	15.10	0.80	7.55	0.50	3	Elephant foot buckling, pipe supports pulled from tank shell	Tanks assumed 50% full, average dimensions	U	Cooper 1997
3	Richmond 3	0.13	18.85	15.10	0.80	7.55	0.50	3	Elephant foot buckling, pipe supports pulled from tank shell	Tanks assumed 50% full, average dimensions	U	Cooper 1997
4	Richmond 4	0.13	18.85	15.10	0.80	7.55	0.50	3	Elephant foot buckling, pipe supports pulled from tank shell	Tanks assumed 50% full, average dimensions	U	Cooper 1997
5	Richmond 5	0.13	18.85	15.10	0.80	7.55	0.50	3	Elephant foot buckling, pipe supports pulled from tank shell	Tanks assumed 50% full, average dimensions	U	Cooper 1997
6	Richmond 6	0.13	18.85	15.10	0.80	7.55	0.50	2	Pipe supports pulled from tank shell	Tanks assumed 50% full, average dimensions	U	Cooper 1997
7	Richmond 7	0.13	18.85	15.10	0.80	7.55	0.50	2	Pipe supports pulled from tank shell	Tanks assumed 50% full, average dimensions	U	Cooper 1997
8	Richmond 8	0.13	18.85	15.10	0.80	7.55	0.50	2	Pipe supports pulled from tank shell	Tanks assumed 50% full, average dimensions	U	Cooper 1997
9	Richmond 9	0.13	18.85	15.10	0.80	7.55	0.50	2	Pipe supports pulled from tank shell	Tanks assumed 50% full, average dimensions	U	Cooper 1997
10	Richmond 10	0.13	18.85	15.10	0.80	7.55	0.50	2	Pipe supports pulled from tank shell	Tanks assumed 50% full, average dimensions	U	Cooper 1997
11	Richmond 11	0.13	18.85	15.10	0.80	7.55	0.50	2	Pipe supports pulled from tank shell	Tanks assumed 50% full, average dimensions	U	Cooper 1997
12	Richmond 12	0.13	18.85	15.10	0.80	7.55	0.50	2	Pipe supports pulled from tank shell	Tanks assumed 50% full, average dimensions	U	Cooper 1997
13	Richmond 13	0.13	18.85	15.10	0.80	7.55	0.50	2	Pipe supports pulled from tank shell	Tanks assumed 50% full, average dimensions	U	Cooper 1997
14	Richmond 14	0.13	18.85	15.10	0.80	7.55	0.50	2	Pipe supports pulled from tank shell	Tanks assumed 50% full, average dimensions	U	Cooper 1997
15	Richmond 15	0.13	18.85	15.10	0.80	7.55	0.50	2	Pipe supports pulled from tank shell	Tanks assumed 50% full, average dimensions	U	Cooper 1997
16	Richmond 16	0.13	18.85	15.10	0.80	7.55	0.50	2	Pipe supports pulled from tank shell	Tanks assumed 50% full, average dimensions	U	Cooper 1997
17	Richmond 17	0.13	18.85	15.10	0.80	7.55	0.50	2	Pipe supports pulled from tank shell	Tanks assumed 50% full, average dimensions	U	Cooper 1997
18	Richmond 18	0.13	13.00	12.00	0.92	6.00	0.50	3	Elephant foot buckling	Tanks assumed 50% full, average dimensions	U	Cooper 1997
19	Richmond 19	0.13	13.00	12.00	0.92	6.00	0.50	3	Elephant foot buckling (incipient)	Tanks assumed 50% full, average dimensions	U	Cooper 1997
20	Richmond 20	0.13	13.00	12.00	0.92	6.00	0.50	1	No apparent damage	Tanks assumed 50% full, average dimensions	U	Cooper 1997
21	Lube 1 of 60	0.13	3.70	7.4	2.00	1.85	0.25	1	No apparent damage		UA	Cooper 1997
22	Lube 2 of 60	0.13	3.70	7.4	2.00	1.85	0.25	1	No apparent damage		UA	Cooper 1997
23	Lube 3 of 60	0.13	3.70	7.4	2.00	1.85	0.25	1	No apparent damage		UA	Cooper 1997
24	Lube 4 of 60	0.13	3.70	7.4	2.00	1.85	0.25	1	No apparent damage		UA	Cooper 1997
25	Lube 5 of 60	0.13	3.70	7.4	2.00	1.85	0.25	1	No apparent damage		UA	Cooper 1997
26	Lube 6 of 60	0.13	3.70	7.4	2.00	1.85	0.25	1	No apparent damage		UA	Cooper 1997
27	Lube 7 of 60	0.13	3.70	7.4	2.00	1.85	0.25	1	No apparent damage		UA	Cooper 1997
28	Lube 8 of 60	0.13	3.70	7.4	2.00	1.85	0.25	1	No apparent damage		UA	Cooper 1997
29	Lube 9 of 60	0.13	3.70	7.4	2.00	1.85	0.25	1	No apparent damage		UA	Cooper 1997
30	Lube 10 of 60	0.13	3.70	7.4	2.00	1.85	0.25	1	No apparent damage		UA	Cooper 1997
31	Lube 11 of 60	0.13	3.70	7.4	2.00	1.85	0.25	1	No apparent damage		UA	Cooper 1997
32	Lube 12 of 60	0.13	3.70	7.4	2.00	1.85	0.25	1	No apparent damage		UA	Cooper 1997
33	Lube 13 of 60	0.13	3.70	15.4	4.16	3.85	0.25	2	Anchor bolts restraining and bending bottom plate		A	Cooper 1997
34	Lube 14 of 60	0.13	3.70	15.4	4.16	3.85	0.25	2	Anchor bolts restraining and bending bottom plate		A	Cooper 1997
35	Lube 15 of 60	0.13	3.70	15.4	4.16	3.85	0.25	1	No apparent damage		UA	Cooper 1997
36	Lube 16 of 60	0.13	3.70	15.4	4.16	3.85	0.25	1	No apparent damage		UA	Cooper 1997
37	Lube 17 of 60	0.13	3.70	15.4	4.16	3.85	0.25	1	No apparent damage		UA	Cooper 1997
38	Lube 18 of 60	0.13	3.70	15.4	4.16	3.85	0.25	1	No apparent damage		UA	Cooper 1997
39	Lube 19 of 60	0.13	3.70	15.4	4.16	3.85	0.25	1	No apparent damage		UA	Cooper 1997
40	Lube 20 of 60	0.13	3.70	15.4	4.16	3.85	0.25	1	No apparent damage		UA	Cooper 1997
41	Lube 21 of 60	0.13	3.70	15.4	4.16	3.85	0.25	1	No apparent damage		UA	Cooper 1997
42	Lube 22 of 60	0.13	3.70	15.4	4.16	3.85	0.25	1	No apparent damage		UA	Cooper 1997
43	Lube 23 of 60	0.13	3.70	15.4	4.16	3.85	0.25	1	No apparent damage		UA	Cooper 1997
44	Lube 24 of 60	0.13	3.70	15.4	4.16	3.85	0.25	1	No apparent damage		UA	Cooper 1997
45	Lube 25 of 60	0.13	3.70	11	2.97	2.75	0.25	1	No apparent damage		UA	Cooper 1997
46	Lube 26 of 60	0.13	3.70	11	2.97	2.75	0.25	1	No apparent damage		UA	Cooper 1997
47	Lube 27 of 60	0.13	3.70	11	2.97	2.75	0.25	1	No apparent damage		UA	Cooper 1997
48	Lube 28 of 60	0.13	3.70	11	2.97	2.75	0.25	1	No apparent damage		UA	Cooper 1997
49	Lube 29 of 60	0.13	3.70	11	2.97	2.75	0.25	1	No apparent damage		UA	Cooper 1997
50	Lube 30 of 60	0.13	3.70	11	2.97	2.75	0.25	1	No apparent damage		UA	Cooper 1997
51	Lube 31 of 60	0.13	3.70	11	2.97	2.75	0.25	1	No apparent damage		UA	Cooper 1997
52	Lube 32 of 60	0.13	3.70	11	2.97	2.75	0.25	1	No apparent damage		UA	Cooper 1997
53	Lube 33 of 60	0.13	3.70	11	2.97	2.75	0.25	1	No apparent damage		UA	Cooper 1997
54	Lube 34 of 60	0.13	3.70	11	2.97	2.75	0.25	1	No apparent damage		UA	Cooper 1997
55	Lube 35 of 60	0.13	3.70	11	2.97	2.75	0.25	1	No apparent damage		UA	Cooper 1997
56	Lube 36 of 60	0.13	3.70	11	2.97	2.75	0.25	1	No apparent damage		UA	Cooper 1997
57	Lube 37 of 60	0.13	6.50	12.3	1.89	3.08	0.25	1	No apparent damage		UA	Cooper 1997
58	Lube 38 of 60	0.13	6.50	12.3	1.89	3.08	0.25	1	No apparent damage		UA	Cooper 1997
59	Lube 39 of 60	0.13	6.50	12.3	1.89	3.08	0.25	1	No apparent damage		UA	Cooper 1997

Table B-15. Loma Prieta 1989 M7, (Page 1 of 3)

No.	Tank ID	PGA (g)	Diameter, D (m)	Height, H (m)	H / D	H Liq (m)	Pct Full	DS	Damage Observed	Remarks	Tank Anchors	Source
60	Lube 40 of 60	0.13	6.50	12.3	1.89	3.08	0.25	1	No apparent damage		UA	Cooper 1997
61	Lube 41 of 60	0.13	6.50	12.3	1.89	3.08	0.25	1	No apparent damage		UA	Cooper 1997
62	Lube 42 of 60	0.13	6.50	12.3	1.89	3.08	0.25	1	No apparent damage		UA	Cooper 1997
63	Lube 43 of 60	0.13	6.50	12.3	1.89	3.08	0.25	1	No apparent damage		UA	Cooper 1997
64	Lube 44 of 60	0.13	6.50	12.3	1.89	3.08	0.25	1	No apparent damage		UA	Cooper 1997
65	Lube 45 of 60	0.13	6.50	12.3	1.89	3.08	0.25	1	No apparent damage		UA	Cooper 1997
66	Lube 46 of 60	0.13	6.50	12.3	1.89	3.08	0.25	1	No apparent damage		UA	Cooper 1997
67	Lube 47 of 60	0.13	6.50	12.3	1.89	3.08	0.25	1	No apparent damage		UA	Cooper 1997
68	Lube 48 of 60	0.13	6.50	12.3	1.89	3.08	0.25	1	No apparent damage		UA	Cooper 1997
69	Lube 49 of 60	0.13	9.20	12.3	1.34	3.08	0.25	1	No apparent damage		UA	Cooper 1997
70	Lube 50 of 60	0.13	9.20	12.3	1.34	3.08	0.25	1	No apparent damage		UA	Cooper 1997
71	Lube 51 of 60	0.13	9.20	12.3	1.34	3.08	0.25	1	No apparent damage		UA	Cooper 1997
72	Lube 52 of 60	0.13	9.20	12.3	1.34	3.08	0.25	1	No apparent damage		UA	Cooper 1997
73	Lube 53 of 60	0.13	9.20	12.3	1.34	3.08	0.25	1	No apparent damage		UA	Cooper 1997
74	Lube 54 of 60	0.13	9.20	12.3	1.34	3.08	0.25	1	No apparent damage		UA	Cooper 1997
75	Lube 55 of 60	0.13	9.20	12.3	1.34	3.08	0.25	1	No apparent damage		UA	Cooper 1997
76	Lube 56 of 60	0.13	9.20	12.3	1.34	3.08	0.25	1	No apparent damage		UA	Cooper 1997
77	Lube 57 of 60	0.13	9.20	12.3	1.34	3.08	0.25	1	No apparent damage		UA	Cooper 1997
78	Lube 58 of 60	0.13	9.20	12.3	1.34	3.08	0.25	1	No apparent damage		UA	Cooper 1997
79	Lube 59 of 60	0.13	9.20	12.3	1.34	3.08	0.25	1	No apparent damage		UA	Cooper 1997
80	Lube 60 of 60	0.13	9.20	12.3	1.34	12.3	1.00	3	Elephant foot buckling. Walkway between this tank and another pulled loose and fell to ground		UA	Cooper 1997
81	San Jose 1 of 32	0.17	23.7	14.8	0.62	14.06	0.95	2	Severe bending and buckling of internal pan	Assumed nearly full	U	Cooper 1997
82	San Jose 2 of 32	0.17	27	14.6	0.54	14.06	0.96	2	Severe bending and buckling of internal pan	Assumed nearly full	U	Cooper 1997
83	San Jose 3 of 32	0.17	19.8	14.6	0.74	U		1	No apparent damage		U	Cooper 1997
84	San Jose 4 of 32	0.17	19.8	14.6	0.74	U		1	No apparent damage		U	Cooper 1997
85	San Jose 5 of 32	0.17	19.8	14.6	0.74	U		1	No apparent damage		U	Cooper 1997
86	San Jose 6 of 32	0.17	19.8	14.6	0.74	U		1	No apparent damage		U	Cooper 1997
87	San Jose 7 of 32	0.17	19.8	14.6	0.74	U		1	No apparent damage		U	Cooper 1997
88	San Jose 8 of 32	0.17	19.8	14.6	0.74	U		1	No apparent damage		U	Cooper 1997
89	San Jose 9 of 32	0.17	19.8	14.6	0.74	U		1	No apparent damage		U	Cooper 1997
90	San Jose 10 of 32	0.17	19.8	14.6	0.74	U		1	No apparent damage		U	Cooper 1997
91	San Jose 11 of 32	0.17	19.8	14.6	0.74	U		1	No apparent damage		U	Cooper 1997
92	San Jose 12 of 32	0.17	19.8	14.6	0.74	U		1	No apparent damage		U	Cooper 1997
93	San Jose 13 of 32	0.17	19.8	14.6	0.74	U		1	No apparent damage		U	Cooper 1997
94	San Jose 14 of 32	0.17	19.8	14.6	0.74	U		1	No apparent damage		U	Cooper 1997
95	San Jose 15 of 32	0.17	19.8	14.6	0.74	U		1	No apparent damage		U	Cooper 1997
96	San Jose 16 of 32	0.17	19.8	14.6	0.74	U		1	No apparent damage		U	Cooper 1997
97	San Jose 17 of 32	0.17	19.8	14.6	0.74	U		1	No apparent damage		U	Cooper 1997
98	San Jose 18 of 32	0.17	19.8	14.6	0.74	U		1	No apparent damage		U	Cooper 1997
99	San Jose 19 of 32	0.17	19.8	14.6	0.74	U		1	No apparent damage		U	Cooper 1997
100	San Jose 20 of 32	0.17	19.8	14.6	0.74	U		1	No apparent damage		U	Cooper 1997
101	San Jose 21 of 32	0.17	19.8	14.6	0.74	U		1	No apparent damage		U	Cooper 1997
102	San Jose 22 of 32	0.17	19.8	14.6	0.74	U		1	No apparent damage		U	Cooper 1997
103	San Jose 23 of 32	0.17	19.8	14.6	0.74	U		1	No apparent damage		U	Cooper 1997
104	San Jose 24 of 32	0.17	19.8	14.6	0.74	U		1	No apparent damage		U	Cooper 1997
105	San Jose 25 of 32	0.17	19.8	14.6	0.74	U		1	No apparent damage		U	Cooper 1997
106	San Jose 26 of 32	0.17	19.8	14.6	0.74	U		1	No apparent damage		U	Cooper 1997
107	San Jose 27 of 32	0.17	19.8	14.6	0.74	U		1	No apparent damage		U	Cooper 1997
108	San Jose 28 of 32	0.17	19.8	14.6	0.74	U		1	No apparent damage		U	Cooper 1997
109	San Jose 29 of 32	0.17	19.8	14.6	0.74	U		1	No apparent damage		U	Cooper 1997
110	San Jose 30 of 32	0.17	19.8	14.6	0.74	U		1	No apparent damage		U	Cooper 1997
111	San Jose 31 of 32	0.17	19.8	14.6	0.74	U		1	No apparent damage		U	Cooper 1997
112	San Jose 32 of 32	0.17	19.8	14.6	0.74	U		1	No apparent damage		U	Cooper 1997
113	Brisbane 1 of 17	0.11	19.8	13.5	0.68	U		1	No apparent damage		U	Cooper 1997
114	Brisbane 2 of 17	0.11	19.8	13.5	0.68	U		1	No apparent damage		U	Cooper 1997
115	Brisbane 3 of 17	0.11	19.8	13.5	0.68	U		1	No apparent damage		U	Cooper 1997
116	Brisbane 4 of 17	0.11	19.8	13.5	0.68	U		1	No apparent damage		U	Cooper 1997
117	Brisbane 5 of 17	0.11	19.8	13.5	0.68	U		1	No apparent damage		U	Cooper 1997

Table B-15. Loma Prieta 1989 M7, (Page 2 of 3)

No.	Tank ID	PGA (g)	Diameter, D (m)	Height, H (m)	H / D	H Liq (m)	Pct Full	DS	Damage Observed	Remarks	Tank Anchors	Source
118	Brisbane 6 of 17	0.11	19.8	13.5	0.68	U		1	No apparent damage		U	Cooper 1997
119	Brisbane 7 of 17	0.11	19.8	13.5	0.68	U		1	No apparent damage		U	Cooper 1997
120	Brisbane 8 of 17	0.11	19.8	13.5	0.68	U		1	No apparent damage		U	Cooper 1997
121	Brisbane 9 of 17	0.11	19.8	13.5	0.68	U		1	No apparent damage		U	Cooper 1997
122	Brisbane 10 of 17	0.11	19.8	13.5	0.68	U		1	No apparent damage		U	Cooper 1997
123	Brisbane 11 of 17	0.11	19.8	13.5	0.68	U		1	No apparent damage		U	Cooper 1997
124	Brisbane 12 of 17	0.11	19.8	13.5	0.68	U		1	No apparent damage		U	Cooper 1997
125	Brisbane 13 of 17	0.11	19.8	13.5	0.68	U		1	No apparent damage		U	Cooper 1997
126	Brisbane 14 of 17	0.11	19.8	13.5	0.68	U		1	No apparent damage		U	Cooper 1997
127	Brisbane 15 of 17	0.11	19.8	13.5	0.68	U		1	No apparent damage		U	Cooper 1997
128	Brisbane 16 of 17	0.11	19.8	13.5	0.68	U		1	No apparent damage		U	Cooper 1997
129	Brisbane 17 of 17	0.11	19.8	13.5	0.68	U		1	No apparent damage		U	Cooper 1997
130	Gilroy 1	0.50	24.4	8	0.33	U	0.95	1	No apparent damage	Water tank assumed nearly full		Cooper 1997
131	PG&E Moss Landing 1	0.24	17	12.2	0.72	U	0.9	4	Failed at floor / shell connection. Junction possibly corroded. Tank drained rapidly. Top shell course buckled	Tank assumed mostly full. Pga based on attenuation	UA	Cooper 1997, USGS 1998
132	PG&E Moss Landing Distilled 1	0.24	17	12.2	0.72	U	0.9	2	failure of pipe couplings	dimensions assumed. PGA based on attenuation	U	Cooper 1997, USGS 1998
133	PG&E Moss Landing Distilled 2	0.24	17	12.2	0.72	U	0.9	2	failure of pipe couplings	dimensions assumed, PGA based on attenuation	U	Cooper 1997, USGS 1998
134	Los Gatos SJ 1	0.28	U	U	U	U	0.95	4	Elephant foot buckling	Bolted water tank, 1966	UA	Cooper 1997, USGS 1998
135	Los Gatos SJ 2	0.28	U	U	U	U	0.95	4	IO pipe underneath tank separated from floor plate	700,00 gal tank welded steel		Cooper 1997, USGS 1998
136	Watsonville 1	0.54	U	U	U	U	0.95	3	Buckled at roof / shell, no leak	1,000,000 gal tank		Cooper 1997
137	Watsonville 2	0.54	U	U	U	U	0.95	1	No damage	600,000 gal tank, AWWA D100		Cooper 1997
138	Santa Cruz 1/ Scotts Valley	0.47	U	U	U	U	0.95	2	Roof damage. Wood roof. Tanks drained due to broken inlet/outlet pipes	750,000 gal	UA	Cooper 1997, USGS 1998
139	Santa Cruz 2 / Scotts Valley	0.47	U	U	U	U	0.95	2	Roof damage. Wood roof. Tanks drained due to broken inlet/outlet pipes	400,000 gal	UA	Cooper 1997, USGS 1998
140	Santa Cruz 3	0.47	U	U	U	U	0.95	1	No damage	1,250,000 gal, AWWA D100 1983		Cooper 1997
141	Hollister	0.1					0.95	1	No damage	Built in 1960s. Pga based on attenuation		USGS 1998
Comments												
Richmond. Gasoline, diesel, turbine fuel, heavy fuel oil. Actual tank dimensions vary from 34 m Dx 14.8m H to 3.7m D x 15.4m H												
Richmond tanks use cone roofs, CIP, F roof systems. Site is marine area with possibly poor soils. All tanks on pile foundations with pile caps												
Richmond. No apparent roof damage at this site												
Lube 1 to 60. Most tanks assumed 25% full (from report which states "less than half full")												
San Jose. Actual tank dimensions vary from 38 m D x 14.6 m H to 7.5 m D x 9.8 m H. Initial construction of these tanks was in 1965												
Brisbane. Located firm ground, hillside location (assumed rock). All tanks have C, F or CF roofs; all tanks built before seismic codes. No damage												
PG&E Moss Landing. DS set to 4, reflecting buckling of top shell, tearing of bottom course and loss of contents". Other tanks at this site had no damage. PGA = 0.24g based on attenuation.												
Several other tanks at this site (include 2 MG oil tank) did not have major damage. PGA = 0.39g suggested in EERI (1990 p210) based on a recording located 15 km away												
The EBMUD water utility operated about 50 water steel tanks at the time of the earthquake. All were shaken with ground motions between PGA = 0.03g and PGA = 0.10g. Most of												
these tanks were anchored and designed per AWWA with seismic provisions. The only reported damage was 2 tanks with internal roof damage (There were no specific seismic designs of the roof systems)												
All these tanks are located on rock with concrete ring foundations. About half have wood roofs and half have integral steel roofs												
Most of the tanks were welded steel; a few were either riveted or bolted steel												
Most of the tanks use bottom entering inlet / outlet pipes. No pipe damage was noted for any tank												
Not all tanks have been inspected for internal damage to roof systems, so some unknown damage to roof systems may have occurred												
San Lorenzo. Near epicentral region. 5 redwood tanks were lost (10,000 to 15,000 gallons each)												
Santa Cruz mountains (in epicentral region). Several small bolted steel tanks failed, broken inlet / outlet pipes, some tanks collapsed [USGS 1998]												
Watsonville. 8 other water storage facilities performed well (unknown types)												
Richmond - Hercules - Rodeo - Martinez - Benicia - Avon locations include about 1,700 flat bottom steel tanks. PGA ranges from about 0.03g (rock outcrop sites) to at most 0.13-0.15g (soft soil sites)												
This report covers only 80 of these 1,700 tanks. All damage to tanks were for tanks at soft soil sites, and nearly full tanks												

Table B-15. Loma Prieta 1989 M7, (Page 3 of 3)

No.	Tank ID	PGA (g)	Diameter, D (m)	Height, H (m)	H / D	H Liq (m)	Pct Full	DS	Damage Observed	Remarks	Tank Anchors	Source
1	701	0.35	44.21	9.76	0.22	9.12	0.93	2	Roof damage, fire caused by tank 792	Welded steel	UA	Ballantyne and Crouse 1997
2	704	0.35	44.21	12.20	0.28	11.52	0.95	2	Roof damage	Welded steel	UA	Ballantyne and Crouse 1997
3	705	0.35	44.21	12.20	0.28	11.52	0.95	2	Roof damage	Welded steel	UA	Ballantyne and Crouse 1997
4	708	0.35	21.16	9.76	0.46	9.30	0.95	3	Elephant foot buckling	Welded steel	UA	Ballantyne and Crouse 1997
5	709	0.35	21.16	9.76	0.46	9.30	0.95	3	Elephant foot buckling	Welded steel	UA	Ballantyne and Crouse 1997
6	715	0.35	29.70	12.20	0.41	11.49	0.94	2	Roof damage	Welded steel	UA	Ballantyne and Crouse 1997
7	717	0.35	17.87	11.43	0.64	11.28	0.99	2	Roof damage	Welded steel	UA	Ballantyne and Crouse 1997
8	725	0.35	17.87	11.43	0.64	11.28	0.99	2	Roof damage	Welded steel	UA	Ballantyne and Crouse 1997
9	726	0.35	17.87	11.43	0.64	11.28	0.99	2	Roof damage, tank lateral movement	Welded steel	UA	Ballantyne and Crouse 1997
10	728	0.35	40.85	12.20	0.30	11.77	0.97	3	Shell buckling near roof, tank lateral movement	Welded steel	UA	Ballantyne and Crouse 1997
11	Unknown	0.35	40.85	12.20	0.30	11.43	0.94	2	Tank lateral movement	Welded steel	UA	Ballantyne and Crouse 1997
12	738	0.35	14.63	9.76	0.67	9.48	0.97	4	Elephant foot buckling	Welded steel. See note below about assumed EFB failure	UA	Ballantyne and Crouse 1997
13	745	0.35	10.37	9.76	0.94	9.45	0.97	3	Elephant foot buckling	Welded steel	UA	Ballantyne and Crouse 1997
14	792	0.35	4.79	4.85	1.01	4.85	1.00	5	Overturned tank, explosion	Welded steel	UA	Ballantyne and Crouse 1997
15	Holanda Chem Plant	0.35	5.53	5.53	1.00			3	Slight Elephant foot buckle	New API 650 tank	UA	Spectra, Vol 7, B, 1991
16	Holanda Chem Plant	0.35	10.06	10.06	1.00			2	Slid 20 cm		UA	Spectra, Vol 7, B, 1991
17	Holanda Chem Plant	0.35						1	No damage		UA	Spectra, Vol 7, B, 1991
18	Holanda Chem Plant	0.35						1	No damage		UA	Spectra, Vol 7, B, 1991
19	Holanda Chem Plant	0.35						1	No damage		UA	Spectra, Vol 7, B, 1991
20	Holanda Chem Plant	0.35						1	No damage		UA	Spectra, Vol 7, B, 1991
21	Holanda Chem Plant	0.35						1	No damage		UA	Spectra, Vol 7, B, 1991
22	Holanda Chem Plant	0.35						1	No damage		UA	Spectra, Vol 7, B, 1991
23	Holanda Chem Plant	0.35						1	No damage		UA	Spectra, Vol 7, B, 1991
24	Holanda Chem Plant	0.35						1	No damage		UA	Spectra, Vol 7, B, 1991
25	Holanda Chem Plant	0.35						1	No damage		UA	Spectra, Vol 7, B, 1991
26	Holanda Chem Plant	0.35						1	No damage		UA	Spectra, Vol 7, B, 1991
27	Transmerquim	0.35	8.66	8.66				3	EFB - severe, no leak	Built 1989	UA	Spectra, Vol 7, B, 1991
28	Transmerquim	0.35	8.66	8.66				3	EFB - severe, no leak	Built 1989	UA	Spectra, Vol 7, B, 1991
29	Transmerquim	0.35						2	Rocking, broken inlent/outlet pipe, loss of some contents		UA	Spectra, Vol 7, B, 1991
30	Transmerquim	0.35						1	No damage		UA	Spectra, Vol 7, B, 1991
31	Transmerquim	0.35						1	No damage		UA	Spectra, Vol 7, B, 1991
32	Transmerquim	0.35						1	No damage		UA	Spectra, Vol 7, B, 1991
33	Transmerquim	0.35						1	No damage		UA	Spectra, Vol 7, B, 1991
34	Transmerquim	0.35						1	No damage		UA	Spectra, Vol 7, B, 1991
35	Transmerquim	0.35						1	No damage		UA	Spectra, Vol 7, B, 1991
36	Transmerquim	0.35						1	No damage		UA	Spectra, Vol 7, B, 1991
37	Transmerquim	0.35						1	No damage		UA	Spectra, Vol 7, B, 1991
38	Transmerquim	0.35						1	No damage		UA	Spectra, Vol 7, B, 1991
Comments												
Tanks 1 - 14 at Recope Refinery, Port of Moin, Costa Rica												
Spillage of oil from at least one tank was confined in a dike. This is arbitrarily assigned to tank 738 (DS=4)												
Holanda Chemical Plant. 2 of 12 tanks were damaged												
Transmerquim plant located next to Holanda. 2 of 12 tanks suffered EFB												
The level of ground shaking at these three sites was considered "moderate" but not instrumental recordings available												
Ground motion for Port of Moin, near Limon, was estimated based on mapped intensity MMI VIII = PGA 0.35g.												

Table B-16. Costa Rica 1991 M7.5

No.	Tank ID	PGA (g)	Diameter, D (m)	Height, H (m)	H / D	H Liq (m)	Pct Full	DS	Damage Observed	Remarks	Tank Anchors	Source
1	BDVWA A	0.56	16.90	7.30	0.43	6.68	0.92	4	EFP around entire tank, failed at shell / bottom plate at 2 locations. 6" overflow pipe failed, lifted 2 feet out of ground. Tank shifted 3" laterally. Failure of side pipe	Welded steel, AWWA D100 1974, 0.25: shell, 0.25" bottom, 3/16" roof	UA	Cooper 1997, Ballantyne and Crouse 1997
2	BDVWA B	0.55	8.10	7.30	0.90	6.95	0.95	2	Minor damage		UA	Cooper 1997, Ballantyne and Crouse 1997
3	BDVWA C	0.55	18.10	7.30	0.40	6.89	0.94	2	Minor damage		UA	Cooper 1997, Ballantyne and Crouse 1997
4	BDVWA 10	0.55	9.90	4.90	0.49	4.45	0.91	2	Minor damage		UA	Cooper 1997, Ballantyne and Crouse 1997
5	BDVWA 22-A	0.54	9.90	4.90	0.49	4.45	0.91	2	Minor damage		UA	Cooper 1997, Ballantyne and Crouse 1997
6	BDVWA 22-B	0.54	9.90	4.90	0.49	4.45	0.91	2	Minor damage		UA	Cooper 1997, Ballantyne and Crouse 1997
7	BDVWA 22-C	0.54	14.00	4.90	0.35	4.45	0.91	2	Minor damage		UA	Cooper 1997, Ballantyne and Crouse 1997
8	BDVWA 22-D	0.54	22.30	4.90	0.22	4.42	0.90	2	Minor damage		UA	Cooper 1997, Ballantyne and Crouse 1997
9	BDVWA 34	0.55	6.40	4.90	0.77	4.48	0.91	2	Minor damage		UA	Cooper 1997, Ballantyne and Crouse 1997
10	HDWD 2 M.G.	0.15	36.60	7.30	0.20	U		1	No significant damage		UA	Cooper 1997, Wald 1998
11	HDWD R-7	0.15	25.90	7.30	0.28	U		1	No significant damage		UA	Cooper 1997, Wald 1998
12	HDWD R-8	0.15	10.00	7.30	0.73	U		1	No significant damage		UA	Cooper 1997, Wald 1998
13	HDWD R-14	0.20	21.30	5.50	0.26	U		1	No significant damage		UA	Cooper 1997, Wald 1998
14	HDWD R-15	0.19	22.90	7.30	0.32	U		1	No significant damage		UA	Cooper 1997, Wald 1998
15	HDWD R-2	0.15	25.90	7.30	0.28	U		1	No significant damage		UA	Cooper 1997, Wald 1998
16	HDWD R-3	0.20	25.90	7.30	0.28	U		1	No significant damage		UA	Cooper 1997, Wald 1998
17	HDWD R-4	0.20	9.10	7.30	0.80	U		1	No significant damage		UA	Cooper 1997, Wald 1998
18	HDWD R-5	0.20	7.90	7.30	0.92	U		1	No significant damage		UA	Cooper 1997, Wald 1998
19	HDWD Upper Ridge	0.10	13.10	7.30	0.56	U		1	No significant damage		UA	Cooper 1997, Wald 1998
20	HDWD Lower Ridge	0.10	5.50	4.9	0.89	U		1	No significant damage		UA	Cooper 1997, Wald 1998
21	HDWD Upper Fox	0.15	24.40	12.2	0.50	U		1	No significant damage		UA	Cooper 1997, Wald 1998
22	HDWD Lower Fox	0.15	10.90	4.9	0.45	U		1	No significant damage		UA	Cooper 1997, Wald 1998
23	HDWD Golden Bee	0.15	14.40	9.8	0.68	U		1	No significant damage		UA	Cooper 1997, Wald 1998
24	HDWD Homestead	0.10	11.80	7.3	0.62	U		1	No significant damage		UA	Cooper 1997, Wald 1998
25	HDWD Hospital Desert Gold	0.15	11.8	7.3	0.62	U		1	No significant damage		UA	Cooper 1997, Wald 1998
26	CSA 70-1	0.47	11.8	7.3	0.62	6.71	0.92	4	EFB all around, shell tearing, pullout of dresser couplings for 2 side attached pipes	Designed per API 12B, 1979, Bolted steel, 10 ga shell 10ga bottom plate	UA	Cooper 1997, Wald 1998
27	Beryl - SCWC	0.14	9.14	7.32	0.80	6.4	0.87	2	Small Leakage of bottom flange	Bolted	U	Ballantune and Crouse 1997
28	Basalt - SCWC	0.14	9.14	7.32	0.80	6.4	0.87	2	Failure of pipe through bottom penetration	Bolted	U	Ballantune and Crouse 1997
29	Arville-N - SCWC	0.14	8.93	12.65	1.42	11.28	0.89	2	Failure of pipe through bottom penetration	Welded (fillet)	U	Ballantune and Crouse 1997
30	Arville-S - SCWC	0.14	8.93	13.56	1.52	12.19	0.90	1	tank lateral movement	Welded	U	Ballantune and Crouse 1997
31	SCE Coolwater 1 of 3	0.53	83.2	15.2	0.18	15.2	1.00	1	No damage	API 650	U	Cooper 1997
32	SCE Coolwater 2 of 3	0.53	83.2	15.2	0.18	13.68	0.90	1	No damage	API 650	U	Cooper 1997
33	SCE Coolwater 3 of 3	0.53	67.2	14.5	0.22	1.45	0.10	1	No damage	API 650	U	Cooper 1997
Comments												
Landers Mw 7.3 followed by Big Bear M 6.5 3 hours later												
All damage in this table due to Landers event												
BDVWA = Bighorn Desert View Water Agency. HDWD = Hi Desert Water District. CSA = San Bernardino County Service Area 70												
SCWC - 4 tanks in Barstow, CA												

Table B-17. Landers 1992 M7.3

No.	Tank ID	PGA (g)	Diameter, D (m)	Height, H (m)	H / D	H Liq (m)	Pct Full	DS	Damage Observed	Remarks	Tank Anchors	Source
1	Van Nuys 1	0.55	8.80	14.60	1.66	7.90	0.54	1	Bolt shearing on tank walkway	Assumed between 1/3 and 2/3 full. API 650 1963	UA	Cooper 1997, Wald 1998
2	Van Nuys 2	0.55	11.00	13.70	1.25	6.85	0.50	1	Bolt shearing on tank walkway	Assumed between 1/3 and 2/3 full. API 650 1963	UA	Cooper 1997, Wald 1998
3	Van Nuys 3	0.55	20.40	14.60	0.72	7.30	0.50	1	Bolt shearing on tank walkway	Assumed between 1/3 and 2/3 full. API 650 1963	UA	Cooper 1997, Wald 1998
4	Van Nuys 4	0.55	21.90	14.60	0.67	7.30	0.50	1	Bolt shearing on tank walkway	Assumed between 1/3 and 2/3 full. API 650 1963	UA	Cooper 1997, Wald 1998
5	Van Nuys 5	0.55	4.60	9.10	1.98	4.55	0.50	1	Bolt shearing on tank walkway	Assumed between 1/3 and 2/3 full. API 650 1963	UA	Cooper 1997, Wald 1998
6	1 of 5	0.55	3.20	10.00	3.13	9.50	0.95	1	Minor damage to walkway	Assumed nearly full	UA	Cooper 1997, Wald 1998
7	2 of 5	0.55	3.20	10.00	3.13	9.50	0.95	1	Minor damage to walkway	Assumed nearly full	UA	Cooper 1997, Wald 1998
8	3 of 5	0.55	3.20	10.00	3.13	0.00	0.00	1	Minor damage to walkway	Assumed nearly full	UA	Cooper 1997, Wald 1998
9	4 of 5	0.55	3.20	10.00	3.13	0.00	0.00	1	Minor damage to walkway	Assumed nearly full	UA	Cooper 1997, Wald 1998
10	5 of 5	0.55	3.20	10.00	3.13	0.00	0.00	1	No significant damage	Assumed other 3 tanks out of service had no liquid	UA	Cooper 1997, Wald 1998
11	A Sepulveda Terminal	0.90	19.80	11.00	0.56	7.32	0.67	1	Slight sloshing	API 650, mid-60s	UA	Cooper 1997, Wald 1998, EERI 1995
12	B	0.90	21.90	11.00	0.50	3.66	0.33	1	Slight sloshing	API 650, mid-60s	UA	Cooper 1997, Wald 1998, EERI 1995
13	C	0.90	18.30	11.00	0.60	3.66	0.33	1	Slight sloshing	API 650, mid-60s	UA	Cooper 1997, Wald 1998, EERI 1995
14	AG 1	0.90	3.70	7.30	1.97	7.30	1.00	1	Minor paint cracks	UL 142, mid-60s	A	Cooper 1997, Wald 1998
15	AG 2	0.90	3.70	7.30	1.97	0.00	0.00	1	No significant damage	UL 142, mid-60s	A	Cooper 1997, Wald 1998
16	Aliso 1	0.70	12.20	7.30	0.60	U		0.75	5	Collapse	Bolted, mostly full based on amount of leakage	U	Cooper 1997, Wald 1998
17	Aliso 2	0.70	12.20	7.30	0.60	U		3	Photo shows some shell damage	Bolted, may be damaged	U	Cooper 1997, Wald 1998
18	Aliso 3	0.70	12.20	7.30	0.60	U		1	No significant damage	Bolted	U	Cooper 1997, Wald 1998
19	Aliso 4	0.70	12.20	7.30	0.60	U		1	No significant damage	Bolted	U	Cooper 1997, Wald 1998
20	Amir	0.90	12.80	9.09	0.71	U		3	EFB		U	Ballantyne and Crouse 1997, Wald 1998
21	Lautenschlager 1	0.90	19.00	6.7	0.35	5.94	0.89	1	No significant damage	Welded, 1965	U	Cooper 1997, Ballantyne and Crouse 1997 Wald 1998
22	Lautenschlager 2	0.90	19.00	7.3	0.38	5.94	0.81	1	No significant damage	Welded 1988	U	Cooper 1997, Ballantyne and Crouse 1997 Wald 1998
23	Tapo	0.90	40.00	9.8	0.25	8.69	0.89	1	No significant damage	Welded 1963	U	Cooper 1997, Ballantyne and Crouse 1997 Wald 1998
24	Crater East	0.75	9.10	7.3	0.80	6.13	0.84	1	No significant damage	Survived, pct full from text in Cooper	U	Cooper 1997, Ballantyne and Crouse 1997 Wald 1998
25	Crater West	0.75	11.90	7.3	0.61	6.13	0.84	1	No significant damage	Survived, pct full from text in Cooper	U	Cooper 1997, Ballantyne and Crouse 1997 Wald 1998
26	Alamo	0.70	30.50	6.3	0.21	6.25	0.99	1	No significant damage	Welded 1964	U	Cooper 1997, Ballantyne and Crouse 1997 Wald 1998
27	Katerine	0.90	12.00	7.3	0.61	6.25	0.86	4	Failed by EFB with loss of contents	Bolted, built 1964	U	Cooper 1997, Ballantyne and Crouse 1997 Wald 1998
28	Rebecca North	0.85	12.00	7.3	0.61	6.86	0.94	4	Failed by EFB with loss of contents	Bolted, built 1964	U	Cooper 1997, Ballantyne and Crouse 1997 Wald 1998
29	Rebecca South	0.85	12.00	7.3	0.61	6.86	0.94	4	Failed by EFB with loss of contents	Bolted, built 1964	U	Cooper 1997, Ballantyne and Crouse 1997 Wald 1998
30	Sycamore North	0.70	9.10	7.3	0.80	5.03	0.69	4	Failed by EFB with loss of contents	Bolted, built 1964	U	Cooper 1997, Ballantyne and Crouse 1997 Wald 1998
31	Sycamore South	0.70	9.10	7.3	0.80	5.03	0.69	4	Failed by EFB with loss of contents	Bolted, built 1964	U	Cooper 1997, Ballantyne and Crouse 1997 Wald 1998
32	SCWC 1 of 4	0.70	15.80	9.8	0.62	U		0.99	1	Survived	Welded	U	Cooper 1997, Wald 1998

Table B-18. Northridge 1994 M6.7 (Page 1 of 3)

No.	Tank ID	PGA (g)	Diameter, D (m)	Height, H (m)	H / D	H Liq (m)	Pct Full	DS	Damage Observed	Remarks	Tank Anchors	Source
33	SCWC 2 of 4	0.70	15.80	9.8	0.62	U		1	Survived	Welded	U	Cooper 1997, Wald 1998
34	SCWC 3 of 4	0.70	27.40	9.8	0.36	U		1	Survived	Welded	U	Cooper 1997, Wald 1998
35	SCWC 4 of 4	0.70	39.00	9.8	0.25	U		1	Survived	Welded	U	Cooper 1997, Wald 1998
36	LADWP Topanga	0.40	11.00	9	0.82	8.08	0.90	2	Replaced broken inlet / outlet valve. Loss of contents	Pct full from B&C. Welded steel, built 1936	UA	Cooper 1997, Ballantyne and Crouse 1997, Brown et al 1995
37	LADWP Zelzah	0.50	21.30	12.2	0.57	9.85	0.81	2	Roof collapsed, local buckling at top, broken valve. Loss of contents	Pct full from B&C. Welded steel built 1948	UA	Cooper 1997, Ballantyne and Crouse 1997, Brown et al 1995
38	LADWP Mulholland	0.40	15.80	10.2	0.65	0	0.00	2	overflow pipe pulled away. Loss of contents	Pct full from B&C. Welded steel built 1931	UA	Cooper 1997, Ballantyne and Crouse 1997, Brown et al 1995
39	LADWP Beverly Glen	0.50	30.50	12.3	0.40	U		2	Roof collapsed, local buckling, dresser coupling pulled out. Loss of contents	Riveted, built 1932. Wood roof replaced with hypalon bladder	UA	Cooper 1997, Brown et al 1995
40	MWD Jensen Clearwell	0.70	42.67	12.19	0.29	11.67	0.96	1	No tank damage		UA	Cooper 1997, Ballantyne and Crouse 1997, Brown et al 1995
41	LADWP Coldwater	0.30	30.48	12.19	0.40	U		2	Roof shifted and collapsed, inlet / outlet pipe failure. Loss of contents	Riveted built 1925. Wood roof shifted and collapsed.	UA	Ballantyne and Crouse 1997, Brown et al 1995
42	LADWP Granada High	1.00	16.80	10.7	0.64	9.66	0.90	5	Tank collapsed and tank removed	Riveted built 1929. Same tank was damaged in the 1971 San Fernando EQ	UA	Cooper 1997, Ballantyne and Crouse 1997, Brown et al 1995
43	LADWP Alta Vista 1	0.60	16.46	8.78	0.53	8.84	1.01	1	No tank damage	Riveted built 1929	UA	Cooper 1997, Ballantyne and Crouse 1997, Brown et al 1995
44	LADWP Alta Vista 2	0.60	28.96	11.13	0.38	9.3	0.84	1	No tank damage	Welded steel, built 1954. Assumed same pga as Alta Vista 1	UA	Cooper 1997, Ballantyne and Crouse 1997, Brown et al 1995
45	LADWP Alta View	0.30	19.81	12.95	0.65	12.5	0.97	1	Settlement		UA	Ballantyne and Crouse 1997, Brown et al 1995
46	LADWP Kittridge 3	0.30	57.90	15.54	0.27	U		1	No tank damage	Welded built 1973	UA	Ballantyne and Crouse 1997, Brown et al 1995
47	LADWP Kittridge 4	0.30	57.90	15.54	0.27	U		1	No tank damage	Welded built 1987	UA	Ballantyne and Crouse 1997, Brown et al 1995
48	LADWP Corbin	0.43	47.50	9.1	0.19	7.62	0.84	2	Minor drain line damage, partially buried	Welded built 1987	UA	Cooper 1997, Ballantyne and Crouse 1997, Brown et al 1995
49	Donick	0.30	37.43	7.32	0.20	6.86	0.94	1	No tank damage		UA	Ballantyne and Crouse 1997, Brown et al 1995
50	Santa Clarita	0.56	24.38	12.19	0.50	11.89	0.98	4	EFB, roof damage	Assumed same PGA as Magic Mountain tanks (also located at Valencia)	U	Cooper 1997, Ballantyne and Crouse 1997, Wald 1998
51	Valencia Round Moutain	0.56	40.30	9.8	0.24	9.07	0.93	1	No tank damage	AWWA D100	U	Cooper 1997, Ballantyne and Crouse 1997, Wald 1998
52	Hasley	0.50	36.60	12.2	0.33	11.29	0.93	1	No tank damage	AWWA D100	U	Cooper 1997, Wald 1998
53	Magic Mountain 2	0.56	22.30	7.3	0.33	6.1	0.84	U	Damaged by outflow of MM 1	Bolted, 1975	U	Cooper 1997, Ballantyne and Crouse 1997, Wald 1998
54	Magic Mountain 1	0.56	18.30	7.3	0.40	6.1	0.84	5	Complete failure, bottom shell torn at base, collapse	Bolted, 1971	U	Cooper 1997, Ballantyne and Crouse 1997, Wald 1998
55	Magic Mountain 3	0.56	24.40	9.8	0.40	9.07	0.93	1	No damage, tank partially buried 2.5 feet	AWWA D100. Welded with external roof rafters	U	Cooper 1997, Ballantyne and Crouse 1997, Wald 1998
56	Presley	0.50	21.30	9.8	0.46	9.07	0.93	1	No damage	AWWA D100	U	Cooper 1997, Wald 1998
57	4 Million	0.55	45.70	9.1	0.20	8.42	0.93	1	No damage	AWWA D100	U	Cooper 1997, Wald 1998
58	Seco	0.43	22.30	7.3	0.33	6.75	0.92	1	No damage	AWWA D100	U	Cooper 1997, Wald 1998

Table B-18. Northridge 1994 M6.7 (Page 2 of 3)

No.	Tank ID	PGA (g)	Diameter, D (m)	Height, H (m)	H / D	H Liq (m)	Pct Full	DS	Damage Observed	Remarks	Tank Anchors	Source
59	Larwin	0.55	18.30	12.2	0.67	9.75	0.80	5	Complete failure, EFB, tie down straps pulled, lifted foundation, nozzle tear outs	AWWA D100 1986. Straps 3/8"x3" at 4" On Center.	A	Cooper 1997, Wald 1998, EERI 1995
60	Poe	0.55	27.40	9	0.33	8.33	0.93	2	Roof rafter damage, sagging roof, no EFB	AWWA D100	U	Cooper 1997, Wald 1998
61	Paragon	0.43	22.30	9.8	0.44	9.07	0.93	1	No damage	AWWA D100	U	Cooper 1997, Wald 1998
62	Newhall 1	0.63	18.29	9.14	0.50	8.23	0.90	5	EFB, collapse, piping damage. Tasnk failed	Welded	UA	Cooper 1997, Wald 1998, EERI 1995
63	Newhall 2	0.63	12.20	9.8	0.80	8.82	0.90	3	Broken piping. EFB, Foundation settling	Built 1954, welded	UA	Cooper 1997, Wald 1998, EERI 1995
64	Newhall 3	0.63	12.20	9.8	0.80	8.82	0.90	3	Broken piping, EFB, Foundation settling	Built 1954, welded	UA	Cooper 1997, Wald 1998, EERI 1995
65	Newhall 4	0.63	12.20	9.8	0.80	8.82	0.90	3	Broken piping, EFB, Foundation settling, Roof rafters pulled out	Built 1962, AWWA	UA	Cooper 1997, Wald 1998, EERI 1995
66	Newhall 5	0.63	19.50	9.8	0.50	8.82	0.90	4	Roof rafter damage, EFB, inlet/outlet piping sheared	Built 1962. DS changed from 3 to 4	UA	Cooper 1997, Wald 1998, EERI 1995
67	Newhall 6	0.63	6.10	6.1	1.00	5.49	0.90	5	EFB, piping failure, plate failure, Tank replaced	Built 1960s	UA	Cooper 1997, Wald 1998, EERI 1995
68	Newhall 7	0.63	27.40	9.8	0.36	8.82	0.90	2	Roof shell seam opened, rafters fell, no EFB	Built 1975. Bottom course t=0.5"	UA	Cooper 1997, Wald 1998, EERI 1995
69	Newhall 8	0.63	18.30	7.3	0.40	6.57	0.90	2	Roof rafters pulled away from the shell, roof damage		UA	Cooper 1997, Wald 1998
70	Newhall 10	0.63	24.40	12.2	0.50	10.98	0.90	1	No apparent damage	Built 1989, AWWA	UA	Cooper 1997, Wald 1998

Comments
City of Simi Water District. 34 tanks in District, about 10 had damage. All damaged tanks were at east end of District (closer to fault). None of these tanks are in the table above
Simi: one tank had a failed underdrain pipe. Visual inspection of 2 tanks showed them unanchored, likely all were unanchored. This data not in above table
SCWC = Southern California Water Company
LADWP = Los Angeles Department of Water and Power
Tanks 51 - 61 are part of the Valencia Water Company
Tanks 62-70 are all welded, built to AWWA D100 or similar criteria
8 Prestressed concrete circular tanks in region with strong shaking (>0.2g) (6 buried or partially buried) performed well, built 1958-1992
There were other steel tanks at industrial sites which had EFB, which are not reported in this table
Tanks A, B, C, AG1, AG2 are at the Sepulveda terminal

Table B-18. Northridge 1994 M6.7 (Page 3 of 3)

No.	Tank ID	PGA (g)	Diameter, D (m)	Height, H (m)	H / D	H Liq (m)	Pct Full	DS	Damage Observed	Remarks	Tank Anchors	Source
1	Fuel Pier Yard. Small craft refuel tank	0.20	10.04	15.06	1.50	7.53	0.50	1			A	Hashimoto 1989
2	Power Plant #3, Tank 4	0.20	5.44	8.15	1.50	6.12	0.75	1			A	Hashimoto 1989
3	Power Plant #3, Tank 5	0.20	5.44	8.15	1.50	6.12	0.75	1			A	Hashimoto 1989
4	Las Ventanas Power Plant	0.25	6.08	9.12	1.50	6.84	0.75	1		Capacity estimated	A	Hashimoto 1989
5	Las Ventanas Power Plant	0.25	6.08	9.12	1.50	6.84	0.75	1		Capacity estimated	A	Hashimoto 1989
6	Las Ventanas Power Plant	0.25	6.08	9.12	1.50	6.84	0.75	1		Capacity estimated	A	Hashimoto 1989
7	LVPP Oil storage day tank	0.25	9.30	13.94	1.50	10.46	0.75	1		Capacity estimated	A	Hashimoto 1989
8	LVPP Oil storage day tank	0.25	9.30	13.94	1.50	10.46	0.75	1		Capacity estimated	A	Hashimoto 1989
9	Kettleman Gas Compressor Stn Lube Oil Fuel Tank 2	0.20	2.85	4.27	1.50	3.21	0.75	1			A	Hashimoto 1989
10	Kettleman Gas Compressor Stn Lube Oil Fuel Tank 3	0.20	2.85	4.27	1.50	3.21	0.75	1			A	Hashimoto 1989
11	Kettleman Gas Compressor Stn Lube Oil Fuel Tank 6	0.20	2.85	4.27	1.50	3.21	0.75	1			A	Hashimoto 1989
12	Pleasant Valley Pump Station Surge Tower	0.56	6.31	48.37	7.66	36.27	0.75	2	All anchor bolts stretched 1.5". No leaks	Anchroed with 1.5" diameter J bolts. PGA from nearby recording	A	Hashimoto 1989
13	San Lucas Canal Pump Station 17-R Surge Tank	0.35	2.85	5.93	2.08	4.45	0.75	4	Tank rocked, stretched or broken most anchors. 24" pipeline failed, likely loss of contents	Average tank dimensions. PGA = 0.35g is average for all pump stations, this one had more damage and may have had more PGA	A	Hashimoto 1989
14	Union Oil Butane Plant Diesel Fuel Oil Tank	0.60	2.42	3.63	1.50	2.72	0.75	1			A	Hashimoto 1989
15	Union Oil Butane Plant Diesel Fuel Oil Tank	0.60	2.42	3.63	1.50	2.72	0.75	1			A	Hashimoto 1989
16	Humboldt Bay 3 Condensate Storage Tank	0.30	4.56	7.99	1.75	5.99	0.75	1		Aluminum tank	A	Hashimoto 1989
17	Humboldt Bay 3 Condensate Storage Tank	0.25	4.56	7.99	1.75	5.99	0.75	1		Aluminum tank	A	Hashimoto 1989
18	Sandia Fuel Oil Tank	0.25	7.43	14.85	2.00	11.14	0.75	3	All 20 Wejit anchors failed. Elephant foot buckling without leak		A	Hashimoto 1989
19	Asososca Lake Surge Tank	0.50	4.86	21.40	4.40	14.70	0.67	2	Stretched 16 anchor bolts, no loss of contents	Capacity estimated	A	Hashimoto 1989
20	Sendai Refinery Fire Water Storage Tank	0.28	11.71	17.57	1.50	15.24	0.87	2	Anchor bolts stretched or pulled 1 to 6 inches, some leaking at a vlave, no buckling or rapid loss of water	Capacity estimated. Shell t = 3/8" est., bttom plate = .25" est. 14 1.25" diam anchor bolts A307, attached by chairs	A	Hashimoto 1989
21	Caxton Paper Mill Chip storage silo	0.40	11.31	16.96	1.50	12.72	0.75	1		Capacity estimated	A	Hashimoto 1989
22	Caxton Paper Mill Hydrogen Peroxide Tank	0.40	2.64	3.95	1.50	2.97	0.75	1		Capacity estimated	A	Hashimoto 1989
23	Caxton Paper Mill Secondary Bleach Tower	0.40	5.44	8.15	1.50	6.85	0.84	1		Capacity estimated	A	Hashimoto 1989
24	New Zealand Distillery Bulk Storage Tank #2	0.50	7.48	5.61	0.75	4.71	0.84	1		Capacity estimated	A	Hashimoto 1989
25	New Zealand Distillery Bulk Storage Tank #5	0.50	4.59	3.44	0.75	2.58	0.75	1		Capacity estimated	A	Hashimoto 1989
26	New Zealand Distillery Bulk Storage Tank #6	0.50	4.59	3.44	0.75	2.58	0.75	1		Capacity estimated	A	Hashimoto 1989
27	New Zealand Distillery Bulk Storage Tank #7	0.50	8.77	6.58	0.75	4.93	0.75	1		Capacity estimated	A	Hashimoto 1989
28	New Zealand Distillery Receiver Tank #9	0.50	3.32	2.49	0.75	1.87	0.75	1		Capacity estimated	A	Hashimoto 1989
29	Whakatane Board Mills Pulp Tank	0.30	7.84	11.76	1.50	8.82	0.75	1		Capacity estimated	A	Hashimoto 1989
30	Whakatane Board Mills Pulp Tank	0.30	7.84	11.76	1.50	8.82	0.75	1		Capacity estimated	A	Hashimoto 1989
31	Whakatane Board Mills Pulp Tank	0.30	7.84	11.76	1.50	8.82	0.75	1		Capacity estimated	A	Hashimoto 1989
32	Glendale power plant Distilled Water tank 1A	0.28	3.62	5.42	1.50	4.07	0.75	1			A	Hashimoto 1989
33	Glendale power plant Distilled Water tank 1B	0.28	3.62	5.42	1.50	4.07	0.75	1			A	Hashimoto 1989
34	Glendale power plant Distilled Water tank 2	0.28	4.01	6.01	1.50	4.51	0.75	1		Capacity estimated	A	Hashimoto 1989
35	Glendale power plant Fuel oil day tank #1	0.28	3.62	5.42	1.50	4.07	0.75	1			A	Hashimoto 1989
36	Pasadena Power plant Unit B1 distilled water tank	0.20	7.28	10.92	1.50	8.19	0.75	1		Capacity estimated	A	Hashimoto 1989
37	Pasadena Power plant Unit B2 distilled water tank	0.20	7.78	9.56	1.23	8.54	0.89	1		A36. t= 5/16" lower course, 1/4" upper course, 1/4" bottom plate. 10 1.25" diam anchor bolts A307 using chairs	A	Hashimoto 1989
38	Pasadena Power plant Unit B3 distilled water tank	0.20	5.46	13.92	2.55	12.19	0.88	1		A283 Gr B. t= 5/16" lower course, 1/4" upper course, .375" bottom plate. 24 1.5" diam. Anchor bolts A307 using chairs	A	Hashimoto 1989
39	Pasadena Power plant Unit B1 distilled water tank	0.17	7.28	10.92	1.50	8.19	0.75	1		Capacity estimated	A	Hashimoto 1989
40	Pasadena Power plant Unit B2 distilled water tank	0.17	7.78	9.56	1.23	8.54	0.89	1	No damage	A36. t= 5/16" lower course, 1/4" upper course, 1/4" bottom plate. 10 1.25" diam anchor bolts A307 using chairs	A	Hashimoto 1989
41	Pasadena Power plant Unit B3 distilled water tank	0.17	5.46	13.92	2.55	12.19	0.88	1	No damage	A283 Gr B. t= 5/16" lower course, 1/4" upper course, .375" bottom plate. 24 1.5" diam. Anchor bolts A307 using chairs	A	Hashimoto 1989

Comments
Tanks 1 - 3. Adak 1986. Tanks 4 - 8. Chile 1985. Tanks 9 - 15. Coalinga 1983. Tank 16. Ferndale 1975. Tank 16. Ferndale 1975.
Tank 18. Greenville 1980. Tank 19. Managua 1972. Tank 20. Miyagi-ken-ogi 1978. Tanks 21 - 31. New Zealand 1987. Tanks 32 - 38 San Fernando 1971. Tanks 39 - 41 Whittier 1987.
Most tanks at least 50% full at time of earthquake. Unless otherwise specified in Hashimoto, set at 75% full

Table B-19. Anchored Tanks, Various Earthquakes

Abbreviation	Description
A	Anchored
API	American Petroleum Institute (API 650 code)
AWWA	American Water Waorks Association (AWWA D100 code)
D	Diameter. For most tanks, the diameter dimension is the inside diameter of the tank
DS	Damage State. See text for descriptions. May be from 1 to 5
EERI	Earthquake Engineering Research Institute
EFB	Elephant Foot Buckling
g	acceleration of gravity (=32.2 ft / sec / sec)
ga	gage thickness
H	Height. Generally the height from the top of the floor to the overflow level. The actual tank may be higher (above the overflow level)
I/O	Inlet / outlet pipe
Liq	Height of Liquid. The estimated (sometimes known) height of fluid contents at the time of the earthquake
m	meter. Note: most tanks in these tables are actually sized to the nearest foot. The metric conversion here does not infer accuracy to the exact dimension in feet.
MMI	Modified Mercalli Intensity
Pct Full	The percent full of the tank (= H Liq / H)
PGA	Peak Ground Acceleration in g
U	Unknown
UA	Unanchored
Z	Design level peak ground acceleration

Table B-20. Legend for Tables B-8 Through B-19

Wood Roof

Overflow Elev 31'-0"

Altitude Valve Control pipe

Overflow pipe

Air Vacuum
Release Pipe

32'-0"

Shell manhole
(typ. of 2)

Hold Down (Typ)

6" min. clearance

75'-0" O.D. Steel Shell

76'-10" O.D. Footing Ring
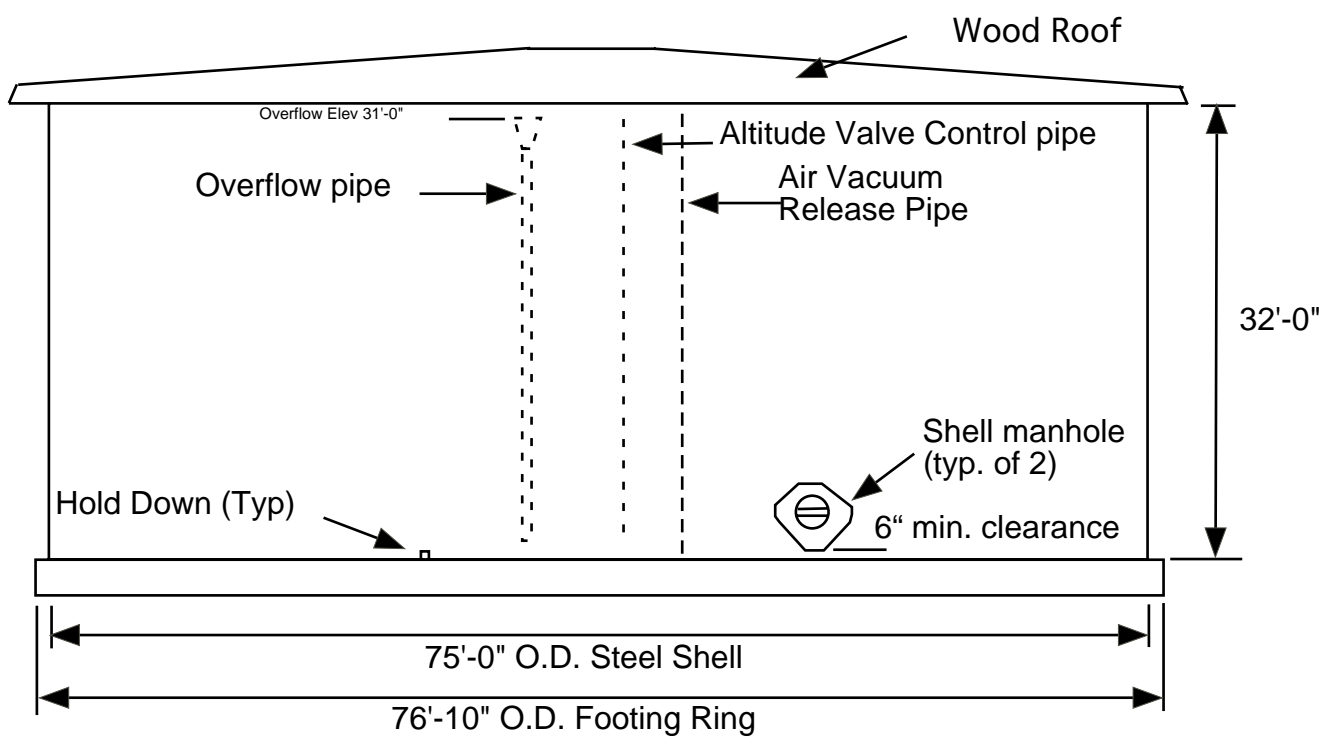
Figure B-1. Elevation of Example Tank

C. Commentary – Tunnels

Section C.1 describes two sets of fragility curves which are in the literature: those in HAZUS, and those in ATC-13.

Sections C.2 through C.5 provide information of the performance of tunnels in past earthquakes.

Section C.6 provides the complete tunnel database, including analyses of tunnels by liner attribute.

C.1 Tunnel Fragility Curves – Prior Studies

C.1.1 HAZUS Fragility Curves

The HAZUS computer program [HAZUS, 1997] includes a number of fragility curves for tunnels. The HAZUS fragility curves are provided for ground shaking and ground failure hazards in the form of landslides or fault offset.

For ground shaking hazards, data from post earthquake reconnaissance of 68 tunnels [Dowding and Rozen, 1978] were reduced to establish fragility parameters. Figure C-1 shows the empirical dataset; Table C-1 provides the specific values; Table C-1 was prepared as follows:

- The tunnel locations in the Dowding and Rozen were located. For each earthquake, the distance from the tunnel to the causative fault was determined. A suitable attenuation model was used (at the median level of shaking, such as using equation 3.3) to estimate the peak horizontal ground motion at the tunnel location.

- Three damage states could be assessed: none, slight and moderate. Descriptions of the damage states are as follows: Minor Damage: minor cracking of tunnel liner, minor rock falls, spalling of shotcrete or other supporting materials. Moderate Damage: moderate cracking of tunnel liner and rock falls.

- The empirical data was binned into three groups – tunnels with no observed damage; tunnels with minor damage, and tunnels with moderate damage.

- The mean and standard deviation were computed for each bin. These are reported directly beneath the empirical data.

- The lognormal median and beta values were computed directly from the mean and standard deviation values (bottom of Table C-1).

Approximately 17 percent of the tunnels were reportedly in competent rock; the remaining were in sheared or broken rock, soil or unknown ground conditions. Tunnels were constructed between 1800 and 1960. For the most part, the older tunnels represent poor to average construction quality; although, the data does not specifically segregate tunnels with respect to quality of construction. For each tunnel, the peak horizontal ground (surface) acceleration at each tunnel location was established using empirical attenuation relationships based on distance from earthquake epicenter to the site.

The data was categorized in three damage states: no damage, minor damage, and moderate damage. Each tunnel has a damage state and associated peak ground acceleration. Nine

"bins" (3 damage states x 3 PGA intervals) were used to sort the tunnels. The results are in Table C-7.

Damage State / PGA	0.0 to 0.2g	0.2 to 0.5g	0.5 to 0.7g	Total
No Damage	30	9	0	39
Minor Damage	1	9	5	15
Moderate Damage	0	5	9	14
Total	31	23	14	68

Table C-7. Number of Tunnels in Each Damage State due to Ground Shaking

The empirical data was then averaged to obtain the mean, median, standard deviation and beta for each damage state within each damage state. The results are provided in Table C-8. Beta in Table C-8 includes uncertainty and randomness (same as β_{total} in equation 5-2).

Damage State / PGA	Mean (g)	Median (g)	Std. Dev (g)	Beta (total)
No Damage	0.183	0.145	0.143	0.689
Minor Damage	0.387	0.353	0.174	0.428
Moderate Damage	0.513	0.500	0.116	0.224

Table C-8. Statistics for Tunnel Damage States

The data in Tables C-7 and C-8 include rock, alluvial, and cut & cover tunnels, but no distinction is made between the three since the ground conditions were not reported in the literature for most of the tunnels.

Dowding [1978] reported that below 0.19g, there is no damage to either lined or unlined tunnels. Also, Owen [1981] concluded that rock tunnels perform better than alluvial or cut and cover tunnels. Specifically, little damage occurs to rock tunnels when accelerations at the ground surface were below 0.4g. Earthquake experience shows that most damage occurs to the tunnel liner, and such damage is well correlated with the quality of construction of the liner. For example, older-designed unreinforced concrete liners using wood sets and lagging for temporary support and without contact grouting are more susceptible to damage than are modern, cast-in-place concrete liners using steel sets and standard contact grouting.

For these reasons, fragility curves developed for HAZUS for ground shaking hazards distinguish between rock tunnels and other tunnels and between poor and good quality construction. No distinction is made in the HAZUS fragility curves between tunnels with or without seismic design, as the empirical database provided no indication of the original design basis; it is likely that seismic design was not included in very many of the tunnels in the empirical database. The resulting HAZUS fragility curves are described in Tables C-9 through C-12.

<u>Alluvial and Cut & Cover Tunnels of poor to average construction</u>. The fragility curves are based on the data in Table C-8 with minor adjustments described below. Beta includes uncertainty and randomness.

Item	Hazard	Damage State	Median PGA (g)	Beta	Median PGD (inch)	Beta
Liner	Ground Shaking	Minor cracking of tunnel liner; minor rock falls; spalling of shotcrete or other supporting material.	0.35	0.4		
Liner	Ground Shaking	Moderate cracking of tunnel liner and rock falls.	0.55	0.6		
Liner	Ground Failure	Moderate cracking of tunnel liner and rock falls			12	0.5
Liner	Ground Failure	Major localized cracking and possible collapse of tunnel liner and rock falls			60	0.5
Portal	Ground Failure	Debris from landslide closes portal			60	0.5

Table C-9. Tunnel – Alluvial or Cut and Cover with Liner of Average to Poor Quality Construction

Minor damage from ground shaking: Median: 0.35g, Beta 0.40. These values are close to the empirical dataset values of Median .353g, Beta .428.

Moderate damage from ground shaking: Median: 0.55g, Beta 0.6. The median value of 0.55g is set 10% higher than the empirical value of 0.50g, based on judgment. The Beta value of 0.6 is set much higher than the empirical value of 0.22; the empirical value is deemed too low due to the small data sample size; in fact, it is felt that the moderate damage state is known with less certainty than the minor damage state, and the state of empirical data (circa 1978) was too incomplete to warrant a lower value.

Damage due to ground failure through the liner. The HAZUS fragility values are set at 12 inches of liner offset to mean moderate damage, and 60 inches of liner offset to mean major damage. This implies that the tunnel diameter is in the range of 8 to 12 feet (typical of water tunnels), and that the materials behind the liner are weak enough to cause some type of debris accumulation in the tunnel. For water tunnels, small amounts of debris will often be carried away by the water flow; whereas large amounts of debris can result in clogging of the tunnel and damage to downstream water system components. If a large amount of debris occurs the tunnel may clog over a long period of time (days to months). No specific fragility curve is provided for fault offset through the liner, but it is understood that a fault offset of about 50% to 75% (or larger) of the inner diameter of the liner can be enough to immediately close off the tunnel. However, it has been noted that larger fault offsets (more than the diameter of the tunnel) can, in some cases, be accommodated the tunnel without loss of flow capacity if the offset is distributed over a reasonable length of the tunnel (on the order of 20 to 50 feet). Current predictive models of fault offset are not so precise as to determine with high confidence whether the fault offset will be like a "knife edge" (leads to tunnel closure if offset approaches of exceeds tunnel diameter)) or distributed over a considerable shear zone (may or may not lead to tunnel closure).

Damage due to ground failure of the portal area. Landslides at portal areas represent a credible hazard to all tunnels. Strong ground shaking can promote landslide movements, especially under saturated soil conditions. The HAZUS fragility model of 5 feet leading to

closure of the portal is based on judgment, and assumes that the tunnel is about 8 to 12 feet in diameter.

Alluvial and Cut & Cover Tunnels of good construction. The median values are increased from those of tunnels with average to poor construction (Table C-9) by one lognormal standard deviation and then rounded. For example: for Minor Damage, 0.35g * exp (0.428) = 0.53g, set to 0.5g; for Major Damage, 0.55g * exp (0.224) = 0.688g, set to 0.7g (Table C-10). Beta includes uncertainty and randomness.

Item	Hazard	Damage State	Median PGA (g)	Beta	Median PGD (inch)	Beta
Liner	Ground Shaking	Minor cracking of tunnel liner; minor rock falls; spalling of shotcrete or other supporting material.	0.5	0.4		
Liner	Ground Shaking	Moderate cracking of tunnel liner and rock falls.	0.7	0.6		
Liner	Ground Failure	Moderate cracking of tunnel liner and rock falls			12	0.5
Liner	Ground Failure	Major localized cracking and possible collapse of tunnel liner and rock falls			60	0.5
Portal	Ground Failure	Debris from landslide closes portal			60	0.5

Table C-10. Tunnel – Alluvial or Cut and Cover with Liner of Good Quality Construction

The HAZUS fragility curves for damage to liners due to ground shaking for tunnels of good quality construction (Table C-10) were developed by increasing the median fragility levels from Table C-9 by about 30% to 40%, representing an increase in the median acceleration levels of one standard deviation above those for tunnels of poor to average quality construction; this is based on judgment and the limited empirical data set. A similar approach was taken to establish fragility curves for rock tunnels (Tables C-11 and C-12).

Rock Tunnels of poor to average construction. The fragility curves are developed based on engineering judgment. (Table C-11), with adjustments taken from rock tunnels of good quality construction. Beta includes uncertainty and randomness.

Item	Hazard	Damage State	Median PGA (g)	Beta	Median PGD (inch)	Beta
Liner	Ground Shaking	Minor cracking of tunnel liner; minor rock falls; spalling of shotcrete or other supporting material.	0.5	0.4		
Liner	Ground Shaking	Moderate cracking of tunnel liner and rock falls.	0.7	0.6		
Liner	Ground Failure	Moderate cracking of tunnel liner and rock falls			12	0.5
Liner	Ground Failure	Major localized cracking and possible collapse of tunnel liner and rock falls			60	0.5
Portal	Ground Failure	Debris from landslide closes portal			60	0.5

Table C-11. Tunnel – Rock without Liner or with Liner of Average to Poor Quality Construction

Rock Tunnels of good construction. The median peak ground acceleration was derived recognizing that little damage occurs below 0.4g. It was assumed that the median PGA for minor damage to rock tunnels of good construction quality would occur one lognormal standard deviation above 0.4g. (Table C-12). Beta includes uncertainty and randomness.

Item	Hazard	Damage State	Median PGA (g)	Beta	Median PGD (inch)	Beta
Liner	Ground Shaking	Minor cracking of tunnel liner; minor rock falls; spalling of shotcrete or other supporting material.	0.6	0.4		
Liner	Ground Shaking	Moderate cracking of tunnel liner and rock falls.	0.8	0.6		
Liner	Ground Failure	Moderate cracking of tunnel liner and rock falls			12	0.5
Liner	Ground Failure	Major localized cracking and possible collapse of tunnel liner and rock falls			60	0.5
Portal	Ground Failure	Debris from landslide closes portal			60	0.5

Table C-12. Tunnel – Rock without Liner or with Liner of Good Quality Construction

As of the time when the tunnel fragility curves were prepared for the HAZUS program (early 1990s), damage due to ground shaking that would results in closure of tunnels was not considered likely; therefore, there is no effect to the functionality of the tunnels due to ground shaking in the damage algorithm. As will be described in subsequent sections, this

"heavy" damage state has in fact been occasionally observed, suggesting that the HAZUS fragility curves might need to be modified.

For ground failures (such as surface faulting through the interior of the tunnel), substantial permanent ground deformations need to occur before appreciable damage occurs. For moderate damage, a permanent ground deformation of one foot is used, and for major damage, a permanent ground deformation of five feet is used. These displacements are based on a typical water tunnel equivalent diameter of about 8 feet. For both moderate and major damage due to ground failure, tunnel closure is possible; tunnel closure could occur immediately, or within a few days of the earthquake, either due to aftershocks, or continued erosion of the geology behind the failed liner.

If the tunnel portals are subjected to PGDs due to landslide, then the same PGDs (five feet) is assumed to cause tunnel major damage and closure. Rockfall type avalanches are not specifically considered in the fragility curves.

C.1.2 Comparison of HAZUS and ATC-13 Fragility Curves

Table C-13 compares the median peak ground accelerations for fragility curves developed in Tables C-10 and C-12 (good quality construction) with the damage algorithms presented in ATC-13 [ATC, 1985]. Only median values are compared because the dispersions in the ATC-13 data do not reflect variability in the ground motion; whereas, the fragility curves developed here do. The damage probability matrices given in the ATC-13 were converted to a cumulative probability distribution using the methodology described in ASCE [1985] and using MMI to PGA conversion suggested by McCann et.al. [1980] (Table C-14).

Tunnel Type / Damage State	HAZUS (PGA)	ATC-13 (PGA)
Rock		
Moderate Damage	0.8 g	0.94 g
Minor Damage **	0.6 g	0.45 g
Cut & Cover or Alluvial		
Moderate Damage	0.7 g	0.74 – 0.84 g *
Minor Damage **	0.5 g	0.40 – 0.44 g *

Table C-13. Comparison of Tunnel Fragility Curves

* ATC-13 gives values for Cut & Cover and Alluvial Tunnels. Both PGAs are given above.
** For *Minor* Damage State shown above, the corresponding ATC-13 Damage State is *Light*.

MMI	PGA Interval	PGA Used
VI	0.09 – 0.15	0.12
VII	0.16 – 0.25	0.21
VIII	0.26 – 0.45	0.36
IX	0.46 – 0.60	0.53
X	0.61 – 0.80	0.71
XI	0.81 – 0.90	0.86
XII	≥ 0.91	1.15

Table C-14. Modified Mercalli to PGA Conversion [after McCann et al, 1980]

As can be seen in Table C-13, the median fragility values for the two damage states agree reasonably well.

C.2 Databases of Owen and Scholl, Sharma and Judd

Owen and Scholl [1981] extended the database of Dowding and Rozen [1978] to a total of 127 cases. Additions to the database included observations from the 1906 San Francisco earthquake, 1971 San Fernando earthquake, and a number of less well documented earthquakes around the world. Based on their examination of the data, Owen and Scholl concluded the following:

- Little damage occurred in rock tunnels for peak ground accelerations below 0.4g.

- Severe damage and collapse of tunnels from shaking occurred only under extreme conditions, usually associated with marginal construction such as brick or plain concrete liners and lack of grout between wood lagging and the overbreak.

- Severe damage was inevitable when the underground structure was intersected by a fault that slipped during an earthquake. Cases of tunnel closure appeared to be associated with movement of an intersecting fault, landslide, or liquefied soil.

- Deep tunnels were safer (i.e., less prone to damage) than shallow tunnels.

- Damage to cut-and-cover structures appeared to be caused mainly by large increases in lateral forces from the surrounding soil backfill.

- Earthquake duration appeared to be an important factor contributing to the severity of damage.

Sharma and Judd [1991] further extended the database to 192 reported cases. In this study, the relationships between observed damage and parameters of the earthquake, tunnel support system, and geologic conditions were examined. Parameters considered in their study included earthquake magnitude, epicentral distance, peak ground acceleration, form of tunnel internal support and lining, overburden depth, and rock type. Sharma and Judd concluded that:

- Damage incidence decreased with increasing overburden depth.

- Damage incidence was higher for colluvium than for harder rocks.

- Internal tunnel support and lining system appeared not to affect damage incidence.

- Damage increased with increasing earthquake magnitude and decreasing epicentral distance (i.e., increasing peak ground acceleration).

- No or minor damage can be expected for peak accelerations at the ground surface less than about 0.15g.

C.3 Database of Power et al

The tunnel studies described in Sections C.1 and C.2, while informative and indicative of generally good tunnel performance during earthquakes, contain some limitations:

- Many of the cases reported were observations from old and/or less well documented earthquakes; the locations and/or magnitudes of a number of the earthquakes were poorly defined.

- The ground shaking levels estimated for the cases were calculated using empirical ground motion attenuation relationships developed in early 1970's. Peak ground accelerations were estimated using distances from earthquake epicenters to the tunnel sites (i.e., epicentral distances). Ground motions calculated using epicentral distance could be misleading for sites located close to a long or extended fault rupture area. Recently developed ground motion attenuation relationships generally use some measure of the closest distance from the site to the fault rupture area. Furthermore, recently developed attenuation relationships are better constrained than the older relationship by more data from many recent earthquakes.

- The damage cases reported and used in the previous studies included damage observations resulting from direct fault rupture through a tunnel and other major ground failure mechanisms, such as landsliding and liquefaction. In examining effects of ground shaking on tunnels, cases of damage due to these other failure mechanisms should not be included.

To consider these limitations, Power et al. [1998] critically examined the previously compiled data bases summarized above and the following revisions were made:

- Data were removed for poorly documented earthquakes, such as earthquakes with unknown magnitudes or locations, or uncertain tunnel performance.

- Data were removed for cases of damage due directly to fault displacement, landsliding, or liquefaction, in order to examine trends for shaking-induced damage in the absence of ground failure.

- Data were not included for cut-and-cover tunnels or tubes, in order to develop trends and a correlation for bored tunnels only.

- Earthquake magnitudes were reported as moment magnitudes (M_w).

- Distances were evaluated as closest distances from the tunnel locations to the fault rupture surfaces of the earthquakes.

- Peak accelerations at the ground surface (at actual or hypothetical rock outcrops) at the tunnel locations were estimated using recently developed ground (rock) motion attenuation relationships.

- Data were added from recent, moderate-to-large magnitude and better-documented earthquakes: 1989 Loma Prieta, 1992 Petrolia, 1993 Hokkaido, 1994 Northridge, and 1995 Kobe earthquakes. Some data were added from case histories from older earthquakes.

Table C-2 (entries 1 through 204) includes the complete database that is summarized in Table 6-1. Included in Table C-2 are information on the earthquake (name, date, and moment magnitude), tunnel (name, owner, function, lining/support system, local geologic conditions, and thickness of geologic cover), level of ground shaking (peak ground acceleration), damage state, and references for data on the tunnels and tunnel performance observations.

In general, peak ground accelerations at the ground surface at tunnel locations were estimated as median (50th percentile) values using rock ground motion attenuation relationships developed by Sadigh et al. [1993, 1997] for earthquakes occurring on crustal faults. The rock relationship of Youngs et al. [1993, 1997] for subduction zone

earthquakes were utilized for the 1964 Alaska earthquake. The median peak accelerations for the 1994 Northridge earthquake were estimated using event-specific ground motion attenuation relationship developed for the Northridge earthquake [Woodward-Clyde Consultants, 1995]. Rock ground motion attenuation relationships were utilized because most of the reported cases in the database involve tunnels founded in rock and also due to the limited information that was available for the local geologic conditions. The actual ground motions experienced at the depth of the tunnels would tend to be less than the values estimated for the ground surface in Table C-2 due to well-known tendencies for ground motions to decrease with depth below the ground surface [e.g. Chang et al., 1986]. The highest median peak rock acceleration estimated for the entire database is about 0.7g, for the 1923 Kanto, 1971 San Fernando, and the 1994 Northridge earthquakes. Many estimated peak rock accelerations for the 1995 Kobe earthquakes are about 0.6g. The Kobe earthquake produced by far the most observations for moderate to high levels of shaking (numerous estimated median peak rock accelerations at the ground surface above the tunnels in the range of about 0.4g to 0.6g).

Damage to the tunnels was categorized into 4 states: none; slight, for minor cracking and spalling of the tunnel lining; moderate, for major cracking and spalling; and heavy for total or partial collapse of a tunnel.

Figure C-2 presents a summary of the observations of the effects of seismic ground shaking on tunnel performance for the case histories 1 through 204 in Table C-2. As indicated previously, the data are for damage due only to shaking and exclude damage that was definitely or probably attributed to fault rupture, landsliding, or liquefaction. Also, the data are for bored tunnels only; data for cut-and-cover tunnels and tubes are not included. Figure C-2 shows the level of damage induced in tunnels with different types of linings subjected to the indicated levels of ground shaking.

The following trends can be inferred from Figure C-2:

- For peak ground accelerations (PGAs) equal to or less than about 0.2g, ground shaking caused very little damage in tunnels.

- For peak ground accelerations (PGAs) in the range of about 0.2g to 0.5g, there were some instances of damage ranging from slight to heavy damage.

- For peak ground accelerations (PGAs) exceeding about 0.5g, there were a number of instances of slight to heavy damage.

- Tunnels having stronger lining system appeared to have performed better, especially those tunnels having reinforced concrete and/or steel linings.

It should be noted that the three instances of heavy damage (solid diamonds in Figure C-2) are all from the 1923 Kanto, Japan earthquake. For the 1923 Kanto earthquake observation with PGA equal to 0.25g (see Table C-2 and Figure C-2), the investigations for this tunnel indicated that the damage may have been due to landsliding. In the other two observed occurrences of heavy damage shown in Figure C-2, collapses occurred in the shallow portions of the tunnels.

The correlations observed in Figure C-2 show similar trends as those observed in the previous study by Dowding and Rozen in Figure C-1. For relatively low ground shaking levels, no or very little damage occurred for PGAs less than about 0.2g. There are relative few instances of moderate to heavy damage for accelerations less than 0.5g, especially for stronger and well-constructed tunnels. This was evident during the 1995 Kobe, Japan

earthquake, where only a few cases of moderate damage and no major damage were reported for bored tunnels for peak ground accelerations of about 0.6g.

Although the number of observations for the seismic performance of cut and cover tunnels are far fewer than those for bored tunnels, the available data including observations from the 1995 Kobe earthquake suggest that cut and cover box-like tunnels are more vulnerable to shaking than bored tunnels with more-or-less circular cross sections. Cut and cover tunnels are vulnerable to racking-type deformations due to ground-imposed displacements of the top of the box structure relative to the base. The higher vulnerability of cut-and-cover tunnels as compared to bored tunnels is also probably due in part to the generally softer geologic materials surrounding the cut-and-cover structures, which are constructed at shallower depths than most bored tunnels.

C.4 Additions to Empirical Database

Asakura and Sato [1998] provided an expanded compilation of tunnel performance data for the 1995 Kobe earthquake. Additional case histories obtained from their database during the present study are summarized in Table C-2 as entries 205 through 217.

As part of U.S./Japanese cooperative research and state-of-the-art studies of tunnel seismic design and performance by Prof. Thomas O'Rourke for MCEER, O'Rourke and Shiba [1997] summarized tunnel performance for 15 different earthquakes in Japan from 1923 to 1993. Table C-3 summarizes tunnel damage observed in these earthquakes. Table C-4 provides an explanation of the Japanese JMA intensity scale that is used in Table C-3. Figure C-3 shows a map of the locations of these earthquakes. The findings in Table C-3 are similar to those described in the Sections C.2 and C.3 and included the following observations:

- Generally the parts of tunnels most significantly damaged were the portals, which was often attributed to landslides.

- Some of the most severe damage occurred due to fault movements.

- Generally, damage to tunnels due to shaking was associated with unreinforced masonry and unreinforced, cast-in-place concrete linings and with tunnel locations where construction difficulties were experienced and poor geologic conditions were encountered.

- Significant damage to Japanese tunnels was observed predominately in locations where seismic intensities of V or higher on the JMA scale occurred (correlating approximately to MMI intensity VIII.

C.5 Tunnels with Moderate to Heavy Damage from Ground Shaking

As previously discussed, the incidence of heavy damage (collapse of at least part of the liner system) in tunnels from ground shaking has been relatively rare. The following sections summarize the specific tunnels which have collapsed, possibly due to ground shaking.

C.5.1 Kanto, Japan 1923 Earthquake

Table C-5 summarizes the earthquake damage observed in 34 tunnels after ten Japanese earthquakes. These tunnels were selected as those displaying the most severe damage for which there is sufficient description in the literature (often in Japanese) to convey a

reasonably clear picture of the tunnel, earthquake, ground conditions, and nature of the damage. The table summarizes information pertaining to tunnel location, use, length, cross-section, lining, geology, overburden, and damage observed either at, within, or beyond 30 m from the portals.

Collapse (damage state 4 in Table C-5) beyond 30 m from the portals was observed in the absence of landslides and faulting at a few tunnels, mostly in the 1923 Kanto earthquake. In all instances, the length of tunnel that experienced collapse was relatively small, ranging from 1.5 to 60 m. The following describes specific tunnel failures:

- The Mineokayama Tunnel (also see also EQID 10 in Table C-2) was under construction during the earthquake, and the collapse occurred in one of the drifts. The type and quantity of temporary support used in the drift were not reported.

- The Yose Railroad Tunnel (also see EQID 19 in Table C-2) was driven in soil for a length of 293 m at a distance from the epicenter of 48 km. The brick masonry lining was 46-69 cm thick, with soil cover ranging mostly from 4 to 21 m. The JMA intensity was V-VI. During construction in 1900, water inflow attributed to a heavy rainfall resulted in the collapse of a 20-m-long section. During the Kanto earthquake, a 60-m-long section collapsed that included the section that failed during construction. The collapsed section was about 55 m from the closest portal.

- The Toke Railroad Tunnel was driven in mudstone for a length of 353 m at a distance of 106 km from the epicenter, The brick masonry lining was 34-46 cm thick, with an overburden of 12 to 20 m. The JMA intensity was IV. There were significant inflows of water into the tunnel that persisted from the time of its construction in 1894-95. During the Kanto earthquake, a section of the brick arch, 2.7 m wide and 5.5 m long, failed, causing 90 m^3 of rock and soil to collapse into the tunnel.

C.5.2 Noto Peninsular Offshore, Japan 1993 Earthquake

Tunnel collapses have been reported more recently for Japanese earthquakes. For example, Kunita, et al. (1994) report on the collapse of the Kinoura Tunnel as a result of the Noto Peninsular Offshore earthquake of 1993. The earthquake magnitude was 6.8, and the tunnel was located 26 km from the epicenter with a JMA intensity of approximately V. This road tunnel was driven in 1965 through alternating strata of tuff and mudstone. The 76-m-long horseshoe-shaped tunnel was 6 m wide and about 4 m high. Timber supports were used during construction, and the final lining was composed of 30-cm-thick concrete. It appears that the lining was unreinforced. After the main shock, a 4.5 x 4.5 m section of the arch lining collapsed at a distance of 21 m form the nearest portal. An aftershock caused the fall zone to expand, and two days after the main shock the tunnel was almost completely blocked with debris.

C.5.3 Kobe, Japan 1994 Earthquake

During the 1994 Kobe earthquake the cut-and-cover tunnel at the Daikai Subway Station collapsed catastrophically. It appears that this is the only instance of tunnel collapse as a result of the Kobe earthquake. The performance of the Daikai Station has been covered in the technical literature. Shear distortion from vertically propagating shear waves caused hinge formation where the central reinforced concrete columns were connected to the roof and invert. There was a lack of adequate confining steel in the central columns, which helped to promote column failure. See Figure C-4.

C.5.4 Duzce, Turkey 1999 Earthquake

Twin tunnels, each 18 m in excavated diameter, were significantly adversely affected by the 1999 Duzce (Turkey) earthquake. They are located on Gurnosova-Gerede portion of the Northern Anatolian Motorway. The tunnels were being driven in a faulted and deformed sequence of rocks, including flysch, shale, sandstone, marble, granite, and amphibolite. Tunneling was performed according to NATM principles, with shotcrete, rock bolts, and light steel sets. The epicenter of the M_w 7.2 earthquake was located about 20 km from the western portals of the tunnels. The surface rupture of the causative fault was within 3 km of these portals. Peak acceleration and velocity recorded at the nearest strong motion station at Bolu (6 km from the causative fault) were 0.81 g and 66 cm/s, respectively. Observations show that the tunnels performed remarkably well, especially in light of their close proximity to the seismic source. Some of the temporary shotcrtete-supported sections, however, collapsed where the worst ground conditions were located, and these sections are discussed below.

- Adjacent twin sections collapsed in a fault zone with weak, intensely slickensided clay gouge and crushed metacrystalline rock with the consistency of silty clay. About 300-m-long sections were affected by full or partial collapse, each located approximated 240 m from the western portals. The tunnels in this location were supported with a 75-mm-thick shotcrete lining with rock bolts and light steel sets. Substantial deformation had been observed in these sections of the tunnel during construction, and it is likely that the initial lining had been subjected to considerable stress under static conditions.

- Partial collapse and severe initial lining deformation was observed near tunnel headings being driven from the eastern portals at the opposite end of the 3.3-km-long highway tunnel. Five-meter-diameter tunnels were being driven as pilot bench tunnels along opposite sides of each 18-m-diameter highway tunnel. The intention was to drive the smaller tunnels initially through a fault zone, and then partially fill them with concrete to act as reaction blocks for the shotcrete arch installed as the remaining parts of the heading were excavated. Each pilot bore tunnel was supported with a 30-cm-thick shotcrete lining, patterned rock bolts, and light steel sets. The pilot bores were driven in a fault zone with weak, intensely slickensided clay gouge. Thirty-meter-long sections of the pilot bores were affected by significant invert heave, ruptured and partially collapsed shotcrete, and buckled steel sets.

C.5.5 Summary Observations

Full or partial collapse of tunnels resulting from earthquakes has occurred under highly localized conditions, involving weak, wet, and highly fractured rock and soil. Collapse has been confined to relatively short sections of tunnel. In Japan, tunnel collapse has occurred in linings with unreinforced masonry or unreinforced concrete. Failure of the Daikai Subway Station (cut and cover tunnel) involved the failure of reinforced concrete columns with inadequate confining steel. The collapsed tunnel sections in Turkey are located in weak, highly fractured clay gouge where construction was in progress and only the initial support system had been installed.

Both the Daikai Subway Station and Bolu Highway Tunnel were affected by near source ground motions, involving high pulses of acceleration and velocity. Peak acceleration and velocity measured at the Kobe Marine Meteorological Observatory (KMMO), which was within several km of the Dakai Station, were 0.81 g and 84 cm/s, respectively. The strong motion recordings at Bolu, which were taken at distances comparable to those separating the Daikai Station and KMMO, show peak acceleration and velocity of 0.81 g and 66 cm/s.

Tunnel damage in these instances is associated with high velocity that would have promoted high transient ground strains.

Accelerations inferred from JMA intensities are much less reliable than strong motion recordings. The accelerations estimated in this way from Table C-5 for the Yose, Toke, and Kinoura Tunnels are 0.25-0.40 g, 0.025-0.08 g, and 0.08-0.25 g, respectively.

In summary, there are two aspects of the strong motion that deserve attention. First, the near source ground motion affecting the Daikai Station and Bolu Tunnel was high. Although both structures were influenced either by remarkably poor ground (Bolu Tunnels) or weakness in structural support (Daikai Station), they were nonetheless subjected to significant peak velocities. Collapsed tunnels, affected by the Kanto and Noto Peninsular Offshore earthquakes, were apparently subjected to a wide range of accelerations, some of which were relatively small. The most prominent features of these tunnels affecting their seismic vulnerability appears to be poor ground conditions in combination with an unreinforced masonry or concrete lining. It seems reasonable, therefore, to conclude that poor ground and weak lining conditions are the most important factors affecting seismic performance leading to moderate to heavy damage. Strong motion in the near field can supply significant excitation that will promote local collapse in tunnel sections influenced by poor ground and lack of either sufficient or final structural support.

C.6 Empirical Basis of the Tunnel Fragility Curves

Table C-2 presents the database of tunnels used in the development of fragility curves presented in Section 6-3 of the main report. Table C-15 summarizes this dataset.

PGA (g)	All Tunnels	DS = 1	DS = 2	DS = 3	DS = 4
0.07	30	30	0	0	0
0.14	19	18	1	0	0
0.25	22	19	2	0	1
0.37	15	14	0	0	1
0.45	44	36	6	2	0
0.57	66	44	12	9	1
0.67	19	3	7	8	1
0.73	2	0	0	2	0
Total	217	164	28	21	4

Table C-15. Complete Bored Tunnel Database (Summary of Table C-2)

Tables C-16 through C-19 summarizes the dataset for based on bored tunnels with specific liner systems. Note that for a tunnel with multiple liner systems, the tunnel is classified according to the "best" liner type in the tunnel, according to the following ranking: unlined, timber / masonry / brick, unreinforced concrete, reinforced concrete / steel.

PGA (g)	Unlined Tunnels	DS = 1	DS = 2	DS = 3	DS = 4
0.05	5	5	0	0	0
0.13	4	4	0	0	0
0.25	10	9	1	0	0
0.35	2	1	0	0	1
0.42	2	0	2	0	0
0.55	2	0	1	1	0
0.66	2	0	1	1	0
0.73	1	0	0	1	0
Total	28	19	5	3	1

Table C-16. Unlined Bored Tunnels

PGA (g)	Timber or Masonry Lined Tunnels	DS = 1	DS = 2	DS = 3	DS = 4
0.26	2	1	0	0	1
0.40	1	1	0	0	1
0.42	4	3	1	0	0
0.60	2	0	0	2	0
0.67	5	0	1	4	0
Total	14	5	2	6	1

Table C-17. Bored Timber and Masonry / Brick Lined Tunnels

PGA (g)	Unreinforced Concrete Lined Tunnels	DS = 1	DS = 2	DS = 3	DS = 4
0.08	13	13	0	0	0
0.13	6	5	1	0	0
0.23	3	2	1	0	0
0.38	8	8	0	0	0
0.45	33	28	3	2	0
0.57	53	39	9	4	1
0.67	8	1	4	3	0
0.73	1	0	0	1	0
Total	125	96	18	10	1

Table C-18. Bored Unreinforced Concrete Lined Tunnels

PGA (g)	Reinforced Concrete / Steel Lined Tunnels	DS = 1	DS = 2	DS = 3	DS = 4
0.07	9	9	0	0	0
0.15	5	5	0	0	0
0.27	6	6	0	0	0
0.35	4	4	0	0	0
0.45	4	4	0	0	0
0.57	6	3	2	1	0
0.66	4	2	1	0	1
Total	38	33	3	1	1

Table C-19. Bored Reinforced Concrete or Steel Lined Tunnels

C.7 References

Asakura, T., and Sato, Y., Mountain tunnels damage in the 1995 Hyogoken-Naubu earthquake, QR of RTRI, Vol. 39, No. 1, 1998.

Dowding, C.H. and Rozen, A., "Damage to Rock Tunnels from Earthquake Shaking", *Journal of the Geotechnical Engineering Division*, American Society of Civil Engineers, New York, NY, Feb. 1978.

ASCE, "Evaluation of Seismic Fragility and Validation of Probabilistic Models", The Fragility Evaluation/Validation Subgroup Joint Working Group on Seismic PRA of the ASCE Dynamic Analysis Committee, Draft Report, April 1, 1985.

Chang, C.-Y., Power, M.S., Idriss, I.M., Somervile, P.G., Silva, W., and Chen, P.C., Engineering characterization of ground motion – Task II: Observational data on spatial variations of earthquake ground motion: Report prepared for U.S. Nuclear Regulatory Commission, NUREG/CR-3805, Vol. 3, 1986.

Dowding, C.H. and Rozen, A., "Damage to Rock Tunnels from Earthquake Shaking", *Journal of the Geotechnical Engineering Division*, American Society of Civil Engineers, New York, NY, Feb. 1978.

HAZUS, Earthquake Loss Estimation Methodology, Technical Manual, Volume II, prepared by the National Institute of Building Sciences for Federal Emergency Management Agency, 1997.

Kunita, M., Takemata, R., and Lai, Y., "Restoration of a tunnel damaged by earthquake," in Tunneling and Underground Space Technology, Vol. 9, No. 4, pp 439-448, 1994.

Kunita, M., et al., "Rehabilitation of Tunnel Damage caused by Noto Peninsula Offshore Earthquake," Tunnels and Underground, Vol.24, No.11, pp.7-13, 1993 (in Japanese).

McCann, M.W., Sauter, F., and Shah, H.C., "A Technical Note on PGA-Intensity Relationship with Applications to Damage Estimation", *BSSA*, Vol. 7, No. 2, pp 631-637, 1980.

O'Rourke, T.D. and Shiba, Y., Seismic performance and design of tunnels: Annual Report, MCEER Highway Project, Sponsored by U.S. Department of Transportation, Federal Highway Administration, FHWA Contract DTFH61-92-C-00106, 1997.

Owen, G.N. and Scholl, R.E., "Earthquake Engineering a of Large Underground Structures", Federal Highway Administration and National Science Foundation, FHWA/RD-80/195, Jan. 1981.

Power, M.S., Rosidi, D., and Kaneshiro, J., Gilstrap, S.D., and Chiou, S.J., Summary and evaluation of procedures for the seismic design of tunnels. Multidisciplinary Center for Earthquake Engineering Research, Technical Report MCEER-98-XXXX. Draft Report, September, 1998.

Sadigh, K., Chang, C.-Y., Abrahamson, N.A., Chiou, S.-J., and Power, M.S., 1993, Specification of long-period ground motions: updated attenuation relationships for rock site conditions and adjustments factors for near-fault effects: Proceedings of Applied Technology Council Seminar on Seismic Isolation, Passive Energy Dissipation, and Active Control, Publication No. ATC-17-1 San Francisco, California, March 11-12, p. 59-70.

Sadigh, K., Chang, C.-Y., Egan, J.A. Makdisi, F.I., and Youngs, R.R., 1997, Atteunuation relationships for shallow crustal earthquakes based on California strong motion data: Seismological Research Letters, Vol. 68, No. 1, p. 180-189.

Sharma, S., and Judd, W.R., 1991, Underground opening damage from earthquakes: Engineering Geology, Vol. 30.

Woodward-Clyde Consultants, 1995, Personal communication.

Tunnel Number	PGA - with No Damage		Tunnel Number	PGA - With Slight Damage		Tunnel Number	PGA - With Moderate Damage
1	0.075		1	0.185		1	0.255
2	0.075		2	0.195		2	0.340
3	0.08		3	0.225		3	0.420
4	0.08		4	0.230		4	0.480
5	0.08		5	0.250		5	0.482
6	0.079		6	0.260		6	0.510
7	0.99		7	0.300		7	0.520
8	0.1		8	0.305		8	0.525
9	0.12		9	0.420		9	0.550
10	0.12		10	0.460		10	0.560
11	0.13		11	0.550		11	0.590
12	0.13		12	0.550		12	0.620
13	0.14		13	0.580		13	0.640
14	0.14		14	0.580		14	0.690
15	0.145		15	0.720		Mean	0.5130
16	0.15		Mean	0.3873		Std Dev	0.1163
17	0.16		Std Dev	0.1738			
18	0.16						
19	0.16					Tunnel Number	PGA - Portal Damage Only
20	0.16					1	0.515
21	0.165						
22	0.165						
23	0.17						
24	0.18						
25	0.185						
26	0.185						
27	0.19		Source Data				
28	0.19		Dowding, C.H. and Rozen, A.,				
29	0.19		"Damage to Rock Tunnels from Earthquake Shaking"				
30	0.19		Journal o fthe Geotechnical Engineering Division, ASCE, Feb. 1978				
31	0.2						
32	0.21						
33	0.21						
34	0.22						
35	0.22						
36	0.22						
37	0.24						
38	0.24						
39	0.31						
Mean	0.1834						
Std Dev	0.1429						

Damage State	Mean	Stnd Dev	CoVariance	Beta**2	Beta	A=-0.5 * BETA**2	Median = Mean * exp(A)
None	0.1834	0.1429	0.779	0.474	0.689	-0.2370	0.145
Minor	0.3873	0.1738	0.449	0.183	0.428	-0.0917	0.353
Moderate	0.5130	0.1163	0.227	0.050	0.224	-0.0251	0.500

Table C-1. Raw Data - Tunnel Fragility Curves

EQID	CASE	EQNAME	DATE	Mw	TNAME	OWNER	FUN	LINER SYSTEM	ROCK SOIL	COVER (M)	PGA (G)	DS	REFERENCE, NOTES
1	1-1	San Francisco, CA	18/4/06	7.8	SF #1	SPRR	RR	4	R	24	0.41	1	Sharma & Judd, 1991
2	1-2	San Francisco, CA	18/4/06	7.8	SF #3	SPRR	RR	4	R	46	0.41	1	Sharma & Judd, 1991
3	1-3	San Francisco, CA	18/4/06	7.8	SF #4	SPRR	RR	4	R	24	0.43	1	Sharma & Judd, 1991
4	1-4	San Francisco, CA	18/4/06	7.8	SF #5	SPRR	RR	4	R	24	0.45	2	Sharma & Judd, 1991
5	1-5	San Francisco, CA	18/4/06	7.8	Corte M. T.	NPC	RR	1	R	60	0.38	1	Sharma & Judd, 1991
6	1-6	San Francisco, CA	18/4/06	7.8	Pilarcitos Res #1	SFWD	WT	4	R	68	0.65	1-3	Schussler, H., 1906
7	1-7	San Francisco, CA	18/4/06	7.8	Pilarcitos Res #2	SFWD	WT	4	R	152	0.65	1-3	Schussler, H., 1906
8	1-8	San Francisco, CA	18/4/06	7.8	Pilarcitos Res #3	SFWD	WT	4	R	137	0.69	1-3	Schussler, H., 1906
9	2-1	Kanto, Japan	1/10/27	7.9	Nagoye	Nat. RW	RR	1		30	0.40	2	Sharma & Judd, 1991
10	2-2	Kanto, Japan	1/10/27	7.9	Meno-Kamiana	Nat. RW	RR	4	R	17	0.60	3	Sharma & Judd, 1991
11	2-3	Kanto, Japan	1/10/27	7.9	Yonegami Yama	Nat. RW	RR	4		50	0.66	2	Sharma & Judd, 1991
12	2-4	Kanto, Japan	1/10/27	7.9	Shimomaki Matsu	Nat. RW	RR	4		29	0.69	3	Sharma & Judd, 1991
13	2-5	Kanto, Japan	1/10/27	7.9	Happon-Matzu	Nat. RW	RR	1	S	20	0.73	3	Sharma & Judd, 1991
14	2-6	Kanto, Japan	1/10/27	7.9	Nagasha-Yama	Nat. RW	RR	4-5		90	0.73	3	Sharma & Judd, 1991
15	2-7	Kanto, Japan	1/10/27	7.9	Hakone #1	Nat. RW	RR	1		61	0.44	2	Sharma & Judd, 1991
16	2-8	Kanto, Japan	1/10/27	7.9	Hakone #3	Nat. RW	RR	1		46	0.56	3	Sharma & Judd, 1991
17	2-9	Kanto, Japan	1/10/27	7.9	Hakone #4	Nat. RW	RR	1		46	0.54	2	Sharma & Judd, 1991
18	2-10	Kanto, Japan	1/10/27	7.9	Hakone #7	Nat. RW	RR	1	R	31	0.63	3	Sharma & Judd, 1991
19	2-11	Kanto, Japan	1/10/27	7.9	Yose	Nat. RW	RR	1	R	20	0.33	4	Sharma & Judd, 1991
20	2-12	Kanto, Japan	1/10/27	7.9	Doki	Nat. RW	RR	4			0.25	4	Sharma & Judd, 1991
21	2-13	Kanto, Japan	1/10/27	7.9	Namuya	Nat. RW	RR	5		75	0.52	4	Sharma & Judd, 1991
22	3-1	Kern County, CA	21/7/52	7.4	Saugus	SPRR	RR	1	R	40	0.06	1	Sharma & Judd, 1991
23	3-2	Kern County, CA	21/7/52	7.4	San Francisquito	SPRR	RR	1	R	160	0.08	1	Sharma & Judd, 1991
24	3-3	Kern County, CA	21/7/52	7.4	Elizabeth	SPRR	RR	1	R	250	0.10	1	Sharma & Judd, 1991
25	3-4	Kern County, CA	21/7/52	7.4	Antelope	SPRR	RR	1	R	30	0.16	1	Sharma & Judd, 1991
26	4-1	Alaska	27/3/64	8.4	Whittier #1		RR	1	R	400	0.22	2	Sharma & Judd, 1991
27	4-2	Alaska	27/3/64	8.4	Whittier #2		RR	1	R	350	0.21	1	Sharma & Judd, 1991
28	4-3	Alaska	27/3/64	8.4	Seward #1		RR	1	R	20	0.25	1	Sharma & Judd, 1991
29	4-4	Alaska	27/3/64	8.4	Seward #2		RR	1	R	20	0.25	1	Sharma & Judd, 1991
30	4-5	Alaska	27/3/64	8.4	Seward #3		RR	1	R	20	0.25	1	Sharma & Judd, 1991
31	4-6	Alaska	27/3/64	8.4	Seward #4		RR	1	R	20	0.25	1	Sharma & Judd, 1991
32	4-7	Alaska	27/3/64	8.4	Seward #5		RR	1	R	20	0.25	1	Sharma & Judd, 1991
33	4-8	Alaska	27/3/64	8.4	Seward #6		RR	1	R	20	0.25	1	Sharma & Judd, 1991
34	5-1	San Fernando, CA	9/3/75	6.6	San Fernando	MWD	WT	5-6-7	S	45	0.69	2	Sharma & Judd, 1991
35	5-2	San Fernando, CA	9/3/75	6.6	Tehachapi #1	SPRR	RR	1	R	30	0.04	1	Sharma & Judd, 1991
36	5-3	San Fernando, CA	9/3/75	6.6	Tehachapi #2	SPRR	RR	1	R	30	0.04	1	Sharma & Judd, 1991
37	5-4	San Fernando, CA	9/3/75	6.6	Tehachapi #3	SPRR	RR	1	R	30	0.04	1	Sharma & Judd, 1991
38	5-5	San Fernando, CA	9/3/75	6.6	Saugus	SPRR	RR	1	R	40	0.30	1	Sharma & Judd, 1991
39	5-6	San Fernando, CA	9/3/75	6.6	San Francisquito	SPRR	RR	1	R	160	0.24	1	Sharma & Judd, 1991
40	5-7	San Fernando, CA	9/3/75	6.6	Elizabeth	SPRR	RR	1	R	250	0.15	1	Sharma & Judd, 1991
41	5-8	San Fernando, CA	9/3/75	6.6	Antelope	SPRR	RR	1	R	30	0.10	1	Sharma & Judd, 1991
42	5-9	San Fernando, CA	9/3/75	6.6	Pacoima Dam		WT	1	R	43	0.69	2	Sharma & Judd, 1991
43	6-1	Loma Prieta, CA	17/10/89	7.1	Fort Baker-Berry	NPS	HW	5	R	61	0.04	1	COE, NPS
44	6-2	Loma Prieta, CA	17/10/89	7.1	Presidio Park	Caltrans	HW	6	R	22	0.04	1	Yashinsky, 1998
45	6-3	Loma Prieta, CA	17/10/89	7.1	Alameda Creek Div	SFWD	WT			300	0.12	1	SFWD
46	6-4	Loma Prieta, CA	17/10/89	7.1	Coast Range	SFWD	WT	5	R	240	0.09	1	SFWD
47	6-5	Loma Prieta, CA	17/10/89	7.1	Pulgas	SFWD	WT	5	R	92	0.09	1	SFWD
48	6-6	Loma Prieta, CA	17/10/89	7.1	Irvington	SFWD	WT	5	R	122	0.10	1	SFWD
49	6-7	Loma Prieta, CA	17/10/89	7.1	Crystal Spr Baypass	SFWD	WT	5-6-7	R	76	0.09	1	SFWD
50	6-8	Loma Prieta, CA	17/10/89	7.1	Downtown S.F.	Caltrain	RR		R		0.05	1	
51	6-9	Loma Prieta, CA	17/10/89	7.1	Stanford Linear Collider	SU	AC	5	R		0.25	1	Rose, 1990; Fisher, 1989
52	6-10	Loma Prieta, CA	17/10/89	7.1	Lomita Mall			5	S		0.14	1	Kaneshiro, 1989
53	6-11	Loma Prieta, CA	17/10/89	7.1	Santa Teresa	SCVWD	WT	7	R		0.26	1	SCVWD
54	6-12	Loma Prieta, CA	17/10/89	7.1	Tunnel #5	SC,BT,PRR	RR	3	R		0.40	1	SC,BT,PR
55	6-13	Loma Prieta, CA	17/10/89	7.1	Tunnel #6	SC,BT,PRR	RR	3	R		0.28	1	SC,BT,PR
56	6-14	Loma Prieta, CA	17/10/89	7.1	Caldecott	Caltrans	HW	6	R	243	0.04	1	Yashinsky, 1998
57	6-15	Loma Prieta, CA	17/10/89	7.1	MacArthur	Caltrans	HW		R	46	0.04	1	Yashinsky, 1998
58	6-16	Loma Prieta, CA	17/10/89	7.1	Stanford	SFWD	WT	5-7	R	23	0.14	1	SFWD
59	6-17	Loma Prieta, CA	17/10/89	7.1	Hillsborough	SFWD	WT	5-7	R	62	0.08	1	SFWD

Table C-2. Bored Tunnel Seismic Performance Database (Page 1 of 4)

EQID	CASE	EQNAME	DATE	Mw	TNAME	OWNER	FUN	LINER SYSTEM	ROCK SOIL	COVER (M)	PGA (G)	DS	REFERENCE, NOTES
60	6-18	Loma Prieta, CA	17/10/89	7.1	Sunol Aqud. #1	SFWD	WT	5	R		0.09	1	SFWD
61	6-19	Loma Prieta, CA	17/10/89	7.1	Sunol Aqud. #2	SFWD	WT	5	R		0.09	1	SFWD
62	6-20	Loma Prieta, CA	17/10/89	7.1	Sunol Aqud. #3	SFWD	WT	5	R		0.09	1	SFWD
63	6-21	Loma Prieta, CA	17/10/89	7.1	Sunol Aqud. #4	SFWD	WT	5	R		0.09	1	SFWD
64	6-22	Loma Prieta, CA	17/10/89	7.1	Sunol Aqud. #5	SFWD	WT	5	R		0.09	1	SFWD
65	7-1	Petrolia, CA	25/4/92	6.9	Tunnel #40	NCRR	RR	5	S		0.13	1	NCRR
66	7-2	Petrolia, CA	25/4/92	6.9	Tunnel #39	NCRR	RR	5-3	R		0.25	1	NCRR
67	7-3	Petrolia, CA	25/4/92	6.9	Tunnel #38	NCRR	RR	5-3	R		0.21	2	NCRR
68	7-4	Petrolia, CA	25/4/92	6.9	Tunnel #37	NCRR	RR	5	R		0.15	1	NCRR
69	7-5	Petrolia, CA	25/4/92	6.9	Tunnel #36	NCRR	RR	5-3	R		0.13	1	NCRR
70	7-6	Petrolia, CA	25/4/92	6.9	Tunnel #35	NCRR	RR	5-3	R		0.12	1	NCRR
71	7-7	Petrolia, CA	25/4/92	6.9	Tunnel #34	NCRR	RR	5-3	R		0.12	2	NCRR
72	7-8	Petrolia, CA	25/4/92	6.9	Tunnel #31	NCRR	RR	5-3	R		0.08	1	NCRR
73	7-9	Petrolia, CA	25/4/92	6.9	Tunnel #30	NCRR	RR	5	R		0.08	1	NCRR
74	7-10	Petrolia, CA	25/4/92	6.9	Tunnel #29	NCRR	RR	5	R		0.06	1	NCRR
75	7-11	Petrolia, CA	25/4/92	6.9	Tunnel #28	NCRR	RR	5-3	R		0.06	1	NCRR
76	8-1	Hokkaido, Japan	0/0/93	7.8	Seikan		HW	6			0.32	1	JTA, 1994
77	9-1	Northridge, CA	17/1/94	6.7	Pershing Sq St.	LAMT	RR	6	R		0.27	1	Tunnels & Tunneling, 1994
78	9-2	Northridge, CA	17/1/94	6.7	McArthur St.	LAMT	RR	6	R		0.27	1	Tunnels & Tunneling, 1994
79	9-3	Northridge, CA	17/1/94	6.7	Civic Center St.	LAMT	RR	6	R		0.27	1	Tunnels & Tunneling, 1994
80	9-4	Northridge, CA	17/1/94	6.7	Tun# 25 @ I-5/14	SPRR	RR	5	R	92	0.67	2	METROLINK
81	9-5	Northridge, CA	17/1/94	6.7	Santa Susana	SPRR	RR	5	R		0.47	1	SPRR
82	9-6	Northridge, CA	17/1/94	6.7	Chatworth	SPRR	RR	5	R		0.50	1	SPRR
83	9-7	Northridge, CA	17/1/94	6.7	Chatworth	SPRR	RR	5	R		0.50	1	SPRR
84	9-8	Northridge, CA	17/1/94	6.7	Near I15 at Cajon Junc	ATSF	RR		R		0.10	1	ATSF
85	9-9	Northridge, CA	17/1/94	6.7	Balboa inlet	MWD	WT	2-5-6-7	R		0.67	1	MWD
86	9-10	Northridge, CA	17/1/94	6.7	Balboa outlet	MWD	WT		R		0.58	1	MWD
87	9-11	Northridge, CA	17/1/94	6.7	Castaic #1	MWD	WT	6-7	R		0.29	1	MWD
88	9-12	Northridge, CA	17/1/94	6.7	Castaic #2	MWD	WT	6-7	R		0.36	1	MWD
89	9-13	Northridge, CA	17/1/94	6.7	Saugus	MWD	WT	6-7	S		0.54	1	MWD
90	9-14	Northridge, CA	17/1/94	6.7	Placerita	MWD	WT	6-7	R		0.62	1	MWD
91	9-15	Northridge, CA	17/1/94	6.7	Newhall	MWD	WT	2-5-6-7	R		0.68	3-4	MWD. Damage attributed to fluid pressure buildup behind tunnel and not to earthquake shaking
92	9-16	Northridge, CA	17/1/94	6.7	San Fernando	MWD	WT	5-6-7	R/S		0.50	1	MWD
93	9-17	Northridge, CA	17/1/94	6.7	Sepulveda	MWD	WT	5-7	R		0.27	1	MWD
94	9-18	Northridge, CA	17/1/94	6.7	Hollywood	MWD	WT		R		0.22	1	MWD
95	9-19	Northridge, CA	17/1/94	6.7	San Rafael #1	MWD	WT	6	R		0.16	1	MWD
96	9-20	Northridge, CA	17/1/94	6.7	San Rafael #2	MWD	WT	6	R		0.18	1	MWD
97	9-21	Northridge, CA	17/1/94	6.7	Pasadena	MWD	WT	6	S		0.15	1	MWD
98	9-22	Northridge, CA	17/1/94	6.7	Siera Madre	MWD	WT		S		0.13	1	MWD
99	9-23	Northridge, CA	17/1/94	6.7	Monrovia #1, #2	MWD	WT	5-6	R		0.09	1	MWD
100	9-24	Northridge, CA	17/1/94	6.7	Monrovia #3	MWD	WT	5-6	R		0.10	1	MWD
101	9-25	Northridge, CA	17/1/94	6.7	Monrovia #4	MWD	WT	5-6	R		0.10	1	MWD
102	9-26	Northridge, CA	17/1/94	6.7	Glendora	MWD	WT	2-5-6-7	R/S		0.07	1	MWD
103	9-27	Northridge, CA	17/1/94	6.7	Oakhill	MWD	WT		R		0.15	1	MWD
104	9-28	Northridge, CA	17/1/94	6.7	Ascat	MWD	WT		R		0.14	1	MWD
105	9-29	Northridge, CA	17/1/94	6.7	Tonner #1	MWD	WT	5-7	R		0.06	1	MWD
106	9-30	Northridge, CA	17/1/94	6.7	Tonner #2	MWD	WT	5-7	R		0.06	1	MWD
107	9-31	Northridge, CA	17/1/94	6.7	LA Aqueduct	LADWP	WT	5		46	0.67	2	LADWP
108	10-1	Kobe, Japan	17/1/95	6.9	Rokkou (#1)	JRN	RR	5		460	0.60	3	Geo. Eng. Assn., 1996
109	10-2	Kobe, Japan	17/1/95	6.9	Kobe (#2)	JRN	RR	5		272	0.57	2	Geo. Eng. Assn., 1996
110	10-3	Kobe, Japan	17/1/95	6.9	Suma (#3)	JRN	RR	5		45	0.53	1	Geo. Eng. Assn., 1996
111	10-4	Kobe, Japan	17/1/95	6.9	Okuhata (#4)	JRN	RR	5		90	0.50	1	Geo. Eng. Assn., 1996
112	10-5	Kobe, Japan	17/1/95	6.9	Takatsukay(#5)	JRN	RR	5		85	0.49	1	Geo. Eng. Assn., 1996
113	10-6	Kobe, Japan	17/1/95	6.9	Nagasaka (#6)	JRN	RR	5		20	0.48	2	Geo. Eng. Assn., 1996
114	10-7	Kobe, Japan	17/1/95	6.9	Daiichinas (#7)	JRN	RR	5		150	0.55	1	Geo. Eng. Assn., 1996
115	10-8	Kobe, Japan	17/1/95	6.9	Ikuse (#8)	JRN	RR	5		250	0.57	1	Geo. Eng. Assn., 1996
116	10-9	Kobe, Japan	17/1/95	6.9	Daiichitaked(#9)	JRN	RR	5		95	0.43	1	Geo. Eng. Assn., 1996

Table C-2. Bored Tunnel Seismic Performance Database (Page 2 of 4)

EQID	CASE	EQNAME	DATE	Mw	TNAME	OWNER	FUN	LINER SYSTEM	ROCK SOIL	COVER (M)	PGA (G)	DS	REFERENCE, NOTES
117	10-10	Kobe, Japan	17/1/95	6.9	Arima (#12)	KBD	RR	5		25	0.46	3	Geo. Eng. Assn., 1996
118	10-11	Kobe, Japan	17/1/95	6.9	Gosha (#13)	KBD	RR	5		40	0.41	1	Geo. Eng. Assn., 1996
119	10-12	Kobe, Japan	17/1/95	6.9	Kitakami (#14)	HOE	RR	6		350	0.51	3	Geo. Eng. Assn., 1996
120	10-13	Kobe, Japan	17/1/95	6.9	Iwataki (#15)	HRP	HW	5		135	0.58	3	Geo. Eng. Assn., 1996
121	10-14	Kobe, Japan	17/1/95	6.9	Nunohiki(#18)	MRP	HW	5		260	0.58	3	Geo. Eng. Assn., 1996
122	10-15	Kobe, Japan	17/1/95	6.9	Daini Nun (#19)	MRP	HW	5		240	0.58	2	Geo. Eng. Assn., 1996
123	10-16	Kobe, Japan	17/1/95	6.9	Hirano (#20)	MRP	HW	5		85	0.58	1	Geo. Eng. Assn., 1996
124	10-17	Kobe, Japan	17/1/95	6.9	K. Daiichi (#21)	MRP	HW	5		32	0.58	1	Geo. Eng. Assn., 1996
125	10-18	Kobe, Japan	17/1/95	6.9	K. Daini (#22)	MRP	HW	5		25	0.58	1	Geo. Eng. Assn., 1996
126	10-19	Kobe, Japan	17/1/95	6.9	Kamoetsu 1(#23)	MRP	HW	5		29	0.55	1	Geo. Eng. Assn., 1996
127	10-20	Kobe, Japan	17/1/95	6.9	Kamoetsu 2(#24)	MRP	HW	5		40	0.55	2	Geo. Eng. Assn., 1996
128	10-21	Kobe, Japan	17/1/95	6.9	Kamoetsu 3(#25)	MRP	HW	5		47	0.55	2	Geo. Eng. Assn., 1996
129	10-22	Kobe, Japan	17/1/95	6.9	Hiyodori (#26)	MRP	HW	5		40	0.54	1	Geo. Eng. Assn., 1996
130	10-23	Kobe, Japan	17/1/95	6.9	Shin-kobe 1(#27)	MRP	HW	5		330	0.49	2	Geo. Eng. Assn., 1996
131	10-24	Kobe, Japan	17/1/95	6.9	Shin-kobe 2(#28)	MRP	HW	5		330	0.49	2	Geo. Eng. Assn., 1996
132	10-25	Kobe, Japan	17/1/95	6.9	Karaki (#29)	MRP	HW	5		145	0.42	3	Geo. Eng. Assn., 1996
133	10-26	Kobe, Japan	17/1/95	6.9	Arino 1 (#30)	MRP	HW	5		25	0.39	1	Geo. Eng. Assn., 1996
134	10-27	Kobe, Japan	17/1/95	6.9	Arino 2 (#31)	MRP	HW	5		35	0.38	1	Geo. Eng. Assn., 1996
135	10-28	Kobe, Japan	17/1/95	6.9	Rokkousan (#32)	MRP	HW	5		280	0.51	2	Geo. Eng. Assn., 1996
136	10-29	Kobe, Japan	17/1/95	6.9	Shinohara (#33)	MRP	HW	5		15	0.55	1	Geo. Eng. Assn., 1996
137	10-30	Kobe, Japan	17/1/95	6.9	Hiyodori (#34)	MRP	HW	5		67	0.59	2	Geo. Eng. Assn., 1996
138	10-31	Kobe, Japan	17/1/95	6.9	Suma (#36)	CDO		5		140	0.44	1	Geo. Eng. Assn., 1996
139	10-32	Kobe, Japan	17/1/95	6.9	Suma ext (#37)	CDO		5			0.58	1	Geo. Eng. Assn., 1996
140	10-33	Kobe, Japan	17/1/95	6.9	Ibuki (#38)	HHP	HW	5		20	0.43	1	Geo. Eng. Assn., 1996
141	10-34	Kobe, Japan	17/1/95	6.9	Taizanji,1E(#39)	HHP	HW	5		53	0.44	1	Geo. Eng. Assn., 1996
142	10-35	Kobe, Japan	17/1/95	6.9	Taizanji,1W(#40)	HHP	HW	5		37	0.44	1	Geo. Eng. Assn., 1996
143	10-36	Kobe, Japan	17/1/95	6.9	Taizanji,2E(#41)	HHP	HW	5		25	0.45	1	Geo. Eng. Assn., 1996
144	10-37	Kobe, Japan	17/1/95	6.9	Taizanji,2W(#42)	HHP	HW	5		17	0.45	1	Geo. Eng. Assn., 1996
145	10-38	Kobe, Japan	17/1/95	6.9	Aina, E(#43)	HHP	HW	5		68	0.46	1	Geo. Eng. Assn., 1996
146	10-39	Kobe, Japan	17/1/95	6.9	Aina, W(#44)	HHP	HW	5		65	0.46	1	Geo. Eng. Assn., 1996
147	10-40	Kobe, Japan	17/1/95	6.9	Nagasaka.,E(#45)	HHP	HW	5		68	0.42	1	Geo. Eng. Assn., 1996
148	10-41	Kobe, Japan	17/1/95	6.9	Nagasaka.,W(#46)	HHP	HW	5		68	0.42	1	Geo. Eng. Assn., 1996
149	10-42	Kobe, Japan	17/1/95	6.9	T.Higa.,TOK(#47)	JHP	HW	5		62	0.58	1	Geo. Eng. Assn., 1996
150	10-43	Kobe, Japan	17/1/95	6.9	T.Higa.,KYU(#48)	JHP	HW	5		59	0.58	1	Geo. Eng. Assn., 1996
151	10-44	Kobe, Japan	17/1/95	6.9	T.Nishi,TOK(#49)	JHP	HW	5		42	0.57	1	Geo. Eng. Assn., 1996
152	10-45	Kobe, Japan	17/1/95	6.9	T.Nishi,KYU(#50)	JHP	HW	5		42	0.57	1	Geo. Eng. Assn., 1996
153	10-46	Kobe, Japan	17/1/95	6.9	Takak.,1TOK(#51)	JHP	HW	5		97	0.59	1	Geo. Eng. Assn., 1996
154	10-47	Kobe, Japan	17/1/95	6.9	Takak.,2TOK(#52)	JHP	HW	5		86	0.59	1	Geo. Eng. Assn., 1996
155	10-48	Kobe, Japan	17/1/95	6.9	Takak.,KYU(#53)	JHP	HW	5		87	0.59	1	Geo. Eng. Assn., 1996
156	10-49	Kobe, Japan	17/1/95	6.9	Tsuki.,TOK(#54)	JHP	HW	5		43	0.60	1	Geo. Eng. Assn., 1996
157	10-50	Kobe, Japan	17/1/95	6.9	Takak.,KYU(#55)	JHP	HW	5		34	0.60	1	Geo. Eng. Assn., 1996
158	10-51	Kobe, Japan	17/1/95	6.9	Omoteyama 1(#61)	KTB	RR	5		41	0.41	1	Geo. Eng. Assn., 1996
159	10-52	Kobe, Japan	17/1/95	6.9	Ochiai (#63)	KTB	RR	5			0.56	1	Geo. Eng. Assn., 1996
160	10-53	Kobe, Japan	17/1/95	6.9	Yokoo, 1 (#64)	KTB	RR	5			0.59	1	Geo. Eng. Assn., 1996
161	10-54	Kobe, Japan	17/1/95	6.9	Yokoo, 2 (#65)	KTB	RR	5			0.60	1	Geo. Eng. Assn., 1996
162	10-55	Kobe, Japan	17/1/95	6.9	Shiroyama (#66)	JRN	RR	5			0.58	1	Geo. Eng. Assn., 1996
163	10-56	Kobe, Japan	17/1/95	6.9	Nashio 2 (#67)	JRN	RR	5			0.48	1	Geo. Eng. Assn., 1996
164	10-57	Kobe, Japan	17/1/95	6.9	Takedo 2 (#68)	JRN	RR	5			0.40	1	Geo. Eng. Assn., 1996
165	10-58	Kobe, Japan	17/1/95	6.9	Douba 1 (#69)	JRN	RR	5			0.40	1	Geo. Eng. Assn., 1996
166	10-59	Kobe, Japan	17/1/95	6.9	Douba 2 (#70)	JRN	RR	5			0.37	1	Geo. Eng. Assn., 1996
167	10-60	Kobe, Japan	17/1/95	6.9	Douba 3 (#71)	JRN	RR	5			0.36	1	Geo. Eng. Assn., 1996
168	10-61	Kobe, Japan	17/1/95	6.9	Keietu (#76)	KBD	RR	5			0.58	1	Geo. Eng. Assn., 1996
169	10-62	Kobe, Japan	17/1/95	6.9	Nakayama(#77)	KBD	RR	5			0.58	1	Geo. Eng. Assn., 1996
170	10-63	Kobe, Japan	17/1/95	6.9	Kadoyama (#78)	KBD	RR	5			0.58	1	Geo. Eng. Assn., 1996
171	10-64	Kobe, Japan	17/1/95	6.9	Kudari (#79)	KBD	RR	5			0.54	1	Geo. Eng. Assn., 1996
172	10-65	Kobe, Japan	17/1/95	6.9	Kik, Nobori(#81)	KBD	RR	5			0.54	1	Geo. Eng. Assn., 1996
173	10-66	Kobe, Japan	17/1/95	6.9	Tanigami (#82)	KBD	RR	6			0.41	1	Geo. Eng. Assn., 1996
174	10-67	Kobe, Japan	17/1/95	6.9	Kobe (#84)	KBD	RR				0.56	1	Geo. Eng. Assn., 1996
175	10-68	Kobe, Japan	17/1/95	6.9	Aina (#85)	KBD	RR				0.48	1	Geo. Eng. Assn., 1996

Table C-2. Bored Tunnel Seismic Performance Database (Page 3 of 4)

EQID	CASE	EQNAME	DATE	Mw	TNAME	OWNER	FUN	LINER SYSTEM	ROCK SOIL	COVER (M)	PGA (G)	DS	REFERENCE, NOTES
176	10-69	Kobe, Japan	17/1/95	6.9	Tetsukaiy (#87)	MRP	HW	5		20	0.60	1	Geo. Eng. Assn., 1996
177	10-70	Kobe, Japan	17/1/95	6.9	Taisanji (#88)	MRP	HW	5		50	0.44	1	Geo. Eng. Assn., 1996
178	10-71	Kobe, Japan	17/1/95	6.9	Kaibara (#89)	MRP	HW	5		20	0.36	1	Geo. Eng. Assn., 1996
179	10-72	Kobe, Japan	17/1/95	6.9	Shimohata (#91)	MRP	HW	5		20	0.60	1	Geo. Eng. Assn., 1996
180	10-73	Kobe, Japan	17/1/95	6.9	Fukuchi (#92)	MRP	HW	5		20	0.36	1	Geo. Eng. Assn., 1996
181	10-74	Kobe, Japan	17/1/95	6.9	Sumadera (#93)	MRP	HW	5		15	0.60	1	Geo. Eng. Assn., 1996
182	10-75	Kobe, Japan	17/1/95	6.9	Shin Arima (#95)	MRP	HW	5		20	0.48	1	Geo. Eng. Assn., 1996
183	10-76	Kobe, Japan	17/1/95	6.9	HigashiAina(#96)	MRP	HW	5		10	0.43	1	Geo. Eng. Assn., 1996
184	10-77	Kobe, Japan	17/1/95	6.9	Fukuyama (#97)	MRP	HW	5		15	0.59	1	Geo. Eng. Assn., 1996
185	10-78	Kobe, Japan	17/1/95	6.9	Minoya (#98)	MRP	HW	5		20	0.40	1	Geo. Eng. Assn., 1996
186	10-79	Kobe, Japan	17/1/95	6.9	Iwayama (#99)	MRP	HW	5		30	0.56	1	Geo. Eng. Assn., 1996
187	10-80	Kobe, Japan	17/1/95	6.9	Tamasaka (#100)	MRP	HW	5		10	0.58	1	Geo. Eng. Assn., 1996
188	10-81	Kobe, Japan	17/1/95	6.9	Fukiage (#101)	MWB	HW	5		30	0.44	1	Geo. Eng. Assn., 1996
189	10-82	Kobe, Japan	17/1/95	6.9	Maesaki (#102)	MWB	HW	5		10	0.43	1	Geo. Eng. Assn., 1996
190	10-83	Kobe, Japan	17/1/95	6.9	Nishikou 2 (103)	MWB	HW	5		20	0.39	1	Geo. Eng. Assn., 1996
191	10-84	Kobe, Japan	17/1/95	6.9	Fusehatagami (104)	MWB	HW	5		30	0.47	1	Geo. Eng. Assn., 1996
192	10-85	Kobe, Japan	17/1/95	6.9	Fusehatashita (105)	MWB	HW	5		30	0.47	1	Geo. Eng. Assn., 1996
193	10-86	Kobe, Japan	17/1/95	6.9	Enoshitayama (109)		WT	4		37	0.60	3	Geo. Eng. Assn., 1996
194	10-87	Kobe, Japan	17/1/95	6.9	Motoyama (110)		WT			96	0.59	3	Geo. Eng. Assn., 1996
195	10-88	Kobe, Japan	17/1/95	6.9	N. of Itayada St.	KMS	RR	6			0.60	1	Japan Society of Civil Eng, 1995
196	10-89	Kobe, Japan	17/1/95	6.9	Near Natani	KMS	RR	5			0.60	1	Japan Society of Civil Eng, 1995
197	10-90	Kobe, Japan	17/1/95	6.9	Koigawa river		WT	6			0.60	1	Geo. Eng. Ass., 1996
198	10-91	Kobe, Japan	17/1/95	6.9	Hosoyadani		WT	5		6	0.59	1	Geo. Eng. Ass., 1996
199	10-92	Kobe, Japan	17/1/95	6.9	Sennomori		WT	5		30	0.59	2	Geo. Eng. Ass., 1996
200	10-93	Kobe, Japan	17/1/95	6.9	Shioyadani		WT	5		25	0.59	2	Geo. Eng. Ass., 1996
201	10-94	Kobe, Japan	17/1/95	6.9	Kabutoyama-Ashiya	HWC	WT	5		25	0.58	1	Geo. Eng. Ass., 1996
202	10-95	Kobe, Japan	17/1/95	6.9	Sannomiya St. 3		UT	6		25	0.59	2	Geo. Eng. Ass., 1996
203	10-96	Kobe. Japan	17/1/95	6.9	NTT @ Chuo-ku	NTT	UT	6	S		0.60	2	Japan Society of Civil Eng, 1995
204	10-97	Kobe. Japan	17/1/95	6.9	Kansai Electric	KEP	UT	5	S		0.60	2	Japan Society of Civil Eng, 1995
205		Kobe, Japan	17/1/95	6.9	HIGASHIYAMA (#10)	KER	RR	4, 5		4-8	0.70	3	Asakura and Sato, 1998
206		Kobe, Japan	17/1/95	6.9	EGEYAMA (#11)	KER	RR	4, 5		2-13	0.68	3	Asakura and Sato, 1998
207		Kobe, Japan	17/1/95	6.9	MAIKO (UP) (#16)	HSB	HW	5		4-50	0.62	2	Asakura and Sato, 1998
208		Kobe, Japan	17/1/95	6.9	MAIKO (DOWN) (#17)	HSB	HW	5		4-50	0.62	2	Asakura and Sato, 1998
209		Kobe, Japan	17/1/95	6.9	SHIOYA-DAN (#35)	KPW	HW	5		4-80	0.70	3	Asakura and Sato, 1998
210		Kobe, Japan	17/1/95	6.9	SEISHIN (2) (#58)	KTB	RR	6		7	0.36	1	Asakura and Sato, 1998
211		Kobe, Japan	17/1/95	6.9	SEISHIN (1) (#59)	KTB	RR	6		3	0.37	1	Asakura and Sato, 1998
212		Kobe, Japan	17/1/95	6.9	OMOTEYAMA (2) (#60)	KTB	RR	6			0.41	1	Asakura and Sato, 1998
213		Kobe, Japan	17/1/95	6.9	KODERA (#62)	KTB	RR	6		7	0.47	1	Asakura and Sato, 1998
214		Kobe, Japan	17/1/95	6.9	OBU (#86)	KPW	HW	5		50	0.55	1	Asakura and Sato, 1998
215		Kobe, Japan	17/1/95	6.9	AINA (#90)	KPW	HW	5		2	0.43	1	Asakura and Sato, 1998
216		Kobe, Japan	17/1/95	6.9	FUTATABI (#94)	KPW		5		20	0.70	1	Asakura and Sato, 1998
217		Kobe, Japan	17/1/95	6.9	SENGARI (#111)	KWS	WT	5		2-25	0.60	3	Asakura and Sato, 1998

Table C-2. Bored Tunnel Seismic Performance Database (Page 4 of 4)

Earthquake	Date and Time	Location of Epicenter	Magnitude, JMA Intensity	Area Most Severely Affected	Tunnel Performance	Selected References
1923 Kanto	Sep. 1 11:58 AM	Sagami Bay 139.3 E, 35.2 N (unknown)	7.90 VI	Kanagawa and Tokyo	Extensive, severest damage to more than 100 tunnels in southern Kanto area	JSCE [1984] Yoshikawa [1979]
1927 Kits-Tango	Mar. 7 6:27 PM	7 km WNW of Miyazu, Kyoto 135.15 E, 35.53 N (0)	7.30 VI	Joint section of Tango Peninsula	Very slight damage to 2 railroad tunnels in the epicentral region	Yoshikawa [1979] Yoshikawa [1984]
1930 Kita-Isu	Nov. 26 4:02 AM	7 km west of Atami, Shizuoka 139.0 E, 35.1 N (0)	7.30 VI	Northerm part of Izu Peninsula	Very severe damage to one railroad tunnel due to earthquake fault crossing	Yoshikawa [1979] Yoshikawa [1982]
1948 Fukui	June 28 4:13 PM	12 km north of Fukui City 136.20 E, 36.17 N (0)	7.10 VI	Fukui Plain	Severe damage to 2 railroad tunnels within 8 km from the earthquake fault	Yoshikawa [1979]
1952 Tokachi-oki	Mar. 4 10:23 AM	Pacific Ocean 90 km ESE of f the Cape Erimo 144.13 E, 41.80 N (0)	8.20 VI - V	Southern part of Hokkaido	Slight damage to 10 railroad tunnels in Hokkaido	Committee Report [1954] Yoshikawa [1979]
1961 Kita-Mino	Aug. 19 2:33 PM	Border of Fukui and Gifu Prefectures 136 46'E, 36 0l'N (0)	7.00 IV	Vicinity along the border of Fuikui and Gifu Prefs.	Cracking damage to a couple of aqueduct tunnels	Okamoto, et al. [1963] Okamoto [1973]
1964 Niigata	June 16 1:01 PM	Japan Sea 50 km NNE of Nugata City 139 ll'E, 38 21'N (40)	7.50 V - VI	Nugata City	Extensive damage to about 20 railroad tunnels and one road tunnel	JSCE [1966] Kawasumi [1968] Yoshikawa [1979]
1968 Tokachi-oki	May 16 9:49 AM	Pacific Ocean 140 km south off the Cape Erimo 143 35~E, 40 44~N (0)	7.90 V	Aomori Prefecture	Slight damage to 23 railroad tunnels in Hokkaido	Committee Report [1969]
1978 Izu-Oshima-kinkai	Jan. 14 12:24 PM	In the sea between Oshima Isl. and Inatori, Shizuoka 139 15'E, 34 46N (0)	7.00 V VI	South-eastern region of Izu Peninsula	Very severe damage to 9 railroad and 4 road tunnels in a limited area	Onoda, et al. [1978] Konda [1978] Yoshikawa [1979][(1982]
1978 Miyagiken-oki	June 12 5:14 PM	Pacific Ocean 115 km east of Sendai City, Miyagi 142 l0'E, 38 09~N (40)	7.40 V	Sendai City and vicinity	Slight damage to 6 railroad tunnels mainly existing in Miyagi Prefecture	Committee Report [1980]
1982 Urakawa-oki	Mar. 21 11:32 AM	Pcific Ocean 18 km SW of Urakawa, Hokkaido 142 36'E, 42 04'N (40)	7.10 IV - V	Urakawa-Cho and Shizunsi-Cho, southern Hokkaido	Slight damage to 6 railroad tunnels near Urakawa	Yoshikawa [1984]
1983 Nihonkai-chubu	May 26 11:59 AM	Japan Sea 90 km west of Noshiro City, Akita 139 04.6'E, 40 21.4'N (14)	7.70 V	Noshiro City and Oga City, Akita	Slight damage to 8 railroad tunnels in Akita, etc.	Yoshikawa [1984] JSCE [1986]
1984 Naganoken-seibu	Sep. 14 8:48 AM	9 km SE of Mt. Ontake, Nagano 137 33.6'E, 35 49.3'N (2)	6.80 VI - V	Otaki Village, Nagano	Cracking damage to one headrace tunnel	Matauda, et al. [1985]
1993 Notohanto-oki	Feb. 7 10:27 PM	Japan Sea 24 km north of Suzu City, Ishikawa 137 18'E, 37 39'N (25)	6.60 V	Suzu City	Severe damage to one road tunnel	Kitaura, et al. [1993] Kunita, et al. [1993]
1993 Hokkaido-nansei-oki	July 12 10:17 PM	Japan Sea 86 km west of Suttsu, Hokkaido 139 12'E, 42 47'N (34)	8 VI - V	Okushiri Isi. and south-western part of Hokkaido	Severe damage to one road tunnel due to a direct hit of falling rock	Miyajima, et al. [1993] Nishikawa, et al. [1993] JSEEP News [1993]

Table C-3. Tunnel Performance in Japanese Earthquakes

JMA	Intensity Scale	Definition	Acceleration (in gals)
0	No feeling	Shocks too weak to be felt by humans and registered only by seismographs.	< 0.8
I	Slight	Extremely feeble shocks felt only by persons at rest, or by those who are observant of earthquakes.	0.8 to 2.5
II	Weak	Shocks felt by most persons; slight shaking of doors and Japanese latticed sliding doors (shoji).	2.5 to 8
III	Rather Strong	Slight shaking of houses and buildings, rattling of doors and shoji, swinging of hanging objects like electric lamps, and moving of liquids in vessels.	8 to 25
IV	Strong	Strong shaking of houses and buildings, overturning of unstable objects, and spilling of liquids out of vessels	25 to 80
V	Very Strong	Cracks in sidewalks, overturning of gravestone and stone lanterns, etc.; damage to chimneys and mud and plaster warehouses	80 to 250
VI	Disastrous	Demolition of houses, but of less than 30% of the total, landslides, fissures in the ground.	250 to 400
VII	Very Disastrous	Demolition of more than 30% of the total number of houses, intense landslides, large fissures in the ground and faults	> 400

Table C-4. Japan Meteorological Agency Intensity Scale

ID	Earthquake	Name of Tunnel	Location	Use	Length (m)	Cross Section Width x Height (m)	Liner System	Liner Thickness (cm)	Geological Feature	Cover (m)	Damage at Portals	Damge within 30 m of portals	Damage to Liner > 30 m from portal	Notes
1	1923 Kanto	Hakone No. 1 (up)	Yamakita-Yaga	RR	284.7	4.3 x 4.7	4	34 - 57	marlstone, soil		2	2	1	
		(down)	(on Tokaido [Gotemba] Line)		285.2	4.6 x 5.0	4	23 - 46						
2	1923 Kanto	Hakone No. 3 (up)	Yamakita-Yaga	RR	312.0	4.3 x 4.7	4	23 - 57		4 - 47	4 - slide	3	1	
		(down)	(on Tokaido [Gotemba] Line)		318.1	4.6 x 5.0	4	23 - 46						
3	1923 Kanto	Hakone No. 4 (up)	Yamakita-Yaga	RR	269.9	4.3 x 4.7	4	23 - 57		4 - 53	4 - slide	3	1	Damage varies from Table C-2.
		(down)	(on Tokaido [Gotemba] Line)		306.8	4.6 x 5.0	4	23 - 57						
4	1923 Kanto	Hakone No. 7 (up)	Yaga - Surugaoyama	RR	211.2	4.6 x 5.0	4	34 - 46			2	4	1	lesser damage to down (mountain side)
		(down)	(on Tokaido [Gotemba] Line)		232.9	4.3 x 4.7	4	34 - 57						Damage varies from Table C-2.
5	1923 Kanto	Nagoe (up)	Kamakura - Zushi	RR	442.6	4.9 x 6.0	4-5	34 - 46	mudstone		1	2	3	Damage varies from Table C-2.
		(down)	(on Yokosuka Line)		344.3	4.3 x 5.6	4-5	23 - 57						
6	1923 Kanto	Komine	Odawara - Hayakawa	RR	260.5	9.1 x 6.0 (box)	4-5	126 - 137	soil	1 - 17	4	4	3	liner type depends on location
			(on Atami Tokaido] Line)			8.5 x 6.9 (tube)					(Box section)	(box section)	(tube section)	
7	1923 Kanto	Fudoyama	Hayakawa - Nebukawa	RR	100.6	8.7 x 6.9	4-5	69 - 114	red agglomerate	4 - 20	2	2	1	
			(on Atami Tokaido Line)											
8	1923 Kanto	Nenoueyama	Hayakawa - Nebukawa	RR	105.6	8.7 x 6.9	4-5	91	black agglomerate,	12 - 17	4 - slide	3	4	steep slope
			(on Atami Tokaido Line)						pyroxene andesite					
9	1923 Kanto	Komekamiyama	Hayakawa - Nebukawa	RR	278.6	8.7 x 6.9	4-5	57 - 103	pyroxene andesite,	2 - 51	4	3	1	liner with invert arch
			(on Atami Tokaido Line)						agglomerate, volcanic ash					
10	1923 Kanto	Shimomakiyayama	Hayakawa - Nebukawa	RR	160.9	8.7 x 6.9	4-5	69 - 103	pyroxene andesite,	14 - 31	4 - slide	4	1	steep slope
			(on Ataini [Tokaido Line)						volcanic ash					Damage varies from Table C-2.
11	1923 Kanto	Happonmatan	Nebukawa - Manazurn	RR	76.4	8.7 x 6.9	4-5	69 - 91	loose agglomerate	< 17	4 - slide	3	1	steep slope
			(on Atami [Tokaidoi Line)											
12	1923 Kanto	Nagasakayama	Nebukawa - Manazurn	RR	673.9	8.5 x 6.9	4-5	57 - 91	agglomerate	11 - 94	2	3	4	Damage varies from Table C-2.
			(on Atami Tokaido] Line)											
13	1923 Kanto	Yose	Sagainiko - Fujino	RR	292.6	4.6 x 5.0	4	46 - 69	soil	4 - 21	1	2	4	collapse accident reported during construction
			(on Chuo Line)											
14	1923 Kanto	Toke	Toke - Ohami	RR	353.3	4.3 x 4.5	4	34 - 46	mudstone	12 - 20	1	1	4	
			(on Boso [Sotobo] Line)											
15	1923 Kanto	Namuya	Iwal - Tomiura	RR	740.3	4.9 x 6.0	4-5	30 - 57	shale, tuffite	9 - 70	2	3	4	steep slope, landslide suspected,
			(on Hojo [Uchibo] Line)											water acceident reported during construction
16	1923 Kanto	Mineokayama	Futorni - Awakamogawa	RR	772.5	4.9 x 6.0	4	30 - 47	sandstone, shale, gabbro		2	3	4	under construction at time of earthquake,
			(on Awa [Uchibo] Line)										of drift	progressive failure after the main shock
17	1930 Kita-Izu	Tanna	Atami - Kannami	RR	7804.0	8.5 x 6.4	4-5	32 - 136	amdesite, agglomerate		1	1	4	under construction at time of earthquake,
			(on Atami [Tokaido] Line)											earthquake fault crossing the tunnel
18	1961 Kita-Mino	I Power Plant	upperstream of Tedori	WT	2538.0	2.1 x 2.2	5	20 - 40	sandstone, soil		1	1	3	cracking 32% of whole length
			River			2.4 x 2.45	5	20 - 40						longitudinal crck dominant
19	1964 Niigata	Budo	Murakami - Buya	HW	320.0	8.6 x 5.8	5	50 - 60	rhyolite, talus, perlite clay		1	2	2	under construction at time of earthquake
			(on Route 7)											cracking on the ground surface
20	1964 Niigata	Terasaka	Nezugaseki - Koiwagawa	RR	79.4		4-5	47 - 107	soft mudstone		1	3	3	landslide area
			(on Uetsu Line)											cracking on the ground
21	1964 Niigata	Nezugaseki	Nezugaseki - Koiwagawa	RR	104.0				soft mudstone		2	2	2	landslide area
			(on Uetsu Line)											
22	1968 Tokachi-oki	Otofuke	Nukabira - Horoka	RR	165.0	4.8 x 5.2	4-5	25 - 60	tuff	< 50	1	1	3	landslide area, slope
			(on Shihoro Line)											
23	1978 Izu-Oshima-kinkai	Inatori	Inatori - haihatna	RR	906.0	4.4 x 5.1	5	40 - 70	metamorphic andesite	< 90	3	2	3	earthquake fault crossing the tunnel
			(on Izu-kyuko Une)						solfataric clay					trouble with geology during construction
24	1978 Izu-Oshima-kinkai	Okawa	Okawa - Hokkawa	RR	1219.5				andesite, fault clay		1	1	2	damage over 60 m long
			(on Izu-kyuko Une)											
25	1978 Izu-Oshima-kinkai	Atagawa	Atagawa - Kataseshirata	RR	1277.0				andesite, solfararic clay		1	1	2	damage over 400 m long
			(on Izu-kyuko Une)											
26	1978 Izu-Oshima-kinkai	Shiroyama	Imaihama - Kawazu	RR							4	1	1	a gigantic rock crashed and blocked
			(on Izu-kyuko Line)											the portal
27	1978 Izu-Oshima-kinkai	Tomoro	Shirata - Inatori	HW	425.5		5		andesite		3	3	3	cracking on the ground surface
			(on Higashi-Izu Toll Road)											
28	1978 Izu-Oshima-kinkai	Shirata	Shirata - Inatori	HW	88.7				audesite		4 - slide	2	3	steep slop
			(on Route 135)											cracking on the ground surface
29	1978 Izu-Oshima-kinkai	Joto	Shirata - Inatori	HW	127.3		4-6		audesite		4 - slide	1	4	steep slope
			(on Route 135)											cracking on the ground surface
30	1978 Izu-Oshima-kinkai	Kurone	Shirata - Inatori	HW	400.0				andesite, scoria		4 - slide	2	1	
			(on Route 135)											
31	1978 Miyagiken-oki	Nakayama No.2	Naruko - Nakayamadaira	RR	262.1	4.9 x 6.1	4-5	59 - 69			1	1	3	
			(on Rikuu-east Line)											
32	1984 Naganoken-seibu	Otakigawa Dam	Otaki, Nagano	UT		2.7 x 3.0	5		sandstone, shale		1	1	2	earthquake fault crossing suspected
33	1993 Notohanto-oki	Kinoura	Orido, Suzu, Ishikawa	HW	76.0	6.8 x 5.1	5		mudstone, tuff	< 26	2	4	3	collapse extended by aftershocks
			Shimamaki Village											
34	1993 Hokkaido-nansei-oki	Shiraito No. 2	(on Route 229)	HW	1463.0		6	60	talus		1	1	4	falling rock hit the exposed tunnel lining

Table C-5. Tunnels with Moderate to Heavy Damage (Japanese)

Table C-6. Legend for Tables C-2, C-5

EQNAME : Earthquake name
Mw: Moment Magnitude
TNAME : Tunnel name
OWNER OR REFERENCE:

ATSF	=	Santa Fe Railroad
CALTRAIN	=	CALTRAIN (Bay Area commuter train)
CALTRANS	=	California Department of Transportation
CDO	=	City Development Office
COE	=	Corps of Engineers
HHP	=	Hanshin Highway Public Corp.
HOE	=	Hokoshin Express
HRP	=	Hyogo Road Public Corp.
HWC	=	Hanshin Waterworks Company
HSB	=	Honsyu Shikoku Bridge Authority
JHP	=	Japan Highway Public Corp.
JRN	=	JR Nishinippon
JTA	=	Japan Tunneling Association
KBD	=	Kobe Dentetsu
KEP	=	Kansai Electric Plant
KER	=	Kobe Electric Railway
KMS	=	Kobe Municipal Subway
KPW	=	Kobe Public Works Bureau
KTB	=	Kobe Transportation Bureau
KWS	=	Kobe Water Supply Bureau
LADWP	=	Los Angeles Department of Water and Power
LAMT	=	Los Angeles Metro
MRP	=	Municipal Road Public Corp.
MWB	=	Municipal Waterworks Bureau
MWD	=	Metropolitan Water District of Southern California
Nat. RW	=	National Railway
NCRR	=	North Coast Railroad
NPC	=	North Pacific Coast Railroad
NPS	=	National Park Service
NTT	=	Nippon Telephone and Telegraph
SC, BT, PR	=	Santa Cruz-Big Trees-Pacific Railway
SCVWD	=	Santa Clara Valley Water District
SFWD	=	San Francisco Water Department
SPRE	=	Southern Pacific Railroad
SU	=	Stanford University

FUN: Function of tunnel

AC	=	Particle accelerator
HW	=	Highway
RE	=	Railroad
UT	=	Utility
WT	=	Water

Liner / support system

1 = Unlined   2 = Rock Bolt   3 = Timber   4 = Masonry/brick
5 = Unreinforced concrete 6 = Reinforced Concrete   7 = Steel pipe   9 = Unknown

Rock / Soil

R = Rock S = Soil

COVER: Depth of cover above tunnel (meters)
PGA : Peak Ground Acceleration in g
DM : Damage State (Table C-3)

1 = None   2 = slight   3 = moderate   4 = heavy

DM : Damage State (Table C-5)

1 = none

2 = slight   (cracks, displacement, deformation)

3 = moderate (severe cracks, falling out, arch hanging down, swelling, invert cut)

4 = heavy (collapse)
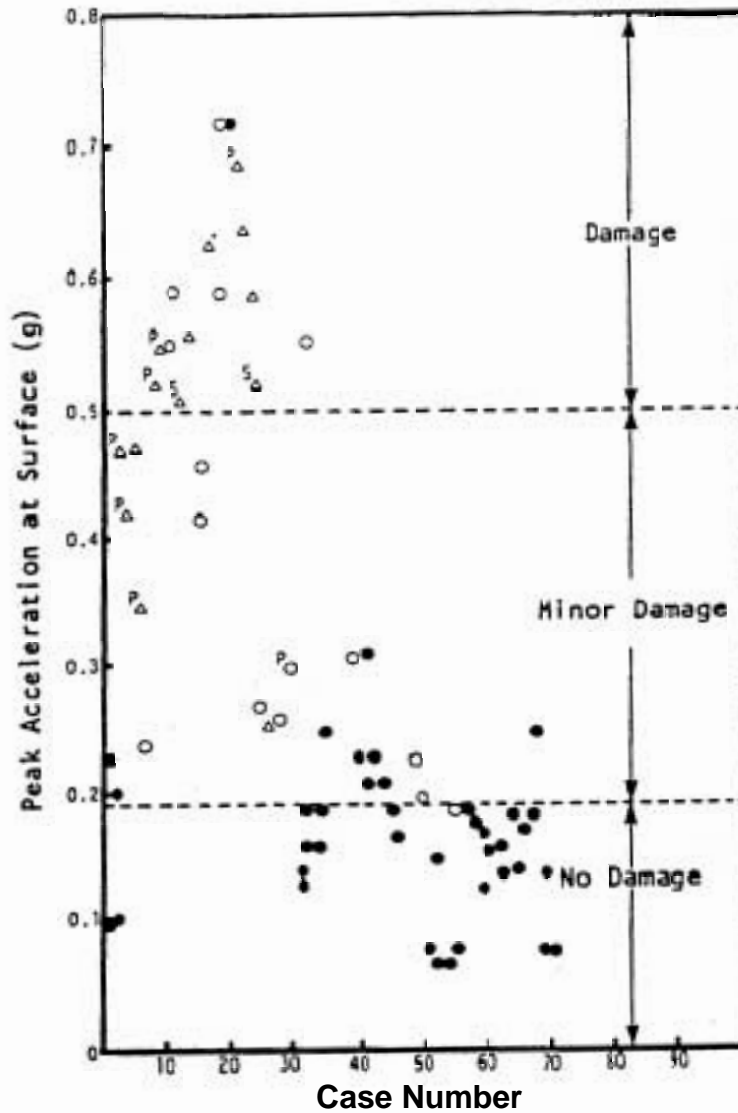
Figure C-1. Peak Surface Acceleration and Associated damage observations for earthquakes (from Dowding and Rozen, 1978)
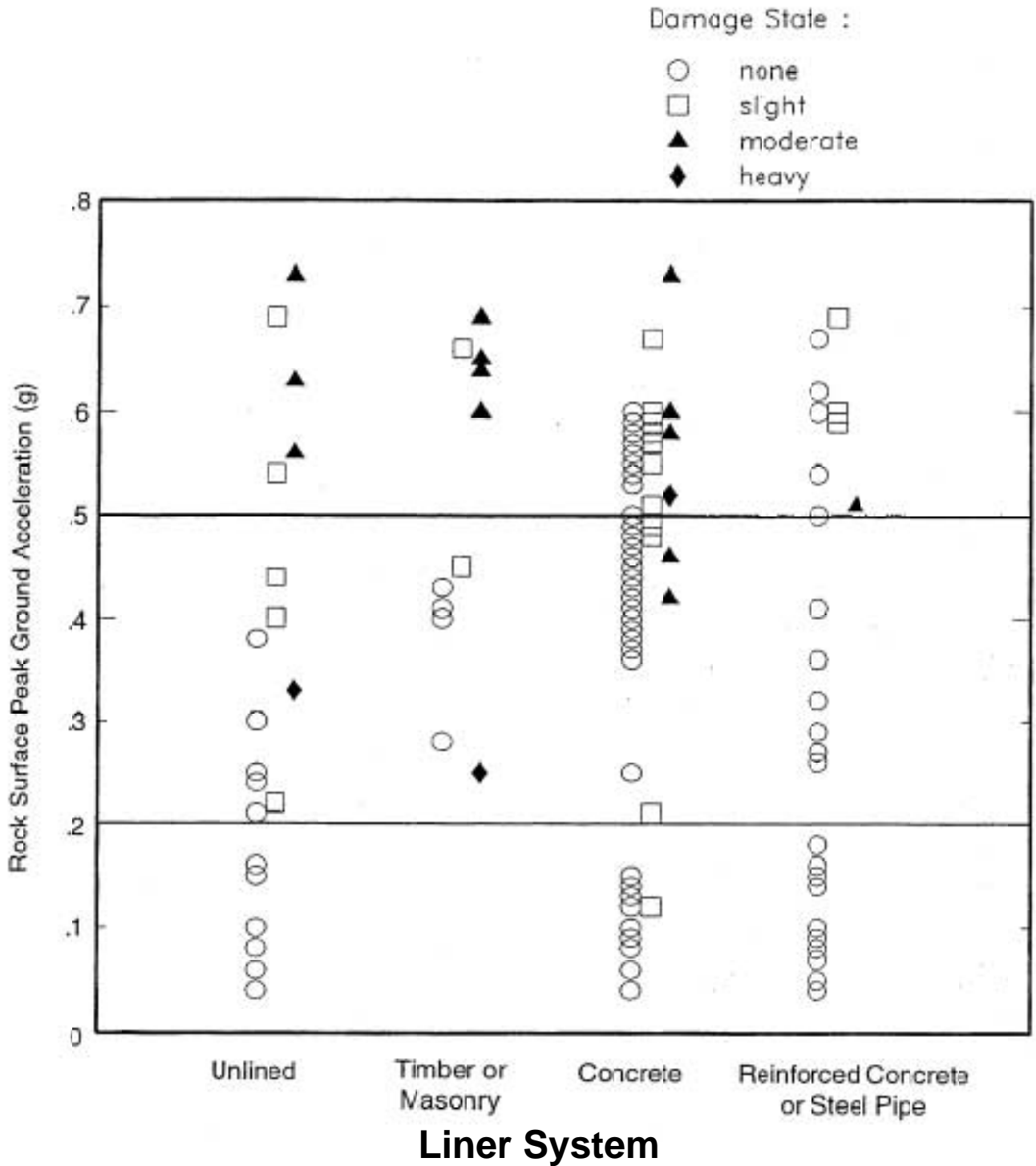
Figure C-2. Summary of empirical observations of seismic ground shaking-induced damage for 204 bored tunnels [after Power et al, 1998]
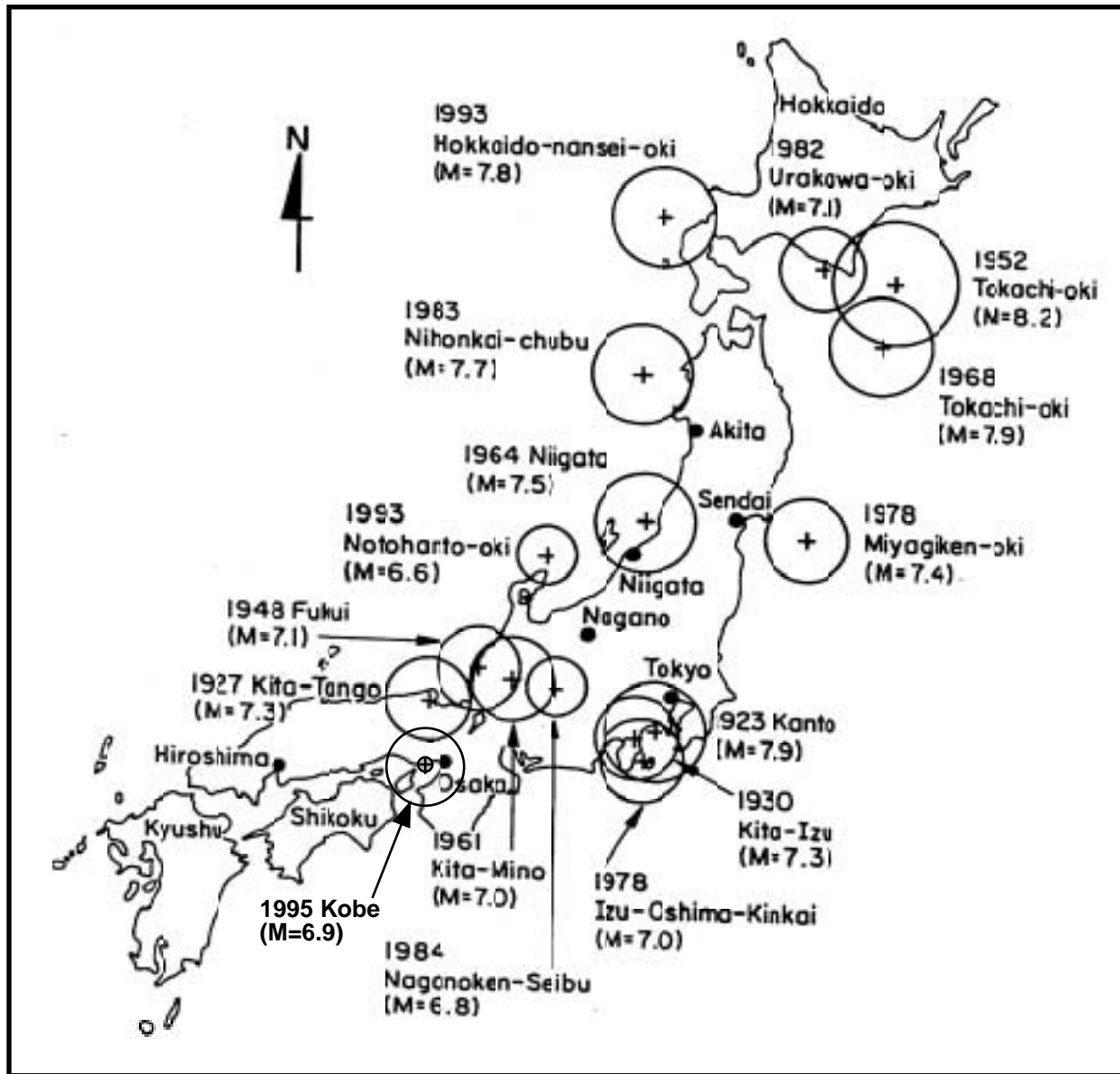
**Figure C-3. Map of Japan showing locations
of 16 earthquakes in Tunnel Database**
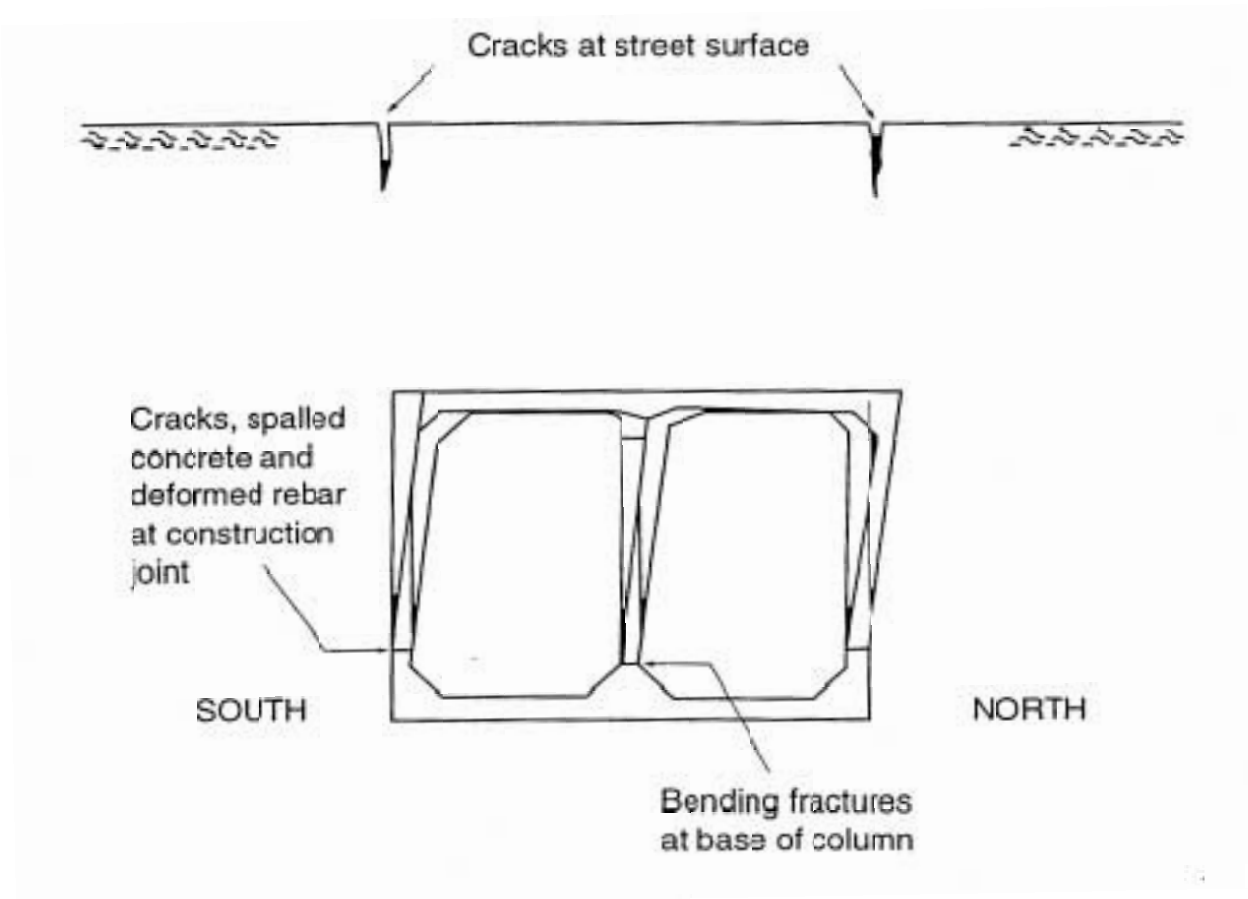
Figure C-4. Deformations of cut and cover tunnel (exaggerated scale) for tunnel of Kobe Rapid Transit Railway between Daikai and Nagata stations [after O'Rourke and Shiba, 1997]

D. Commentary - Canals

D.1 1979 Imperial Valley Earthquake

The 1979 Imperial Valley M 6.5 earthquake caused widespread damage to irrigation canals. The following descriptions are adapted from [Dobry et al].

The Imperial Valley is located near the U.S. – Mexico border in Southern California. The area is flat, and thus landslide movements are not significant in this area. Water for domestic, industrial and irrigation purposes originates at the Colorado River and is transported to a network of canals by the All American Canal. The canals are either lined with unreinforced concrete or unlined.

The most extensively damaged canal was the All American Canal, constructed in the late 1930s. The total damage to the canal was estimated to be about $982,000 [Youd and Wieczorek]. Settlements, slumps, incipient slumps, and incipient lateral spreads occurred along a 13 km long section between Drop No. 5 near the Ash Canal and the East Highline Canal. The damage was concentrated on a 1.5 km long section of the All American Canal, near the Alamo River. The repairs were made rapidly, preventing detailed mapping of the embankment deformations. Rotational earth slumps threatened to breach the canal, incipient slumps, lateral spreads, and many undifferentiated fissures caused extensive cracks on the embankment and also in the compacted fill around the structures. Along the All American Canal, the damage was distributed as far as 10 km east and 3 km west of the causative Imperial fault. Youd and Wieczorek reported that there was no evidence of large scale liquefaction around the canal, but localized liquefaction may have contributed to failure in some places.

Slumping and incipient slumping extended for about 500 m along the east side of the Highline Canal.

Both sides of the South Alamo Canal were badly cracked for a length of about 100 m; crack widths were about 15 mm and vertical crack offsets were 50 to 100 mm. At another location, the east bank showed fissures in a 500 m length. These fissures were caused by incipient slumping or lateral spreading towards the canal. The cracks at this site showed as much as 100 mm of opening and vertical offset.

The Barbara Worth Drain canal was also damaged in this earthquake.

In 1940, a M 7.1 earthquake occurred on much of the same fault as in the 1979 event. In the 1940 earthquake, damage to canals included: Holtville Main Drain, All American, Central Main, Alamo and Solfatara, for a total length of 119.7 km of damaged canal. The damage to these canals in the 1940 event was more severe than in the 1979 event. Although damage to canals in the 1940 event was not clearly associated with the occurrence of liquefaction, the soil in the affected areas did contain sand layers, whereas the soils in the areas without canal damage did not.

Based on damage to the canal and irrigation ditch network in the 1979 earthquake, the authors analyzed the repair rate as a function of distance and recorded PGAs at representative distances from the nearest fault rupture. The results are shown in Figure D-1. In Figure D-1a, "conduit" represents either canal or irrigation ditch. The following trends are noted:

- The repair rate is highest for locations closest to the fault. For PGAs in the range of 0.5g to 0.8g, with corresponding PGVs of 22 in/sec to 35 in/sec, repair rates are

about 0.15 to 0.25 repairs per kilometer. Repair rates drop to about one-tenth this rate when PGAs / PGVs have attenuated to about 0.2g / 9 in/sec.

- Due to the lack of detailed design information for each canal or ditch in the area, we do not attempt to provide a fragility curve based on this information.

With regards to operation of the All American Canal in the 1979 earthquake, it was reported [EERI, 1980] that at the time of the earthquake, 3,700 cubic feet per second (cfs) of water was flowing in the canal. The bulk of this water was used for irrigation. Due to damage in the canal, flow was reduced to about 700 cfs, in order to prevent flooding over damaged levees of the canal. As repairs were made to the canal, flow was increased, reaching the required flow of 4,100 cfs by October 19 (4 days after the earthquake). During this 4 day operation of the canal at low flows, there was sufficient raw water in an open cut reservoir for the City of El Centro's water treatment plant, and therefore the damage to the canal did not directly affect treated water deliveries to customers in the City of El Centro (although damage to distribution pipelines did affect treated water deliveries).

D.2 1980 Greenville Earthquake

Contra Costa Canal. This canal is operated by the Contra Costa Water District. It transports raw water from the Delta to the City of Concord, California, and other nearby localities.

This canal underwent minor levels of ground shaking in the 1980 Greenville earthquake. PGAs were on the order of 0.02g to 0.10g. Minor damage was observed due to earth sloughing from adjacent earthen banks.

D.3 1989 Loma Prieta Earthquake

Contra Costa Canal. This canal underwent minor levels of ground shaking in the 1989 Loma Prieta earthquake. PGAs were on the order of 0.02g to 0.10g. No damage was observed.

South Bay Aqueduct. This canal is operated by the State of California, Division of Water Resources. It transports water from the Delta to the Cities of Livermore, Pleasanton and San Jose, California. This canal underwent moderate levels of ground shaking in the 1989 Loma Prieta earthquake. However, no canal lining damage was sustained. A bridge adjacent to the canal received moderate damage.

D.4 References

Dobry, R., Baziar, M. H., O'Rourke, T. D., Roth, B. L., and Youd, T. L., Liquefaction and Ground Failure in the Imperial Valley, Southern California During the 1979, 1981 and 1987 Earthquakes, *in* Case studies of liquefaction and lifeline performance during past earthquakes, Volume 2, United States Case Studies, Eds. T. D. O'Rourke and M. Hamada, NCEER Report 92-0002, February 17, 1992.

EERI, Imperial County, California Earthquake Reconnaissance Report, Earthquake Engineering Research Institute, G, Brandow Coordinator, D. Leeds, Editor, February, 1980.

Youd T.L. and Wieczorek G.F., Liquefaction and secondary ground failure in the Imperial Valley California earthquake Oct 15, 1979, *in* The Imperial Valley California Earthquake Oct. 15, 1979, U.S. Geological survey, Professional Paper 1254, pp. 223-246, 1982.
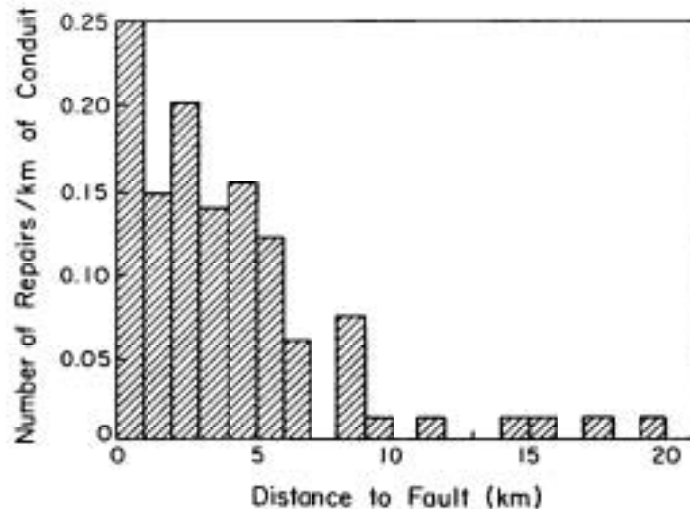
D-1a. Repair Rate versus Distance to Nearest Fault
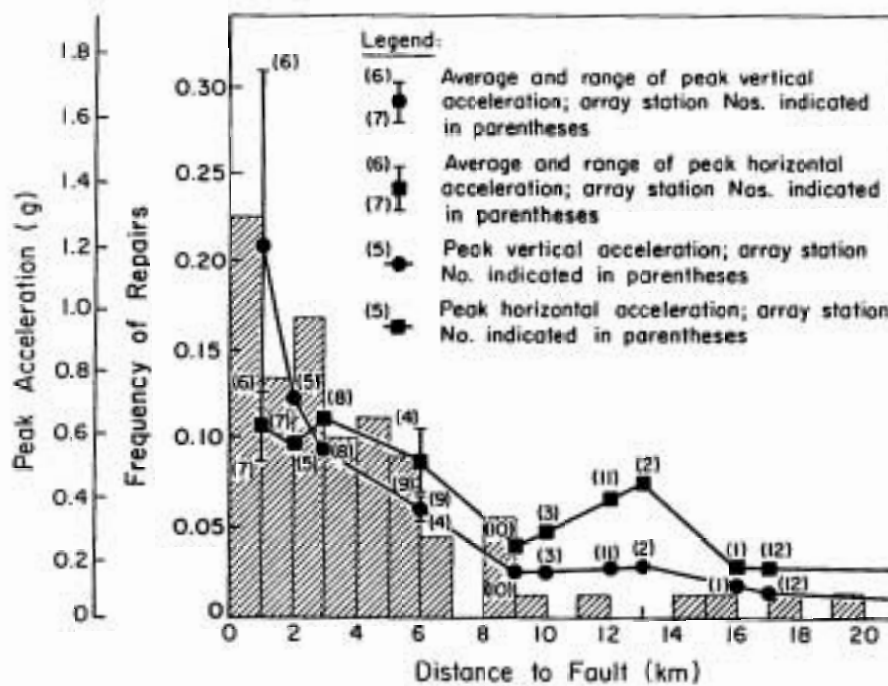
D-1b. Repair Rate versus PGAs Recorded at
Similar Distances to the Nearest Fault

Figure D-1. Canal and Ditch Repair Rates,
1979 Imperial Valley Earthquake [after Dobry et al]

E. Basic Statistical Models

Appendix E describes the general process used in establishing fragility curves.

E.1 The Options

There are three general approaches that can be used in developing fragility curves. These are:

- The empirical approach. This involves use of observed damage / non-damage from past earthquakes.

- The analytical approach. This involves the use of specific engineering characteristics of a component to assess its seismic capacity, in a probabilistic way.

- The engineering judgment approach. This involves the review of available information by cognizant engineers, and making an informed judgment as to the capacity of a component.

The main report uses all three approaches in developing fragility curves for the various components. Appendix E provides the mathematical models that are used in this process. Appendix G provides an alternate approach, called Bayesian Analysis, to standard regression analysis.

E.2 Randomness and Random Variables

Randomness in a parameter means that more than one value is possible. In other words the actual value, to some degree, is unpredictable. Mathematical representation of a random variable is thus a primary task in any probabilistic formulation.

In a loss estimation study, a prediction of the future is made using information from the past, including experience and judgment whenever possible. Thus, it is necessary to collect all relevant information from the past for this purpose. A typical flow chart of the steps involved is shown in Figure E-1. The information collected will constitute the sample space.

Appendices A-D provide empirical information (sample space) for some of the water system components. The empirical information is likely not complete, and further effort in reviewing the performance of water transmission system components would likely yield additional information that could be added to the sample space. It was not feasible in the current effort to consider every possible known piece of information. By expanding the data in the sample space, it is hoped that better fragility curves can be developed in the future.

The randomness characteristics of any sample space can be described graphically in the form of a histogram, or a frequency diagram, as shown in Figure E-2. For a more general representation of the randomness, the frequency diagram can be fitted to some theoretical probability density function (PDF) $f_x(x)$. By integrating the probability density function thus obtained, a cumulative distribution function (CDF) $F_x(x)$ can be obtained.

To describe the PDF or CDF uniquely, some parameters of the distribution need to be estimated. The estimation of these parameters, which are called statistics, is a key step in the development of fragility curves.

E.2.1 The Normal Distribution

A random variable usually can be described mathematically by a distribution. A random variable can be discrete or continuous. Most commonly used discrete random variable are described by the binomial distribution, Poisson, distribution, geometric distribution, etc. Continuous random variables are generally described by the normal distribution, lognormal distribution, exponential distribution, Gamma distribution, Beta distribution, Chi-Square distribution, etc. The reader is referred to Benjamin and Cornell [1970] for a more complete description of various distributions.

Amongst the most important statistical parameters are the mean value, μ, which denotes the average of expected value of the random variable, and the standard deviation, σ, which denotes the dispersion of a random variable with respect to the mean value. The coefficient of variation (COV) is the ratio of the standard deviation and the mean value.

For a discrete random variable, the mean and unbiased variance can be calculated as follows:

$$\mu_x = \frac{1}{n}\sum_{i=1}^{n} x_i$$

$$Var(x) = \frac{1}{n-1}\sum_{i=1}^{n}\left(x_i - \mu\right)^2$$

The standard deviation and COV are calculated from the following relationships once the mean and variance of a random variable are known.

$$\sigma_x = \sqrt{Var(x)}$$

$$COV = \frac{\sigma_x}{\mu_x}$$

E.2.2 Which Distribution Model?

To develop a probabilistic model, the underlying distribution of a random variable needs to be known, as well as its statistics. The methods to empirically determine the distribution model is discussed in this section.

In practice, the choice of the probability distribution if often dictated by mathematical convenience. In many (most?) engineering evaluations of damage to water system components from past earthquakes, the functional form of the required probability distribution may not be easy to determine, or more than one distribution may fit the available data. The basis of the properties of the physical process may suggest the form of the required distribution.

The required probability distribution may be determined empirically, based entirely on the available observed data., A frequency diagram for the set of data can be constructed and a distribution model can be selected by visual comparison as shown in Figure E-2.

When the distribution model is obtained using this method, or when two or more distributions appear to be plausible probability distribution models, statistical tests (known as goodness-of-fit tests for distributions) can be carried out to verify the distribution model. Two such tests commonly used for this purpose are the Chi-Square χ^2 and the Kolmogorov-Smirnov (K-S) tests. For this report, the lognormal distribution is assumed in essentially all fragility formulations. This has been done as the lognormal distribution is

mathematically convenient; Section E.6 provides further details. Other researchers may find that other dispersion models are better suited for specific applications.

E.2.3 Lognormal Variables

In some special cases, suppose

$$Y = X_1 \bullet X_2 \mathrm{L} \bullet X_n$$

where X_i's are statistically independent lognormal variables with means μ_{X_i} and standard deviation σ_{X_i}; then Y is also a lognormal variable.

From an engineering point of view, for loss estimation of water system components, the form of the lognormal distribution has some advantages. The total response, Y, can be represented as the deterministic response value multiplied by a series of correction factors that are random and associated with various uncertainties. Irrespective of the proper distribution of these individual variables X_i, the product of the variable will be approximately lognormal. Another advantage of the lognormal function is that a variable cannot take negative values. For these reasons, it is commonly adopted to model a variable as a lognormal variable rather than a normal variable. Note that whether or not the real world is really "lognormal" is often ignored in the evaluation – but it is convenient that it should be.

Knowing the mean and variance for a random variable X, μ_X and σ_X the two parameters of the lognormal distribution λ_X (logarithmic mean) and ς_X (logarithmic standard deviation, beta, β) can be obtained as follows:

$$\lambda_X = \ln(\mu_X) - \frac{1}{2}\varsigma_X^2$$

and

$$\varsigma_X^2 = \ln\left(1 + \frac{\sigma_X^2}{\mu_X^2}\right)$$

Say that x_m is the median (x_{50}) of the variable X. Then,

$$\lambda = \ln(x_m)$$

and the 84th percentile value of X (i.e., one standard deviation higher than the median) is

$$x_{84} = x_{50}e^{\beta} = x_m e^{\varsigma}$$

Since X_i's are lognormal, then $\ln(X_i$'s) are normal and

$$\lambda_Y = Expected\_Value(\ln Y) = \sum_{i=1}^{n} \lambda_{X_i}$$

and

$$\varsigma_Y^2 = Var(\ln Y) = \sum_{i=1}^{n} \varsigma_{X_i}^2$$

E.2.4 Regression Models

Some of the regression models used in this report for buried pipe are of the logarithmic regression form. In other words, if Y_i is the repair rate per 1,000 feet and Xi is the PGV in inches/sec, then:

$$Y_i = \alpha X_i^B z_i$$

where α and B are constants to be determined from a regression analysis, and z_i is the error term. The solution for α and B using least squares methods can be found in many statistics textbooks. Appendix G provides an alternative approach, called Bayesian analysis.

This model can be simplified into the standard linear regression model by taking the log of the equation, thus:

$$\ln Y_i = \ln \alpha + B \ln X_i + e_i$$

E.3 Simulation Methods

When performing loss estimates for water system components, the analyst can employ the Monte Carlo simulation technique. The Monte Carlo simulation technique is readily adapted to computer techniques. One advantage of the technique is that many independent variables can be processed on an individual basis, and the distribution of the dependent variable can be examined by reviewing the results of many independent trials.

The number of simulations to be used will affect the accuracy of the final results. A larger number of simulations will reduce the effects of the tails of the derived distribution.

E.4 Risk Evaluation

Using the procedures described in the previous sections, the uncertainties associated with the random resistance R and the random load S can be quantified. This is graphically shown in Figure E-3. The shaded region in Figure E-3 indicates the region where the loading function (S) is greater than the resistance function (R). The risk that the damage state R occurs is the area represented by the shaded region. Mathematically,

$$Risk = P(\text{damage state R occurs}) = P(R \leq S)$$

$$= \int_0^\infty \left[\int_0^s f_R(r)dr \right] f_S(s)ds$$

E.5 Fragility Curve Fitting Procedure

For the fragility curves developed for tanks and tunnels (Tables 5-7 and 6-3), a best fit regression analysis was performed. The approach was as follows:

The tanks and tunnels were "binned" into PGA bins. Each bin was for typically for a range of 0.1g, with the exception of PGAs over 0.7g. The higher g bins were wider, as there were fewer tunnels in this PGA range. The PGA for each bin was set at the average of the PGA values for each tunnel in that bin. The percent of tunnels reaching or exceeding a particular damage state was calculated for each bin.

A lognormal fragility curve was calculated for each of the damage states. A fragility curve was calculated for all tanks or tunnels which reached damage state 2 (DS2) or above, DS3 or above, DS4 or above, and DS5 (as applicable). The fragility curve uses two parameters:

the median acceleration to reach that damage state or above; and a lognormal dispersion parameter, β. The "best fit" fragility curve was selected by performing a least square regression for all possible fragility curves in the range of A=0.01g to 5.00g (in 0.01g steps) and β=0.01 to 0.80 (in 0.01 steps).

Since there are an unequal number of tanks or tunnels in each bin, the analysis was performed using just an unweighted regression analysis (eight data points for the eight bins), and also a weighted regression analysis (the number of data points in each bin reflecting the actual number of tanks or tunnels in each bin). The weighted analysis is considered a better representation.

E.6 Randomness and Uncertainty

In developing or updating fragility curves, this report often separately characterizes "randomness" from "uncertainty".

Randomness reflects the variabilities in the real world, for which we do not have an adequate explanation using our current technology. In other words, no reasonable amount of additional study of the problem will reduce randomness. For example, there is randomness in the level of ground motion at two nearby sites, even if they have very similar soil profiles and distances from the fault rupture. We characterize Randomness using a logarithmic dispersion parameter:

$$\beta_R$$

β_R can be determined by doing regressions for ground motion attenuation functions for the suitable parameter (PGA for tanks and tunnels, PGV and PGD for buried pipelines). There are many published references for these values, and it varies based on earthquake magnitude, type of faulting mechanism, type of soil, etc. Recent work by Geomatrix (Power, Wells and Coppersmith, et al) can be used to provide β_R for permanent ground deformations (PGDs), for fault offset, liquefaction, and landslide.

Uncertainty reflects the uncertainty in our predictions, given the level of simplification taken in the analysis. For example, suppose a water utility wanted to do a "quick and dirty" earthquake loss estimate for buried transmission pipelines, without having to do a detailed effort to ascertain exactly what type of buried pipelines are in use at which locations, how old they are, what is their leak history, which soils are most susceptible to corrosion, which soils are most susceptible to (PGDs), what level of corrosion protection has been taken for a particular pipeline, etc. In such a case, the fragility curve used should take into account that there is uncertainty in the pipeline inventory, as well as how that inventory would respond to a given level of ground motion. We characterize Uncertainty using a logarithmic dispersion parameter:

$$\beta_U$$

The total uncertainty is then expressed as:

$$\beta_T = \sqrt{\beta_R^2 + \beta_U^2}$$

E6.1 Total Randomness and Uncertainty

The method by which randomness and uncertainty is tabulated for this report considers the following:

- A possible update of the water pipeline / transmission system component fragilities in the HAZUS computer program. HAZUS makes many simplifying assumptions in order to get a computer program that is both easy to use and easy to program. Thus, only a single dispersion parameter is allowed in HAZUS, which is the equivalent of β_T.

- Depending upon the source datasets used to establish the uncertainty parameters, the underlying uncertainty in the empirical data may or may not include β_R. (A good quality data set using GIS techniques on a well document earthquake would primarily reflect β_U). In either case, the fragility curves in the main report must be clear as to whether the dispersion parameter includes (or does not include) β_R. By so doing, an the results in the main report can be suitably interpreted to allow for separation of uncertainty in ground motion and inventory response.

- To summarize, it would be ideal to present three measures of uncertainty: β_T (if used in HAZUS or HAZUS-like programs); β_R so that this could be varied by the type of earthquake and by future advances in geotechnical descriptions of ground motion; and β_U so that this can be used in programs that are more sophisticated than HAZUS, and for end users who take the effort to establish a high quality inventory database.

E.7 The Model to Estimate Fragility of a Structure or Piece of Equipment

The variability of how a structure or piece of equipment can respond can be described by a probability density function (PDF), as shown in Figure E-3 (f_R(r.)). In the great preponderance of application, the engineer rarely considers the shape of the PDF of the item he/she is designing; instead, the engineer designs the item to "code". For convenience, we call designing to "code" a "deterministic" design. Generally conservative parameters are used in deterministic design so that only a low probability exists that the actual (random) seismic demand S exceeds the actual (random) seismic capacity. It is neither necessary nor desirable for the deterministic design to be so conservatively performed that the probability of failure is negligibly low (i.e., very close to zero).

In deterministic analysis, the deterministic factor of safety, F_D, is defined as the ratio of the deterministic code capacity, C_D, to the deterministic computed response, R_D, i.e.,

$$F_D = \frac{C_D}{R_D}$$

In probabilistic analysis, both the capacity C and the response R are random variables. Thus, the factor of safety is given by:

$$F = \frac{C}{R}$$

which is also a random variable. A capacity factor, F_C, can be defined as the ratio of the actual capacity, C, to the deterministic code capacity, C_D. Similarly, a response factor, F_R, is defined as the ratio of the deterministic computed response, R_D, to the actual response R, i.e.,

$$F_C = \frac{C}{C_D}; \qquad F_R = \frac{R_D}{R}$$

Thus, the probabilistic factor of safety, F, can be defined in terms of the deterministic factor of safety, F_D, by:

$$F = F_C \bullet F_R \bullet F_D$$

The probability of failure is the probability that the factor of safety, F, is less than 1. The reliability is the probability that the factor of safety, F, is 1 or greater.

Computation of the probability of failure is tractable mathematically when the capacity and the response factors, F_D and F_R, are assumed to be lognormally distributed random variables. F is a lognormal random variable if F_D and F_R, are lognormal random variables. The median value, $\hat{F}$, and the logarithmic standard deviation, β_F of F are given by:

$$\hat{F} = \hat{F}_C \bullet \hat{F}_R \bullet F_D$$

$$\beta_F^2 = \beta_C^2 + \beta_R^2$$

where $\hat{F}_C$ and $\hat{F}_R$ are the median values and β_C and β_R and the logarithmic standard deviations for the capacity F_C, and response F_R, factors. The probability of failure is then given by:

$$P_f = \Phi\left(\frac{\ln\left(1/\hat{F}\right)}{\beta_F}\right)$$

where Φ is the standard cumulative distribution function.

Section E.7 is concerned with estimating the capacity factor random variable, F_C, that, when combined with the response random variable, F_R, and a code-specified deterministic factor of safety, F_D, can be used to estimate a probabilistic factor of safety F, and a probability of failure.

Section 3 of the main report provides a brief introduction as to how to compute F_R. It is beyond the scope of the current effort to examine the issues with how to compute the seismic response at a location.

Under dynamic loading, the capacity factor is assumed to be made up of two parts:

$$F_C = F_S \bullet F_\mu$$

where F_S represents the strength factor for an equivalent static loading and F_μ represents the added capacity due to the ductility (inelastic energy-absorbing capability) of the structure and the fact that the loading has limited energy content (short duration, cyclic loading).

E.8 References

Benjamin, J. R. and Cornell, C. A., Probability, Statistics and Decision for Civil Engineers, McGraw-Hill.
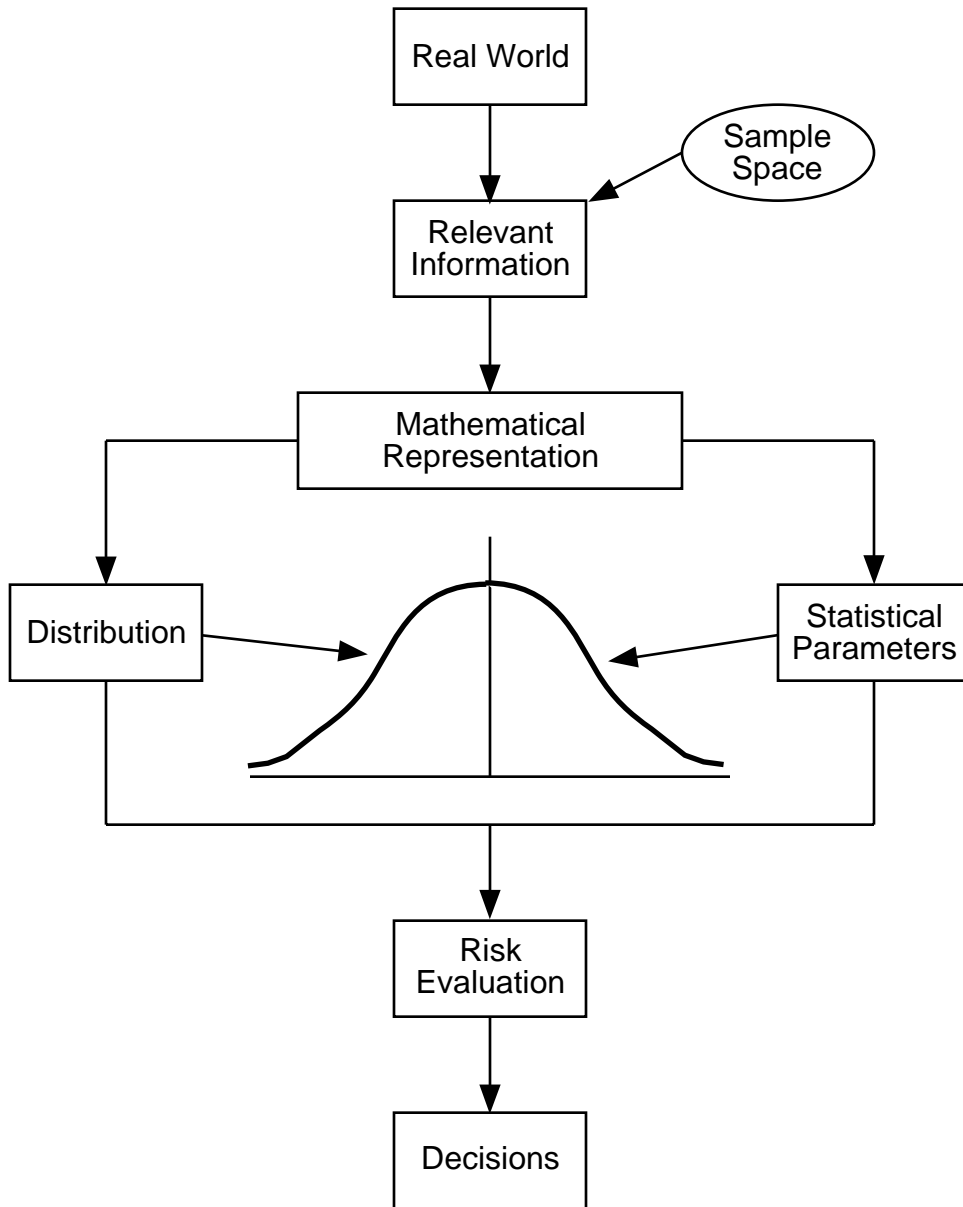
Figure E-1. Steps in a Probabilistic Study
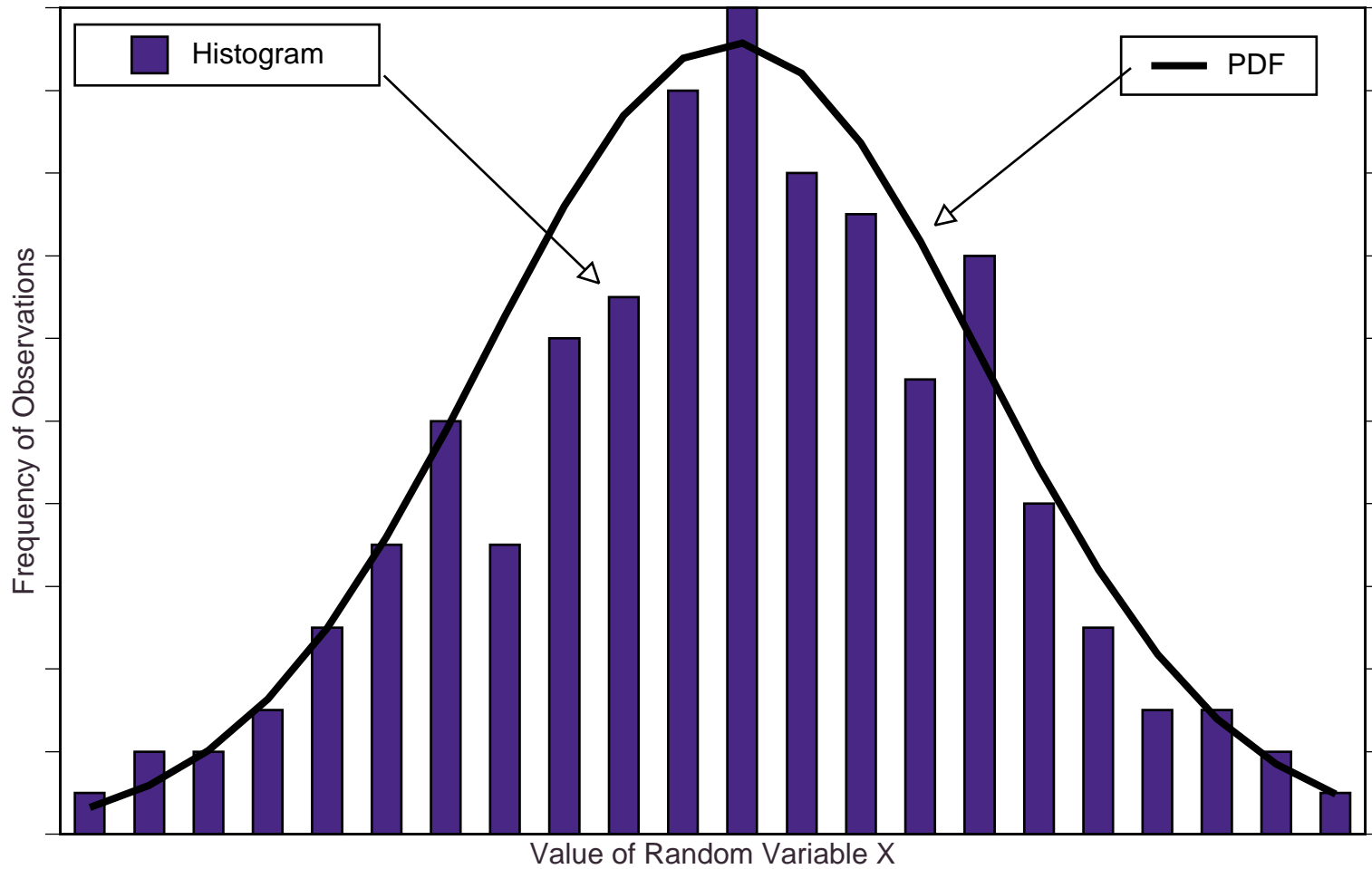
Figure E-2. Typical Histogram or Frequency Diagram
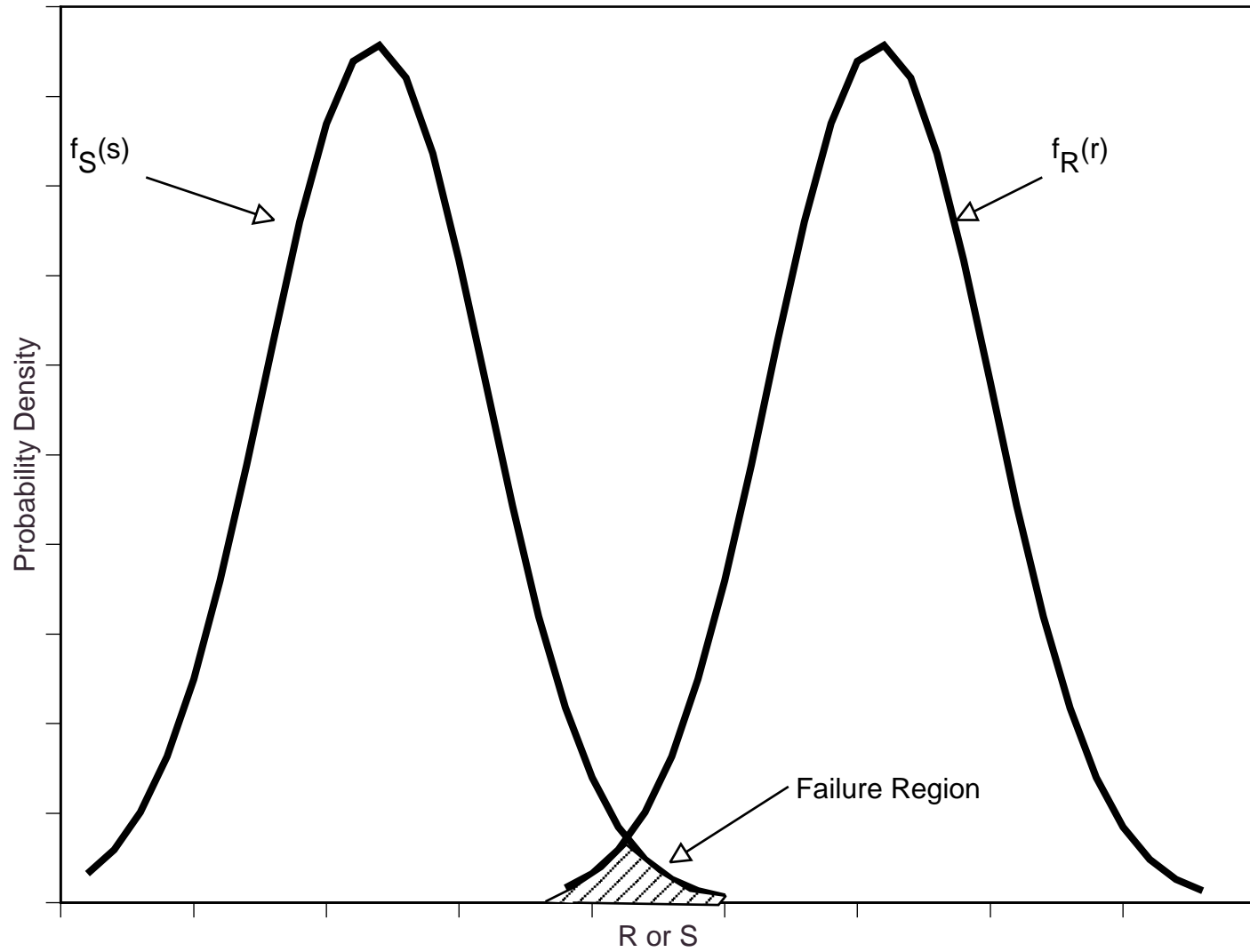
Figure E-3. Risk Evaluation

F. Example

A portion of a California water transmission aqueduct built in 1930's is examined in Appendix F. It consists of 33,400 feet of 62-inch diameter concrete pipe (with steel cylinder) and 48,000 feet of 66-inch diameter welded steel pipe.

For the purpose of illustrating how to apply the guideline procedures, this portion of pipeline is further divided into the following four segments according to their surface geological conditions:

Segment	Length	Material	Joint	Avg. Dist. from Fault Considered	Surface Geology
1	7,200 ft	Conc. w/ steel cyl.	Welded	2.3 mi.	Rock-like soils
2	30,500 ft	Steel	Welded	0.6 mi.	Firm soils
3	17,500 ft	Steel	Welded	1.5 mi.	Firm Soils
4	26,200 ft	Conc. w/ steel cyl.	Welded	3.7 mi.	Rock-like soils

Table F-1. Water Transmission Aqueduct Example

Figure F-1 shows a simplified map of the water transmission system of Table F-1. The issue at hand is to estimate the number of repairs may be required for this portion of the pipeline during an earthquake with Richter moment magnitude of 7.1 ($M_w7.1$) generated by the fault near the pipeline.

Tables F-2a and F-2b provides the summary results of the analysis.

Segment	PGA	Number of Repairs				
		Ground Shaking	Liquefaction		Landslide	Total
			Settlement only	With Lateral Spread		
1 [1]	0.58g	0.18		-	-	0.18
2 [2]	0.55g	0.24	0.23	-	-	0.47
3 [3]	0.40g	0.0		2.73	-	2.73
4 [4]	0.40g	0.60		-	1.49	2.09
Total	-	1.02	0.23	2.73	1.49	5.47

Table F-2a. Summary Results (Dry Conditions)

Notes.
[1]. Detailed calculation provided in Section F.1.
[2]. Detailed calculation provided in Section F.2.
[3]. Detailed calculation provided in Section F.3.
[4]. Detailed calculation provided in Section F.4.

Segment	PGA	Number of Repairs				
		Ground Shaking	Liquefaction		Landslide	Total
			Settlement only	With Lateral Spread		
1 [1]	0.58g	0.18		-	-	0.18
2 [2]	0.55g	0.24	0.23	-	-	0.47
3 [3]	0.40g	0.0		2.73	-	2.73
4 [4]	0.40g	0.50		-	15.1	15.6
Total	-	0.92	0.23	2.73	15.1	19.0

Table F-2b. Summary Results Wet Conditions)

Notes [1] to [4]. See Notes for Table F-2a.

F.1 Calculations – Segment 1

Segment 1. This segment of welded steel pipeline is subject to strong ground shaking from the nearby fault. The pipe traverses an area best characterized as rock or rock-like material without potential for liquefaction or landslide.

Ground Shaking

Step 1. Obtain anticipated earthquake magnitude generated from an active fault. Calculate the site specific peak ground acceleration (PGA) from this earthquake.

Assume $M_w = 7.1$ and average PGA for this segment = 0.58g. The selection of the moment magnitude is beyond the scope of this report. Section 3.2 of the main report provides some guidance, differentiating between deterministic and probabilistic definitions of earthquakes. Absent of input from knowledgeable seismologists, a rational approach would be to evaluated the pipeline for a specific scenario earthquake. Select the moment magnitude M_w for the scenario earthquake based on the length of the fault (L_r in km), using an expression like:

$$\log_{10} L_r = -2.36 + 0.58 M_w$$

Once the magnitude of the scenario earthquake is selected, calculate the median horizontal ground acceleration (PGA) such as by using equation F.1 (other equations might be more suitable, depending upon location in the United States, type of fault mechanism, etc.). This assumes the pipeline is underlain by rock or rock-like soils.

$$\ln Z = -1.274 + 1.1M - 2.1\left[\ln\left(R + e^{-0.48451 + 0.524 M}\right)\right] \qquad \text{(eqn. F.1)}$$

Assuming the average distance to the fault is 2.3 miles (= 3.7 km), gives ln Z = -0.543, or Z = 0.58g.

Step 2: Calculate peak ground velocity (PGV) with suitable attenuation relationship.

For M=7.1 and rock-like soil conditions, assume PGV = 49.4 cm/sec = 19.4 inch/sec.

Step 3: Calculate number of repairs per 1000 ft. based on PGV, pipe material, pipe joints, soil corrosiveness and pipe diameter.

From Table 4-4, the repair rate for the "backbone" pipe fragility curve is RR = 0.00187 * PGV = 0.0363 repairs per 1,000 feet. From Table 4-5, apply K1 = 0.7 (large diameter concrete cylinder pipe with lap welded joints), so the total repair rate is 0.0254 repairs per 1,000 feet.

Step 4: Calculate total number of repairs in this segment due to ground shaking

N = 0.0254 * 7200 / 1000 = 0.18.

F.2 Calculations – Segment 2

Segment 2. This segment of welded steel pipeline is subject to strong ground shaking from the nearby fault. This segment also traverses reasonably competent soils which are subject to localized liquefaction.

Ground Shaking

Step 1. Obtain anticipated earthquake magnitude generated from an active fault. Calculate the site specific peak ground acceleration (PGA) from this earthquake.

Calculate the median horizontal ground acceleration (PGA) using an attenuation model such as in Equation F.2 (others may be more suitable). This assumes the pipeline is underlain by firm soils.

$$\ln Z = -2.17 + 1.0M - 1.7\left[\ln\left(R + 0.3825 e^{0.5882 M}\right)\right] \qquad\qquad \text{(eqn. F.2)}$$

Assuming the average distance to the fault is 0.6 miles (= 1 km), gives Z = 0.55g.

Step 2: Calculate peak ground velocity (PGV) with suitable attenuation relationship.

For M=7.1 and firm soil conditions, PGV = 73.7 cm/sec = 29 inch/sec.

Step 3: Calculate number of repairs per 1000 ft. based on PGV, pipe material, pipe joints, soil corrosiveness and pipe diameter.

From Table 4-4, the repair rate for the "backbone" pipe fragility curve is RR = 0.00187 * PGV = 0.0543 repairs per 1,000 feet. From Table 4-5, apply K1 = 0.15 (large diameter single lap welded steel pipe), so the total repair rate is 0.00814 repairs per 1,000 feet.

Step 4: Calculate total number of repairs in this segment due to ground shaking

N = 0.00814 * 30500 / 1000 = 0.25. But note that this value (N=0.25) assumes that the entire length of Segment 2 is not subject to liquefaction. As described below, about 4% of the length is subject to liquefaction. So, the damage in the ground shaking zone is 96% of this value (=0.96 * 0.25).

Liquefaction

Step 1: For a scenario earthquake, calculate the level of shaking (PGA) at the particular location of the component being evaluated.

M = 7.1, PGA = 0.55g (same as the value from the ground shaking calculations)

Note: Steps 2 through 5 below are to be used only when no detailed geotechnical investigation is available. In any case, geotechnical investigation done by knowledgeable professionals is strongly recommended.

Step 2: Establish the geologic unit for the near surface environment at the component location.

From a site-specific geotechnical report or USGS or CDMG's publications:

- Type of deposit: Alluvial.

- Age of deposit: Holocene

Chance of susceptibility to liquefaction is "Low".

Step 3: Given the PGA, geologic unit and liquefaction susceptibility description, the estimated ground water depth and the magnitude of the earthquake, calculate the probability that liquefaction occurs at the location.

For this PGA level, earthquake magnitude and ground water table, assume the probability of liquefaction is 80% for liquefiable deposits. Assume 5% of the deposits are liquefiable. Thus, the probability that a spcific location liquefies is 4% (=0.8 * 0.05).

Step 4: Given that the site liquefies, calculate the maximum permanent ground deformation (settlement) or the probabilities for different settlement ranges.

Assume the settlement ranges in Table F-3 are prepared using techniques outside the scope of this report.

Settlement Range (in.)	Probability of settlement due to 4% probability of liquefaction
≤ 1	4% * 35% = 1.4%
1 – 3	4% * 60% = 2.4%
3 – 6	4% * 4% = 0.16%
6 -12	4% * 1% = 0.04%

Table F-3. Settlement Ranges – Segment 2

Step 5: If there is no lateral spread (for example, the pipe is not adjacent to an open cut or a slope), calculate the repair rates per 1000 ft. using the vertical ground settlement.

From Table 4-4 and 4-6, the repair rate for the "backbone" pipe fragility curve is RR = K2 * 1.06 * PGD repairs per 1,000 feet. From Table 4-6, apply K2 = 0.15 (large diameter single lap welded steel pipe). The vertical displacement will be the total estimated PGD parameter.

The average values of the settlement ranges in the first column of Table F-3 are used as the estimated PGDs.

Assumed estimated PGD (in.)	Number of repairs per 1000 ft. (Assume 100% probability for each estimated PGD)	Number of repairs per 1000 ft.
1	n = 0.15 * 1.06 * $(1)^{0.319}$ = 0.16	n = 0.16 * 1.4% = 0.00224
2	n = 0.15 * 1.06 * $(2)^{0.319}$ = 0.20	n = 0.20 * 2.4% = 0.0048
4	n = 0.15 * 1.06 * $(4)^{0.319}$ = 0.25	n = 0.25 * 0.16% = 0.00040
9	n = 0.15 * 1.06 * $(9)^{0.319}$ = 0.32	n = 0.32 * 0.04% = 0.00013

Table F-4. Pipe Repair Rates – Segment 2

Repair rate per 1000 feet = 0.00224 + 0.0048 + 0.00040 + 0.00013 = 0.0076.

Step 6: Calculate total number of repairs in this segment due to liquefaction.

N = .0076 * 30,500 / 1000 = 0.23.

Note. The PGD algorithm already includes damage due to PGV.

Step 7: Total Repairs (Ground Shaking and Liquefaction) for Segment 2

The total number of repairs for Segment 2:

Liquefaction zone: N = 0.23

Ground shaking zone without liquefaction:

N = 0.25 * 0.96 = 0.24

Total = 0.23 + 0.24 = 0.47.

F.3 Calculations – Segment 3

Repair rates for liquefaction (with and without lateral spread) are calculated. Assume M = 7.1 and average PGA for this segment = 0.5g. The pipeline is assumed to be buried and traverse through liquefiable soils near a body of water. It is also assumed that the pipe has been installed using typical cut and cover trench techniques without special soil improvement to address liquefaction hazards. While the soil within the pipeline trench may be of various materials, the native soils underlying and adjacent to the pipe trench are assumed to control the overall potential for PGDs along the length of pipeline.

Liquefaction

Step 1: For a scenario earthquake, calculate the level of shaking (PGA) at the particular location of the component being evaluated.

M = 7.1, PGA = 0.40g. Note that for this segment, the pipe traverses modern young soils, and moderately high values of PGA (0.4g) may still have very high values of PGV (over 35 inches / sec).

Note: Steps 2 through 6 below are to be used only when no detailed geotechnical investigation is available. In any case, geotechnical investigation done by knowledgeable professionals is strongly recommended.

Step 2: Establish the geologic unit for the near surface environment at the component location.

From a site-specific geotechnical report or USGS or CDMG's publications:

- Type of deposit: Delta.

- Age of deposit: Modern

Chance of susceptibility to liquefaction is "Very High".

Step 3: Given the PGA, geologic unit and liquefaction susceptibility description, the estimated ground water depth and the magnitude of the earthquake, calculate the probability that liquefaction occurs at the location.

For this PGA level, earthquake magnitude and ground water table, assume the probability of liquefaction is 95% for liquefiable deposits. Assume 25% of the deposits are liquefiable. Thus, the probability that a specific location liquefies is 24% (=0.95 * 0.25).

Step 4: Given that the site liquefies, calculate the maximum permanent ground deformation (settlement and lateral spread) and the probabilities for different PGD ranges.

Step 4a. No Lateral Spread. Table F-5 provides a range of settlements for the specific soil deposits and earthquake conditions.

Settlement Range (in.)	Probability of settlement due to 24% probability of liquefaction
1 - 3	24% * 5% = 1.2%
3 - 6	24% * 25% = 6%
6 - 12	24% * 50% = 12%
> 12	24% * 20% = 4.8%

Table F-5. Settlement Ranges – Segment 3

Step 4b. With Lateral Spread. Assume an analysis is performed that determines that a lateral spread with PGD = 82 inches is possible at locations so susceptible.

Step 5: For areas with no lateral spread, calculate the repair rates per 1000 ft. using the vertical ground settlement.

From Table 4-4 and 4-6, the repair rate for the "backbone" pipe fragility curve is RR = K2 * 1.06 * PGD repairs per 1,000 feet. From Table 4-6, apply K2 = 0.15 (large diameter single lap welded steel pipe). The vertical displacement will be the total estimated PGD parameter.

The average values of the settlement ranges in the first column of Table F-6 are used as the estimated PGDs.

Assumed estimated PGD (in.)	Number of repairs per 1000 ft. (Assume 100% probability for each estimated PGD)	Number of repairs per 1000 ft.
2	$n = 0.15 * 1.06 * (2)^{0.319} = 0.20$	$n = 0.20 * 1.2\% = 0.0024$
4	$n = 0.15 * 1.06 * (4)^{0.319} = 0.25$	$n = 0.25 * 6.0\% = 0.015$
9	$n = 0.15 * 1.06 * (9)^{0.319} = 0.32$	$n = 0.32 * 12\% = 0.038$
12	$n = 0.15 * 1.06 * (12)^{0.319} = 0.35$	$n = 0.35 * 4.8\% = 0.017$

Table F-6. Pipe Repair Rates – Segment 3

Repair rate per 1000 feet = 0.0024 + 0.015 + 0.038 + 0.017 = 0.072 (settlement only)

Step 6: For area adjacent to an open cut (lateral spread possible), calculate the repair rates per 1000 ft. using the vector sum of the ground settlement and the lateral displacement.

The vector sum of the ground settlement and the lateral spread displacement should be used for PGD when lateral spread is possible. Assume the most probable settlement range is 6 to 12 inches. Conservatively, use the high value to calculate PGD.

$$\therefore PGD = \sqrt{(12)^2 + (82)^2} = 83 \text{ in.}$$

$K_2 = 0.15$ (steel pipe with welded joints) per Table 4-6.

Repair rate per 1000 feet = $0.15 * 1.06 * (83)^{0.319}$ = 0.65 (lateral spread and settlement)

As the repair rate with lateral spread (0.65) is higher than the repair rate from settlement only (0.072), use the higher value in zones with liquefaction with potential for lateral spread.

Step 7: Total Repairs (Ground Shaking and Liquefaction) for Segment 3

The total number of repairs for Segment 3:

Liquefaction zone: N = 0.24 * 0.65 * 17,500 / 1,000 = 2.73

Check damage rate if there were no liquefaction.

Assume PGV = 35 inches per second. RR = 0.15 * 0.00187 * 35 = 0.0098 per 1,000 ft

N = 0.76 * .0098 * 17,500 / 1,000 = 0.13. since 0.13 << 2.73, liquefaction rate controls.

F.4 Calculations – Segment 4

Repair rates for Segment 4 include the potential for landslide hazard along this length of pipeline. It is assumed that the entire Segment 4 length is located in sloped terrain.

Landslide

Step 1: For a scenario earthquake, calculate the level of shaking (PGA) at the particular location of the component being evaluated.

Assume average PGA for this segment = 0.4g, and the typical soil profile is rock. While landslide zones may be characterized as having up to a few tens of feet of colluvial material, it is still reasonable to use a rock-type attenuation model to estimate ground motions at the pipe locations.

$$\therefore A_{is} = 0.4g$$

Note: Steps 2 thru 4 below are to be used only when no detailed geotechnical investigation is available. In any case, geotechnical investigation done by knowledgeable professionals is strongly recommended.

Step 2: Determine slope angle and geologic group of the region or subregion being evaluated.

Slope: 20° to 30° (based on site survey). Geologic Group: Weakly cemented rock.

Step 3: Determine the susceptibility category, the critical acceleration, a_c and the percentage of the landslide susceptibility area that is expected to be susceptible to landslide during dry and wet conditions.

Dry condition : $\Rightarrow a_c = 0.30g$
Wet condition : $\Rightarrow a_c = 0.10g$

Assume the following percentage of the pipeline lengths that are within susceptible soils:

Dry condition: $\Rightarrow$ Percentage of Map Area with Landslide Susceptible Deposit = 8%
Wet condition: $\Rightarrow$ Percentage of Map Area with Landslide Susceptible Deposit = 25%

Step 4: Estimate amount of PGD due to landslide based the critical acceleration (a_c), the induced acceleration (a_{is}), and the expected number of cycles.

Dry condition:

E[PGD] = 0.57 in.

Wet condition:

E[PGD] = 23 in.

Step 5: Calculate the repair rates for dry and wet conditions.

Dry condition:

N = 0.8 * 1.06 * (0.57)$^{0.319}$ = 0.71 per 1000 ft (covers 8% of pipe length)

N = 0.08 * 0.71 * 26,200 / 1,000 = 1.49 repairs.

Wet condition:

N = 0.8 * 1.06 * (23)$^{0.319}$ = 2.31 per 1000 ft (covers 25% of pipe length)

N = 0.25 * 2.31 * 26,200 / 1,000 = 15.1 repairs.

Step 6: Total Repairs (Ground Shaking) for Segment 4

The total number of repairs for Segment 4:

Assume PGV = 0.4g * 85 cm/g = 13.4 inches per second.

RR = 1.0 * 0.00187 * 13.4 = 0.025 per 1,000 ft

N = 0.92 * 0.025 * 26,200 / 1,000 = 0.60 (dry conditions)

N = 0.75 * 0.025 * 26,200 / 1,000 = 0.50 (wet conditions)

Segment 4

Lake

Fault

Hills

Segment 3

Segment 2

Segment 1
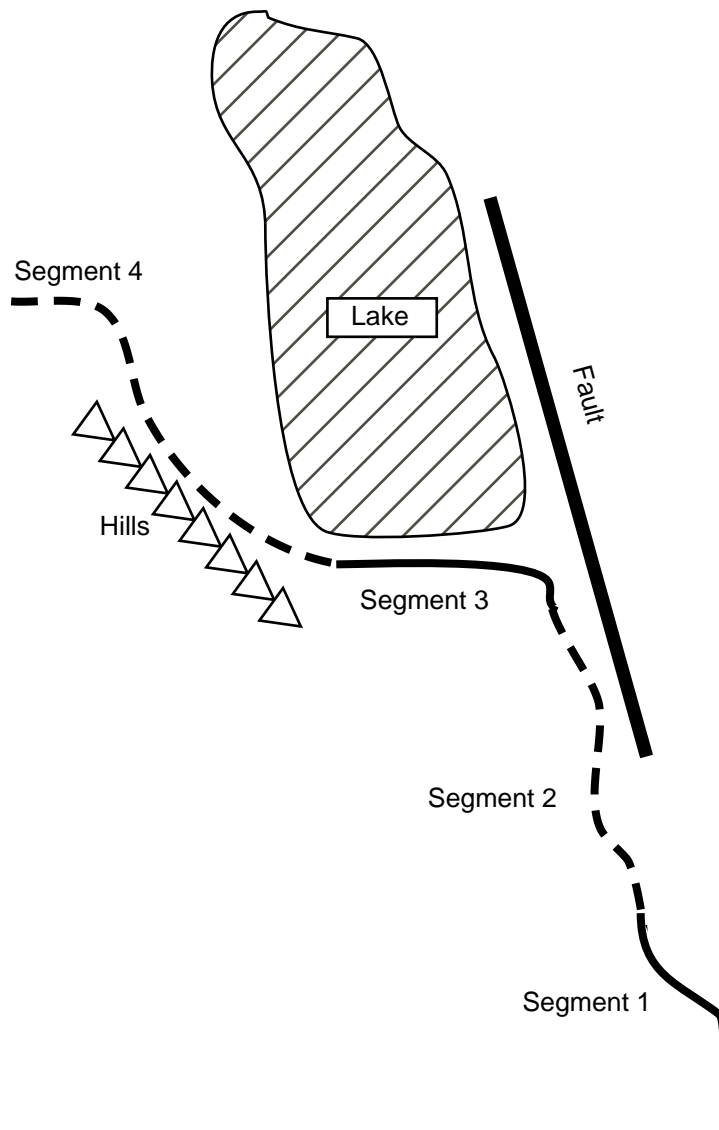
Figure F-1. Example Water Transmission System

G. Bayesian Estimation of Pipe Damage

G.1 Introduction

Appendix G provides an alternative approach for developing fragility curves for estimating damage potential for buried pipelines.

As described in Section 4.6.2 of the main report, the complete empirical dataset exhibits a lot of scatter. It is the judgment of the authors of the report that the form of the fragility function used to describe damage to buried pipelines due to wave passage effects is to use a straight line through the entire dataset. Alternative approaches were investigated in the main report, including a power model. The decision to use a straight line through the dataset, fitted so that 50% of the empirical data points lied below and 50% lied above the curve, was selected for the following reasons:

- The scatter in the empirical dataset is large. Many different types of curves can be fitted through the dataset, but no one would be much better than the other, other than mathematical convenience.

- The theoretical basis for estimating strain in the ground from wave propagation is that it is linearly correlated with maximum ground velocity. For wave propagation, pipe strain is often assumed to be the same as the ground strain, which basically assumes that the pipe does not slide relative to the ground.

- The desired accuracy of the fragility model for ground shaking is perhaps not as important as that for permanent ground deformations. This is because the rate of pipeline damage in soils prone to PGDs is often an order of magnitude larger than the rate of pipeline damage in soils not prone to PGDs.

- Regression analyses which use weighted damage data (Figure A-15) shows that the best fit curve through the empirical data has an exponent of 0.99 (RR = 0.001795 * $PGV^{0.99}$), which is essentially linear.

- Bayesian analyses presented in Section G.10 for cast iron pipe with diameters 6" and 8" (the most common type) show a linear trend (exponent of 0.9942).

Any method used to fit a fragility function through the pipeline empirical database must deal with the form of the empirical database. Specifically, the empirical database has the following issues which might influence how one fits a fragility function through it:

- The empirical data is expressed in terms of repairs per length of pipeline (repairs per 1,000 feet or repairs per km). Each empirical data point is ideally developed by calculating the actual PGV for each pipe of homogeneous attribute. A homogeneous attribute for a pipe mean that the pipe has the same material, same joinery, same diameter, same lay lengths, same installation method, same age, same corrosion protection system, same level of ground shaking, etc. The repair rate is calculated by adding up the entire length of pipe that experienced the same (or nearly the same) level of ground motion, and by adding up all the repairs made to that length of pipe, and taking the ratio = total repairs / total length of pipe with homogeneous attributes.

- For the empirical database presented in Section 4 of the main report, only pipe repairs from the 1994 Northridge earthquake for the LADWP and the 1989 Loma Prieta earthquake for EBMUD have used rigorous GIS techniques to present the empirical

data as homogeneous data points. Even so, the only attributes that the homogeneous data points were evaluated at were pipe barrel material, pipe diameter and level of ground shaking.

- When combining empirical data points using regression analysis, a limitation is that each data point is treated equally in the regression analysis. For example, a data point which represents 2 pipe repairs for 20 km of pipe at PGV = 15 inch/sec is 0.1 (=2/20). Another data point that represents 200 pipe repairs for 1,000 km of pipe at PGV = 15 inch/sec is 0.2 (=200/1,000). It is obvious that doing a regression analysis which incorporates these two data points should weight the 1,000 km inventory higher than the 20 km inventory; however, standard regression analysis equally weights the data points.

Recognizing these issues, Appendix G introduces an alternative way to fit fragility curves through the empirical dataset. The method is called "Bayesian Estimation."

Sections G.2 through G.9 use a portion of the entire empirical dataset for purposes of sample application of the method. This introduces the following limitations on the results presented in these sections:

1. The empirical data sample is derived for only the Northridge earthquake for the LADWP water system, and only for cast iron, ductile iron and asbestos cement type pipes.

2. The empirical data sample uses a different parameter for ground motion than what is used in the main report. Specifically, the data sample in Sections G.2 through G.9 uses the highest of the peak PGV of two horizontal directions, whereas the main report uses mean PGV of two horizontal directions. The differences in these two forms of PGV is about 21%.

3. The empirical data sample excludes known damage to pipelines for cases where the repair records had missing attributes. In other words, it is known that a pipe repair was made, but perhaps it is unknown as to what was the pipe barrel material, or what was the pipe diameter. This causes an undercount of pipe repairs by about 8%.

4. Section G.10 addresses these limitations by including additional empirical data from the Loma Prieta earthquake and making the necessary adjustments to allow combination of the Northridge and Loma Prieta datasets into one analysis.

G.2 Background

Bayesian methods provide an alternative to statistical analysis of data that can be particularly effective for the assessment of seismic fragility based on field or laboratory observations. This approach has several features, including (a) the possibility to incorporate engineering expert opinion through a prior distribution, (b) the ability to handle all types of information, including direct measurements, measurement of bounds, and indirect observations, (c) the feasibility to properly and fully account for all types of aleatory (meaning random in the sense of Section E.6) and epistemic (meaning uncertain in the sense of Section E.6) uncertainties, and (d) the ease with which parameter estimates can be updated when new data become available.

Appendix G describes an application of the Bayesian approach to estimate the mean rate of damage along buried pipes caused by seismic ground shaking. The pipe damage data is the same as presented in Tables A.3-14, A.3-15 and A.3-16, but subdivided by pipe diameter; the data is given in Tables G-1, G-2 and G-3.

The Bayesian approach recognizes that uncertainties are always present in estimation of parameters. Accordingly, the state of information about a set of parameters is expressed in terms of a probability distribution. The less dispersed this distribution, the more information it conveys about the parameters. As new information becomes available, the distribution is updated it could become more informative (less dispersed). As seen in the main report, the collection of pipeline damage data across different earthquakes has not yet shown this trend, possibly because of non-homogenous sampling methods.

The Bayesian parameter estimation method is based on the following updating rule:

$$f(\theta) = kL(\theta)p(\theta) \qquad\qquad\qquad \text{[G.1]}$$

which has the following elements:

$\theta = [\theta_1, \theta_2, \Kappa\ ]^T$ is the vector of parameters to be estimated

$p(\theta)$ is the prior distribution reflecting our state of knowledge about θ before new data is obtained. This distribution can be based on engineering expert opinion, which is subjective information. A non-informative prior should be used if no prior information about the parameters is available.

$L(\theta)$ is the likelihood function and represents the objective information contained in the new data. This function is proportional to the conditional probability of observing the data, given the parameters θ. Specific formulations of this function are given later in this appendix.

$k = \left[\int L(\theta)p(\theta)d\theta \right]^{-1}$ is a normalizing factor.

$f(\theta)$ is the posterior distribution representing our updated state of knowledge about θ. This distribution combines the information contained in the prior, which can be subjective in nature, with the objective information contained in the likelihood.

Once the posterior distribution $f(\theta)$ is determined, the posterior mean vector of the parameters is obtained as:

$$M_\theta = \int \theta\ f(\theta)\ d\theta \qquad\qquad\qquad \text{[G.2]}$$

and the posterior mean-square matrix is obtained as:

$$E\left[\theta\theta^T\right] = \int \left(\theta\theta^T\right)f(\theta)d\theta \qquad\qquad\qquad \text{[G.3]}$$

where the superimposed T is the vector transpose. The posterior covariance matrix is computed as:

$$\Sigma_{\theta\theta} = E\left[\theta\theta^T\right] - M_\theta M_\theta^T \qquad\qquad\qquad \text{[G.4]}$$

The diagonal elements of $\Sigma_{\theta\theta}$ are the variances σ_i^2 of the parameters, where σ_i denotes the standard deviation of θ_i, and the off-diagonal elements are the covariances $\rho_{ij}\sigma_i\sigma_j$ from which the correlation coefficients ρ_{ij} are obtained after division by the two standard deviations. The coefficient of variation (c.o.v.) of θ_i is defined as $\delta_i = \sigma_i / \mu_i$. The integrals

in [G.2] and [G.3] are carried out over the applicable domain of θ. A method for computing these integrals is described in Section G.9.

G.3 Poisson Model for Pipe Damage

It can be conveniently assumed that damage along a length of buried pipe due to ground shaking can be modeled as a homogeneous Poisson process. According to this model, the probability that damage occurs at exactly *n* points along a pipe of length *L* is given by:

$$P(n,L) = \frac{(\lambda L)^n}{n!} \exp(-\lambda L), \ \ n = 0,1,2,\text{K}$$

[G.5]

This model has a single parameter λ which is equal to the mean rate of events. Thus, the mean number of damage points along a pipe of length *L* is given by λL. The objective of the Bayesian analysis is to estimate parameter λ.

G.4 Pipe Damage Data

Tables G-1, G-2 and G-3 present pipeline damage data for Cast Iron (CI), Ductile Iron (DI) and Asbestos Cement (AC) pipe from the LADWP, from the 1994 Northridge earthquake. Section G-1 presents some limitations to this data which would be required in order to combine it with data from the other sources presented in this report.

Each data point is for a homogeneous length of pipeline *L* with diameter D that experienced a range (bin) of peak ground velocity centered on PGV (cm / s) and that experienced *n* known pipe repairs. Blank entries in the tables indicate that there were no pipes of the specified diameter that were located in an area that experienced ground motion PGV in the specified bin.

The mean rate of damage along a buried pipe may depend on such variables as the intensity of the ground motion, the material of the pipe, the pipe diameter and wall thickness, the depth of soil cover, the lay length of the pipe, the corrosivity of the soil, the corrosion protection system for the pipe, the number and type of laterals, etc. Determining the mean rate of damage as a function of all these variables would require a large matrix of observed pipe damage data for each set of these variables, which is not available at this time. As a result, one has to "bin" the data together to make estimates of the mean rate as a function of only a subset of these variables.

The data in Tables G-1 to G-3 is used in the following sections to estimate λ as a function of the PGV for each pipe type. In the case of CI pipes with diameters in the range of 4-12 inches, the data is sufficiently rich to allow inferring a dependence of λ on the pipe diameter as well (but note Figure A-11 using another dataset does not show the same dependence on diameter). For larger diameter CI pipes, or for DI and AC pipes, the data is not sufficiently rich to allow inferring the dependence of λ on the pipe diameter.

As is the case with any statistical estimate, the results and conclusions derived in the following analyses are conditioned on the data base. If the data is changed or modified, the results and conclusions may also vary.

G.5 Estimation of λ for Cast Iron Pipes

Examination of the data for CI pipes in Table G-1 reveals that there is a fairly uniform data available for pipe sizes 4-12 inch in diameter, except for pipes of 10 inch diameter.

Specifically, for these pipe sizes, observations for relatively long pipe segments (tens or hundreds of kilometers) have been made. In contrast, the data for pipe sizes 16-24 inch diameter is relatively sparse. If we were to combine the data for all pipe sizes together, obviously the smaller pipes with larger data would dominate the result. For this reason, we perform separate analyses for these two ranges of pipe diameters.

G.5.1 Cast Iron Pipes with 4-12" Diameter

In order to estimate λ as a function of the PGV and the pipe diameter, we need an interpolation model. We select the relation:

$$\lambda = a * V^b * D^{-c} \qquad\qquad [G.6]$$

were V is PGV is in cm/sec and D is the pipe diameter in inches and a, b, and c are the parameters to be estimated. Note that by selecting the form of equation [G.6], the Bayesian model assumes that pipe damage increases with increasing PGV, and decreases with increasing D (that is, if parameters b and c are positive). The issue as to whether pipe damage increases with PGV seems to be well accepted. The issue as to whether pipe damage rate should decrease with increasing D seems to be indicated in some datasets (Tables G-1 through G-3), but not in other datasets (see Figure A-11). For purposes of Sections G.2 through G.9, the [G.6] model is presented as illustrative of the technique using the particular datasets of Tables G-1, G-2 and G-3, with recognition that the smoothness inferred from this model is not well represented in the more complete empirical database currently available; Section G.10 examines this issue in more detail.

Using this relation in [G.5], the probability that a pipe of length *L*, having diameter *D*, will experience *n* damage points due to a ground motion with PGV equal to *V*, is given by:

$$P(n,L) = \frac{(aV^b D^{-c} L)^n}{n!} \exp(-aV^b D^{-c} L) \qquad\qquad [G.7]$$

As mentioned earlier, the likelihood function is proportional to the conditional probability of the data, given the set of parameters. The data in this case consists of observations V_i, D_i, L_i and n_i, $i = 1, K, N$, as listed in Table G-1 for the considered pipe sizes. Assuming statistical independence between the observations and using [G.7], the likelihood function takes the form:

$$L(a,b,c) = \prod_{i=1}^{N} \left[\frac{(aV_i^b D_i^{-c} L_i)^{n_i}}{n_i!} \exp(-aV_i^b D_i^{-c} L_i) \right] \qquad\qquad [G.8]$$

For Bayesian updating analysis, we also need to select a prior distribution. If prior information on the parameters were available, we could include it through this distribution. For purposes of Appendix G, we use a non-informative prior, which for the case of positive-valued parameters is proportional to their reciprocals [see Box and Tiao 1992], i.e.,:

$$p(a,b,c) \propto \frac{1}{abc} \qquad\qquad [G.9]$$

With the likelihood function and the prior distribution formulated, the Bayesian analysis is carried out by use of the updating rule in [G.1]. Once the posterior density is determined, the posterior means, standard deviations and correlation coefficients are computed using

[G.2]-[G.4]. Sections G.9 and G.11 describes the computational method used for this purpose.

Table G-4 lists the posterior means, standard deviations and correlation coefficients of the model parameters obtained for this case. These are computed with an accuracy of 5% c.o.v. in the estimated means (see Section G.9). It is important to note that these parameter estimates are for the units indicated in parenthesis in the title of the table.

Parameter	μ_i	σ_i	ρ_{ij}		
			a	*b*	*c*
a	0.0631	0.0205	1.000	−0.640	0.720
b	0.8424	0.0547	−0.640	1.000	0.021
c	1.4568	0.1378	0.720	0.021	1.000

Table G-4. Posterior statistics of parameters a, b and c for CI pipes of diameter 4 to 12 inches (for V in cm/s, D in inches, and λ per km^{-1}).

With the posterior statistics of the parameters available, we can now estimate the mean and coefficient of variation of λ. Using first-order approximations [Ang and Tang 1975], the mean of λ is given by:

$$\mu_\lambda \cong \mu_a V^{\mu_b} D^{-\mu_c} \tag{G.10}$$

and its c.o.v., δ_λ, is given by:

$$\begin{aligned}
\delta_\lambda^2 &\cong \frac{1}{\mu_\lambda^2}\sum_i\sum_i\frac{\partial\lambda}{\partial\theta_i}\frac{\partial\lambda}{\partial\theta_j}\rho_{ij}\sigma_i\sigma_j \\
&= \delta_a^2 + (\ln V)^2\sigma_b^2 + (\ln D)^2\sigma_c^2 \\
&\quad + 2(\ln V)\delta_a\sigma_b\rho_{ab} - 2(\ln D)\delta_a\sigma_c\rho_{ac} - 2(\ln V)(\ln D)\sigma_b\sigma_c\rho_{bc}
\end{aligned} \tag{G.11}$$

These values are plotted in Figures G-1 and G-2 (solid curves) as functions of the PGV (in in/sec) for different diameter pipes. The estimates for the mean are multiplied by 0.3048 to find the mean rate of damage per 1000 ft of pipe.

It is noted in Figure G-1 that for these pipes the mean rate of damage is strongly influenced by the pipe diameter. The mean rate of damage shows a steady increase with the PGV for all pipe sizes. The c.o.v. of λ, which is a measure of the epistemic uncertainty in measuring the mean rate of damage, is of the order of 10-15%. Note that the percent difference between the estimated mean rates for different pipe sizes is much greater than the estimated c.o.v., which would appear to justify the use of the pipe diameter as a variable for estimating λ, at least for this dataset; even though other datasets do not seem to support this hypothesis (for example, see Figure A-11).

G.5.2 Cast Iron Pipes with 16-24" Diameter

For this group of pipes, the data in Table G-1 is rather sparse. Analysis with the 3-parameter formula in [G.6] leads to results that cannot be justified. Specifically, the percent difference between estimates of the mean rate of damage for different pipe sizes is smaller than the estimated c.o.v. of λ. This implies that, based on the present data, the differentiation of the pipe sizes is not justified. Therefore, for these pipes, we use the 2-parameter formula:

$$\lambda = aV^{b} \tag{G.12}$$

where a, b are the parameters to be estimated. The likelihood function in this case takes the form:

$$L(a,b) = \prod_{i=1}^{N} \left[\frac{(aV_i^{b}L_i)^{n_i}}{n_i!} \exp(-aV_i^{b}L_i) \right] \tag{G.13}$$

We also select the non-informative prior:

$$p(a,b) \propto \frac{1}{ab} \tag{G.14}$$

Table G-5 lists the posterior means, standard deviations and correlation coefficients of the model parameters for this case. These are estimated with an accuracy of 5% or less c.o.v. of the estimated means. Note again that these parameter estimates are valid for the units indicated in parenthesis in the title of the table.

Parameter	μ_i	σ_i	ρ_{ij}	
			a	b
a	0.0230	0.0139	1.000	-0.686
b	0.1658	0.2270	-0.686	1.00

Table G-5. Posterior statistics of parameters a and b for CI pipes of diameter 16 to 24 inches (for V in cm/s and λ per km^{-1}).

The mean and c.o.v. of λ are computed, based on first-order approximations, from:

$$\mu_{\lambda} \cong \mu_a V^{\mu_b} \tag{G.15}$$

$$\delta_{\lambda}^2 \cong \delta_a^2 + (\ln V)^2 \sigma_b^2 + 2(\ln V)\delta_a\sigma_b\rho_{ab} \tag{G.16}$$

The results are shown in Figures G-1 and G-2, respectively, as dashed lines. The c.o.v. of λ is around 50% to 90%, indicating a high level of epistemic uncertainty in the estimation. This could be due to the sparseness of the data for this range of pipe sizes, or other unknown factors. It is noted that the mean of λ only mildly increases with the PGV for this type of pipe.

G.6 Estimation of λ for Ductile Iron Pipes

The data for DI pipes in Table G-2 is rather sparse for all pipe sizes. Hence, we cannot justify using the 3-parameter formula [G.6]. Instead, we use the 2-parameter formula in [G.12] with $\theta = (a,b)$ as the set of parameters. Table G-6 lists the posterior statistics of the parameters.

Parameter	μ_i	σ_i	ρ_{ij}	
			a	b
a	0.0073	0.0071	1.000	-0.840
b	0.6770	0.2510	-0.840	1.00

Table G-6. Posterior statistics of parameters a and b for DI pipes
(for V in cm/s and λ per km^{-1})

The mean and c.o.v. of λ are computed by use of [G.15] and [G.16]. These are plotted in Figures G-3 and G-4, respectively, as functions of the PGV (in in/sec). The estimates for the mean are multiplied by 0.3048 to find the mean rate of damage per 1000 ft of pipe. The c.o.v. of λ is around 50% to 70%, signifying a large epistemic uncertainty in the estimation. This could be due to the sparseness of the data for the DI pipes or other factors. A rapid increase in the mean of λ with the PGV is observed in Figure G-3.

G.7 Estimation of λ for Asbestos Cement Pipes

The data for AC pipes in Table G-3 is rather sparse for all pipe sizes. Hence, we cannot justify using the 3-parameter formula [G.6]. Instead, we use the 2-parameter formula in [G.12] with $\theta = (a,b)$ as the set of parameters. Table G-7 lists the posterior statistics of the parameters.

Parameter	μ_i	σ_i	ρ_{ij}	
			a	b
a	0.0044	0.0038	1.000	-0.860
b	0.6625	0.2477	-0.860	1.00

Table G-7. Posterior statistics of parameters a and b for AC pipes
(for V in cm/s and λ per km^{-1})

The mean and c.o.v. of λ are computed by use of [G.15] and [G.16]. These are plotted in Figures G-5 and G-6, respectively, as functions of the PGV (in in/sec). The estimates for the mean are multiplied by 0.3048 to find the mean rate of damage per 1000 ft of pipe. The c.o.v. of λ is around 45% to 65%, signifying a large epistemic uncertainty in the estimation. This might be due to the sparseness of the data for the AC pipes, or other factors. The mean of λ shows a rapid increase with the PGV in Figure G-5.

G.8 Comparison of Results for Different Pipe Materials

Figures G-7 and G-8 compare the mean and c.o.v. estimates of λ for all the pipes, respectively. Solid lines are for CI pipes of different diameter, as indicated, the dotted lines are for the DI pipes with 4-20" diameter, and the dashed lines are for the AC pipes with 4-12" diameter. It is clear from Figure G-8 that the estimation is most accurate for the CI pipes with 4-12" diameter, for which a large amount of data is available. The estimates for the CI pipes with 16-24" diameter, and for the DI and AC pipes are a lot more uncertain.

The mean estimates in Figure G-1 indicate that large diameter CI pipes and AC pipes have the lowest mean damage rates. However, this conclusion should be used with caution, particularly for AC pipes, due to the large epistemic uncertainty that is present in the estimation. Further data collection can help reduce this uncertainty.

If and when new data becomes available, the posterior statistics obtained in Appendix E can be used to formulate a prior distribution for the parameters. The updating procedure can then be used to derive posterior statistics of the parameters that incorporate the information gained from the new data.

G.9 Integration by Importance Sampling

Determination of the normalizing factor in the Bayesian updating rule [G.1] and the posterior statistics in [G.2] and [G.3] require multi-dimensional integral calculations. Conventional numerical integration methods may not be effective for more than 2 parameters. Section G.9 presents a method for evaluation of these integrals by importance sampling that is effective for any number of parameters. Section G.11 provides computation routines to apply this method.

The integrals to be computed can all be written in the unified form:

$$I = \int K(\theta)L(\theta)\,p(\theta)\,d\theta \qquad\qquad [G.17]$$

For $K(\theta) = 1$, the integral yields the reciprocal of the normalizing factor k; for $K(\theta) = k\theta$, the integral yields the posterior mean vector $\mathbf{M}_\theta$; and for $K(\theta) = k\theta\theta^{\mathrm{T}}$, the integral yields the posterior mean-square matrix $\mathrm{E}[\theta\theta^{\mathrm{T}}]$, from which the posterior covariance matrix is computed as in [G.4]. In the following, we describe the computation of a typical integral as in [g.17].

Let $h(\theta)$ denote a suitable sampling probability density function that has a non-zero value within the domain of θ. We can rewrite [G.17] as:

$$\begin{aligned}
I &= \int \frac{K(\theta)L(\theta)\,p(\theta)}{h(\theta)} h(\theta)\,d\theta \\
&= \mathrm{E}\!\left[\frac{K(\theta)L(\theta)\,p(\theta)}{h(\theta)}\right]
\end{aligned} \qquad\qquad [G.18]$$

where E[•] denotes expectation. It is clear that the integral of interest is equal to the mean of $K(\theta)L(\theta)\,p(\theta)/h(\theta)$ with respect to the sampling density $h(\theta)$. Therefore, a simple method for computing the integral I is:

1. Generate a sample of parameter values θ_i, $i = 1,2,\mathrm{K}\,,N$, according to the probability density function $h(\theta)$.

2. Compute the corresponding values $I_i = K(\theta_i)L(\theta_i)\,p(\theta_i)/h(\theta_i)$.

3. Compute the sample mean $\bar{I} = \sum_{i=1}^{N} I_i/N$.

4. As N becomes large, $\bar{I}$ asymptotically approaches the integral I. A measure of accuracy of the computation is given by the c.o.v. of $\bar{I}$. This is computed as $\delta I/\sqrt{N}$, where δI is the c.o.v. of the sampled values I_i, $i=1,2,\mathrm{K}\,,N$.

Matlab routines for computing the posterior statistics of the 3-parameter model [G.6] are presented in Section G.11. For the sampling density function $h(\theta)$, owing to the non-negativeness of the parameters, a joint lognormal distribution is used. For faster convergence, it is important that the sampling density have a mean vector and a covariance matrix that are close to the posterior mean vector and covariance matrix of the parameters. Since these values are not known in advance, we use an adaptive approach. That is, one starts with an assumed mean vector and covariance matrix for the sampling density $h(\theta)$ and makes a first estimate of the posterior statistics of the parameters. The mean vector and covariance matrix of the sampling density are then replaced by the estimated posterior mean and covariance matrix and the calculation is repeated. This process is continued until sufficiently small c.o.v. values of the estimated posterior mean values are obtained. For numerical stability, it is also important that the normalizing factor k be neither too small nor too large. A scale parameter for the likelihood function is provided in the Matlab code that can be adjusted to control the magnitude of the normalizing factor.

G.10 Updated Bayesian Analyses

The analytical results presented in Sections G.1 through G.8 are based on application of the Bayesian model using data only from the 1994 Northridge earthquake, Tables G-1, G-2 and G-3. To further examine the Bayesian model, the analyses were repeated, this time also using the data from the 1989 Loma Prieta earthquake, Tables A.3-7, A.3-8 and A.3-9.

As described elsewhere in this report, the available empirical datasets from these two earthquakes do not use precisely the same definitions of PGV. The differences are: Northridge dataset uses peak of two horizontal directions versus Loma Prieta dataset uses median of two horizontal directions; Northridge dataset excludes 7.9% of main damage (see Section A.3.12).

Table G-8 provides a summary of the computed mean *a*, *b* and *c* values from the updated Bayesian analyses. For small diameter cast iron pipe, the parameters are for the model in equation G.6. for other entries, the parameters are for the model in equation G.12.

Pipe Material	Diameter	a	b	c
Cast Iron	4-12"	0.0324	0.9942	1.3188
Cast Iron	16-24"	0.0187	0.2454	
Asbestos Cement	4-12"	0.0016	0.8804	
Ductile Iron	4-20"	0.0073	0.677	
Welded Steel	4-30"	0.000213	1.8678	

Table G-8. Summary of Updated Bayesian Analysis Parameters a, b, c. Units are: (for V in cm/s, D in inches, and λ repairs per km^{-1}).

Table G-9 compares the updated Bayesian analysis results with those presented elsewhere in this report. The most common pipe material in the empirical dataset is 6 and 8 inch diameter cast iron pipe. The Bayesian analysis assumes an explicit diameter value (D^{-c}) in equation G.6. to make comparisons, we evaluate this factor and adjust the Bayesian "a" value accordingly. The results are in Table G-9. As can be seen the Bayesian analysis predicts parameter "b" to be 0.9942, which is essentially unity (linear model). By averaging the most common empirical data, the Bayesian analysis would suggest a model of:

$RR = 0.0197 \, (PGV)^{0.9942}$, with RR = repairs per 1,000 feet and PGV in inches per second.

This model is very similar to that derived using a slightly wider dataset (Figure A-15) using weighted regression, and also very similar to the small diameter Cast Iron fragility model provided in the main report (Table 4-4, with K1 = 1.0 from Table 4-5).

Pipe Material	Diameter	Adjusted Parameter a	Parameter b	Notes
Cast Iron	6"	0.00234	0.9942	Bayesian, LP+NR
Cast Iron	8"	0.00160	0.9942	Bayesian, LP+NR
Cast iron	Avg 6", 8"	0.00197	0.9942	Bayesian Average, LP+NR
Cast Iron	All diameters	0.00180	0.99	Weighted Regression, Fig A-15, LP+NR
Cast Iron	Up to 12"	0.00187	1.00	Tables 4-4, 4-5

Table G-9. Comparison of Fragility Models for Small Diameter Cast Iron Pipe

G.11 Matlab Routines

Section G.11 provides the Matlab source code and data input files used to compute the statistic presented in Appendix G.

Posterior2.m: Computes the posterior statistics of the parameters for the 2-parameter model (CI pipes 16-24" diameter, DI pipes, AC pipes). It calls Loglhood2.m.

Posterior3.m: Computes the posterior statistics of the parameters for the 3-parameter model (CI pipes 4-12" diameter). It calls Loglhood3.m.

Loglhood2.m: Computes the natural logarithm of the likelihood function for the 2-parameter model. It calls Data2.m.

Loglhood3.m: Computes the natural logarithm of the likelihood function for the 3-parameter model. It calls Data3.m.

Data2.m: Contains the pipe damage data for the 2-parameter model (listed data is for DI pipes)

Data3.m: Contains the pipe data for the 3-parameter model (listed data is for CI pipes 4-12" diameter)

Note: in Data2.m, the lengths of pipe segments and the number of damage points at each PGV level are combined.

Data_CI_16_24.m   Contains the combined data for CI pipes 16-24" diameter

Data_AC.m   Contains the combined data for AC pipes

To run the Matlab routine for the 2-parameter model, do the following:

1. Put all *.m files in a single directory on the path of Matlab.

2. Copy the data file of interest into Data2.m. Right now, Data2.m has the data for DI pipes.

3. Adjust the input parameters in Posterior2.m. Read the heading for guidelines. The parameters are now set for the DI pipes.

4. Issue the command "Posterior2" in the Matlab environment.

5. The computation will take quite some time. To do a quick check without high accuracy, change parameter "nmax" to something small, say nmax=1000. The posterior results will appear on the screen. They will also be stored in the file Results2.mat. Read the guidelines regarding the accuracy of estimation.

To run the program for the 3-parameter model (CI pipes with 4-12" diameter), do as above but replace 2 with 3. The Data3.m file now contains the data for the CI pipes with diameter 4-12".

Posterior2.m

```
%%%%%%%%%%%%%%%%%%%%%%%%%%%%%%%%%%%%%%%%%%%%%%%%%%%%%%%%%%%%%%%%%%%%%%%%
%
% This program computes the posterior means, standard deviations  and
% correlation matrix of the parameters of a 2-parameter model describing
% the mean rate of damage points along a pipe. It uses importance sampling
%  to carry out the necessary integrations over the Bayesian kernel. The
%  joint lognormal distribution with specified means, standard deviations
%  and correlation matrix is used for the sampling distribution.
%  Convergence will be faster if these statistics of the sampling
%  distribution are close to the corresponding statistics of the
%  posterior distribution that are to be computed. The program may be
%  run several times to adjust the statistics of the samplingdistribution.
%
%  For numerical stability, it is important that the normalizing factor
%  k in the Bayesian updating formula be neither too small nor too large.
%  This factor can be adjusted by scaling the likelihood function. In this
%  program this is done by adjusting the "scale" parameter.
%
%  Run the program with trial estimates of the means, standard deviation
%  and correlation matrix of the sampling density, and of the scale
%  parameter.  This will give a first estimate of the reciprocal of the
%  normalizing factor k and the posterior statistics of the parameters.
%  Make sure that the sampling density has sufficiently large standard
%  deviations (no smaller than the posterior standard deviations estimated).
%  Use the first posterior estimates as the new means, standard deviations
%  and correlation matrix of the sampling distribution and adjust the
%  scale parameter (decrease it if k is too large, increase it if k is too
%  small). Run the program again to obtain a second set of posterior estimates.
%  Repeat this process until sufficient accuracy in the posterior estimates
```

```
%  is achieved.
%
%  The accuracy is measured in terms of the coefficients of variation of
%  the posterior mean estimates (denoted cov_p_mean in this program).
%  A value less than 5% for each element of cov_p_mean is a good level
%  of accuracy.
%
%  The results of the computation are stored in the file "Results2.mat"
%  as follows:
%
%         nmin    minimum number of simulations
%         nmax    maximum number of simulations
%         npar    number of parameters
%            k    normalizing factor in the updating formula
%       p_mean    posterior mean vector
%   cov_p_mean    c.o.v. of the posterior mean estimates
%     p_st_dev    vector of posterior standard deviations
%        p_cov    vector of posterior c.o.v.'s
%        p_cor    posterior correlation matrix
%
%%%%%%%%%%%%%%%%%%%%%%%%%%%%%%%%%%%%%%%%%%%%%%%%%%%%%%%%%%%%%%%%%%%%%%%%%%%

clear

%----- Specify the means, standard deviations and correlation matrix
%----- of the sampling density

M    = [0.0081;              % mean vector of sampling density
        0.657];

D = [0.01 0.00;             % diagonal matrix of standard deviations of
     0.00 0.30];       % the sampling density

R = [ 1.00 -0.80;    % correlation matrix of the sampling density
     -0.80  1.00];

%----- Specify the scale parameter

scale = 20;

%----- Set minimum and maximum number of simulations:

nmin = 50000;
nmax = 200000;

%----- Begin calculations

d = diag(D);                % vector of standard deviations
cov = d ./ M;               % c.o.v.'s
z = sqrt(log(1+(cov).^2));  % zeta parameters of lognormal distribution
LAM = log(M) - 0.5 * (z).^2; % lambda parameters of lognormal dist.
Z = diag(z);                % diagonal matrix of zeta's
S = Z*R*Z;                  % covariance matrix of transformed normals
L= chol(S)';                % lower choleski decomposition of S
iS = inv(S);                % inverse of S

%----- Initialize integral values:
```

```
I1 = 0;
I2 = 0;
I3 = 0;
I4 = 0;

npar = length(M);            % number of parameters
i_counter = 0;
flag = 1;
constant = 1/( (6.28318531)^(npar/2) * sqrt(det(S)) );

%----- Begin importance sampling:

for i = 1:nmax

        %-- simulate standard normal random variables;
        u = random('Normal',0,1,npar,1);
        theta = exp( LAM + L*u);      % simulated lognormal theta's

        %-- define three kernels
        K1 = 1;% this is for computing the normalizing constant k
        K2 =  theta;           % this is for computing the mean
        K3 =  theta*theta';     % this is for computing the mean squares

        %-- compute the scaled likelihhod function
         lhood = exp(Loglhood2(theta)+scale);

        %--- compute the prior distribution (non-informative):
         p = 1/(theta(1)*theta(2));

        %--- compute the sampling probability density
        h = constant * exp(-0.5*(log(theta)-LAM)'*iS*(log(theta)-LAM));
        h = h/(theta(1)*theta(2));

        %--- compute (kernel*likelihood*prior)/sampling-density:
        I1 = I1 + K1*lhood*p/h;
        I2 = I2 + K2*lhood*p/h;
        I3 = I3 + K3*lhood*p/h;

         I4 = I4 + (K2*lhood*p/h).^2;  % this is for computing cov_p_mean

        %--- reciprocal of the normalizing constant
        k = I1/i;

        %--- posterior mean and its c.o.v.
        p_mean = I2/I1;
        cov_p_mean = sqrt(( 1/i*(I4/(k^2*i)-(I2/(k*i)).^2) ))./abs(p_mean);

        %--- posterior covariance matrix
        p_cov = I3/I1 - p_mean*p_mean';

         % check if c.o.v is <= 0.05 for all the posterior means, but
        % make sure that at least nmin simulations are performed.
         % flag = 0 means that convergence has been achieved.
         i_counter = i_counter+1;
         if max(cov_p_mean) <= 0.05 &  i_counter>nmin
                flag = 0;
                break
         end
```

```
end


%----- display results:
%
disp('--- Number of simulations')
disp(i_counter);

disp('--- Number of parameters')
disp(npar)

disp('========== Bayesian Posterior Estimates ==========')

disp('--- Reciprocal of normalizing factor k')
disp(k);

disp('--- Posterior means')
disp(p_mean');

disp('--- c.o.v.s for the posterior means')
disp(cov_p_mean')

for i=1:npar
        p_st_dev(i) = sqrt(p_cov(i,i));
        p_c_o_v(i) = p_st_dev(i)/abs(p_mean(i));
end
disp('--- Posterior standard deviations')
disp(p_st_dev)
disp('--- Posterior c.o.v.s')
disp(p_c_o_v)
for i=1:npar
        for j=1:npar
                p_cor(i,j)=p_cov(i,j)/(p_st_dev(i)*p_st_dev(j));
        end
end
disp('--- Posterior correlation matrix')
disp(p_cor);

%--- save results
save Results2 i_counter npar k p_mean cov_p_mean p_st_dev p_c_o_v p_cor
```

Posterior3.m

```
%%%%%%%%%%%%%%%%%%%%%%%%%%%%%%%%%%%%%%%%%%%%%%%%%%%%%%%%%%%%%%%%%%%%%%%%
%
%  This program computes the posterior means, standard deviations  and
%  correlation matrix of the parameters of a 3-parameter model describing
%  the mean rate of damage points along a pipe. It uses importance sampling
%  to carry out the necessary integrations over the Bayesian kernel. The
%  joint lognormal distribution with specified means, standard deviations
%  and correlation matrix is used for the sampling distribution.
%  Convergence will be faster if these statistics of the sampling
%  distribution are close to the corresponding statistics of the
%  posterior distribution that are to be computed. The program may be
%  run several times to adjust the statistics of the sampling distribution.
%
%  For numerical stability, it is important that the normalizing factor
%  k in the Bayesian updating formula be neither too small nor too large.
%  This factor can be adjusted by scaling the likelihood function. In this
```

```
% program this is done by adjusting the "scale" parameter.
%
% Run the program with trial estimates of the means, standard deviation
% and correlation matrix of the sampling density, and of the scale
% parameter.  This will give a first estimate of the reciprocal of the
% normalizing factor k and the posterior statistics of the parameters.
% Make sure that the sampling density has sufficiently large standard
% deviations (no smaller than the posterior standard deviations estimated).
% Use the first posterior estimates as the new means, standard deviations
% and correlation matrix of the sampling distribution and adjust the
% scale parameter (decrease it if k is too large, increase it if k is too
% small). Run the program again to obtain a second set of posterior estimates.
% Repeat this process until sufficient accuracy in the posterior estimates
% is achieved.
%
% The accuracy is measured in terms of the coefficients of variation of
% the posterior mean estimates (denoted cov_p_mean in this program).
% A value less than 5% for each element of cov_p_mean is a good level
% of accuracy.
%
% The results of the computation are stored in the file "Results3.mat"
% as follows:
%
%         nmin    minimum number of simulations
%         nmax    maximum number of simulations
%         npar    number of parameters
%            k    normalizing factor in the updating formula
%       p_mean    posterior mean vector
%   cov_p_mean    c.o.v. of the posterior mean estimates
%     p_st_dev    vector of posterior standard deviations
%        p_cov    vector of posterior c.o.v.'s
%        p_cor    posterior correlation matrix
%
%%%%%%%%%%%%%%%%%%%%%%%%%%%%%%%%%%%%%%%%%%%%%%%%%%%%%%%%%%%%%%%%%%%%%%%%%

clear

%----- Specify the means, standard deviations and correlation matrix
%----- of the sampling density

M     = [0.06;          % mean vector of sampling density
         0.8;
         1.5];

D = [0.03 0.00 0.00;  % diagonal matrix of standard deviations of
     0.00 0.06 0.00;     % the sampling density
     0.00 0.00 0.14];

R = [ 1.00 -0.60  0.70;      % correlation matrix of the sampling density
     -0.60  1.00  0.00;
      0.70  0.00  1.00];

%----- Specify the scale parameter

scale = 310;

%----- Set minimum and maximum number of simulations:
```

```
nmin = 50000;
nmax = 200000;


%----- Begin calculations

d = diag(D);                    % vector of standard deviations
cov = d ./ M;                   % c.o.v.'s
z = sqrt(log(1+(cov).^2));      % zeta parameters of lognormal distribution
LAM = log(M) - 0.5 * (z).^2;    % lambda parameters of lognormal dist.
Z = diag(z);                    % diagonal matrix of zeta's
S = Z*R*Z;                      % covariance matrix of transformed normals
L= chol(S)';                    % lower choleski decomposition of S
iS = inv(S);                    % inverse of S


%----- Initialize integral values:
I1 = 0;
I2 = 0;
I3 = 0;
I4 = 0;


npar = length(M);               % number of parameters
i_counter = 0;
flag = 1;
constant = 1/( (6.28318531)^(npar/2) * sqrt(det(S)) );

%----- Begin importance sampling:

for i = 1:nmax

        %-- simulate standard normal random variables;
        u = random('Normal',0,1,npar,1);
        theta = exp( LAM + L*u);     % simulated lognormal theta's

        %-- define three kernels
        K1 = 1;% this is for computing the normalizing constant k
        K2 =   theta;          % this is for computing the mean
        K3 =   theta*theta';     % this is for computing the mean squares

        %-- compute the scaled likelihhod function
         lhood = exp(Loglhood3(theta)+scale);

        %--- compute the prior distribution (non-informative):
         p = 1/(theta(1)*theta(2)*theta(3));

        %--- compute the sampling probability density
        h = constant * exp(-0.5*(log(theta)-LAM)'*iS*(log(theta)-LAM));
        h = h/(theta(1)*theta(2)*theta(3));

        %--- compute (kernel*likelihood*prior)/sampling-density:
        I1 = I1 + K1*lhood*p/h;
        I2 = I2 + K2*lhood*p/h;
        I3 = I3 + K3*lhood*p/h;

         I4 = I4 + (K2*lhood*p/h).^2;  % this is for computing cov_p_mean

        %--- reciprocal of normalizing constant
        k = I1/i;
```

```
        %--- posterior mean and its c.o.v.
        p_mean = I2/I1;
        cov_p_mean = sqrt(( 1/i*(I4/(k^2*i)-(I2/(k*i)).^2) )),./abs(p_mean);


        %--- posterior covariance matrix
        p_cov = I3/I1 - p_mean*p_mean';

        % check if c.o.v is <= 0.05 for all the posterior means, but
        % make sure that at least nmin simulations are performed.
        % flag = 0 means that convergence has been achieved.
        i_counter = i_counter+1;
        if max(cov_p_mean) <= 0.05 &  i_counter>nmin
                flag = 0;
                break
        end
end

%----- display results:
%
disp('--- Number of simulations')
disp(i_counter);

disp('--- Number of parameters')
disp(npar)

disp('========= Bayesian Posterior Estimates =========')

disp('--- Reciprocal of normalizing factor k')
disp(k);

disp('--- Posterior means')
disp(p_mean');

disp('--- c.o.v.s for the posterior means')
disp(cov_p_mean')

for i=1:npar
        p_st_dev(i) = sqrt(p_cov(i,i));
        p_c_o_v(i) = p_st_dev(i)/abs(p_mean(i));
end
disp('--- Posterior standard deviations')
disp(p_st_dev)
disp('--- Posterior c.o.v.s')
disp(p_c_o_v)
for i=1:npar
        for j=1:npar
                p_cor(i,j)=p_cov(i,j)/(p_st_dev(i)*p_st_dev(j));
        end
end
disp('--- Posterior correlation matrix')
disp(p_cor);

%--- save results
save Results3 i_counter npar k p_mean cov_p_mean p_st_dev p_c_o_v p_cor


Loglhood2.m

%  FUNCTION STATEMENT
```

```
%  Loglhood2 is a string containing the name of a function that computes
%  the logarithm of the likelihood function for the 2-parameter model
%  of the mean rate of pipe damage. This function reads the necessary
%  data stored in array "x" from the file named "Data2.m".

%  ** VARIABLE DESCRIPTION **
%  theta = model parameters;
%  Loglhood2 = logarithm of the likelihood function.

function[Loglhood2] = Loglhood2(theta)

% load data stored in array x:

Data2

[nobsrv] = size(x);
a = theta(1);
b = theta(2);

% Log-likelihood calculation
Loglhood2 = 0;

for i = 1 : nobsrv

        Vi = x(i,1);    %  PGV in cm/s
        Li = x(i,2);    %  Pipe length in km
        Ni = x(i,4);    %  Number of damage points

        lambdaL = a * (Vi^b) * Li;
        if Ni==0
        LogP = -lambdaL;
        elseif Ni>0
        LogP = Ni*log(lambdaL) - log(factorial(Ni)) - lambdaL;
        end

         Loglhood2 = Loglhood2 + LogP;

end
```

Loglhood3.m

```
%  FUNCTION STATEMENT
%  Loglhood3 is a string containing the name of a function that computes
%  the logarithm of the likelihood function for the 3-parameter model
%  of the mean rate of pipe damage. This function reads the necessary
%  data stored in array "x" from the file named "Data3.m".

%  ** VARIABLE DESCRIPTION **
%  theta = model parameters;
%  Loglhood3 = logarithm of the likelihood function.

function[Loglhood3] = Loglhood3(theta)

% load data stored in array x:

Data3

[nobsrv] = size(x);
a = theta(1);
b = theta(2);
```

```
c = theta(3);

% Log-likelihood calculation
Loglhood3 = 0;

for i = 1 : nobsrv

        Vi = x(i,1);     %  PGV in cm/s
        Li = x(i,2);     %  Pipe length in km
        Di = x(i,3);     %  Pipe diameter in inches
        Ni = x(i,4);     %  Number of damage points

        lambdaL = a * (Vi^b) * (Di^(-c)) * Li;
        if Ni==0
        LogP = -lambdaL;
        elseif Ni>0
        LogP = Ni*log(lambdaL) - log(factorial(Ni)) - lambdaL;
        end

         Loglhood3 = Loglhood3 + LogP;

end
```

Data2.m

```
%  This file contains failure data on pipes damaged in past earthquakes.
%   This data is for Ductile Iron pipes and was collected by O'Rourke
%   and Jeon after the Northridge 1994 earthquake.
%
%   V = Peak Ground Velocity, cm/s
%   L = Pipe segment length, km
%   D = Range of pipe diameters (not used in the calculation)
%   N = Number of damage points in the pipe segment.

%     V    L      D   N
x = [ 5    42.2   420  0;
      15   116.7  420  1;
      25   92.7   420  6;
      35   40.3   420  2;
      45   32.2   420  3;
      55   18.1   420  1;
      65   12.8   420  4;
      75   7.5    420  2;
      85   5.3    420  1;
      95   16.1   420  1;
      105  7.4    420  0;
      115  15.6   420  1;
      125  5.8    420  0;
      135  5.4    420  0;
      145  5.7    420  0;
      155  5.4    420  1;
      165  3.3    420  1];
```

Data3.m

```
%  This file contains failure data on pipes damaged in past earthquakes.
%  and Jeon after the Northridge 1994 earthquake.
%  This data is for Cast Iron pipes with diameters  4-12 inches.
%
%   V = Peak Ground Velocity, cm/s
%   L = Pipe segment length, km
%   D = Pipe diameter, in
%   N = Number of damage points in the pipe segment.
%
%     V    L     D  N

x = [ 5   33.8   4  0;
      15  263.8  4  7;
      25  387.2  4  64;
      35  129.5  4  29;
      45  52.3   4  24;
      55  23.3   4  18;
      65  22.4   4  15;
      75  9.4    4  6;
      85  10.4   4  2;
      95  8.0    4  0;
      105 9.9    4  0;
      115 9.2    4  0;
      125 7.5    4  0;
      135 4.8    4  0;
      145 3.3    4  4;
      155 3.6    4  0;
      165 4.1    4  5;
      5   126.5  6  0;
      15  768.7  6  24;
      25  878.8  6  66;
      35  536.9  6  58;
      45  427.7  6  22;
      55  276.0  6  23;
      65  195.5  6  45;
      75  84.7   6  21;
      85  72.4   6  10;
      95  48.2   6  1;
      105 53.1   6  1;
      115 47.7   6  3;
      125 40.4   6  4;
      135 28.5   6  0;
      145 33.9   6  2;
      155 30.9   6  9;
      165 32.0   6  19;
      5   47.5   8  0;
      15  379.5  8  5;
      25  574.1  8  25;
      35  298.5  8  14;
      45  230.5  8  9;
      55  140.0  8  10;
      65  90.9   8  18;
      75  62.0   8  11;
      85  42.1   8  11;
      95  21.0   8  1;
      105 23.1   8  1;
```

```
        115 22.8   8   2;
        125 17.0   8   1;
        135 24.4   8   2;
        145 19.8   8   3;
        155 15.6   8   5;
        165 24.8   8   20;
        5    3.7    10  0;
        15   16.5   10  0;
        25   30.6   10  3;
        35   3.0    10  0;
        5    23.3   12  0;
        15   193.0  12  6;
        25   263.0  12  7;
        35   125.0  12  8;
        45   84.7   12  4;
        55   56.0   12  5;
        65   34.9   12  7;
        75   19.7   12  1;
        85   8.4    12  1;
        95   10.7   12  0;
        105 7.9     12  0;
        115 4.0     12  0;
        125 6.4     12  1;
        135 7.5     12  0;
        145 4.6     12  1;
        155 6.8     12  2;
        165 5.4     12  0];
```

Data_AC.m

```
%  This file contains failure data on pipes damaged in past earthquakes.
%   This data is for Asbestos Cement pipes and was collected by O'Rourke
%   and Jeon after the Northridge 1994 earthquake.
%
%  V = Peak Ground Velocity, cm/s
%  L = Pipe segment length, km
%  D = Range of pipe diameters, in (not used in the analysis)
%  N = Number of damage points in the pipe segment.
%
%    V    L     D    N

x = [ 5   157.3  412  0;
      15   307.9  412  2;
      25   235.5  412  15;
      35   117.7  412  2;
      45   37.8   412  0;
      55   34.1   412  0;
      65   24.4   412  7;
      75   10.9   412  0;
      85   3.0    412  0;
      95   1.2    412  0;
      105 4.8     412  0;
      115 1.6     412  0;
      125 3.9     412  0;
      135 7.2     412  0;
      145 5.0     412  0;
      155 5.8     412  0;
      165 3.5     412  0];
```

Data_CI_16_24.m

```
%  This file contains failure data on pipes damaged in past earthquakes.
%   This data is for Cast Iron pipes and was collected by O'Rourke
%   and Jeon after the Northridge 1994 earthquake.
%
%   V = Peak Ground Velocity, cm/s
%   L = Pipe segment length, km
%   D = Range of pipe diameters, in (not used in the analysis)
%   N = Number of damage points in the pipe segment.
%
%    V    L      D    N

x = [ 5   15.9   1624  0;
     15   67.6   1624  2;
     25   59.8   1624  1;
     35   27.2   1624  2;
     45   9.8    1624  0;
     55   6.9    1624  0;
     65   12.6   1624  2;
     75   2.8    1624  0;
     85   6.8    1624  1;
     95   4.3    1624  0;
    105   2.0    1624  0;
    115   2.9    1624  0;
    125   4.9    1624  0;
    135   6.2    1624  0;
    145   2.7    1624  0;
    155   2.9    1624  0;
    165   0.0
```

G.12 References

Ang, A. H-S., and W-H. Tang. *Probability concepts in engineering planning and design, vol. I - basic principles*. John Wiley & Sons, New York, N.Y, 1975.

Box, G.E.P., and Tiao, G.C. *Bayesian Inference in Statistical Analysis,* Addison-Wesley, Reading, Mass, 1992.

PGV	Pipe Diameter, Inches																	
cm / sec	4		6		8		10		12		16		18		20		24	
	L	n	L	n	L	n	L	n	L	n	L	n	L	n	L	n	L	n
5	33.8	0	126.5	0	47.5	0	3.7	0	23.3	0	7.8	0	0.2	0	8	0		
15	263.8	7	768.7	24	379.5	5	16.5	0	193	6	32.4	2	2.3	0	32	0	0.8	0
25	387.2	64	878.8	66	574.1	25	30.6	3	263	7	43.8	0	4.4	1	11	0	0.5	0
35	129.5	29	536.9	58	298.5	14	3	0	125	8	19.7	1	0.2	0	5.3	1	1.9	0
45	52.3	24	427.7	22	230.5	9			84.7	4	9.2	0			0.6	0		
55	23.3	18	276	23	140	10			56	5	6.9	0						
65	22.4	15	195.5	45	90.9	18			34.9	7	11.9	2			0.7	0		
75	9.4	6	84.7	21	62	11			19.7	1	2.3	0			0.6	0		
85	10.4	2	72.4	10	42.1	11			8.4	1	3.9	0			2.9	1		
95	8	0	48.2	1	21	1			10.7	0	3	0			1.2	0		
105	9.9	0	53.1	1	23.1	1			7.9	0	1.8	0			0.2	0		
115	9.2	0	47.9	3	22.8	2			4	0	2.4	0			0.4	0		
125	7.5	0	40.4	4	17	1			6.4	1	4.3	0			0.6	0		
135	4.8	0	28.5	0	24.4	2			7.5	0	5	0			1.2	0		
145	3.3	3	33.9	2	19.8	3			4.6	1	2.7	0						
155	3.6	0	30.9	9	15.6	5			6.8	2	2.1	0			0.9	0		
165	4.1	5	32	19	24.8	20			5.4	0								
Total	982.5	173	3682.1	308	2033.6	138	53.8	3	861.3	43	159.2	5	7.1	1	65.6	2	3.2	0
Notes																		
L = length of pipeline in km, within the specified PGV bin																		
n = number of repairs																		
See Section G.1 for further description of the data																		

Table G-1. Cast Iron Pipe Damage, 1994 Northridge Earthquake, LADWP

PGV	Pipeline Diameter, Inches											
cm / sec	4		6		8		12		16		20	
	L	n	L	n	L	n	L	n	L	n	L	n
5	0.9	0	19.9	0	11.6	0	5.3	0	3.4	0	1.1	0
15	2.2	0	53.2	1	32.4	0	21.4	0	4.6	0	2.9	0
25	2.5	1	47.5	5	33	0	8	0	1.7	0		
35	1.3	1	16	0	12.8	1	6.5	0	2.3	0	1.4	0
45	1.7	1	10.8	1	10.6	1	8.4	0	0.7	0		
55	2.1	0	6.2	1	8.5	0	1.3	0	0	0		
65	2.1	0	5.6	3	3.4	1	1.4	0	0.2	0	0.2	0
75	1.3	1	1.7	0	2.3	1	2.3	0				
85	0.3	0	2	1	0.4	0	2.6	0				
95	2.6	0	6.2	0	4.5	0	2.7	0	0.1	1		
105	0.6	0	2.8	0	2.1	0	0.2	0	1.7	0		
115	1.5	0	3.9	0	6.5	0	2.2	1	1.4	0	0.2	0
125	0.8	0	2.5	0	1.3	0	0.7	0			0.6	0
135	0.5	0	2.7	0	0.4	0	0.7	0	0.8	0	0.3	0
145	0.3	0	3.2	0	1.4	0			0.7	0	0.1	0
155			4.3	0	0.1	1	0.7	0	0.3	0		
165			2.6	1			0.7	0				
Total	20.7	4	191.1	13	131.3	5	65.1	1	17.9	1	6.8	0
Notes												
L = length of pipeline in km, within the specified PGV bin												
n = number of repairs												
See Section G.1 for further description of the data												

Table G-2. Ductile Iron Pipe Damage, 1994 Northridge Earthquake, LADWP

PGV	Pipeline Diameter, Inches									
cm / sec	4		6		8		10		12	
	L	n	L	n	L	n	L	n	L	n
5	9.5	0	79.3	0	53.4	0			15.1	0
15	14.1	0	180.5	2	88.1	0	1.9	0	23.2	0
25	12.5	6	129.7	7	82.1	2			11.2	0
35	8	0	73.2	1	32.2	1			4.3	0
45	1.1	0	22.6	0	13.1	0			1	0
55	2.8	0	25.1	0	5.4	0			0.7	0
65	2.6	7	17.6	0	3.9	0			0.2	0
75	2.4	0	7	0	1.5	0				
85	0.7	0	2.1	0	0.1	0				
95	0.3	0	0.9	0						
105	0.5	0	3.2	0	1.2	0				
115	0.2	0	1	0	0.4	0				
125	0.3	0	3.4	0	0.1	0				
135	0.6	0	5.5	0	1.1	0				
145	0.2	0	3	0	1.8	0				
155	0.5	0	3.4	0	1.9	0				
165	0.1	0	2.6	0	0.9	0				
Total	56.4	13	560.1	10	287.2	3	1.9	0	55.7	0
Notes										
L = length of pipeline in km, within the specified PGV bin										
n = number of repairs										
See Section G.1 for further description of the data										

Table G-3. Asbestos Cement Pipe Damage, 1994 Northridge Earthquake, LADWP
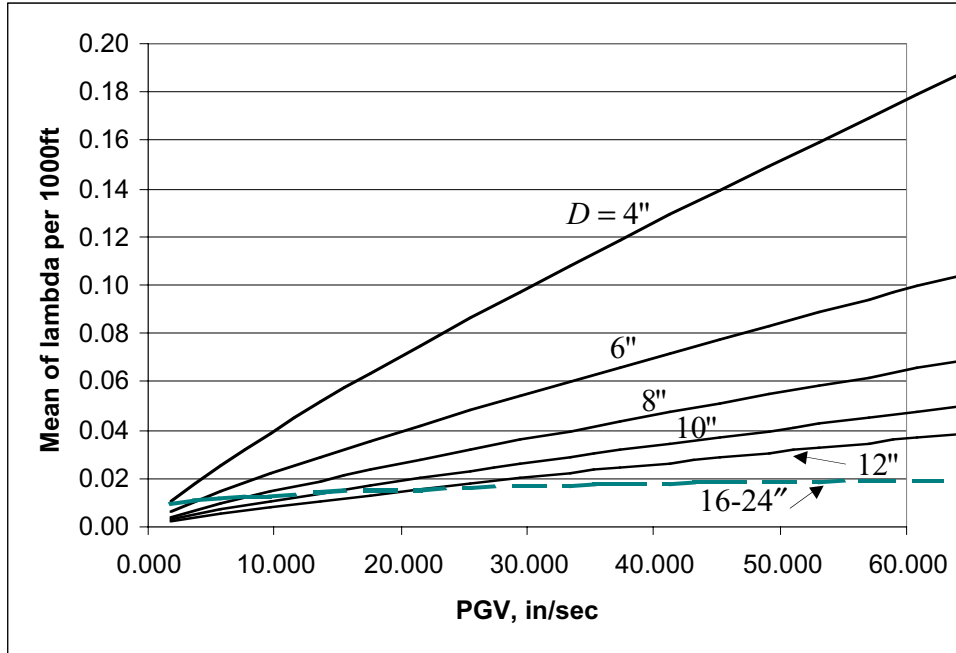
Figure G-1. Mean of λ for Cast Iron Pipes: 3-parameter formula for pipes with
4-12" diameter; 2-parameter formula for pipes with 16-24" diameter.
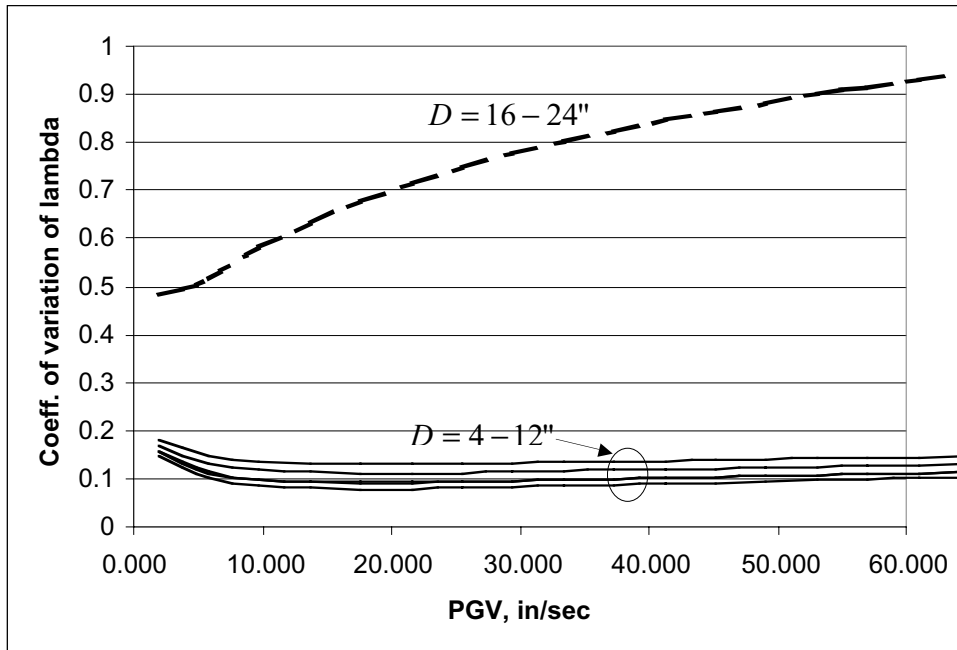
Figure G-2. Coefficient of variation of λ for Cast Iron Pipes:
3-parameter formula for pipes with 4-12" diameter;
2-parameter formula for pipes with 16-24" diameter.
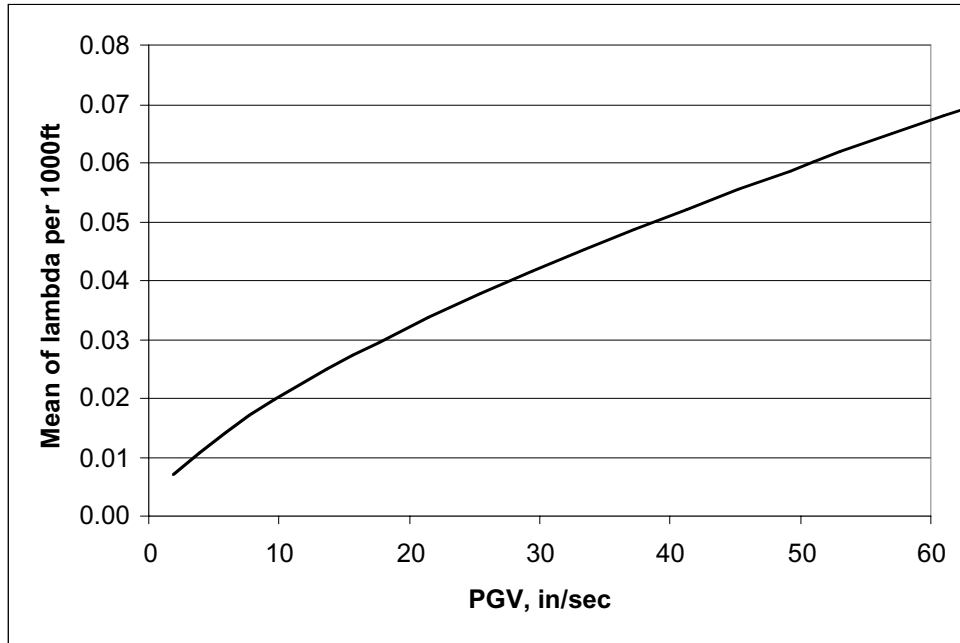
Figure G-3. Mean of λ for Ductile Iron pipes with 4-20" Diameter.
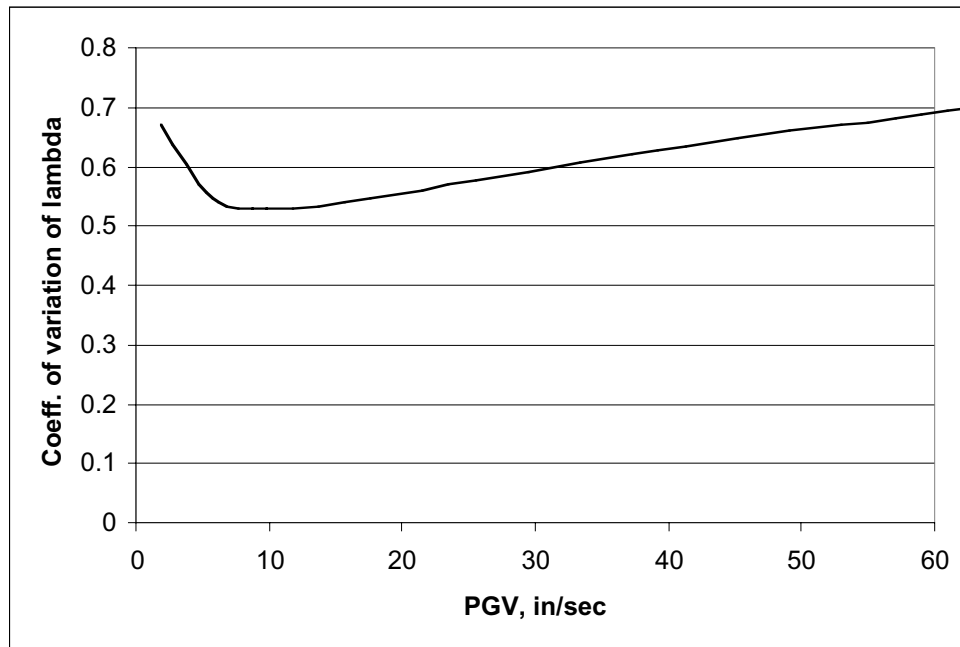
Figure G-4. Coefficient of Variation of λ for Ductile Iron Pipes with 4-20" Diameter.
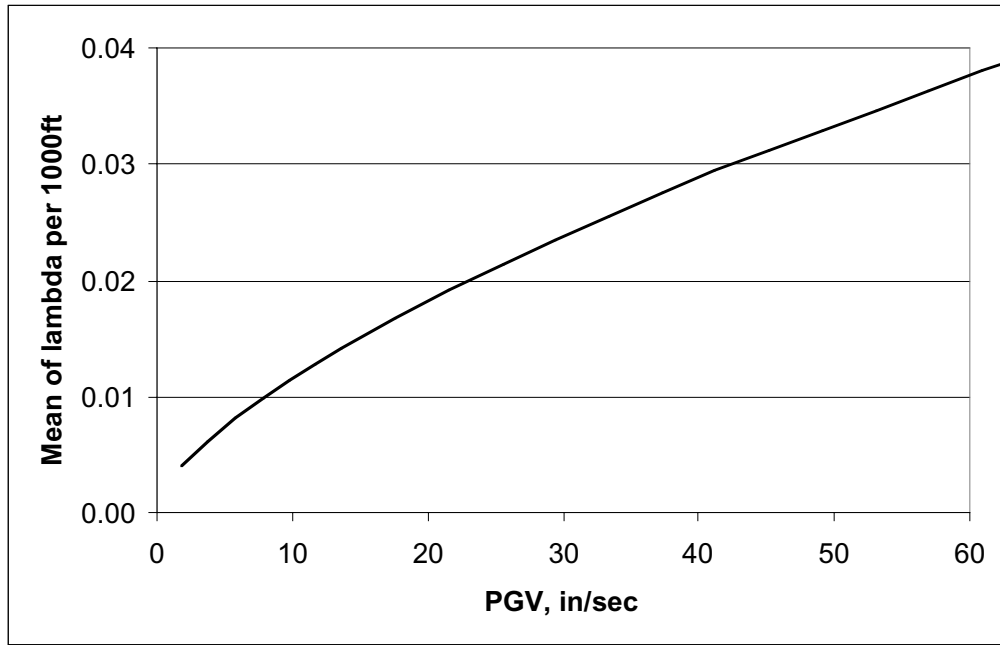
Figure G-5. Mean of λ for Asbestos Cement pipes with 4-12" Diameter.
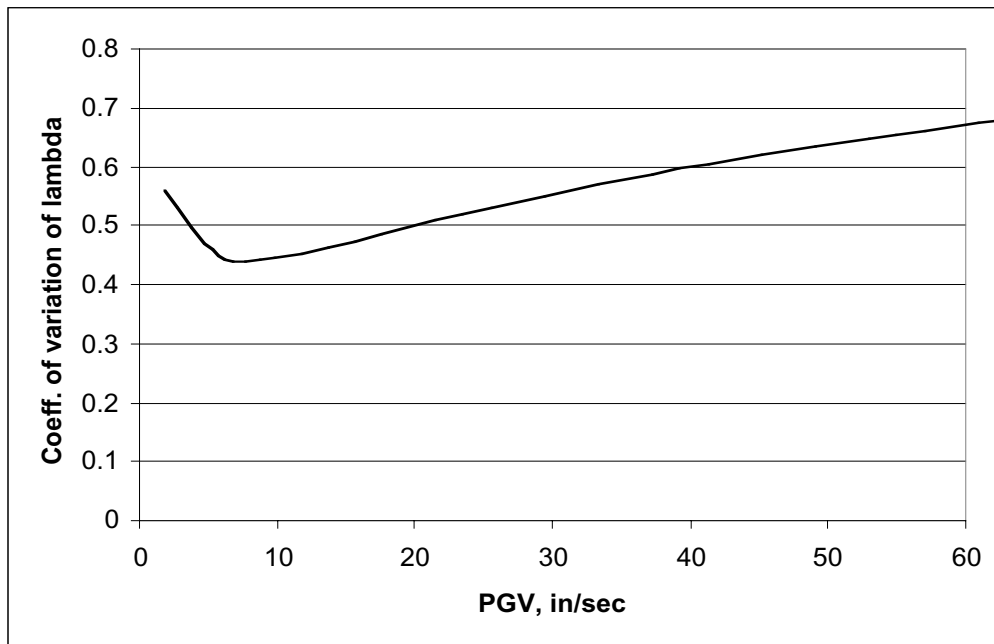
Figure G-6. Coefficient of Variation of λ for AC Pipes with 4-12" Diameter.
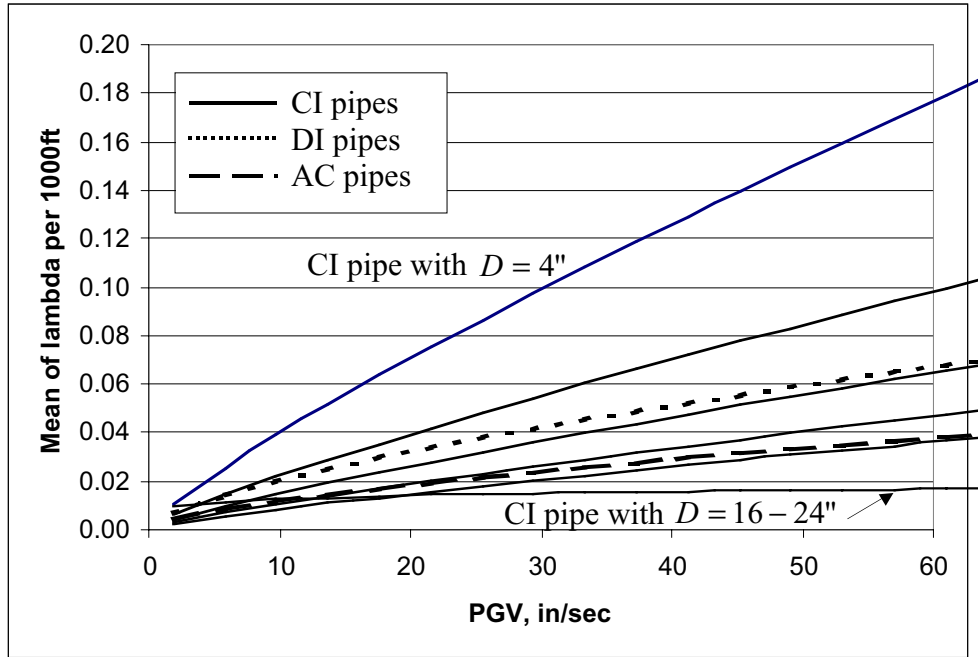
Figure G-7. Comparison of Mean of λ for Pipes of Different Material and Diameter.
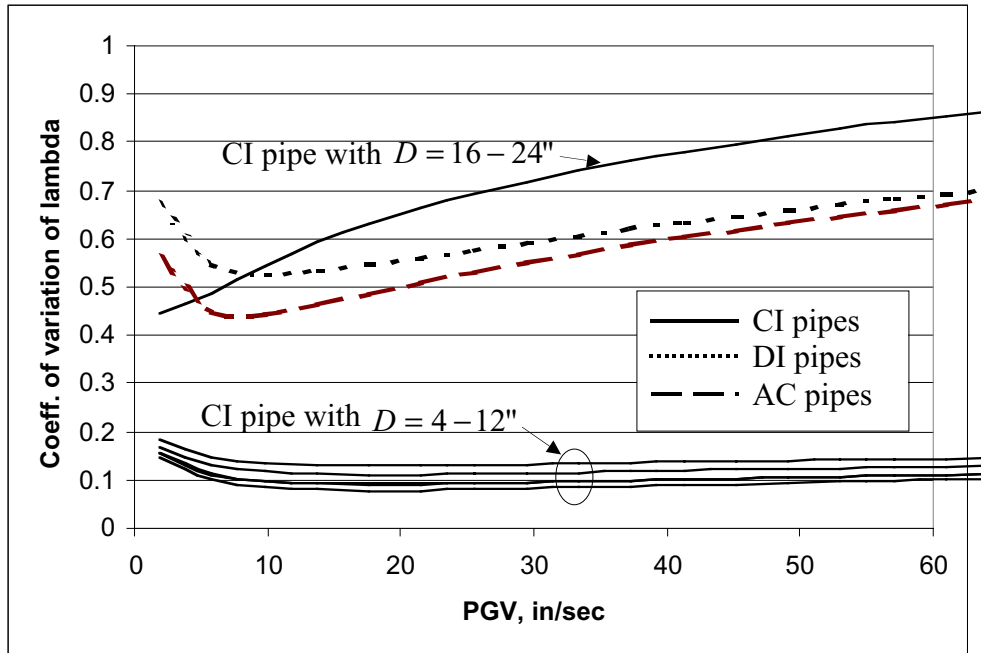

Figure G-8. Comparison of C.O.V. of λ for Pipes of Different Material and Diameter.